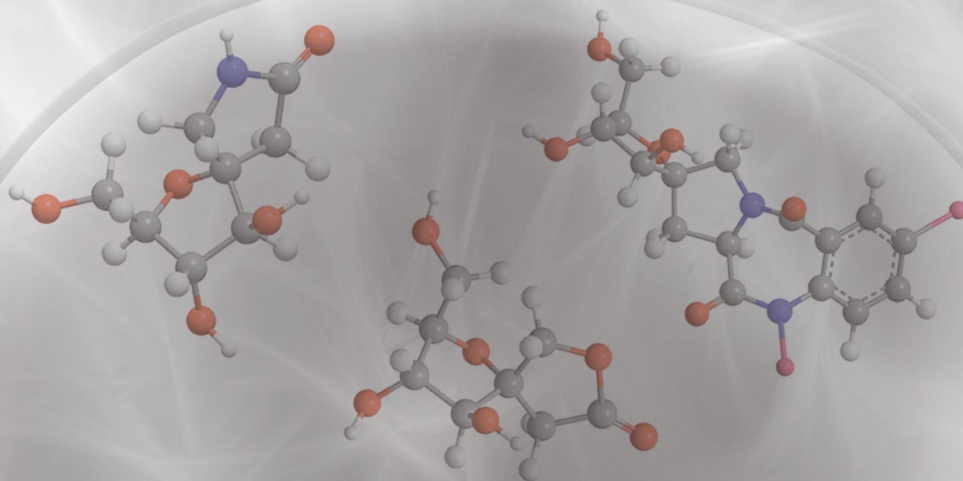


UNIVERSIDADE DE LISBOA
FACULDADE DE CIÊNCIAS
DEPARTAMENTO DE QUÍMICA E BIOQUÍMICA



**POLYFUNCTIONALIZED CARBOHYDRATE-DERIVED
SCAFFOLDS FOR THE PRODUCTION
OF LIBRARIES OF BIOACTIVE COMPOUNDS**

Ana Catarina de Araújo Silva

DOUTORAMENTO EM QUÍMICA
(Química Orgânica)

2009

UNIVERSIDADE DE LISBOA
FACULDADE DE CIÊNCIAS
DEPARTAMENTO DE QUÍMICA E BIOQUÍMICA



POLYFUNCTIONALIZED CARBOHYDRATE-DERIVED SCAFFOLDS FOR THE PRODUCTION OF LIBRARIES OF BIOACTIVE COMPOUNDS

Ana Catarina de Araújo Silva

SUPERVISED BY:

Amélia Pilar Rauter

(Professora Associada com Agregação,
Departamento de Química e Bioquímica,
Faculdade de Ciências da Universidade de Lisboa)

Francesco Nicotra

(Professore Ordinario di Chimica Organica,
Dipartimento di Biotecnologie e Bioscienze,
Università degli Studi di Milano-Bicocca)

DOUTORAMENTO EM QUÍMICA

(Química Orgânica)

2009

To my parents...

*The most beautiful experience we can have is the mysterious –
the fundamental emotion which stands at the cradle of true art and true
science.*

*Living Philosophies, 1931
Albert Einstein*

ACKNOWLEDGMENTS

*“A adversidade desperta em nós capacidades que,
em circunstâncias favoráveis, teriam ficado adormecidas.”*

Quintus Horatius Flaccus

De uma forma pouco convencional quero iniciar este texto agradecendo a todos aqueles que de modo directo ou indirecto contribuíram para as minhas desventuras científicas. Obrigada aos ‘obstáculos’ que ao longo deste percurso académico se fizeram notar, para eles uma mensagem:

*“Pedras no caminho?
Guardo todas, um dia vou construir um castelo...”*

Fernando Pessoa

A nível académico os meus agradecimentos vão, em primeiro lugar, para os meus orientadores, Professora Amélia Pilar Rauter e *Professore* Francesco Nicotra. Tendo sido este doutoramento muito mais do que uma experiência académica, tenho a agradecer não só o contributo científico mas todo o carinho e inspiração que recebi de ambos. Professora Amélia, obrigada pela sua acurada orientação e afectuosa dedicação.

Um agradecimento aos meus colegas de laboratório (FCUL), Nuno, Joana, Susana, Caio, Miguel e Rui, que com extrema paciência me apoiaram e contribuíram de modo sempre espirituoso para o ‘desenrascar’ à Catarina. Ao meu casal *target*, João e Filipa, quero agradecer a disponibilidade constante para as minhas pequenas/grandes dúvidas.

Ao meu colega de laboratório (UNIMIB) e amigo Marcos quero agradecer todo o apoio nos primeiros Km desta aventura. Uns anitos mais tarde tive a oportunidade de trabalhar com uma menina muito especial, a Íris. Obrigada pela tua doçura e a tua sincera disponibilidade em passar a ferro as minhas roupas (Incrível!).

OBRIGADA Anabela, Ana Elisa, Isabel e Verinha (por ordem alfabética); vocês são as *gaiijas, mulheris*, químicas da FCUL, doceiras, mães, voluntárias, e outras características *in press....* do meu coração. Devo salientar contudo que contribuíram de modo significativo na minha incessante busca de novos psicofármacos as noitadas de poker, o *cheesecake* (ou bolo de laranja), aquele filme na casa da Vera (cabos para quê?!), os petiscos da Anabela (e a piscina...não esquecer!), os croissants quentes de Famalicão, as latas de feijão e grão, os telefonemas ao domingo de manhã, e muitos, muitos outros momentos. A vossa amizade forneceu-me os sacos para guardar todas as pedras que fui encontrando ao longo deste caminho, e o vosso apoio e estímulo deram-me as forças para construir as paredes do meu castelo. Muito obrigada.

Isabel, agradeço te a ti em especial todo o apoio científico e emocional que me deste nesta aventura. Lado a lado iniciámos este percurso, e muitas foram as aventuras e desventuras. A tua sensatez foi muitas vezes uma espécie de barómetro na minha vida, ao apaziguar muitos dos meus impulsos irracionais, típicos da minha essência taurina. Obrigada pela tua amizade.

Um especial agradecimento ao meu amigo Rodrigo que generosamente realizou a capa desta tese. Para além do seu contributo gráfico, agradeço a sua protecção quase 'paternal' e enorme afecto. Sei que poderei contar sempre contigo para aliviar o peso de algumas pedras.

Tânia e Susana, OBRIGADA *migas!* O meu trabalho por vezes torna-se a minha vida e nem sempre consigo estar presente como gostaria nos vossos projectos de vida, mas mesmo assim a vossa compreensão é total. Agradeço-vos por não deixarem a minha vida ser normal.

Para ti Miguel sei que palavras valem muito pouco, mas nestas páginas não posso colar actos. Obrigada pelo teu amor....

PedeSenos.... ou é do nome ou realmente sou mesmo eu que sou CHATA. Porque será que estou sempre a PEDIR-te favores?? Não há palavras que descrevam o teu contributo nesta tese, foi só PEDE, PEDE e tu sempre disponível para as inúmeras tarefas que te solicitava. Ora foram correcções, ora boleias à FCUL, ora foi imprimir a tese, 'arranjar' material informático vital para o desenvolvimento do projecto, etc. Tens um segundo emprego e ele é: fazer-me FELIZ. Obrigada por tornares as minhas pedras mais leves!

....*And the winner is: Francisco Cadorna!!* O que este rapaz aturou, eu não devia agradecer, devia pedir desculpa, no mínimo... Admiro a tua perseverança e determinação, mas adoro quando me deixas levar a bicicleta para casa. Sabemos ambos que nem uma página chega para agradecer TUDO o que fizeste por mim. A aprendizagem no laboratório foi importante mas cruciais foram as experiências de vida. Aspirar ou varrer podem colocar a minha integridade moral em risco! Obrigada por me aturares.

To Oscar.... *tack min älskade för ditt ovärderliga stöd.*

Por fim, agradeço aos pilares da minha vida, os meus pais. OBRIGADA pelo infinito apoio. O vosso amor incondicional permitiu-me construir os alicerces do meu castelo e viver nele como uma princesa. A vocês dedico esta tese, porque sem o vosso afecto nada seria possível.

OBRIGADA

“Sono buona fino a che non divento cattiva”.

A Milano ho cominciato questo progetto di ricerca e sono tante le persone con cui ho lavorato o che ho avuto l'opportunità di conoscere. GRAZIE a tutti, è stata fino ad ora una dell'esperienza più bella della mia vita.

Il mio primo ringraziamento va al Professore Nicotra, che più che un professore di chimica organica è stato un professore di filosofia di vita. Lei mi ha insegnato che 'abbinare' è possibile anche nel modo di vivere. Il suo carattere mi è stato di ispirazione. Grazie per il buon vino e la piscina sempre disponibile...

Ringrazio Cristina Redaelli, la mia prima 'supervisora' i primi tempi in laboratorio, che in modo sempre dolce mi ha insegnato a fare le prime reazioni. Alla mia seconda 'supervisora', Ingrid, grazie per l'amicizia e tutto l'appoggio scientifico che mi hai dato. Voglio ringraziare Laura Cipolla per il suo atteggiamento, che mi ha sempre spinto a fare più e più ricerca. Un'enorme riconoscenza anche a Barbara Costa, Pietro e Prof. Gabriella Giagnoni per tutta l'assistenza nel lavoro e per l'affetto.

I 'mie' studenti e amici: Krama, Betta, Rossella e Junior. A loro voglio esprimere gratitudine per tutto l'aiuto che mi hanno dato. Siete un contributo molto importante della mia tesi. Krama, a te più che per le sintesi delle *benzo*, ti ringrazio per le lezioni di italiano.

In laboratorio 4014, Barbara, 'Autista', Dario, Cristiano, 'Brasuca', in laboratorio 4018, Simone (VIVA il trenino), Paolino, Nasrin, Elena e in laboratorio 4048, Peri, Sissi, Square e Luca, a tutti voi GRAZIE per tutto.

Laboratorio 4054: 'Paradise Girl', Erika e 'Ragazzino', voglio dirvi: MI MANCATE tanto, comunque RITORNERÒ...

Chiara e Maria grazie per il viaggio della mia vita: I LOVE NY.

Ale (o Alexandre per il volo RYANAIR), senza di te non riuscivo a sopravvivere neanche cinque minuti a Milano. Grazie per tutte le volte che mi hai aiutato....sono state TANTISSIME. Sei un bravo ragazzo!

Cristina e Russo, GRAZIE amiche mie! Quella serata MERAVIGLOSA non la SCORDERÒ mai... perciò (Attenzione!) possiamo cancellare il video? Grazie Cristina per la vera amicizia e per l'aiuto nella tesi. Russo.... FA MALEEEEEEEEEEE ma vicino a te il dolore diminuisce. Grazie per le belle serate!

'Tesoro' mio e Paty, a voi voglio dire che siete stati la mia luce in quegli ultimi mesi a Milano, in cui io non ce la facevo più. Vi ADORO (Viva Partanna).

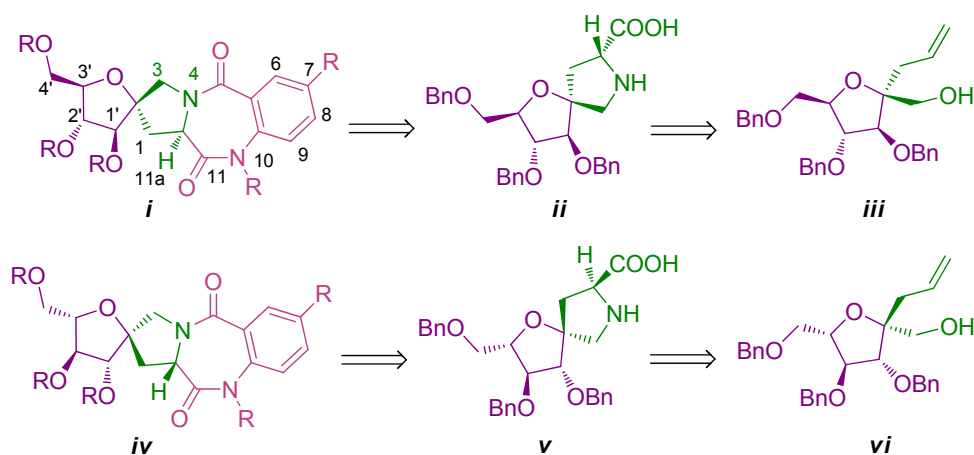
GRAZIE MILLE

ABSTRACT

Inspired by the role of carbohydrates as natural scaffolds, we exploited the sugar skeleton to generate new libraries of polyfunctionalized compounds as GABA_A receptor ligands. Hybrids of benzodiazepines, γ -butyrolactone and -lactam derivatives, and a GABA analogue were developed. The incorporated sugar moiety offered the possibility of diverse and controlled functionalization, modulating physicochemical and structural properties, namely solubility and rigidity, and consequently biological activity of the synthesized scaffolds.

1,4-Benzodiazepine-2,5-dione scaffolds (**i** and **iv**) derived from spiro bicyclic D- or L-proline analogues (**ii** and **v**), containing a D- or a L-fructose moiety were synthesized in the present work. The D-proline analogue **ii** was prepared in a sixteen-step synthesis in 24% overall yield, adopting a methodology which used D-fructose as starting material and 3-*C*-(3,4,6-tri-*O*-benzyl- α -D-fructofuranos-2-yl)propene **iii** as key intermediate. Instead, the L-fructose moiety, required for the preparation of the corresponding L-proline analogue **v**, was obtained using a new synthetic pathway. The key intermediate of this synthesis, the 3-*C*-(3,4,6-tri-*O*-benzyl- α -L-fructofuranos-2-yl)propene **vi**, was effectively obtained from L-arabinose through a seven steps pathway in 13.5% overall yield. This starting material embodies the furanose ring with the appropriate configuration. Hence, a one carbon chain elongation at the anomeric position lead to the desired L-fructose derivative, compound **vi**. For that purpose, oxidation to arabinonolactone, formyl group introduction *via* a dithiated intermediate and reduction to the primary alcohol were performed. The subsequent eleven-step synthesis afforded the new spiro bicyclic L-proline analogue **v** in 24% overall yield. In addition, a procedure previously reported for L-fructose synthesis was also used to obtain 3-*C*-(3,4,6-tri-*O*-benzyl- α -L-fructofuranos-2-yl)propene **vi**. Starting from L-sorbose, diisopropylidene protection, mesylation, selective deprotection, oxirane formation and opening led to inversion of configuration at C-3 and C-4

affording the stereochemistry of L-fructose. The key intermediate **vi** was obtained by this eight-step synthesis with a 8.5% overall yield.

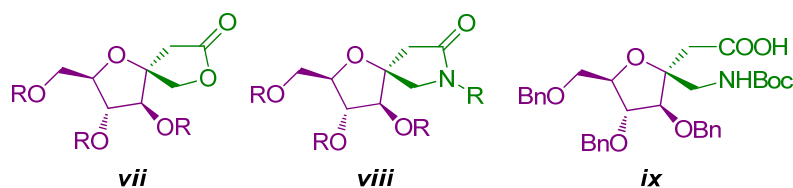


Molecular modelling calculations, NMR studies at variable temperature (dynamic NMR–DNMR) and preliminary biological studies were also performed on these compound libraries of enantiomeric fructose–proline–benzodiazepine derivatives (**i** and **iv**). The proline moiety linked to the fructose derivative through a spiro junction and consequent fusion of this bicyclic structure to the benzodiazepine ring promoted high conformational rigidity to the hybrid scaffold. Therefore, the conformational equilibrium normally occurring with (*P*) and (*M*) benzodiazepine conformers was not observed. The benzodiazepine derivatives synthesized adopted a rigid conformation in which the C-11a substituent was always pseudo-equatorial.

The diverse and controlled functionalization of these molecules (**i** and **iv**) was achieved using different isatoic anhydride types which are commercially available. Coupling of D- or L-proline analogues, **ii** and **v**, respectively, with the suitably functionalized isatoic anhydride, afforded the desired sugar-based pyrrolobenzodiazepine library (**i** and **iv**). These compounds were functionalized not only with electronegative substituents, such as –Cl, –Br and –NO₂, but also with –NH₂ at position seven, while at position ten the presence of –CH₃ is expected to give a more appropriate binding affinity, as suggested by reported QSAR studies. The ability of

these compounds to displace the [^3H]flunitrazepam from the GABA_A receptor was measured with a competition binding assay using rat cortical membrane. It was observed that substitution on both positions are crucial for binding affinities, being particularly effective $-\text{NO}_2$ and $-\text{NH}_2$ groups. The free $-\text{OH}$ or $-\text{CH}_2\text{Ph}$ groups on the sugar offered the possibility to balance hydrophilic/lipophilic for tuning the pharmacokinetic properties and the binding affinities of the potential drug. As expected, water soluble sugar-based pyrrolobenzodiazepine derivatives, i.e. with $-\text{OH}$ groups, presented highest binding affinities. The effect of conformational changes in the 1,4-benzodiazepine-2,5-dione ring and of different substituents allowed an evaluation of binding affinities at the benzodiazepine site on the GABA_A receptor.

Additionally, was developed the synthesis of β -disubstituted D-fructose-based γ -butyrolactone **vii** and γ -butyrolactam analogues **viii**, and that of a lipophilic D-fructose-based GABA analogue **ix**, where the pharmacophore is engineered into the carbohydrate scaffold through a spiro junction. The ability to bind GABA_A receptor, using a radioligand binding technique, was evaluated for all these compounds. GABA lactones **vii** were synthesized *via* the key intermediate 3-C-(3,4,6-tri-O-benzyl- α -D-fructofuranos-2-yl)propene **iii**, while γ -butyrolactams **viii** and GABA analogue **ix** took advantage of the allyl group and an amino functionality replacing the hydroxyl group in **iii**. The fructose moiety acted as versatile scaffold, rich in stereochemistry and with a relatively rigid skeleton. Thus, additional hydroxyl derivatization was used to increase lipophilicity, as well as to modulate the activity of pharmacophores or the receptor specificity, since benzyl groups could facilitate blood-brain barrier (BBB) crossing, which is one of the main issues to be addressed for central nervous system (CNS) directed drugs.



KEY WORDS

Carbohydrates

Fructose

Spiro Proline Analogues

1,4-Benzodiazepine-2,5-diones

Pyrrrolobenzodiazepines

γ -Butyrolactones

γ -Butyrolactams

GABA analogues

GABA_A Receptor

Radioligand Techniques

Compounds Libraries

Molecular Modelling

Dynamic NMR

RESUMO

Os hidratos de carbono constituem uma família única de compostos polifuncionais com primordial importância em química e biologia. Funcionalidade, quiralidade e diversidade estrutural são algumas das suas características mais relevantes. Neste contexto, dirigimos esta investigação para a síntese de novas estruturas que possuem unidades monossacarídicas com rigidez estrutural e ainda uma complexidade e diversidade tais que permitiram a construção de novas bibliotecas de compostos bioactivos.

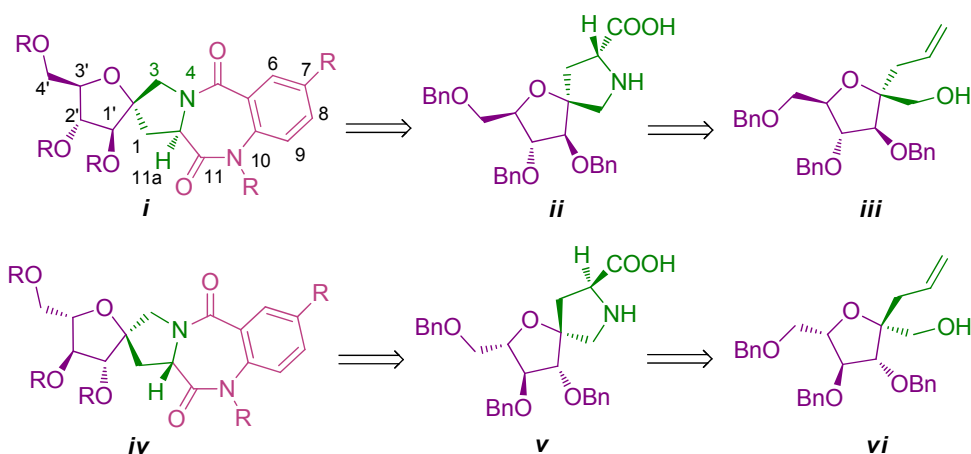
Inspirados pela proeminente utilidade dos hidratos de carbono como *scaffolds* em química medicinal, foram sintetizadas duas bibliotecas de potenciais ligandos do receptor GABA_A, geradas a partir da D-fructose e de um derivado da L-fructose. A primeira biblioteca de compostos inclui várias estruturas análogas às benzodiazepinas e a segunda contém γ -butirolactonas, γ -butirolactamas e um análogo do ácido gama-aminobutírico (GABA). Todos estes compostos foram submetidos a ensaios biológicos, nomeadamente utilizando a técnica que investiga a competição entre o composto e o radioligando correspondente relativamente à afinidade para a ligação ao receptor no seu local específico.

O GABA é um neurotransmissor inibidor do sistema nervoso central. Os seus efeitos resultam principalmente da sua ligação ao receptor GABA_A, que constitui uma estrutura macromolecular em volta de um canal iónico permeável ao cloreto. A fixação do GABA ao receptor GABA_A causa um aumento da condutância da membrana celular ao cloreto, que habitualmente existe em maior concentração no exterior do que no interior da célula. O movimento de aniões para dentro da célula aumenta a diferença de potencial entre a face externa e a interna da membrana celular e reduz a excitabilidade neuronal. O GABA funciona como uma molécula reguladora de efeitos tais como ansiedade, depressão, insónias, convulsões, tensão ou relaxamento muscular, actividade epiléptica, memória, euforia e disforia. O receptor GABA_A tem

locais específicos de ligação para distintas moléculas que influenciam a actividade do GABA, tais como benzodiazepinas, barbitúricos, etanol, esteróides, etc. As benzodiazepinas são um grupo de fármacos ansiolíticos utilizados no tratamento sintomático da ansiedade, insónia, depressão e distúrbios mentais em geral. Estas moléculas ligam-se a um local próprio, denominado receptor das benzodiazepinas, e aumentam a afinidade do GABA para o receptor GABA_A. Os barbitúricos, por exemplo, fixam-se também ao receptor GABA_A e provocam uma abertura prolongada do canal do cloreto. Diferem das benzodiazepinas porque a abertura do canal não exige a presença de GABA, ao contrário das benzodiazepinas que se limitam a potenciar o efeito do GABA endógeno. Além disso a abertura é mais prolongada, enquanto que as benzodiazepinas aumentam a frequência das aberturas sem prolongarem a duração de cada uma delas.

Especificamente, no presente trabalho é apresentada a síntese de uma biblioteca de enantiómeros análogos das benzodiazepinas, *i* e *iv*, desenvolvidos a partir da D-frutose e de um derivado da L-frutose, respectivamente. A estratégia adoptada centrou-se na síntese de um novo análogo da D- e da L-prolina, *ii* e *v*, respectivamente, com uma estrutura bicíclica espiro que contém a unidade sacarídica. A junção espiro reduziu significativamente a flexibilidade molecular, induzindo restrições conformacionais ao anel da prolina e conseqüentemente a toda a estrutura da molécula final (comprovado por NMR a temperaturas variáveis e estudos de modelação molecular).

A escolha do monossacárido frutose resultou do facto deste açúcar oferecer potencialidades interessantes devido à presença de grupos hidroximetilo (em C-1 e C-6) e devido à reactividade única do seu carbono anomérico. A síntese de derivados protegidos da frutose baseia-se na ramificação no carbono C-2 (*iii* e *vi*) e posterior reacção de ciclização entre uma função amina e um grupo alilo ligado à posição anomérica dando origem ao anel de pirrolidina seguidamente transformado no aminoácido *ii* e *v*.



O plano de síntese para o análogo da D-proline **ii**, envolveu a metilação da posição anomérica e benzilação das restantes posições utilizando a metodologia clássica (NaH, BnBr, DMF). Seguidamente foi introduzido um grupo alilo na posição anomérica através da formação de uma ligação C-C com aliltrimetilsilano mediada por um ácido de Lewis. A reacção dá-se geralmente por intermédio de um ião oxocarbénio cíclico, o qual sofre um ataque nucleófilo estereoquimicamente controlado, conduzindo a uma elevada estereoselectividade tanto em anéis de piranose como em anéis de furanose. Consequentemente, o tratamento de 1,3,4,6-tetra-*O*-benzilfrutofuranósido de metilo com aliltrimetilsilano na presença de eterato de trifluoreto de boro originou 3-*C*-(1,3,4,6-tetra-*O*-benzilfrutofuranos-2-il)propeno. A relação espacial entre a ligação dupla e o oxigénio do grupo benziloxi do carbono C-1 favorece a ocorrência da ciclização 5-*exo* por tratamento com iodo, desprotegendo selectivamente o grupo hidroxilo primário de C-1. A introdução da amina foi realizada através da oxidação a aldeído do álcool primário, formação de oxima e redução com hidreto de alumínio e lítio. Uma segunda iodociclização, desta vez envolvendo a função amina, protegida com um grupo carbamato, e o grupo alilo, conduziu à formação do anel pirrolidina. Tratamento com hidróxido de sódio permitiu, através da formação de uma oxazolidinona intermediária, obter o composto que possui a função álcool primário e a estereoquímica desejada. A sua oxidação conduziu à síntese do aminoácido prolina.

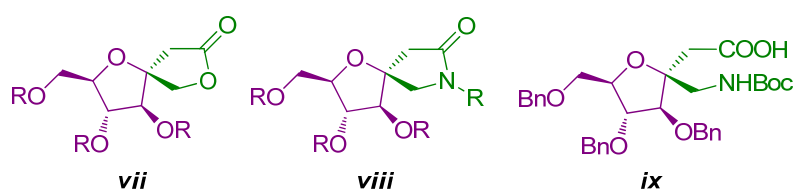
O plano de síntese do análogo da L-proline *v* envolveu a preparação de um derivado da L-frutose, uma vez que este açúcar não natural é comercializado a um preço bastante elevado. Foram desenvolvidas duas metodologias para a formação do intermediário-chave, o composto 3-*C*-(3,4,6-tetra-*O*-benzil- α -L-frutofuranos-2-il)propeno, uma das quais se baseou num procedimento descrito em literatura para a síntese da L-frutose, o qual usa a L-sorbose como composto de partida. Esta estratégia baseia-se na inversão da configuração das posições três e quatro para obter assim o intermediário-chave com a configuração do açúcar desejada. A estratégia alternativa desenvolvida partiu da L-arabinose, a qual possui a estereoquímica pretendida, resultou no alongamento da cadeia carbonada em C-1. Esta síntese é mais directa e permite obter a molécula-alvo com um rendimento ligeiramente superior (13,5% rendimento total) do que a utilizada inicialmente (8,5% rendimento total).

O uso do aminoácido prolina na produção de pirrolobenzodiazepinas foi estabelecido como sendo um dos processos sintéticos mais eficazes e rentáveis, através do uso de anidrido isotóico em DMF e refluxo. O reagente anidrido isotóico pode ser diversamente substituído permitindo a obtenção de uma variada biblioteca de compostos, nomeadamente benzodiazepinas substituídas na posição sete com halogéneos (Br e Cl), grupos amina ou nitroílo e metiladas em *N* (posição dez). O nosso contributo singular na estrutura das benzodiazepinas consistiu na incorporação de um açúcar de modo a funcionalizar os grupos hidroxilo e modular as propriedades físico-químicas e estruturais, nomeadamente a solubilidade e a rigidez, e consequentemente a actividade biológica do potencial fármaco.

A síntese destas estruturas rígidas teve como objectivo, não só permitir o estudo da relação estrutura-actividade, mas também uma análise acurada da especificidade conformacional do local de ligação no receptor das benzodiazepinas. Conforme descrito na literatura, o anel diazepina das benzodiazepinas tem um equilíbrio conformacional entre os confórmeros (*M*) e (*P*) e a ligação das mesmas ao receptor é dependente da conformação adoptada por estas. Embora existam estudos prévios que demonstraram que o receptor é favorável à conformação (*M*), a investigação

desenvolvida no âmbito desta tese, utilizando enantiómeros conformacionalmente rígidos no anel diazepam, permitiu concluir que ambas as conformações apresentam actividades biológicas semelhantes para estes compostos. As actividades biológicas determinadas demonstraram que a contribuição mais significativa para a ligação específica ao receptor provém dos substituintes no anel do benzeno, nomeadamente os grupos amina e nitroílo (posição sete), bem como a *N*-metilação. Os grupos hidroxilo do açúcar também contribuíram para um aumento da actividade biológica.

Paralelamente a estes análogos das benzodiazepinas, desenvolvemos uma segunda biblioteca de compostos, igualmente potenciais ligandos do receptor GABA_A. Foram sintetizadas γ -butirolactonas e γ -butirolactamas β -disubstituídas, *vii* e *viii*, respectivamente, e um derivado do GABA *ix*. Estas estruturas bicíclicas possuem uma junção espiro com um derivado da D-frutose. Os resultados de estudos farmacológicos, envolvendo radioligandos através de ensaios de competição entre o composto e o muscimol marcado, indicaram que as lactamas são os compostos com maior actividade biológica, seguidas das lactonas. O açúcar mostrou ser uma estrutura esteroquimicamente não impeditiva para a ligação ao receptor e até mesmo os compostos benzilados tiveram actividades biológicas interessantes, o que reforça a importância de estruturas lipofílicas para atravessar a barreira hemato-encefálica (BHE).



Em resumo podemos assumir que o trabalho desenvolvido conduziu ao desenvolvimento de novas estruturas glucídicas para a produção de novas bibliotecas de compostos com interesse farmacológico, que são excelentes candidatos para investigações de estrutura-actividade no receptor GABA_A.

PALAVRAS – CHAVE

Hidratos de Carbono

Frutose

Prolina

1,4-Benzodiazepinas-2,5-dionas

Pirrol benzodiazepinas

γ -Butirolactonas

γ -Butirolactamas

Análogos do GABA

Receptor GABA_A

Actividades biológicas

Radioligandos

Biblioteca de compostos

Modelação Molecular

RMN Dinâmico

LIST OF ABBREVIATIONS

- Ac** acetyl
AlSi(CH₃)₃ allyltrimethylsilane
Aq. aqueous
Ar aryl
b broad
BBB blood-brain barrier
BF₃·Et₂O boron trifluoride etherate
B_{max} (or **R₀**) maximum binding
Bn benzyl
Boc *tert*-Butyloxycarbonyl
BSA bovine serum albumin
BTSFA bis(trimethylsilyl)trifluoroacetamide
Bu butyl
BZ benzodiazepine(s)
ca. *circa*, approximately
Calcd calculated
CCK-A peripheral cholecystokinin
Ci curie
CNS central nervous system
conc concentrated
cpm cycles per minute
δ chemical shift(s)
d doublet
DBMMH 1,3-dibromo-5,5-dimethylhydantoin
dd doublet of doublets
ddd doublet of doublet of doublets
de diastereoisomeric or diastereoisomer excess
DIPEA *N,N*-diisopropylethylamine

DIS diazepam-insensitive
DMF *N,N*-dimethylformamide
DMS dimethylsulphide
DMSO dimethylsulfoxide
DME 1,2-dimethoxyethane
DMP 2,2-dimethoxypropane
DNA deoxyribonucleic acid
DNMR dynamic nuclear magnetic resonance
dpm disintegrations per minute
DS diazepam-sensitive
dt doublet of triplets
EPSP excitatory postsynaptic potential (EPSP)
Eq. equation
eq. equivalent(s)
Et ethyl
f fento (factor 10^{-15})
Fmoc 9-fluorenylmethoxycarbonyl
GABA gamma-aminobutyric acid
GABA-T gaba transaminase
GAD L-glutamic acid decarboxylase
GBL gamma-butyrolactone(s)
GBP-L gabapentin-lactam
GHB γ -hydroxybutyrate(s)
HIV Human immunodeficiency virus
Hz hertz
IAA imidazole-4-acetic acid [IUPAC name: 2-(1*H*-imidazol-4-yl)acetic acid]
IBX iodoxybenzoic acid
IC₅₀ inhibitory concentration (50%)
IUPAC International Union of Pure and Applied Chemistry
J coupling constant
K Kelvin

K_a ligand affinity/equilibrium constant
K_i equilibrium constant (for the competitor)
L ligand
M molar (1M = 1 mol/L)
M conformation minus
m milli (factor 10⁻³) or multiplet
MALDI-TOF Matrix Assisted Laser Desorption /Ionization- Time Of Flight
MHz megahertz
mmol milimole
min minute(s)
M.p. melting point
MS mass spectrometry
Ms mesyl
ms molecular sieves
m/z masse-to-charge ratio
n nano (factor 10⁻⁹)
NMO *N*-methylnmorpholine oxide
NMR nuclear magnetic resonance
NOE nuclear overhauser effect
NOESY nuclear overhauser effect spectroscopy
NP neurotoxic pesticides
s singlet
n.s. not statistically significant
nsb nonspecific binding
OAc acetate
p pico (factor 10⁻¹²)
P conformation plus
P Probability
PCC pyridinium chlorochromate
Pd/C palladium on charcoal
Ph phenyl

PIOL 5-(4-piperidyl)isoxazol-3-ol
ppm parts per million
PTX picrotoxin(s)
PTZ pentylenetetrazole
P4S piperidine-4-sulfonic acid
q quaternary ou quartet
QSAR Quantitative Structure-Activity Relationship
R receptor(s)
R_f retention factor
RL receptor–ligand complex
rt room temperature
sat. saturated
SEM standard error of the mean
soln. solution
SSA succinic semialdehyde
t time or triplet
TBDMSCI *tert*-butyldimethylchlorosilane
TBPS *tert*-butyl bicyclophosphorothionate
TFA trifluoroacetic acid
THF tetrahydrofuran
THIP 4,5,6,7-tetrahydroisoxazolo[5,4-*c*]pyridin-3-ol
THPO 4,5,6,7-tetrahydroisoxazole[4,5-*c*]pyridin-3-ol
TLC thin layer chromatography
TM transmembrane
TMSOTf trimethylsilyl trifluoromethanesulfonate
Ts *p*-toluenesulfonyl
μ micro (factor 10⁻⁶)
VGAT vesicular neurotransmitter transporter
v/v volume per unit volume
vs *versus*
w/w weight per unit weight

CONTENTS

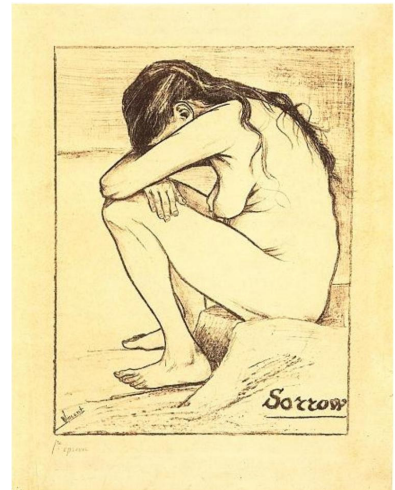
Acknowledgements.....	iii
Abstract	ix
Key Words	xiii
Resumo	xv
Palavras Chave	xxi
List of Abbreviations.....	xxiii
1. INTRODUCTION.....	1
1.1. Neurobiology: An Overview	5
1.1.1 The Synaptic Mechanism.....	7
1.1.2 Neurotransmitters – The Chemical Messengers	9
1.1.3 Receptors	10
1.1.3.1 Neurotransmitter Receptors	11
1.1.4 Drugs Action on the CNS.....	12
1.2. GABA and GABA Receptors.....	14
1.2.1 GABA – from Metabolite to Neurotransmitter.....	16
1.2.2 GABA _A Receptors	18
1.2.2.1 GABA _A Receptor Binding Sites.....	19
1.2.2.1.1 Convulsant Binding Site	22
1.2.2.1.2 Butyrolactone Site	22
1.2.3 GABA Binding Site for GABA _A R.....	23
1.2.4 GABA Analogues.....	25
1.2.4.1 γ -Butyrolactones (GBLs).....	27
1.2.4.2 γ -Butyrolactams.....	29
1.2.4.3 QSAR Modelling for Selective Anticonvulsants	30
1.3. Benzodiazepines.....	31
1.3.1 A Chemical Perspective – Structure and Synthesis.....	31
1.3.2 Benzodiazepine as a Privileged Scaffold in Medicinal Chemistry	33
1.3.3 Benzodiazepine as a Commercial Psychoactive Drug.....	34
1.3.4 Benzodiazepine Binding Site on GABA _A Receptors.....	36
1.3.4.1 Classification of BZs and Their Congeners	37
1.3.4.2 Conformational Equilibrium in Benzodiazepine Ring.....	38
1.3.4.3 SAR studies.....	41

1.4. Carbohydrates as Natural Scaffolds.....	42
1.4.1 Sugar Derived Polyfunctional Scaffolds–GABA Analogues and Bzs.....	45
1.5. Radioligand Technique.....	47
1.5.1 Ligand Binding: Simple Theory	48
1.5.1.1 Equilibrium Binding: Saturation Analysis	49
1.5.1.1.1 Nonspecific Binding.....	52
1.5.1.1.2 Analysis of Saturation Binding Isotherms: Scatchard Plot ...	53
1.5.1.2 Equilibrium Binding: Competition Studies	55
1.5.1.3 Limits on the Interpretation of Equilibrium Radioligand Binding Studies.....	57
1.5.2 Radiolabelled Ligand Binding Studies: Separation of Free From Bound Ligand.....	59
2. RESULTS AND DISCUSSION	61
2.1 Synthesis of the Spiro D- and L-Proline Analogues.....	65
2.1.1 Synthesis of the Spiro D-Proline Analogue	67
2.1.2 Synthesis of the Spiro L-Proline Analogue.....	72
2.1.2.1 Synthesis of Compound 111 - Pathway <i>a</i>	73
2.1.2.2 Synthesis of Compound 111 - Pathway <i>b</i>	78
2.1.2.3 Synthesis of Compound 112	83
2.1.3 Novel Rigid 1,4-Benzodiazepine-2,5-dione Scaffolds	85
2.1.3.1 Synthesis	86
2.1.3.2 Molecular Modelling and DNMR Experiments	89
2.1.3.3 Biological Assays	99
2.1.3.3.1 Evaluation of Total, Non-Specific and Specific Binding – Saturation Studies	99
2.1.3.3.2 GABA _A R Binding Assays - Competition Studies.....	101
2.1.4 Fructose-Based γ -Butyrolactones and γ -Lactams, and a GABA analogue.....	110
2.1.4.1 Synthesis	110
2.1.4.2 Biological Evaluation	114
2.1.4.2.1 Evaluation of Total, Non-Specific and Specific binding – Saturation Studies	114
2.1.4.2.2 GABA _A R Binding Assays – Competition Studies.....	115
3. CONCLUSIONS	119

4.EXPERIMENTAL SECTION.....	125
4.1 Organic Synthesis.....	127
4.1.1 General Methods.....	127
4.1.2.1 Dry Solvents and Reactions	127
4.1.2.2 Preparation of 2-Iodoxtbenzoic acid (IBX)	127
4.1.2.3 Thin-Layer Chromatography.....	127
4.1.2.4 Flash Column Chromatography	127
4.1.2.5 Mass Spectroscopy.....	128
4.1.2.6 NMR Spectroscopy.....	128
4.1.2 Synthesis of the Spiro D-Proline Analogue	128
4.1.3 Synthesis of the Spiro L-Proline Analogue.....	144
4.1.3.1 Synthesis of Compound 111 - Pathway <i>a</i>	144
4.1.3.2 Synthesis of Compound 111 - Pathway <i>b</i>	152
4.1.3.3 Synthesis of Compound 112	158
4.1.4 Synthesis of the 1,4-Benzodiazepine-2,5-dione Scaffolds	167
4.1.5 Synthesis of the Pyrrolobenzodiazepines.....	197
4.1.6 Synthesis of the Fructose-Based γ -Butyrolactones and γ -Lactams, and a GABA analogue.....	199
4.2 Molecular Modelling and DNMR Experiments.....	211
4.3 <i>In Vitro</i> Pharmacology: GABA _A R Binding Assays.....	211
4.3.1 Chemicals	211
4.3.2 Instruments.....	212
4.3.3 Methods	212
4.3.3.1 Benzodiazepine Derivatives	213
4.3.3.1.1 Membrane Preparation	213
4.3.3.1.2 Radioligand Binding Assay	214
4.3.3.1.3 Data analysis	214
4.3.3.2 GABA Derivatives	214
4.3.3.2.1 Membrane Preparation	214
4.3.3.2.2 Radioligand Binding Assay	215
4.3.3.2.3 Data analysis	216
4.3.3.3 Lowry Protein Assay.....	216
5. REFERENCES.....	219

*Matar o sonho é matarmo-nos.
É mutilar a nossa alma.
O sonho é o que temos de realmente nosso,
de impenetravelmente e inexpugnavelmente nosso.*

Fernando Pessoa



*Sorrow, 1882
Vincent van Gogh*

INTRODUCTION

HIGHLIGHTS

Globally, it is estimated that 450 million people suffer from mental or behavior disorders.

In developed countries, 8 of the 10 leading causes of disability are related to mental illness.

Mental disorders are one of the most prominent and treatable causes of suicide; every year about 800 000 people commit suicide.

According to the World Health Organization,^[1] Mental Health is defined as:

"A state of complete physical, mental and social well-being and not merely the absence of disease."

Problems related to mental health, as anxiety and depression disorders, should be a public priority. The social and economic impact of depression, for example, is enormous in modern society. Moreover, there is not health without a good mental health.

Mental health is influenced by a wide range of factors, such as individual biological and psychological factors, social interaction, societal structures or resources and cultural values. Certain mental illnesses are known to be linked to structural abnormalities or chemical dysfunction of the brain. Others are inherited, but often the cause is unknown. Likewise, injuries to the brain and chronic drug or alcohol abuse can trigger also some mental illnesses.^[1]

A 2004 report from European Communities^[2] describes and compares the state of mental health in the European Union and Norway. The report showed the percentage of psychological distress and the positive mental health in 10 EU countries (Fig. 1). Portugal and Italy have the highest incidence of mental health problems and the lowest positive mental health. These values were not the motivation for my research work; however are a curious coincidence.

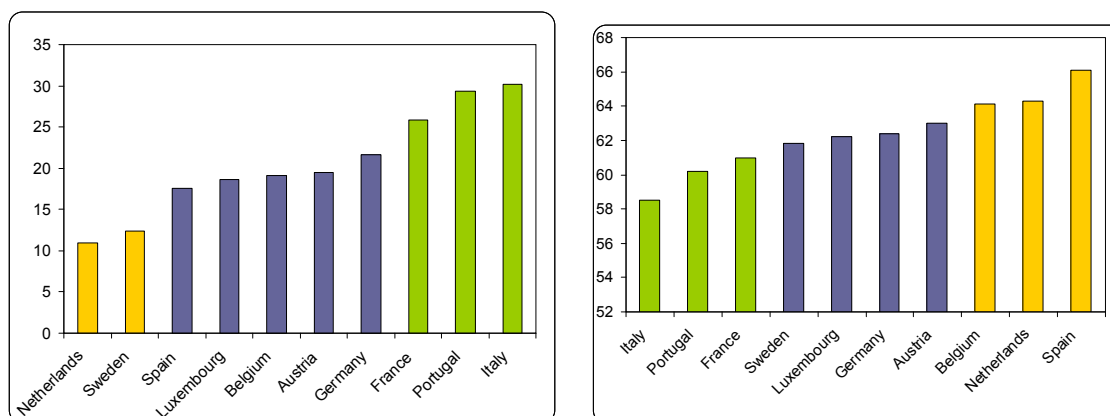


Figure 1. Psychological distress (*left*) and positive mental health (*right*) in ten EU countries.^[2]

Thus, having consciousness that Mental Health is a global problem, the research and development of new psychoactive drugs, which act primarily into the central nervous system (CNS), becomes a relevant issue. Hence, drugs that interact with CNS receptors are amongst the most important in medicine, providing treatment for diseases such as pain, depression, Parkinson's disease, psychosis, heart failure, asthma, and many others.

In the present work, two novel classes of **GABA receptor ligands** were developed. Inspired by the role of carbohydrates as natural scaffolds, a sugar skeleton was exploited to develop a library of new **benzodiazepine** and **GABA derivatives (γ -butyrolactones, γ -butyrolactams and a GABA analogue)** of biological relevance. Derivatization and introduction of several substituents provided different pharmacophores,ⁱ allowing the construction of small libraries of the respective scaffold.

ⁱ **Pharmacophores** are atoms and functional groups required for a specific pharmacological activity, and their relative positions in space.

1.1 Neurobiology: An Overview

In a complex organism, cells have to get along with their neighbours. A communication system and its control is essential, and comes primarily from the brain and spinal column – the central nervous system (CNS), which receives and sends messages *via* a vast network of nerves. These messages are electrical pulses which travel down the nerve cell, the **neuron** (Fig. 2), towards a target, whether that be a muscle cell or another nerve.^[3]

There are two main classes of cells in the nervous system: neurons and glial cellsⁱⁱ (glia). Neurons are cells entirely different from other cells in the body. They are typically highly polarized, and their cell functions are compartmentalized. The main functional compartments of neurons can be defined into four morphologically distinctive regions: the cell body (soma), the dendrites, the axonsⁱⁱⁱ (covered with sheaths of lipids – myelin sheath), and axon terminals; which are usually separated by considerable distances (Fig. 2).

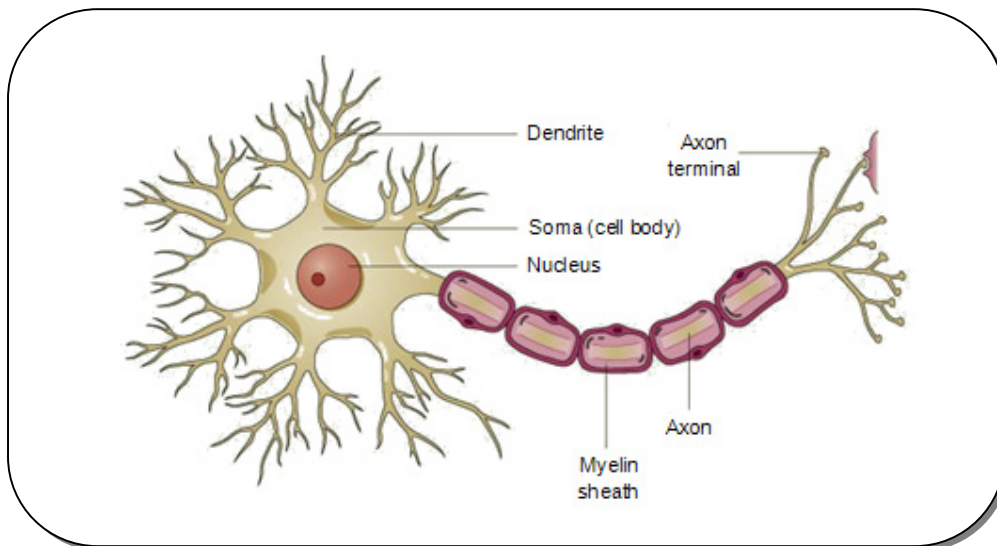


Figure 2. Cartoon showing the structure of a typical neuron.^[4]

ⁱⁱ **Glial cells** provide support and nutrition to neurons. As far as is known, glia are not directly involved in information processing. They surround the cell bodies, axons, and dendrites of neurons, providing structure to the brain.

ⁱⁱⁱ **Axon** is the main conducting unit for carrying out signals (electrical impulses) away from a neuron cell body.

The electrical excitability is among the most important and characteristic properties of neurons and is due to the presence of voltage-sensitive ion channels in the neuronal plasma membrane (Fig. 3).^[4, 5] Depolarization is a decrease in the absolute value of a cell's membrane potential, which is caused by influx of Na^+ through Na^+ channels (or influx of Ca^{2+} through Ca^{2+} channels), and the effect is to stimulate the nerve. Contrary, hyperpolarization is an increase absolute value of a cell's membrane potential, which is caused by out-flux of K^+ through K^+ channels (or influx of Cl^- through Cl^- channels) and the effect is to destimulate the nerve. This cell's electrical signals (nerve impulses), called **action potentials**, allow neurons to carry a signal over a certain distance (Fig. 3). The brain receives, analyzes, and transmits information through these signals.

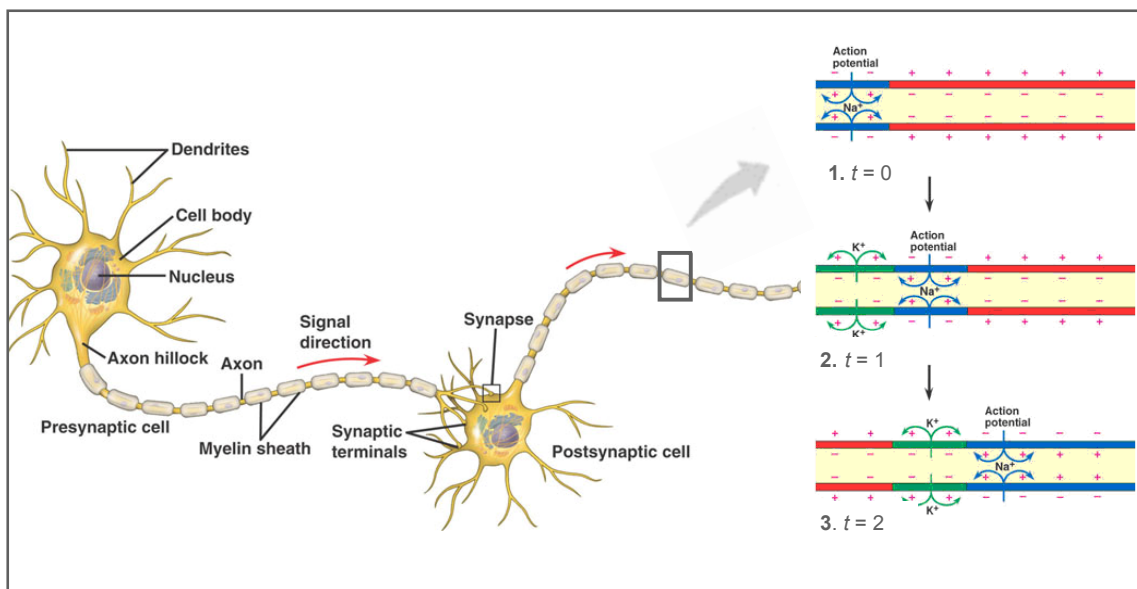


Figure 3. Cartoon showing a communication system between two neurons. The action potential, i.e. the cell's conducting signal, is initiated either at the axon hillock (the initial segment of the axon) or in some cases slightly further down and moves towards the presynaptic cells. Then, from a specific region of the axon of one neuron, the presynaptic terminal cells, messages are transmitted to another neuron, the postsynaptic cells – synapse. Most presynaptic terminals ends on the postsynaptic neuron's dendrites, but the terminals may also end on the cell body or, less often, at the beginning or end of the axon of the receiving cell.^[4]

The correct functioning of the CNS is based on the generation, propagation, and coordination of signals between different neurons. However, neurons do not connect directly to their target cells. The distance between them is minimal, about 100 Å, but it is a space that the electrical pulse is unable to jump. Therefore, there has to be a method of carrying the message across the gap between the neuron ending and the target cell. The problem is solved by the release of a chemical messenger called a **neurotransmitter** (see also chapter 1.1.2). Thus, the transference of information between neurons is achieved neither by direct contact nor electrically but chemically in a process called **synaptic mechanism** (see also chapter 1.1.1). This communication between individual neurons is performed at a morphologically and functionally highly specialized region named the **synapse** (Fig. 3). Once released, the neurotransmitter diffuses across the gap to the target cell, where it binds and interacts with a specific protein – a **receptor** (see also chapter 1.1.3), embedded in the cell membrane. This process of binding results either in a flow of ions across the cell membrane or in the switching on (or off) of enzymes inside the target cell. A biological response then arises, namely the contraction of a muscle cell or the activation of fatty acid metabolism in a fat cell.^[3]

1.1.1 The Synaptic Mechanism

Communication between neurons happens when chemical signals, the neurotransmitters, are transmitted across a gap between the membranes of the pre- and post-synaptic cells, the synaptic cleft. This chemical transmission is known as the synaptic mechanism, and can be divided into four steps, in which two are presynaptic and the other two postsynaptic (Fig. 4). The dendrites act as small arms radiated from the cell body that received messages from other nerves. These messages either stimulate or destimulate the nerve. The cell body ‘collects’ the total sum of the received messages (neurotransmitters), and ‘stores’ them in vesicles.^{iv}

^{iv} **Vesicle** is a small, intracellular, membrane-enclosed pocket that stores and transports substances within a cell, as neurotransmitters.

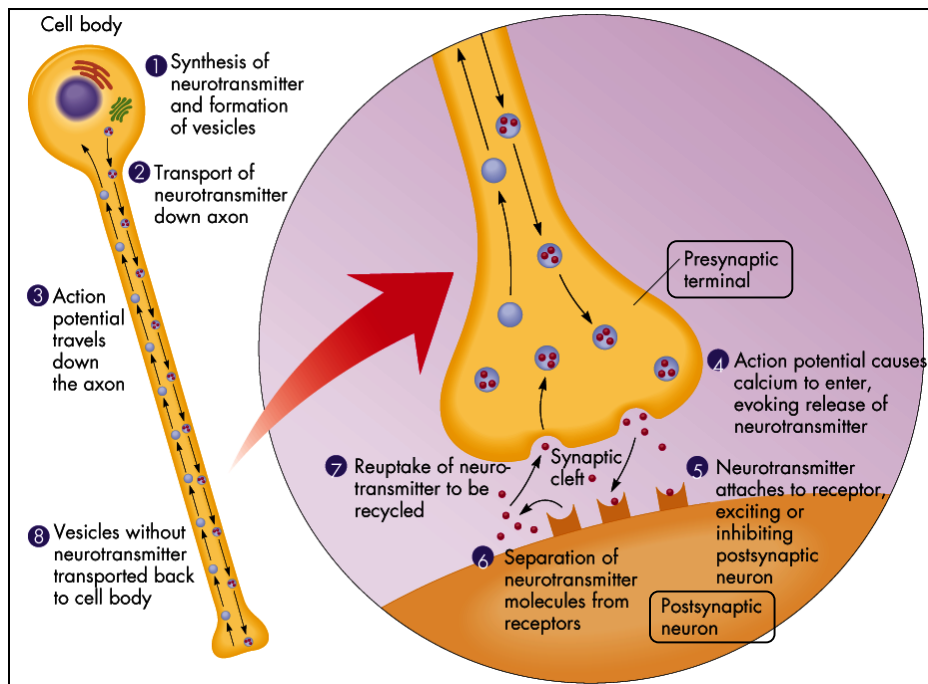


Figure 4. Cartoon showing a synaptic mechanism between two neurons. The primary steps of this process are: the synthesis of the neurotransmitter; the storage and release of the neurotransmitter; the transmitter's interaction with a receptor in the postsynaptic membrane; and the removal of the neurotransmitter from the synaptic cleft.^[6]

The synthesis of the neurotransmitters and the subsequent formation of the vesicles can be considered the starting point of the synaptic mechanism. So, assuming that the overall stimulation of the nerve by the received messages is great enough, an electrical signal is fired down the axon. The myelin sheaths insulate the signal as it passes down the axon. This transportation of the vesicles down the axon is achieved due to the action potential (Fig. 3). These vesicles conducting signals traveled down the axon to the presynaptic terminal, considered the synaptic button (knob-shaped swelling). The depolarization of the presynaptic terminal membrane, i.e. the opening of the calcium channels and consequent influx of Ca^{2+} ions, results on the stimulation of the nerve. These generated action potential influences the vesicles "full to the limit" of neurotransmitters to fuse with the presynaptic terminal membrane. The neurotransmitters are then released from the vesicles into the synaptic cleft, and it targets its reciprocal receptor on the postsynaptic membrane of the next neuron. The effect of the neurotransmitter on the postsynaptic membrane will depend on the

nature of the neurotransmitter, the nature of the postsynaptic receptors, and whether the postsynaptic ion channels are voltage-gated or chemically-gated. Most neurotransmitters are removed from the synaptic cleft by neurotransmitter transporters in a process called reuptake (uptake). Without reuptake, neurotransmitters can continue to stimulate or inhibit the firing of the postsynaptic neurons.

1.1.2 Neurotransmitters – The Chemical Messengers

There is a large variety of messengers that interact with receptors and that differ quite significantly in structure and complexity. Some neurotransmitters are simple in structure, such as monoamines (e.g. acetylcholine, noradrenaline, dopamine and serotonin) or amino acids [e.g. **γ -aminobutyric acid – GABA** (see also chapter 1.2.1), glutamic acid and glycine]. Other chemical messengers are more complex in structure and include lipids, purines, neuropeptides, peptide hormones, and even enzymes.^[3] Thus, different neurotransmitters operate at different parts of the nervous system and have different effects. Some neurotransmitters promote the transmission of impulses while others inhibit it.^[7] In general, a nerve releases mainly one type of neurotransmitter, and the receptor which awaits it on the target cell will be specific for that messenger. However, that does not mean that the target cell has only one type of receptor protein. Each target cell has a large number of nerves communicating with it and they do not all use the same neurotransmitter. Therefore, the target cell will have other types of receptors specific for those other neurotransmitters.

1.1.3 Receptors

A receptor (Rs) is a protein molecule, usually embedded within the cell membrane with part of its structure facing the outside of the cell (Fig. 5). The protein surface has a complicated shape containing hollows, ravines, and ridges, and somewhere within this complicated geography there is an area that has the correct shape to accept the incoming messenger. This area is known as the **binding site** and is analogous to the active site of an enzyme. The molecule which binds to this site is called a **ligand** and may be a peptide (such as a neurotransmitter), a hormone, a pharmaceutical drug, or a toxin. When the ligand fits into the binding site, it 'switches on' the receptor molecule and a message is received. In this process, ligand does not undergo a chemical reaction. It fits into the binding site of the receptor protein, passes on its message, and then leaves unchanged. This process depends highly on shape; i.e. the messenger binds to the receptor and induces it to change shape. This change subsequently affects other components of the cell membrane and leads to a biological effect.

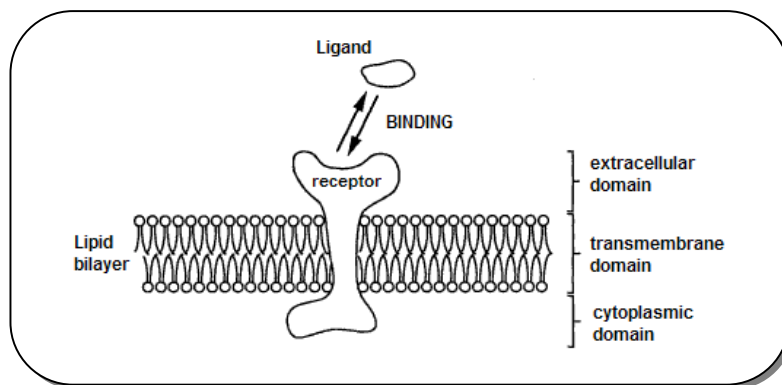


Figure 5. Cartoon showing a schematic structure of a receptor. Cell surface receptors possess an extracellular domain for binding ligands (e.g., growth factors, adhesion molecules), a transmembrane domain, and an intracellular or cytoplasmic domain. Receptors may be unbound, bound, or coupled with other membrane-associated molecules.^[8]

1.1.3.1 Neurotransmitter Receptors

Most neurotransmitter receptors can be divided into two types, on the basis of their structure and function (Fig. 6):

- **Ion channel receptors or ligand-gated ion channel^v – ionotropic receptors** [e.g. **GABA_A Rs** (see also chapter 1.2.2)]: They are part of a five-protein ion channel structure, a glycoprotein which cross the cell membrane. This receptor is part of the ion channel structure, so the binding of a chemical messenger leads to the rapid response that is crucial to the speed and efficiency of nerve transmission. When the receptor binds a ligand, it changes shape and this has a specific effect on the protein complex which leads to the channel opening – a process called gating. Ions channels can select between different ions. There are cationic ion channels for sodium (Na⁺), potassium (K⁺), and calcium (Ca²⁺) ions. When these channels are open, they are generally excitatory and lead to depolarization of the cell. There are also anionic ion channels for chloride ion (Cl⁻), controlled by the **GABA_A** and glycine receptors. These ion channels generally have an inhibitory effect when they are open, hyperpolarization of the cell. There are at least three families of receptors involved in the control of ion channels and these are classified by the number of transmembrane (TM) domains that they contain (4-TM, 3-TM, 2-TM). The **4-TM** ion channels include the **GABA_A receptor**.
- **G-protein-coupled receptor – metabotropic receptors** (or 7-TM Rs): They are receptors which do not directly affect ion channels or enzymes. Instead, they active a signalling protein called G-protein^{vi} which then initiates a signalling cascade involving a variety of enzymes. G-protein coupled receptors are known as metabotropic or slow receptors, due to their indirect action. Examples include GABA_B, glutamate and dopamine receptors.

^v Ion channels controlled by chemical messengers are called **ligand-gated ions channels**. Ion channels in excitable cells such as nerves are controlled by the membrane potential of the cell, and are called **voltage-gated ion channels**.

^{vi} **G proteins** are guanine nucleotide-binding proteins which are important signal transducing molecules in cells.

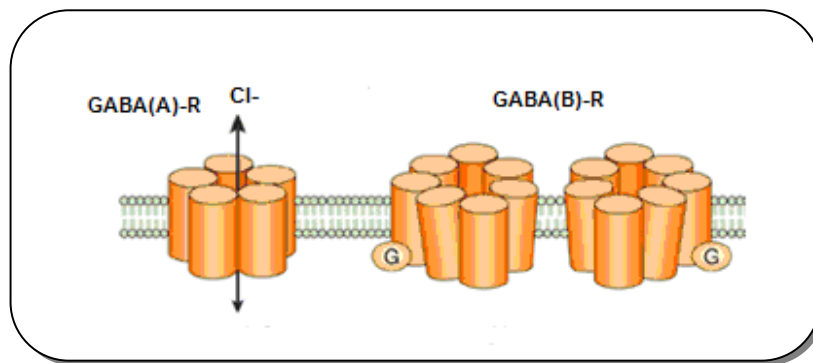


Figure 6. Cartoon showing a ligand-gated ion channel 4-TM receptor (GABA_A R) and a G-protein-coupled receptor (GABA_B R).^[6]

1.1.4 Drugs Action on the CNS

A communication system is clearly essential for a normal function of the human body and it is crucially dependent on a chemical messenger, the neurotransmitter. Hence, it should be possible for other chemicals, like drugs, to interfere or interact with this system. If this communication should become defective, it could lead to a variety of ills such as depression, heart problems, schizophrenia, muscle fatigue, and many other problems.

What sort of things could go wrong? One problem would be if too many messengers were released. The target cell could (metaphorically) start to overheat. Alternatively, if too few messengers were sent out, the cell could become slow or inert. It is at this point that drugs can play a role by either acting as replacement messengers (if there is a lack of the body's own messengers), or by blocking the receptors for the natural messengers (if there are too many host messengers).

Drugs that interact with receptors are amongst the most important in medicine. They can be characterized as:

- **Agonist:** A drug that produces the same response at a receptor as the natural messenger. An agonist should have the following characteristics: i) the correct binding groups; ii) the binding groups properly positioned; iii) the right size for the binding site.

- **Antagonist:** A drug that binds to the receptor without activating it, and which prevents an agonist or a natural messenger from binding. The antagonist may bind to a totally different part of the receptor. This process could alter the shape of the receptor protein leading to the distortion of the neurotransmitter receptor which is then unable to recognize the natural neurotransmitter. This form of antagonism is non-competitive, as the antagonist is not competing with the neurotransmitter for the same binding site.

- **Inverse agonist:** An inverse agonist has the same effect as an antagonist; it binds to a receptor, fails to activate it, and prevents the normal chemical messenger from binding. In addition, it is capable of preventing the inherent activity of a receptor. Some receptors (e.g. the **GABA** and dihydropyridine receptors) are found to have an inherent activity even in the absence of the chemical messenger.

- **Uptake inhibitor:** A drug that inhibits the transport of neurotransmitters into axon terminals or into storage vesicles within terminals. For many transmitters, uptake determines the time course of transmitter action so that inhibiting uptake prolongs the activity of the transmitter. Many clinically important drugs are uptake inhibitors although the indirect reactions of the brain, rather than the acute block of uptake itself, are often responsible for the therapeutic effects.

- **Partial agonist:** A drug which acts like an antagonist by blocking an agonist, but which retains some agonist activity itself. There are several possible explanations for this behaviour: i) the partial agonist binds to the receptor in order to have an agonist effect. However, it may bind in such a way that the conformation change induced is not ideal and subsequent effects of receptor activation are decreased; ii) the partial agonist may be capable of binding to a receptor in two different ways by using different binding regions in the binding site. One of them activates the receptor (agonist effect), but the other does not (antagonist effect); iii) the partial agonist may be capable of distinguishing between different types of receptor. Receptors which bind a particular chemical messenger are not all the same, and there are various receptor types and subtypes. A partial agonist might distinguish between them, acting as an agonist at one subtype, but as an antagonist at another one.

1.2 GABA and GABA Receptors

γ -Aminobutyric acid or GABA (**1**, Fig. 7), is an amino acid neurotransmitter widely distributed throughout the neuraxis.^{vii}

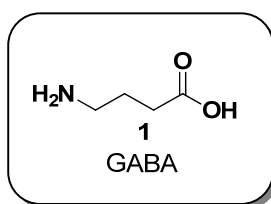


Figure 7. γ -Aminobutyric acid (GABA).

While GABA **1** is found in some peripheral tissues, and there is evidence that it may regulate neuronal activity in the intestines, lungs, and bladder, its predominant effects are in the CNS. GABA **1** activity is mediated by GABA receptors (GABA Rs). Because activation of neuronal GABA R generally results in hyperpolarization, this amino acid is considered an inhibitory neurotransmitter. Given the number of GABAergic

^{vii} **Neuraxis** is the long axis of the spinal cord and brain.

neurons^{viii} in the brain, and their widespread distribution, GABA **1** is the major inhibitory neurotransmitter in the CNS. So, given its ubiquity, and relatively high concentrations in the CNS, GABA **1** plays a major role in mediating or modulating most, if not all, CNS functions. Evidence for this is provided by the fact that GABA R agonists and antagonists display a wide variety of pharmacological effects such as anxiolysis, hypnosis, muscle relaxation, amnesia, cognitive enhancement, stimulant, and anticonvulsant activities.^[9] It is this ubiquity that has hindered drug development because non selective GABA R agonists and antagonists have generalized effects on CNS function.

GABA Rs have been traditionally classified into two distinct types, the ionotropic **GABA_A R** and the metabotropic GABA_B R. These two classes of receptors are functionally, molecularly and pharmacologically different. GABA_A Rs are pentameric, ligand-gated ion channels composed of different subunits which are highly permeable to chloride. GABA_B Rs, in contrast, are heterodimers coupled to G-proteins. GABA_C Rs are the most recent and the least studied of the three major classes of GABA Rs. They are ligand gated ion channels, but their physiological roles are still being unravelled and the pharmacology of these receptors is also under development. The fast-inhibitory actions of GABA **1** are mediated by the activation of GABA_A Rs in the brain^[10] and GABA_C Rs in the retine,^[11] whereas its slow and prolonged actions are mediated by GABA_B Rs.^[12, 13]

^{viii} **GABAergic neurons** are neurons that produce and degrade GABA.

1.2.1 GABA – from Metabolite to Neurotransmitter

Gamma-aminobutyric acid **1** or zwitterion gamma-aminobutyric acid (at physiologic pH) was first identified in the mammalian brain in 1950's by three research groups.^[14-16] Nowadays, it is believed to be the primary endogenous^{ix} inhibitory neurotransmitter in the mammalian CNS, being perhaps the most comprehensively studied inhibitory neurotransmitter in the mammalian CNS. It has been estimated that about 40% of synapses in the brain are GABAergic.^[17]

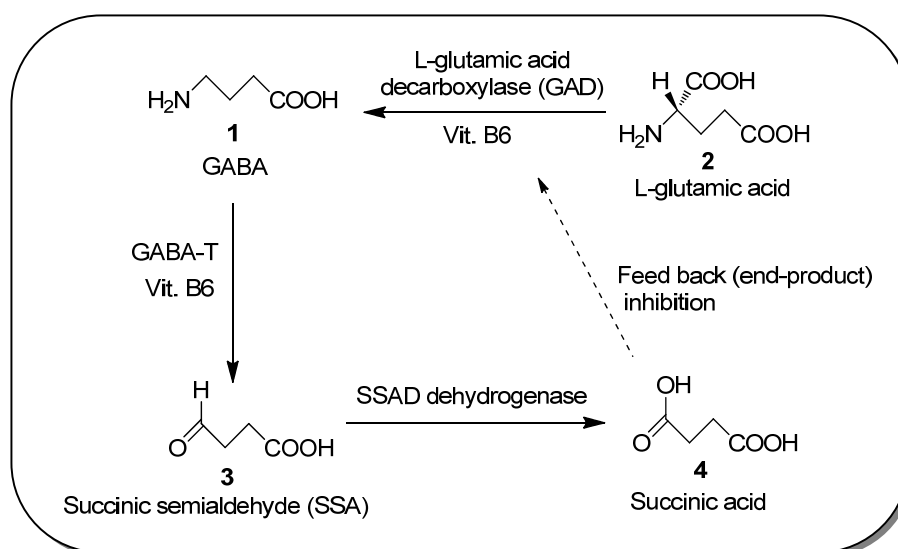


Figure 8. Biosynthetic pathway and metabolism of GABA.

GABA **1** is synthesized in GABAergic neurons by alpha-decarboxylation of the L-glutamic acid **2** (or of glutamate, which is the carboxylate anions and salts of glutamic acid) (Fig. 8). The rate-determining enzyme which catalyzes this step is the L-glutamic acid decarboxylase (GAD). GAD requires vitamin B₆ (active form: pyridoxal phosphate) as a cofactor, which can be used to regulate the levels of GABA **1**. After being synthesized, GABA **1** is transported into vesicles by a vesicular neurotransmitter transporter (VGAT) (Fig. 9). GABA **1** can be released either vesicularly or non-vesicularly (by reverse transport). GABA **1** is degraded by a transamination reaction

^{ix} **Endogenous** substances are those that originate from within an organism, tissue, or cell.

that is catalysed by GABA transaminase (GABA-T). This enzyme also depends on pyridoxal phosphate as its cofactor. The resulting product, succinic semialdehyde **3** (SSA) is converted to succinic acid **4**, which has negative-feedback inhibition on the enzyme GAD, thereby decreasing the conversion of L-glutamic acid to GABA **1**. Therefore, if insufficient quantities of GABA **1** are present, GAD is activated due to the lack of end-product inhibition resulting from a lower concentration of the end-product, succinic acid. [14, 18, 19]

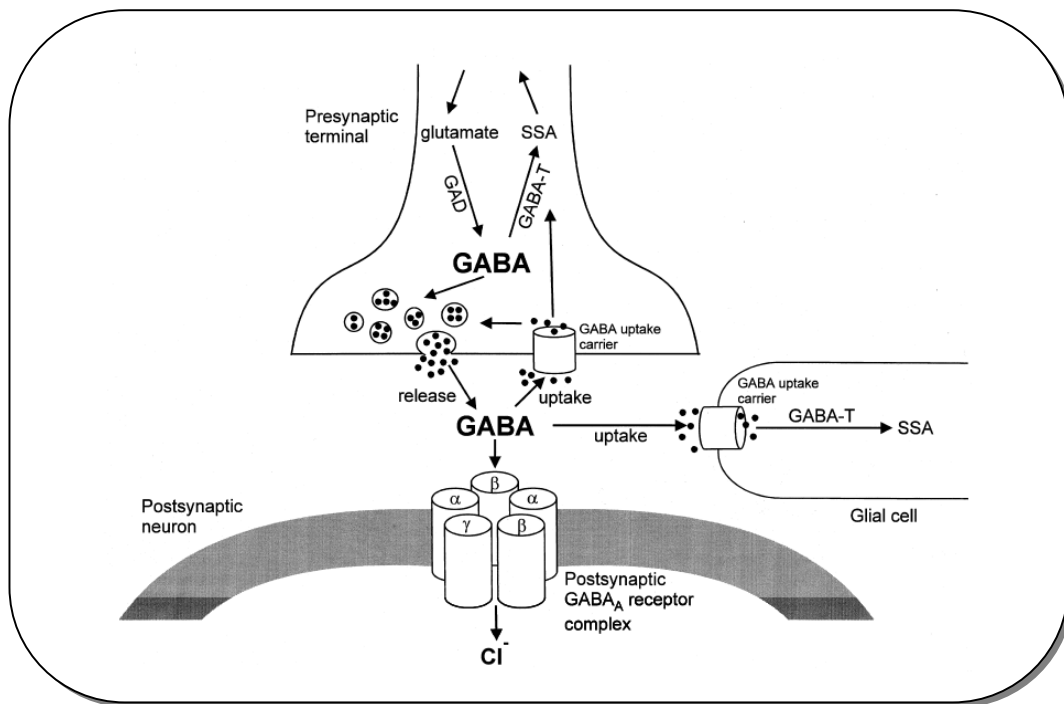


Figure 9. Cartoon showing the GABA-mediated inhibition.[20]

GABA-mediated action is an inhibitory ion channel synapse (Fig. 9). Glutamate (or L-glutamic acid, **2**) is synthesized in the presynaptic terminal, and consequently transformed in GABA **1**. GABA **1** is stored in synaptic vesicles and released into the synapse, upon presynaptic depolarization. Reuptake by GABA-T occurs by surrounding neurons in the axon or by glial cells from the extracellular space. GABA Rs are located at pre- and postsynaptic sites. Postsynaptically, GABA **1** activates the GABA_A Rs, which

stimulate the influx of chloride ions through the GABA-gated chloride channel, and GABA_B Rs (not in the picture). GABA_B R cause presynaptic inhibition by suppressing calcium influx and reducing transmitter release, and achieve postsynaptic inhibition by activating potassium currents that hyperpolarize the cell.^[14, 18, 19, 21]

1.2.2 GABA_A Receptors

GABA_A Rs are the most important inhibitory neurotransmitter receptors in the mammalian CNS. They are allosteric proteins^x members of the ligand-gated ion channel superfamily. GABA_A Rs are heteromeric^{xi} chloride channels composed of five homologous subunits that share a common structure: a large amino-terminal extracellular domain and four TM domains, with a large intracellular domain between TM3 and TM4 (Fig. 10). GABA_A Rs have structural and functional homology with a superfamily of cys-loop ligand-gated ion channel receptors.

GABA_A Rs are activated by brief releases of GABA **1** into the synaptic cleft.^[22] The activation of GABA_A R by GABA **1** opens the intrinsic ion channel, enabling flux of chloride through the channel into the cell, leading to subsequent hyperpolarization of neurons. Thus, occurs an increase of the intraneuronal concentration of chloride ion, and thereby a reduction in neuronal activity. GABA_A Rs besides GABA **1** activation are also modulated by a variety of different drugs. GABA_A Rs are clinically relevant drug targets for anti-convulsant, anxiolytic and sedative-hypnotic agents. Moreover, deficits in the functional expression of GABA_A Rs are critical in epilepsy, anxiety disorders, cognitive deficits, schizophrenia, depression and substance abuse. Understandably, there has been considerable interest in determining the cellular mechanisms that regulate GABA_A R accumulation on the neuronal plasma membrane.^[23] This receptor has an inherent activity; it does not have a 'fixed' inactive conformation, is continually changing shape such that there is equilibrium between the active conformation and

^x **Allosteric proteins:** a protein whose shape is changed when it binds a particular molecule. In the new shape the protein's ability to react to a second molecule is altered.

^{xi} **Heteromeric:** consisting of more than one kind of structural subunit.

different inactive conformations. In that equilibrium, most of the receptor population is in an inactive conformation but a small proportion of the receptor is in the active conformation.^[3]

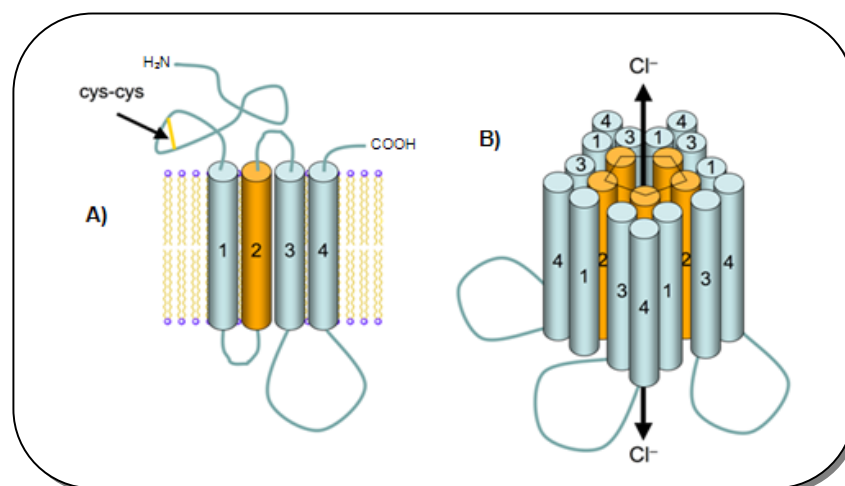


Figure 10. Cartoon showing the structure of a GABA_A R. **(A)** Structure of the 4-TM domains of a single subunit of the GABA_A R in a lipid bilayer (yellow lines connected to blue sphere): TM domain 2 is shown as the shaded barrel that lines the pore of the ion channel. The disulfide bond in the C-terminal extracellular domain, characteristic of the family of cys-loop receptors is depicted as a yellow line. **(B)** Schematic plan view of a GABA_A R containing five subunits with the pore in the centre of the heteromeric molecule.^[24]

1.2.2.1 GABA_A Receptor Binding Sites

GABA_A receptors have a rich pharmacology in that they have a number of separate allosteric binding sites^{xii} for a variety of drugs that can modulate the activity of GABA **1** (Fig. 11). These includes: barbiturates, e.g. thiopental **5**; non-barbiturate intravenous anesthetics, e.g. (*R*)-(+)-etomidate **6**; neuroactive steroids, e.g. lanosterol **7**; sedatives, e.g. loreclezole **8**; benzodiazepines (BZ), (see also chapter 1.3), e.g. clonazepam **9**; ethanol and other alcohols; volatile anesthetics, e.g. (*S*)-isoflurane **11**; channel blockers or picrotoxin (PTX) site, e.g. picrotoxinin **10** and ionic zinc (Fig. 12). A distinct binding site that mediates the stimulatory actions of lactones (see also

^{xii} **Allosteric Site** refers to a protein binding site other than the one used by the normal ligand, which affects the activity of the protein. An allosteric inhibitor that binds to an allosteric binding site induces a change of shape in the protein which disguises the normal binding site from its ligand.

chapter 1.2.4.1) is presumed to exist, although no definitive evidence to support this claim exists.^[25, 26] GABA_A Rs are antagonized by bicuculline (BMC) **12** and insensitive to (*R*)-(-)-baclofen (**13**, Fig. 13).^[27]

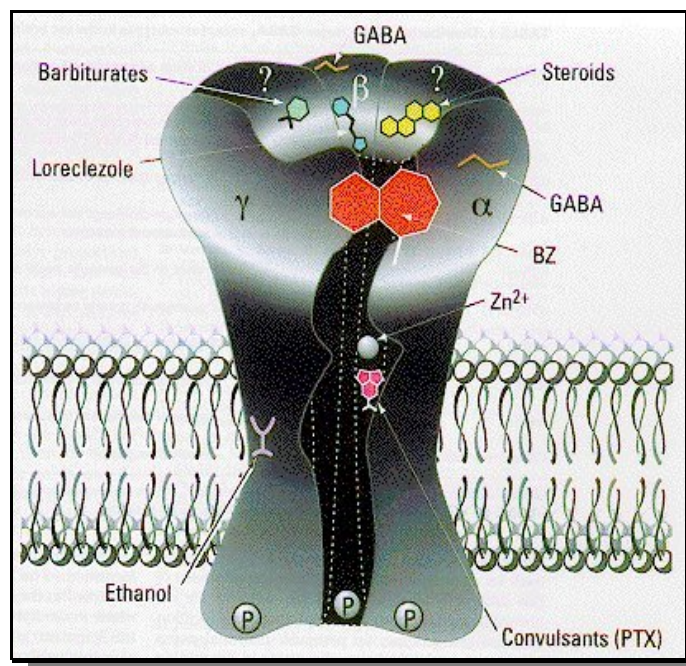


Figure 11. Three-dimensional cartoon of the GABA_A R on the plasma membrane with ligand-binding sites indicated: GABA site, barbiturate site [e.g. barbiturates and loreclezole **8**, benzodiazepine site (BZs and non-BZs), general anaesthetics site (e.g. steroids and ethanol) and convulsant site (PTX).^[10]

Until now, only nineteen GABA_A receptor subunits, molecularly distinct, have been identified. Based on sequence homology, they are divided into eight subunit classes (designed α , β , γ , δ , ϵ , θ , π and ρ), some of which have multiple isoforms (designed numerically): $\alpha(1-6)$, $\beta(1-3)$, $\gamma(1-3)$, δ , ϵ , θ , π and $\rho(1-3)$.^[28] The subunit composition influences fundamental features of the receptor, including sensitivity to GABA, channel kinetics and desensitization^{xiii}, neuronal location and pharmacological properties. GABA_A receptors with different subunit composition have different physiological and pharmacological properties, are differentially expressed throughout

^{xiii} **Desensitization**, in pharmacology, is the loss of responsiveness (i.e. the response to stimulation) to the continuing or increasing dose of a drug. For medical purposes, is a method to reduce or eliminate an organism's negative reaction to a substance or stimulus.

the brain and are targeted to different subcellular regions. For instance, receptors composed of $\alpha 1$, $\alpha 2$, $\alpha 3$ or $\alpha 5$ subunits together with β and γ subunits are benzodiazepine-sensitive, which are largely synaptically located and mediate most phasic inhibition in the brain.^[29] By contrast, those composed of $\alpha 4$ or $\alpha 6$ subunits together with β and δ subunits formed a specialized population of predominantly extrasynaptic receptor subtypes that mediate tonic inhibition and are insensitive to benzodiazepine modulation.^[30]

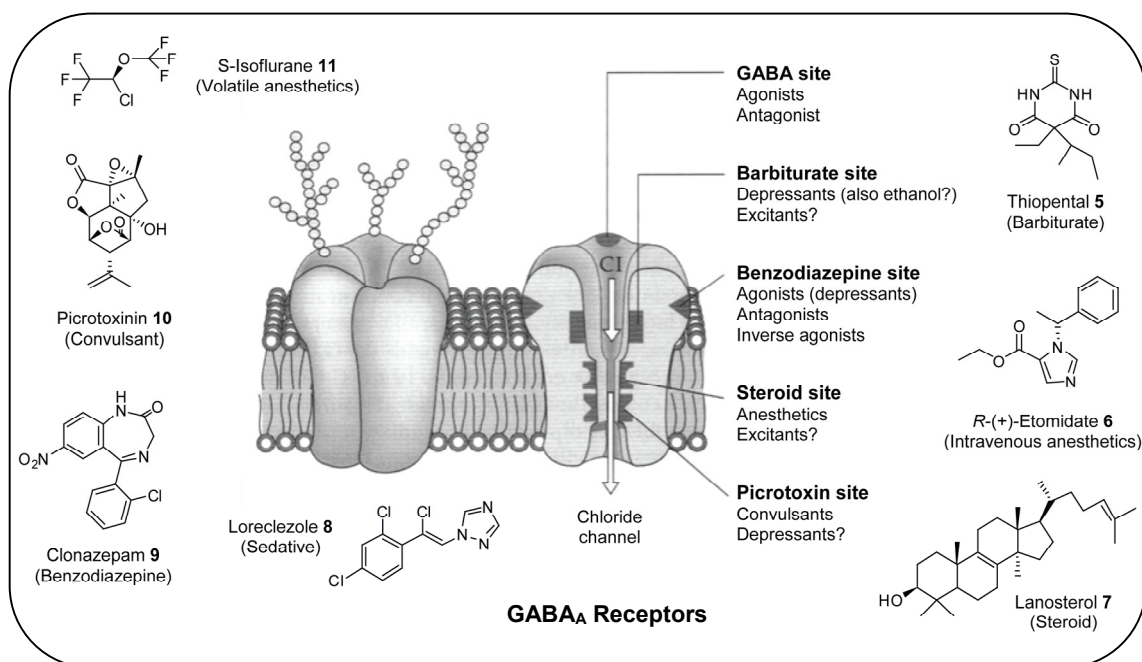


Figure 12. Drug binding sites and respective ligand drugs of the GABA_A R.

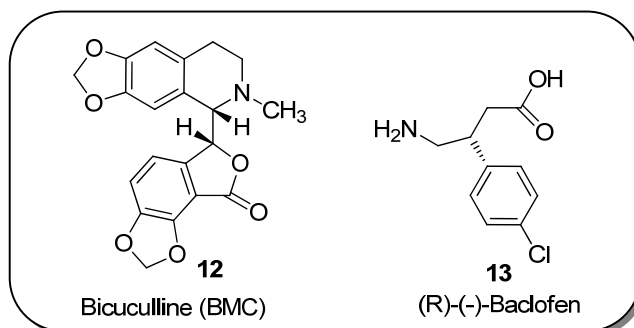


Figure 13. Chemical structure of BMC **12** and (R)-(-)-baclofen **13**.^[27]

1.2.2.1.1 Convulsant Binding Site

The channel blockers are commonly described as the picrotoxin site, since picrotoxin is most often used as a research tool in the comprehension of this binding site. Picrotoxin (picrotoxinin **10** in Fig. 12, is the active component) acts as a non-competitive antagonist of GABA_A channel, likewise, other ligands as bicyclic phosphates [such as *tert*-butyl bicyclic phosphorothionate (TBPS)], pentylentetrazole (PTZ) and other tetrazoles, penicillin and other β -lactam antibiotics, thiobutyrolactones and neurotoxic pesticides (NP). All these agents have cyclic structures and share a substantial similarity in chemical and conformational structure, allowing to consider them as a common group of “cage convulsants”. Until now this convulsant-binding pocket of GABA_A Rs is poorly understood.^[31]

1.2.2.1.2 Butyrolactone Site

Earlier reports on competitive inhibitors of TBPS binding by convulsant butyrolactones suggested that they bind to a common TBPS/picrotoxin convulsant ionophore site. This is also in line with similar chemical structures of these ligands (e.g. picrotoxinin molecule contains a butyrolactone ring). Likewise, butyrolactones share similar physiological and pharmacological mechanisms of action with PTZ and are able to allosterically modulate TBPS binding. Collectively, this implies that picrotoxin, PTZ, TBPS and butyrolactones may bind to overlapping ionophore binding sites. Although butyrolactone binding site is not yet identified, the sensitivity of butyrolactone binding to point mutations^{xiv} in residue 6 indicates its location within a common binding area for the convulsant. Since mutations affecting picrotoxin binding also affect that of butyrolactones, it is indeed likely that binding sites for picrotoxin and butyrolactones significantly overlap. In contrast, other studies have demonstrated anticonvulsant effects of some butyrolactones, suggesting either antagonism of the picrotoxin receptor, or a second positive (modulatory) “lactone” site.^[31]

^{xiv} A **point mutation**, or **single base substitution**, is a type of mutation that causes the replacement of a single base nucleotide with another nucleotide of the genetic material, DNA or RNA. Often the term point mutation also includes insertions or deletions of a single base pair.

1.2.3 GABA Binding Site for GABA_A R

GABA_A R binding site for GABA, commonly referred to as GABA_A site, is located at the interface of an α and a β subunit. Currently, only a few different classes of compounds are known as ligands for the GABA binding site.^[32] Studies on recombinant GABA_A R have indicated that the currently known full agonists or antagonists at the GABA binding site of these receptors seem not to exhibit significant receptor subtype selectivity. In addition, the use of these compounds is associated with severe side effects. Full GABA agonists open all GABA_A R associated chloride channels indiscriminately, cause inhibition of most neuronal systems, and severely interfere with the function of the brain, whereas GABA antagonists promote anxiety and convulsions.^[9]

The basically inhibitory nature of the central GABA neurotransmission encouraged the design and development of different structural types of GABA_A R agonists. The conformational restrictions of various parts of the GABA **1** molecule and bioisosteric replacements of the functional groups of the amino acid have led to a broad spectrum of specific GABA_A R agonists. The majority of compounds showing agonist activity at the GABA_A site are structurally derived from the GABA_A R agonist, namely muscimol **14**, 4,5,6,7-tetrahydroisoxazolo[5,4-c]pyridin-3-ol (**15**) (THIP or Gaboxadol) or isoguvacine **16**, which are illustrated in Figure 14.

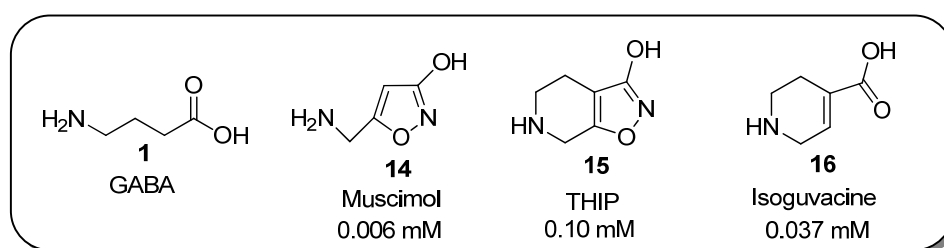


Figure 14. Chemical structure and data binding (IC_{50} , mM)^{xv} of some GABA_A R agonists.^[9]

^{xv} The **half maximal inhibitory concentration (IC_{50})** indicates how much of a particular drug or other substance (inhibitor) is needed to inhibit a given biological process (or component of a process) by half. In other words, it is the half maximal (50%) inhibitory concentration (IC) of a substance (50% IC, or IC_{50}).

Muscimol **14**, a constituent of the mushroom *Amanita muscaria*, was extensively used as a molecule leader for the design of different classes of GABA **1** analogues. The 3-isoxazolol carbonyl group bioisostere^{xvi} of muscimol **14** can be replaced by 3-hydroxyisoxazoline or 3-isothiazolo group to give dihydromuscimol **17** and thiomuscimol **18**, respectively, without significant loss of GABA_A R agonism (Fig 15). However, the structurally related muscimol analogues, isomuscimol **19** and azamuscimol **20** are virtually inactive, emphasizing the very strict structural constraints imposed on agonist molecules by the GABA_A R (Fig. 15).^[33]

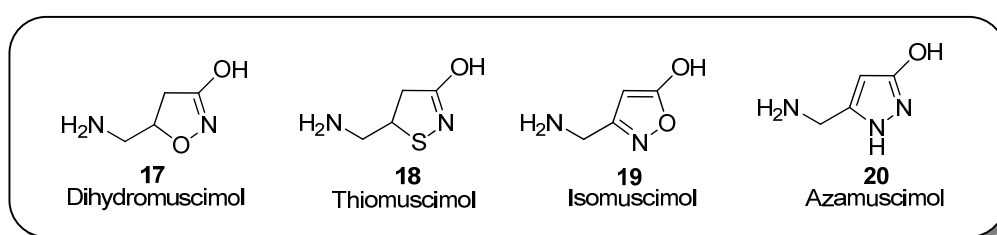


Figure 15. Chemical structure of some GABA_A agonists, highly potent such as dihydromuscimol **17** and thiomuscimol **18** and very weak such as isomuscimol **19** and azamuscimol **20**, derived from muscimol.^[9]

The conversion of muscimol into THIP **15** and the isomeric compound 4,5,6,7-tetrahydroisoxazole[4,5-*c*]pyridin-3-ol (**26**) (THPO) effectively separated GABA_A R and GABA uptake affinity, THIP **15** being a specific GABA_A R agonist and THPO **26** a GABA uptake inhibitor. Using THIP **15** as a lead, a series of specific GABA_A R agonists, as the monoheterocyclic isoguvacine **16** and isonipecotic acid **22**, and Thio-THIP **21** were developed. The non-fused THIP, compound 5-(4-piperidyl)isoxazol-3-ol (**23**) (4-PIOL), is a low-affinity GABA_A agonist and has been characterized as a partial GABA_A agonist.^[34] Likewise, piperidine-4-sulfonic acid (**24**) (P4S) and imidazole-4-acetic acid (**25**) (IAA) are partial GABA_A R agonists. A series of cyclic acids derived from THPO **26**, including Thio-THPO **27**, nipecotic acid **28**, and guvacine **29** were also developed as GABA uptake inhibitors (Fig. 16).

^{xvi} **Bioisostere** is a compound resulting from the exchange of an atom or of a group of atoms with another, broadly similar, atom or group of atoms. The objective of a bioisosteric replacement is to create a new compound with similar biological properties to the parent compound. The bioisosteric replacement may be physicochemically or topologically based.

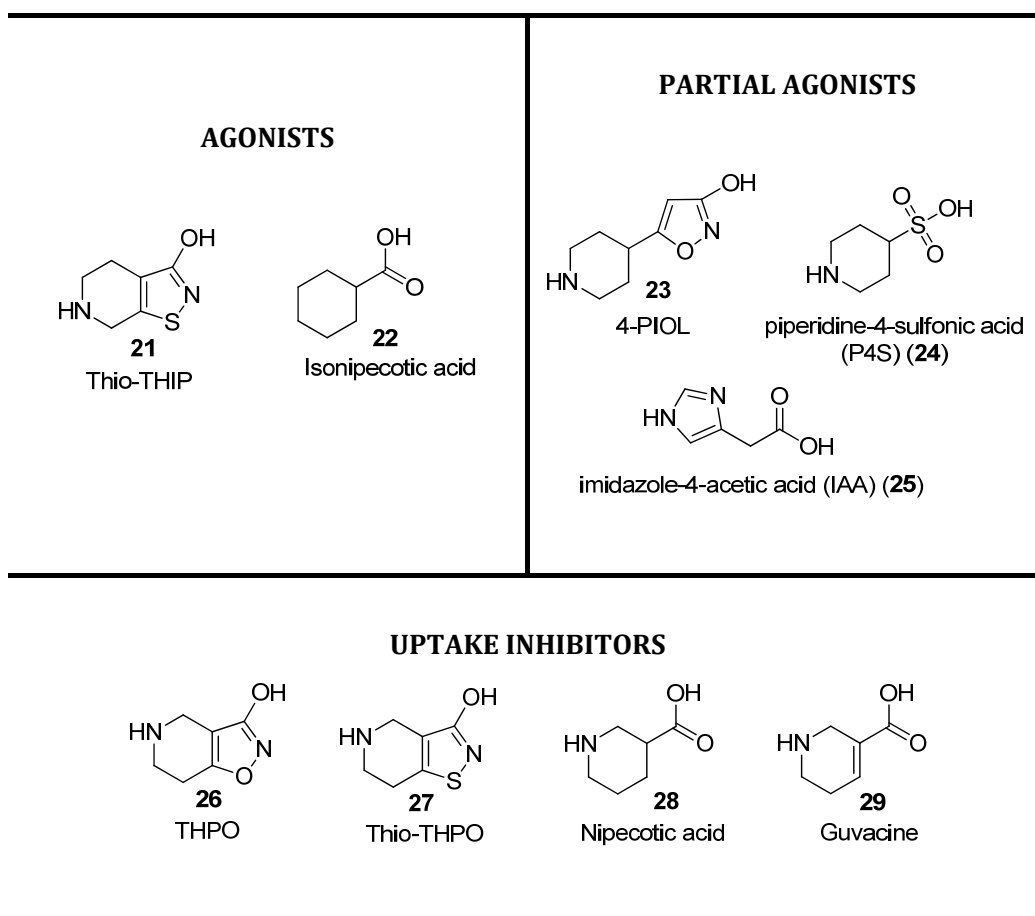


Figure 16. Chemical structure of some GABA_A R agonists, partial agonists and uptake inhibitors.^[9]

1.2.4 GABA Analogues

The ability of compounds to penetrate the blood-brain barrier^{xvii} (BBB) is of fundamental importance in drug discovery and design. High BBB permeability is needed for CNS-active drugs, while low BBB permeability may be desirable to minimize CNS-related side effects of drugs with peripheral sites of action. It seems that moderate levels of both relative hydrophobicity and lipophilicity values are required for compounds to be able to cross the BBB; more lipophilic compounds must be more sensitive toward their aqueous environment to cross the BBB.^[35] GABA

^{xvii} The **blood-brain barrier** (BBB) is a metabolic or cellular structure in the CNS that restricts the passage of various chemical substances and microscopic objects (e.g. bacteria) between the bloodstream and the neural tissue itself, while still allowing the passage of substances essential to metabolic function (e.g. oxygen).

analogues of pharmacological interest do not easily penetrate the BBB and after their administration, some are found in the periphery NS, where they may cause adverse effects.^[36] Therefore, manipulation of GABA **1** chemical structure is required to increase lipophilicity thus enabling compounds access to the CNS by crossing the BBB.

As mentioned before, compounds that act on GABA_A R have considerable therapeutic interest for use in a variety of neurological disorders such as epilepsy,^[37, 38] anxiety,^[38, 39] schizophrenia,^[38, 40] stiff-person syndrome,^[38, 41] and Huntington's chorea.^[42] While GABA **1** itself has not shown to be pharmacologically useful,^[43, 44] many attempts have been made to produce GABAergic drugs and prodrugs.^{xviii} Several GABA_A R ligands derived from GABA have been developed over the years.^[31, 36, 45-49] Some of them, such as the anticonvulsants progabide **30**, Gabapentin **31** (GBP) and vigabatrin **32**, containing a GABA substructure, have been already commercialized as antiepileptic drugs (Fig. 17).^[50] Based on the restriction of the conformation of the structure of GABA **1**, a large number of cyclic GABA analogues have been developed,^[51] namely **γ-butyrolactones 33** (GBLs) (IUPAC name: oxolan-2-ones) and **γ-butyrolactams 34** (IUPAC name: pyrrolidin-2-ones), with biological relevance as GABA_A R ligands.^[26, 52-54]

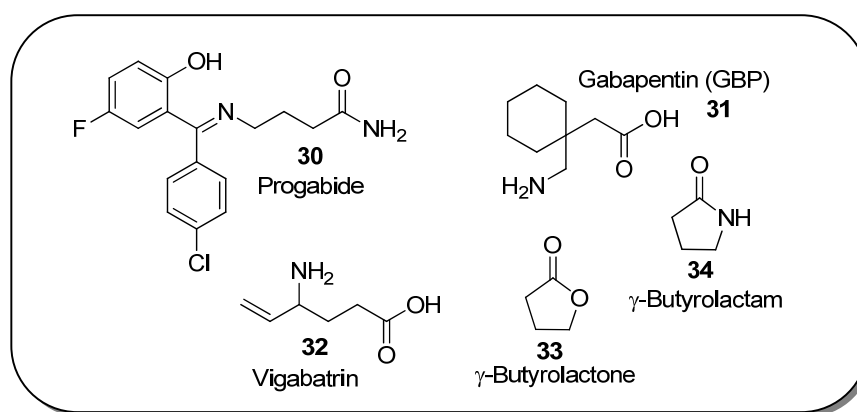


Figure 17. Chemical structure of some GABAergic ligands.

^{xviii} A **prodrug** is a pharmacological substance (drug) that is administered in an inactive (or significantly less active) form. Once administered, the prodrug is metabolized *in vivo* into an active metabolite. Prodrugs are usually designed to improve oral bioavailability, with poor absorption from the gastrointestinal tract usually being the limiting factor.

1.2.4.1 γ -Butyrolactones (GBLs)

GBLs **33** are metabolic precursors (or produgs) of γ -hydroxybutyrate (GHB **35**, Fig. 18). GHB **35** occurs naturally in the brain, and is both a precursor and a metabolite of GABA **1**. It is an emerging drug of abuse, possessing anxiolytic, hypnotic and anaesthetic effects, being capable of inducing amnesia, sedation, absence seizures, and, at very large doses, coma and death. In the beginning, GHB **35** was just related to the increase growth hormone, and until recently, was available in various prodrugs indicated for weight loss, muscle building and sleep induction. However, increasing reports of marked sedation, anaesthesia and coma following ingestion of GHB **35** have lead to restrictions on its availability, including classification in the US as Schedule I (Controlled Substances Act). The behavioural effects of GHB **35** and its precursors, as GBLs **33**, are similar though not identical, is the conversion of the precursors to GHB **35** *in vivo* that might suggest that GHB **35** is responsible for the behavioural effects of the precursors.^[55] Regardless the similarities between GBLs **33** and GHB **35**, several reports show that GBL **33** has common structural motifs encountered in a number of naturally occurring compounds possessing therapeutic properties,^[56-60] and in particular some of their derivatives are GABA_A R modulator agents of great interest^[25, 61-64] possessing potent anticonvulsant activity *in vivo*.^[65-67]

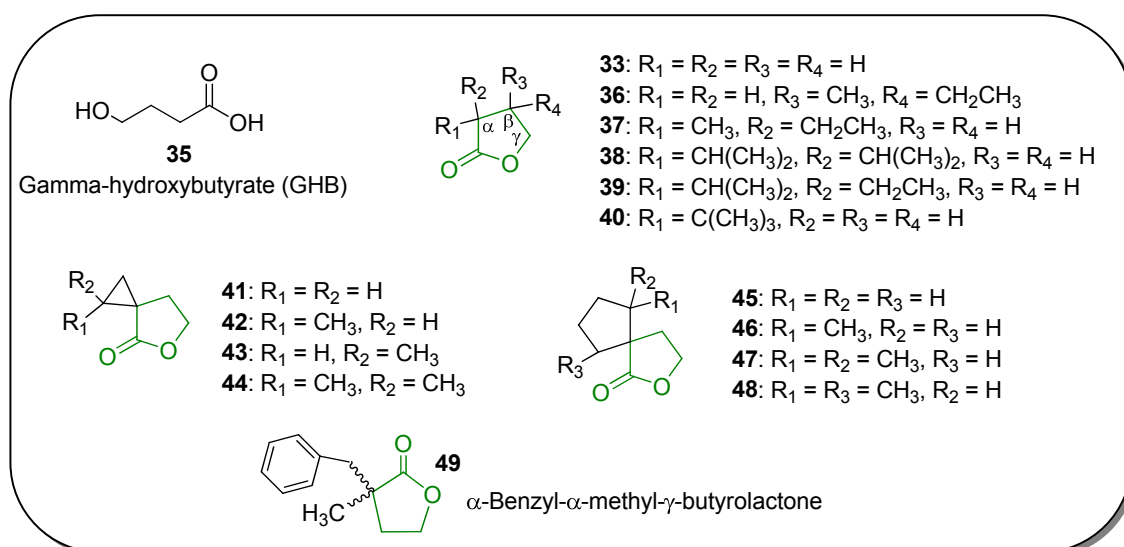


Figure 18. Chemical structure of GHB and some α - and β -substituted γ -butyrolactones as GABA R ligands.

In the attempt to explore GBL possible binding site more closely, conformationally unconstrained (compounds **36–40**) and constrained (compounds **41–48**) derivatives of GBLs were synthesized and evaluated by several research groups (Fig. 18). The data collected from literature revealed that lactones have either positive or negative modulatory activity, depending on the size and location of the substituent incorporated in the lactone ring. For example, alkyl-substituted GBLs, compounds **36–40** (Fig. 18), have shown to affect neural activity, but unfortunately, the distinction between the biological activities of β - (compound **36**) and α -substituted GBLs (compounds **37–40**) is not clear. Some compounds can cause both inhibitory and stimulatory effects on GABA_A Rs. The convulsant activity (GABA current-inhibiting) is presumed to be due to the ability of lactones to act as positive modulators on the PTX site and their anti-convulsant (stimulatory) activity (GABA current-enhancing), acting as negative modulators, is presumed to exist through the **lactone site**.^[25, 64, 68] Evidence from binding and electrophysiology studies have supported the hypothesis that the butyrolactone site on the GABA_A R is distinct from that for the BZ or the barbiturates, and that this site is closely related to the site of action of PTX.^[25, 69]

In addition, when comparing data obtained for α -spirocyclopropyl- γ -butyrolactones (compounds **41–44**) and α -spirocyclopentyl- γ -butyrolactones (compounds **45–48**) with data previously reported for unconstrained compounds **37–40**, it appears that cyclic substituents on the α - carbon of GBLs do not enhance anticonvulsant activity.^[67]

A more recent study on substituted GBLs enantiomers [compounds (*R*)-**49** and (*S*)-**49**, Fig. 18] showed enantioselective preference which supported the existence of a lactone binding site on GABA_A Rs. Targets that prefer one chiral form of the enantiomers are thus likely to have a specific binding site for the parent molecule.^[25]

1.2.4.2 γ -Butyrolactams

γ -Butyrolactams **34**, often referred as pyrrolidones, are GABA derivatives (Fig. 19) with close chemical correlations to the GABA molecule **1**. In general, γ -lactams have shown to possess anticonvulsant and antioxidant activity, and can be useful as key intermediates for the synthesis of pyrrolidines, the biosynthetic precursors of GABA analogues.^[70-73] γ -Butyrolactams **34** are more lipophilic than GABA **1**, therefore they could penetrate more easily the BBB. Hence, they can be used as a GABA prodrug in the treatment of neurological and neuropsychiatric disorders associated with a decrease in GABA levels in CNS. In this context, several α - and β -substituted- γ -butyrolactams have been developed as GABA_A R ligands, namely compounds **50-56** (Fig 19), described below.

As mentioned before, GABA-pentin (**31**, Fig. 17), is currently used as therapeutic agent against epilepsy as well as neuropathic pain. However, its derivative GABA-pentin-lactam (GBP-L) (**50**, Fig. 19), was found to be a more effective anticonvulsive agent than the free amino acid GABA-pentin **31**. In addition it also shows a pronounced neuroprotective activity in retinal ischemia.^[74] Another β -substituted-pyrrolidin-2-one, rolipram **51**, was also developed as an antidepressant drug and is commercialized in Europe by Schering AC.^[75] Another example of an α -substituted-pyrrolidin-2-one is the 3,3-diethylpyrrolidin-2-one (**52**, Fig. 19) which increases GABA-induced currents in cultured hippocampal neurons. *N*-nicotinoyl-pyrrolidin-2-one (**53**) and 1-(2-propyl-1-pentanoyl)-pyrrolidin-2-one (**54**) are also examples of GABA receptor ligands. Finally, two known commercial antiepileptic pyrrolidones, the piracetam **55** (Nootropil®) and levetiracetam **56** (Keppra®) are also illustrated in Figure 19.^[54, 65, 70, 76-78]

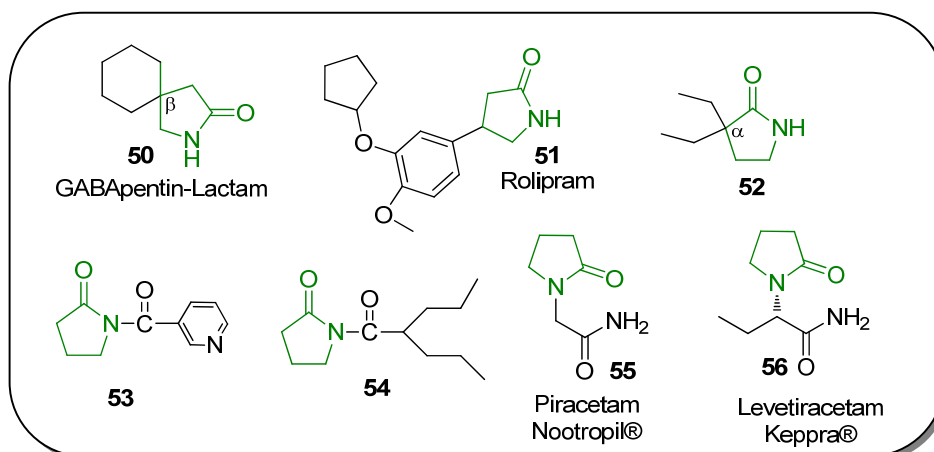


Figure 19. Chemical structure of some α - and β -substituted γ -butyrolactams as GABA R ligands.

1.2.4.3 QSAR Modelling for Selective Anticonvulsants

Evaluation and comparison of some Quantitative Structure-Activity Relationship^{xix} (QSAR) models provided additional understanding for the binding and anticonvulsant activity of some GABA_A R binding ligands. Derivatives of butyrolactones **33**, thiobutyrolactones, pentanones, hexanones, pyrrolidones **34** and piperidinones were used for the construction of these models. All the compounds study share a common structural pattern, changing in ring size, heteroatom and chain length.^[79]

Based on an overview of several QSAR models, the following conclusions were made:

- Substituent side chain affects anticonvulsant activity, while electronic factors have no direct consequences; e.g. polar side chains in the molecule enhance hydrophilicity and increases the anticonvulsant activity; the more electronegative elements in the molecule, the higher probability of being convulsant.

^{xix} **QSAR** study is the search for quantitative relations between the chemical structure, i.e. physicochemical and structure properties and the biological activity.

- It can be also speculated that both convulsant and anticonvulsant sites compete for the molecules and they have the choice of binding to any of the sites.
- Anticonvulsant activity can be increased by bulky side chains with constrained flexibility, i.e. having ring structures or unsaturated bonds.

1.3. Benzodiazepines

1.3.1 A Chemical Perspective – Structure and Synthesis

The parent structure of a benzodiazepine, e.g. 1,4-benzodiazepine (**57**, Fig. 20) consists on a benzene ring (A) fused to a seven-membered ring containing two nitrogen atoms (diazepine) (B) and is known to be a highly flexible structure. There are numerous types of benzodiazepines which includes 1,4-benzodiazepin-2-one, 1,4-benzodiazepin-3-one, 1,4-benzodiazepin-5-one, 1,4-benzodiazepine-2,5-dione **58**, 1,4-benzodiazepine-3,5-dione, 1,5-benzodiazepine, 1,5-benzodiazepin-2-one and pyrrolo[2,1-c][1,4]benzodiazepine-5,11-dione^{xx} (**59**, Fig. 20). 1,4-Benzodiazepine-2,5-dione **58** is one of the most studied benzodiazepines framework. In particular, pyrrolo[2,1-c][1,4]benzodiazepine-5,11-diones **59** which are proline substituted 1,4-benzodiazepine-2,5-dione scaffolds.^[80]

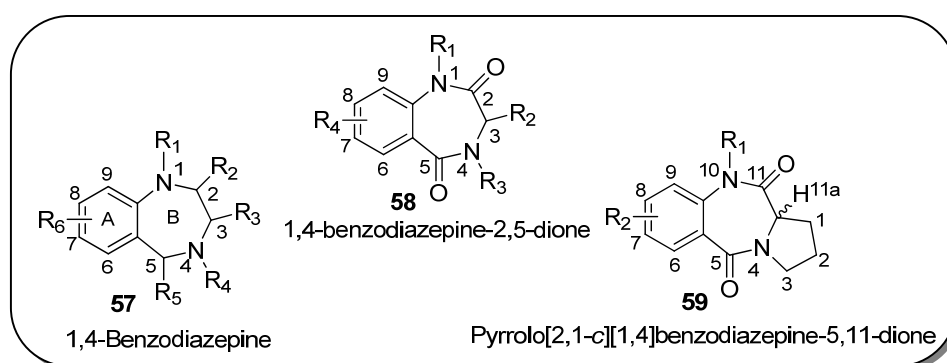


Figure 20. Chemical structure of 1,4-benzodiazepine **57**, 1,4-benzodiazepine-2,5-dione **58** and pyrrolo[2,1-c][1,4]benzodiazepine-5,11-dione **59**.

^{xx} IUPAC Nomenclature for Fused Polycyclic Hydrocarbons, Rule A - 21.5.

Among the numerous methods reported in the literature for the preparation of pyrrolo[2,1-*c*][1,4]benzodiazepine-5,11-diones **59**, one of the eldest and efficient synthetic approach is the condensation of isatoic anhydride **60** with proline **61** or proline derivatives (α -amino acids). This reaction is usually performed in polar aprotic solvents like DMSO/DMF at high temperatures (115-150 °C) (Fig. 21).^[81-84]

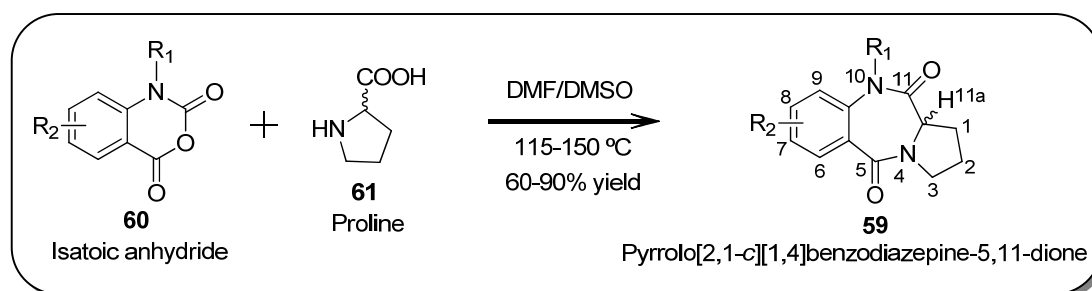


Figure 21. General synthesis of a pyrrolo[2,1-*c*][1,4]benzodiazepine-5,11-dione.

Unnatural amino acids have found considerable use as building blocks in medicinal, peptide and protein chemistry.^[85, 86] In particular, stereochemically and conformationally constrained amino acids, such as proline **61** strongly favour specific backbone conformations. L-Proline is unique among the twenty natural amino acids since it has the side-chain cyclized onto the backbone nitrogen atom, i.e. the C_α-N bond is a part of the pyrrolidine ring. Due to these unique structural properties, proline **61** has been used in the development of numerous D- and L-proline mimetics and analogues and applied in the synthesis of biologically relevant peptides and other molecules over the past years.^[85, 86] Nowadays its completely established that α -amino acids are the key starting materials which provide the configuration at C-11a of pyrrolo[2,1-*c*][1,4]benzodiazepines.

The most interesting chemistry related to isatoic anhydride is the result of nucleophilic attack on its oxazine ring (Fig. 22). In fact, isatoic anhydride **60** has two carbonyl groups susceptible to the attack of nucleophiles, namely the C-2 and C-4, and a nucleophilic nitrogen atom on the oxazine. The majority of the attacks occur at C-4 and the transformation is accompanied by carbon dioxide evolution, leading to the

formation of a second amide bond when the nucleophile is proline (e.g. pyrrolo[2,1-c][1,4]benzodiazepine-5,11-dione, **59**).

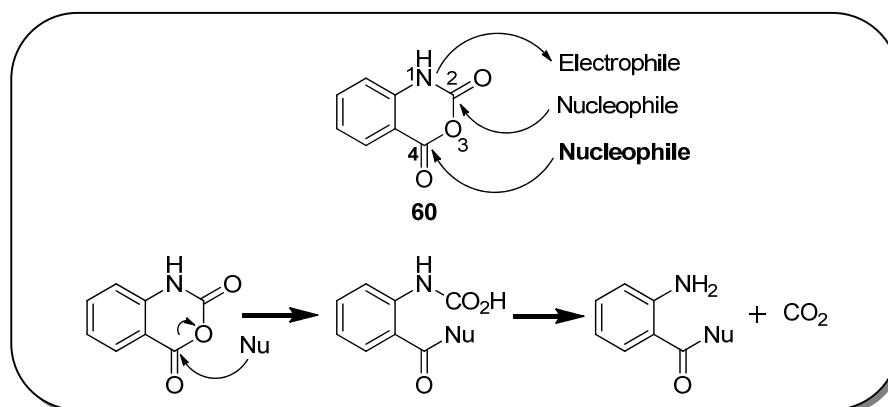


Figure 22. Proposed mechanism for the studied reactivity of isatoic anhydride.^[87]

1.3.2 Benzodiazepine as a Privileged Scaffold in Medicinal Chemistry

BZs are considered a prototypical privileged substructure or privileged scaffold.^{xxi} It was with this class of compounds that the term “privileged structure” was first applied in 1988.^[88] BZs are among the most widely dispensed drugs. Besides the well known anxiolytic, sedative, anticonvulsant myorelaxants and hypnotics activities,^[10] BZs have been shown to act as peripheral cholecystokinin (CCK-A) receptor agonists,^[89-91] α -thrombin inhibitors,^[92] antitubercular drugs,^[93] endothelin receptor antagonists^[94] and can be cytotoxic against transformed T-cells.^[95] Indeed, several of these nitrogen-containing heterocycles have been identified as antitumour antibiotics,^[96] anti-HIV^[97] and antithrombotic agents.^[98] Moreover, because of both their structural motifs and physicochemical properties, the BZ scaffold has been considered among novel non-peptide peptidomimetics, acting as a mimic of peptide secondary structures such as γ - and β -turns.^[99-101] Particularly useful in medicinal

^{xxi} **Privileged scaffolds** are scaffolds that are commonly present in established drugs.

chemistry are proline-derived benzodiazepines (pyrrolo[2,1-*c*][1,4]benzodiazepines),^[102-104] showing promise as anxiolytic drug candidates (i.e. compound **62**, Fig. 23) and as starting materials for the synthesis of anthramycin-inspired anticancer drugs (e.g. compound **63**),^[105] DNA-cross-linking agents (e.g. compound **64**),^[106] and $\alpha 5$ -selective GABA_A receptor ligands (e.g. compound **65**).^[107] Our interest in compounds with this structure, the pyrrolobenzodiazepines, was directed to their anxiolytic activity.

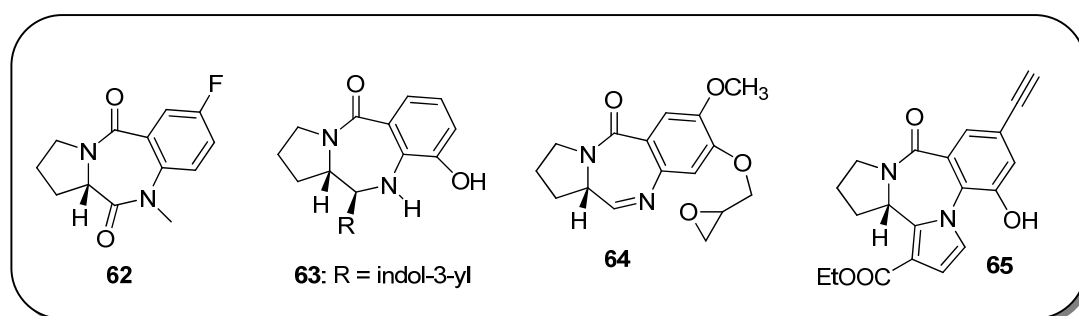


Figure 23. Chemical structure of some biologically active pyrrolo[2,1-*c*][1,4]benzodiazepines.

1.3.3 Benzodiazepine as a Commercial Psychoactive Drug

BZs, first discovered by their anxiolytic activity, became recognized as privileged scaffolds in medicinal chemistry due to their wide range of biological activities and therapeutic uses. The first BZ, chlordiazepoxide (Librium®) (**66**, Fig. 24), was introduced into clinical practice by Hoffmann-La Roche in the sixties. Some years later, diazepam (Valium®) (**67**, Fig. 24) was synthesized, again by Hoffmann-La Roche. Nowadays, one of the most famous BZs is alprazolam (Xanax®) (**68**, Fig. 24). The selection of the most appropriated BZ depends obviously on the specific clinical situation. Thus, within this class of compounds longer-acting (with long-lived pharmacologically active metabolites), or shorter-acting (without active metabolites, they have shorter half-live) drugs are available. Recently there has been a shift to the prescription of shorter-acting agents, such as the well known bromazepam (Lexotam®) **69** and lorazepam (Ativan®) **70**, although the most widely studied and utilized BZs are still the longer-acting agents, namely chlordiazepoxide **66** and diazepam **67**, all illustrated in Figure 24.^[108]

BZs have a sedative, hypnotic, anxiolytic, muscle relaxant and anticonvulsant action and, from a therapeutic perspective, it would certainly be highly desirable to have BZs selective for each of these different actions. Their wide pharmacological behaviour is due to the ability to bind to specific sites on the GABA_A receptor, *via* the benzodiazepine receptor site. BZs enhance the action of GABA on GABA_A Rs by increasing the GABA-induced frequency of opening the chloride channel, allosterically modulating these receptors.^[107, 109] Unlike neurosteroids and barbiturates, BZs can not increase the channel open time in the absence of GABA 1.

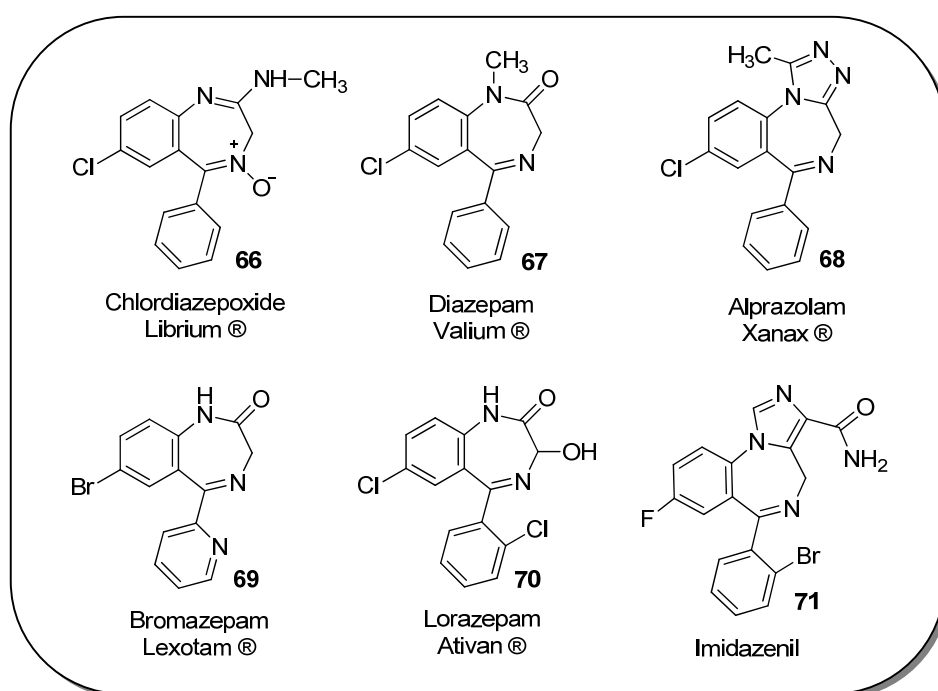


Figure 24. Chemical structure of some commercial benzodiazepines.

Since the discovery of the first BZ as tranquilizer, barbiturates were completely replaced. These drugs have acquired certain relevance in clinical practice because they are or have been used in psychiatry (anxiety disorders), neurology (anticonvulsants) and anaesthesia. By virtue of their selective ability to amplify GABA action at GABA_A Rs and because of their limited toxicity, BZs are the drugs of choice to treat convulsive and anxiety disorders. Regardless the limited clinical utility of

classical BZs because of their tremendous side effects, namely tolerance and abuse potential, they are amongst the most widely used drugs.^[10] The onset of tolerance requires frequent increase in dosages to maintain BZ therapeutic efficacy. Tolerance is followed by dependence, and dependence leads to addiction in worst cases. That is why the future use of BZs in therapy is linked to the development of partial allosteric modulators, as imidazenil (**71**, Fig. 24), which is devoid of the typical side effects of BZs.

1.3.4 Benzodiazepine Binding Site on GABA_A Receptors

The BZ R site on GABA_A Rs does not only recognizes or reacts with BZs but also accepts other ligands of very different structures (Fig. 25) such as imidazobenzodiazepines, e.g. imidazenil **71**, imidazo-pyrrolobenzodiazepines, e.g. bretazenil **72**, β -carboline, e.g. FG 7142 **73**, pyrazoloquinolinones, e.g. CGS-8216 **74** and triazolopyridazines, e.g. CL 218872 **75**. The BZ site is known for its heterogeneity, having therefore different efficacies.^[36]

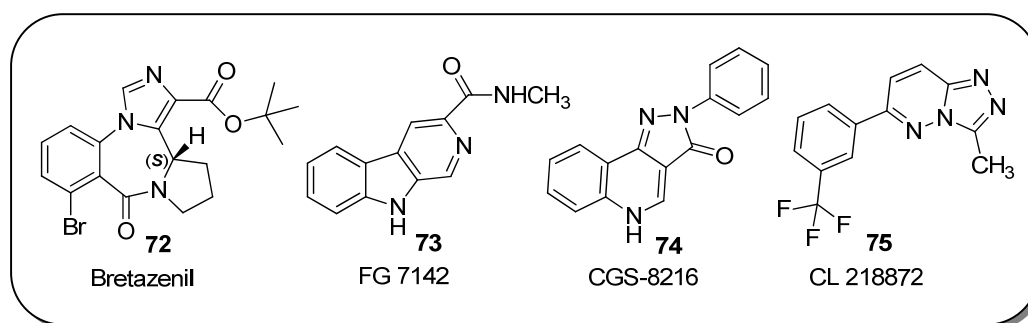


Figure 25. Chemical structure of some compounds which interact with BZ R site.

BZs and their congeners are supposed to bind to the extracellular domain of different GABA_A R subtypes at the border interface between the α and γ 2 or γ 3 subunits expressed in any given GABA_A R subtype. Since the BZ binding site on GABA_A Rs is located at the interface of two subunits, α and γ , its binding properties are influenced by the types of the subunits forming the interface. Since there are six different α

subunits and three different γ subunits in the mammalian CNS, up to eighteen different GABA_A R-associated BZ binding sites may exist. Most compounds interacting with BZ binding site are inactive or only weakly active at receptors containing γ 1 subunits. Although there seems to be some activity of BZ ligands at receptors containing γ 3 subunits, these receptors exhibit a very low abundance in the brain. Thus, the currently prescribed BZs, such as diazepam (**67**, Fig. 24), and most of the structurally unrelated compounds bind to GABA_A Rs containing α 1, α 2, α 3 or α 5 (α 1 β γ 2, α 2 β γ 2, α 5 β γ 2) subunits and are commonly described as diazepam-sensitive (DS) receptors. However, the corresponding binding site of GABA_A Rs containing either an α 4 or α 6 subunit (α 4 β γ 2, α 6 β γ 2), does not bind the classical BZs and therefore they are known as diazepam-insensitive (DIS) receptors.^[9, 110]

1.3.4.1 Classification of BZs and Their Congeners

BZs and their congeners that bind to the BZ recognition site can act:

- As full, selective or partial positive allosteric modulators (anxiolytic, anticonvulsant, hypnotic, sedative and muscle relaxant effects);
- As negative allosteric modulators (anxiety, proconflict, convulsant and/or proconvulsant or nootropic^{xxii});
- Neutralizing the positive or negative allosteric modulation of GABA action at GABA_A R (often named pure “antagonists”).

BZs are strictly allosteric modulators of the GABA_A Rs. Hence this is a more accurate terminology than “agonist” or “inverse agonist” to describe the action of BZs on GABA_A R.^[111] BZs that act as positive allosteric modulators increase the channel function in response to GABA or a GABA_A agonist. However they do not have any effect when GABA binding to its separate agonist binding site is absent. Therefore, in the presence of BZs that act as positive allosteric modulators, less GABA is needed for the induction of a given GABA-gated Cl⁻ conductance. BZs with full positive allosteric

^{xxii} **Nootropics**, also referred to as smart drugs, memory enhancers, and cognitive enhancers, are able to improve human cognitive abilities.

modulatory activity (e.g. diazepam **67**, Fig. 24) can maximize the action of very small concentrations of GABA in many receptor subtypes, without increasing the intensity of GABA maximal response. Whereas partial allosteric modulators (e.g. imidazenil **71**, Fig. 24) never maximize the actions of GABA but only modestly increase the actions of various doses of GABA.^[9, 22]

Negative allosteric modulators exert the opposite effect of the positive allosteric modulators by decreasing the channel function. “Antagonists” or neutralizers allosteric modulators, such as flumazenil (**72**, Fig. 24), occupy the binding site without influencing GABA-induced chloride flux but antagonize the action of agonists or inverse agonists.^[46]

1.3.4.2 Conformational Equilibrium in Benzodiazepine Ring

Benzodiazepine anxiolytics, contrary to GABA **1**, do not open directly the channel gate and are known to display an interesting conformational enantiomerism which influences their ability to bind to the benzodiazepine binding site.^[112, 113] This high-affinity and stereospecific binding site of benzodiazepines at the GABA_A Rs was always subject of enormous concern. Several reports showed that binding affinities at the GABA_A R are exquisitely sensitive to the helical chirality of the 1,4-benzodiazepine ring. The chirality of these compounds is determined by determining the screw sense of the helix. 1,4-Benzodiazepine’s seven-membered ring has a boat conformation, assigned *P* (plus) or *M* (minus) on the basis of the sign of the torsion angle around C3-N4. If the screw (twist) is right handed the chirality is ***P*** (plus), if it is left handed the chirality is ***M*** (minus). Figure 26 illustrates an example of these conformational equilibrium, (*M*) and (*P*), present in the (*3R*) and (*3S*)-1,4-benzodiazepine-2,5-dione ring.^[113, 114]

The effect of the benzodiazepine conformational changes on their binding ability has been investigated by several groups, which highlighted that (*3R*)- and (*3S*)-1,4-benzodiazepines have a different effect on binding affinities to the GABA_A R.^[114, 115] From single crystal X-ray analyses and computational studies of 1,4-benzodiazepines

ring inversion it was observed that both enantiomers have a preferred conformation in which R_2 is pseudo-equatorially oriented (Fig. 26). Moreover, because (3*S*)-enantiomer preferentially adopts (*M*)-helicity, since this conformation places the R_2 in the pseudo-equatorial orientation, and (3*R*)-enantiomer preferentially adopts (*P*)-helicity for the same reason, the (3*S*)-enantiomer has shown to be more active in binding assays and *in vivo* pharmacological tests than the corresponding (3*R*)-enantiomer.^[113, 116] Therefore, it was suggested that the primary source of binding selectivity of 1,4-benzodiazepine enantiomers was the differential recognition of ligand conformations by the receptor, with a preferred recognition of (*M*)-1,4-benzodiazepine conformation.

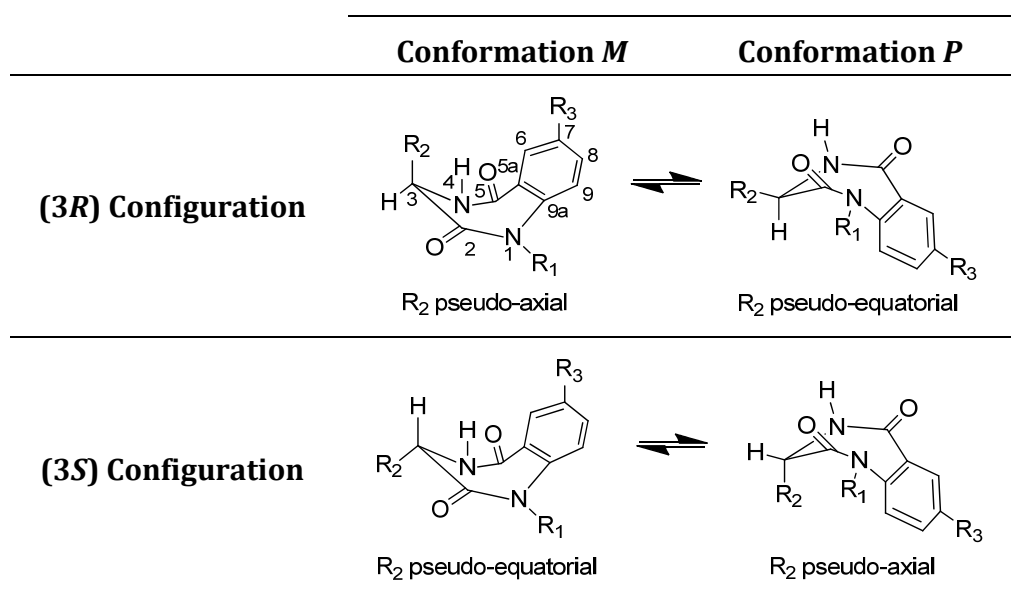


Figure 26. Conformational equilibrium in (3*R*)- and (3*S*)-1,4-benzodiazepine-2,5-dione. (*M*) and (*P*) helical descriptors of configuration are assigned on the basis of the sign of the C2-N1-C9a-C5a dihedral angle. This dihedral angle has the same sign as the C2-C3-N4-C5 dihedral which historically has been used to designate the sense of conformational chirality of the benzodiazepine ring.^[117]

Hence, benzodiazepine ring helical chirality and consequent stereospecific GABA_A receptor binding is important for the development of new lead compounds. Thus, great efforts have been devoted to the synthesis of conformationally constrained

benzodiazepine derivatives, since these conformational changes in the benzodiazepine ring system have a strong effect on binding affinities to the receptor complex.^[102, 116, 118] The conformational equilibrium of the benzodiazepine ring can be locked through the control of the absolute stereochemistry of carbon C-3, by the formation of a fused pyrrolidine ring. Synthesis of 1,4-benzodiazepine-2,5-diones derived from proline (pyrrolo[2,1-*c*][1,4]benzodiazepine-5,11-diones **59**, Fig. 27) showed that the use of this specific amino acid allows the control of the absolute stereochemistry of carbon C-11a. All reported proline-derived quaternary BZs retained a single conformation of the seven-membered ring.^[102] As illustrated in Figure 27, (11a*R*)-enantiomer **59** preferentially adopts (*P*)-helicity and (11a*S*)-enantiomer **59** preferentially adopts (*M*)-helicity, since this conformation places the H-11a in the pseudo-axial orientation. However, the ability of these heterocycles to bind to GABA_A R, and their behaviour as anxiolytic agents has been scarcely studied so far. Our aim was to synthesize new enantiomeric constrained sugar-based pyrrolobenzodiazepine derivatives and to study their ability on binding to GABA_A R.

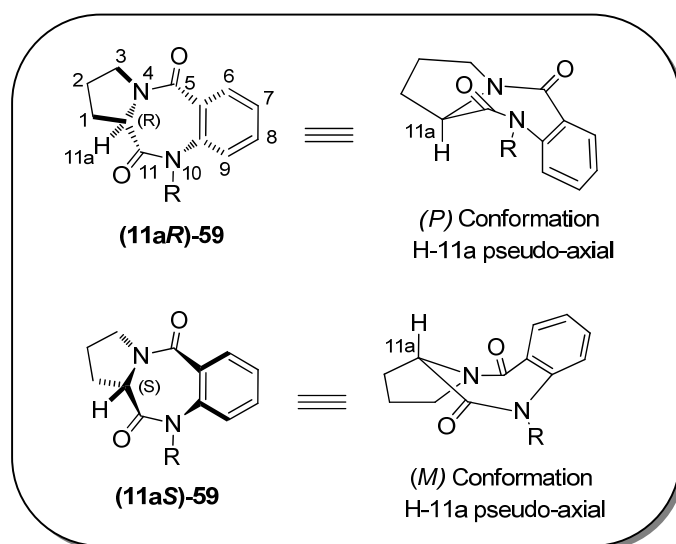


Figure 27. Conformationally constrained (11a*R*)- and (11a*S*)-pyrrolo[2,1-*c*][1,4]benzodiazepine-5,11-diones. Atom numbering is according to standard pyrrolobenzodiazepines.

1.3.4.3 SAR studies

Structure-activity relationship (SAR) studies have been carried out by a number of research groups on structurally diverse classes of ligands and have resulted in the formulation of several different pharmacophore/receptor models for the BZ R. Several models which attempt to explain ligand efficacy as a function of ligand-receptor interaction at the molecular level have been developed.^[119]

Early SAR studies concerning the basic structure of a classical anxiolytic 1,4-benzodiazepin-2-one (**76**, Fig. 28), showed that the seven-membered imino ring B was essential for its affinity towards BZ-binding. In addition, these studies have demonstrated that all BZ ligands share the presence of an aromatic or heteroaromatic A ring, believed to undergo π/π stacking with aromatic amino acid residues within the receptor, as well as the presence of a proton-accepting group as substituent of the aromatic ring A interacting with a histidine residue on the receptor.^[120] Additionally, the carbonyl group at position two, and the N(4)-C(5) double bond within the ligand have been shown to contribute to the binding affinity of the compound. Also substituents at positions one and seven contribute to high receptor binding affinity. Position seven is the most effective location in these molecules for enhancing the affinity of the compound for the BZ-binding site. So, an increase in the lipophilicity and electronic charge of substitutions at position seven are directly related to an increased affinity of the ligand for the binding site.^[121]

Optimal functional groups at positions one and seven are:

- position one: OH > F > NH₂ > H > NHOH > CH₃ > Cl > CF₃ > Br
- position seven: C > H₂CF₃ > I > Br > CF₃ > Cl > C(CH₃) > NO₂ > F > N₃ > CH=CH₂

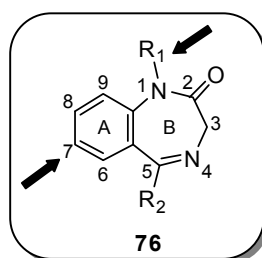


Figure 28. Chemical structure of a 1,4-benzodiazepin-2-one.

In this work was used not only electronegative substituents at position seven, such as -Cl, -Br and -NO₂, but also -NH₂, and at position one was used -CH₃ in order to have a suitable binding affinity.

Further QSAR and SAR studies indicated that the molecular lipophilicity properties of numerous BZs played a significant role in their corresponding receptor affinity. In order to further evaluate the lipophilic/hydrophilic balance, was developed new pyrrolobenzodiazepines, where the pharmacophore is spiro-linked to a carbohydrate moiety. The free hydroxyl groups on the sugar moiety offer the possibility of functionalisation for tuning the pharmacokinetic properties and the biological activity.

1.4 Carbohydrates as Natural Scaffolds

The abundance of carbohydrates in nature and their diverse roles in biological systems makes them attractive molecules for chemical and biological research. They are found as monomers, oligomers or polymers, or as components of biopolymers and other naturally occurring substances. As natural products, they play important roles in conferring certain physical, chemical, and biological properties. Furthermore, they have been implicated in many cellular processes, including cell-cell recognition, cellular transport, and adhesion; they appear in all cells in some form or another, for example, as peptide- and proteoglycans, glycoproteins, nucleic acids, lipopolysaccharides or glycolipids.^[122]

Thus, carbohydrates are of great interest due to their unique characteristics as polyfunctional molecules, which occur in enantiomerically pure forms and have some conformational rigidity. So, functionality, chirality, structural diversity and availability are features that make this class of compounds particularly appealing as scaffolds and as a challenging synthetic platform with application in the areas of pharmaceutical and medicinal chemistry.^[123]

Indeed, the last decade has witnessed the importance of carbohydrate chemistry in drug discovery processes. Sugar templates have been used as tools for the production of new drugs by first mimicking non-carbohydrate structures such as peptides. The possibility to elaborate the functional groups, together with the rigid molecular structure, render carbohydrates well suited as molecular templates to display pharmacophoric groups in well defined spatial orientation. Steric and conformational aspects play an important role in drug action, since the correct orientation of the pharmacophoric group is necessary for the interaction with specific receptors. Hence, recent efforts have focused on developing efficient methods of selective protection, deprotection, and functionalization, both in solution and on solid supports, to build up libraries of compounds based on carbohydrate scaffolds. It has also been reported that, according to Lipinski's 'rule of five',^[124] the high number of hydrogen bond acceptors and donors in carbohydrate scaffolds can decrease their cellular and tissue absorption.^[125] This problem is often bypassed in the case of monosaccharide-derived drugs by the presence of specific biological transporters that improve cellular uptake.^[125]

Monosaccharides and particularly hexoses are ideal chiral scaffolds, less expensive and containing five functionalized positions. In principle, various substituents can be appended at each position and the configuration of each stereogenic center can be altered. Particularly, D-fructose (**77**, Fig. 29), also referred to as fruit sugar, is one of the most abundant natural sugars and is highly attractive due to the presence of two hydroxymethyl groups (C-1 and C-6) and the unique reactivity of the anomeric position, which is part of a hemiketal functional group.

Fructose is a six-carbon polyhydroxy ketone which forms ring structures, the cyclic hemiketals, as opposed to the cyclic hemiacetals formed by aldoses such as glucose. The five-membered ring form (D-fructofuranose) results from reaction of OH-5 with the carbonyl group, while reaction of OH-6 leads to a six-membered ring (D-fructopyranose).

In this context, chemical modification of this sugar can afford original, stable and possibly more rigid compounds. As a result, fructose scaffolds provide an unparalleled opportunity to generate libraries of structurally diverse and highly functionalized molecules.

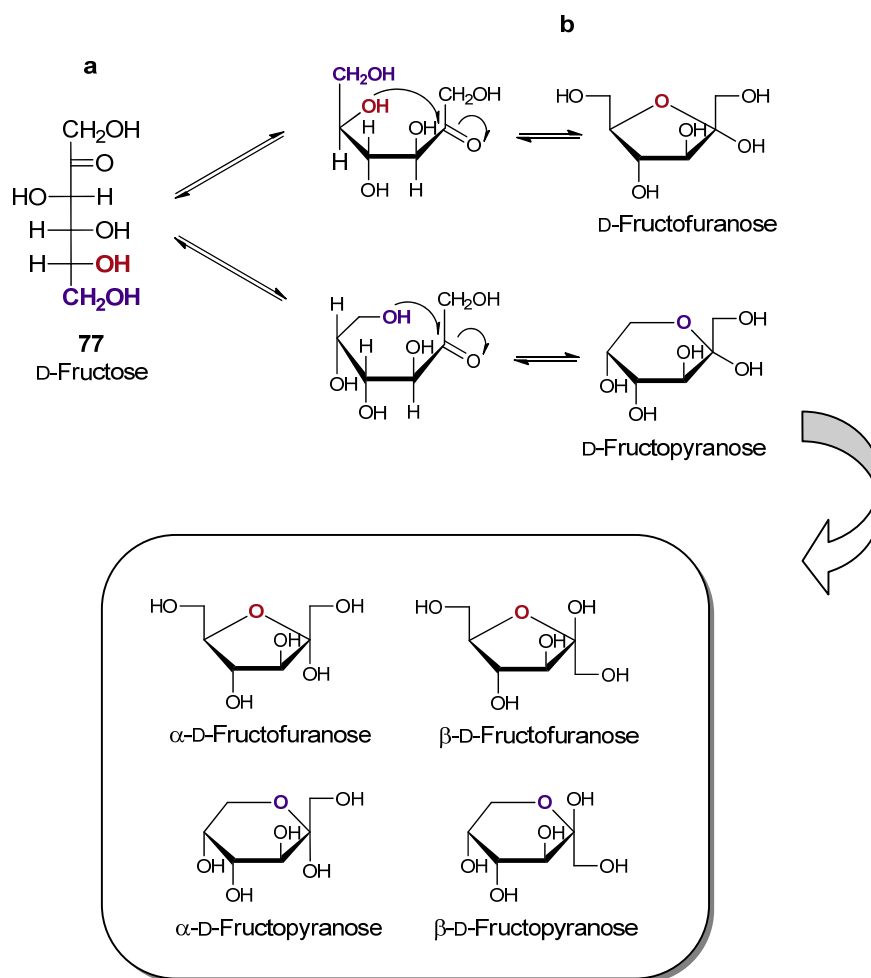


Figure 29. Isomeric forms of D-fructose **77**, Fischer (a) and Haworth (b) projections.

1.4.1 Sugar Derived Polyfunctional Scaffolds– GABA Analogues and Benzodiazepines

The generation of novel polyfunctional scaffolds from monosaccharides is increasing significantly the number of privileged scaffolds available in medicinal chemistry. Recently, several new scaffolds such as hybrids of benzodiazepines have been developed. Examples of these sugar-based benzodiazepine scaffolds are compounds **78–82** represented in Figure 30. [126-131] The low hydrosolubility of classical BZ restricts significantly their applications. Thus, attaching a sugar moiety (e.g. galactose, ribose or glucose) to this structure increases the water solubility and confers amphiphilic properties to the final compound. Contrary to sugar-based benzodiazepines, only few examples of sugar-based GABA analogues were reported in literature. Carbohydrates such as galactose **83** and glucose **84**, showed in Figure 31, were used as platforms for the design of GABA derivatives. However no biological evaluation was reported so far. [132, 133]

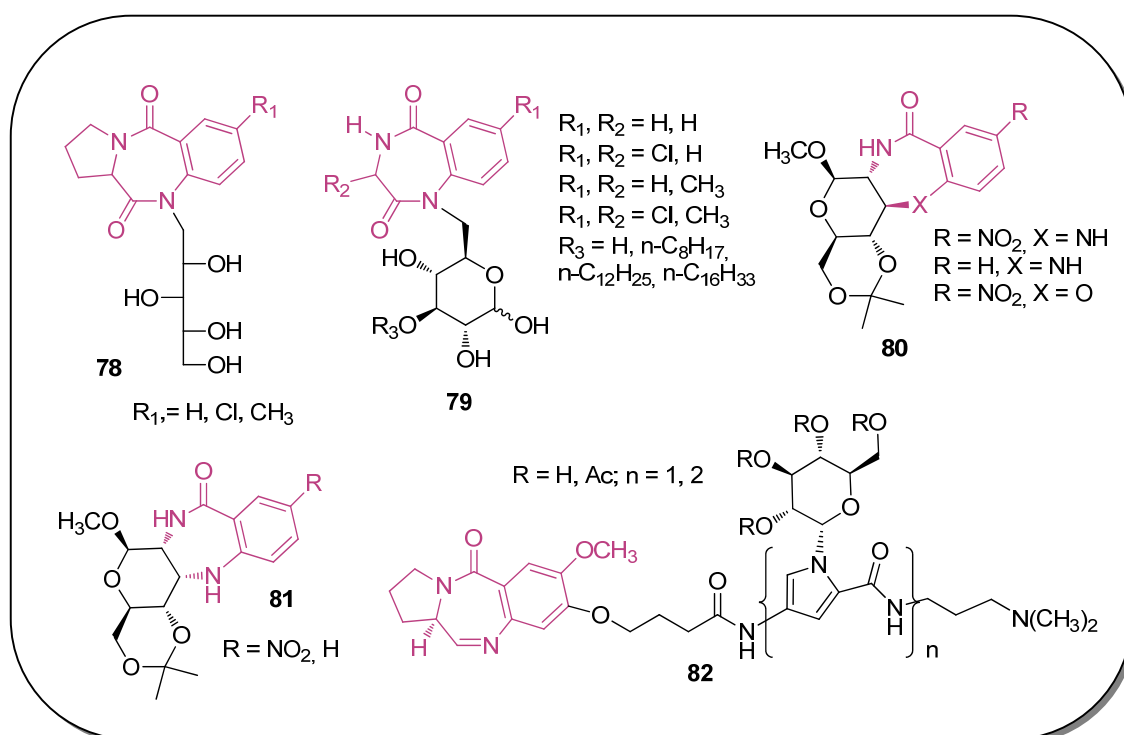


Figure 30. Examples of sugar-based benzodiazepines.

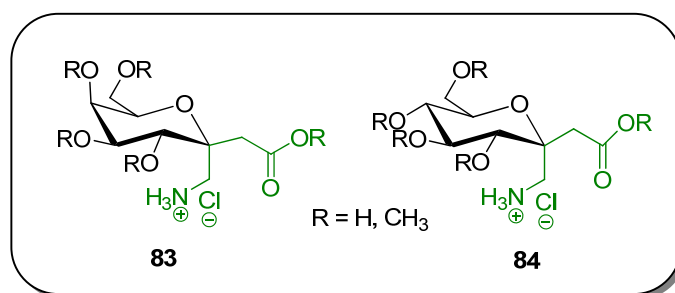


Figure 31. Examples of galactose- and glucose-based GABA-analogues.

Attempts to develop anticonvulsive agents from GABA related compounds, amino acid derivatives, and structurally modified drugs, have long been pursued. Many GABA-mimetic substances such as GABA receptor agonists, GABA reuptake inhibitors and GABA metabolism inhibitors have been introduced. However, these compounds have difficulties when entering the CNS in pharmacologically effective amounts after peripheral administration due to their low lipophilicity, that limits effective passage through the blood-brain barrier.^[50] Therefore, the additional hydroxyl derivatization of the polyol scaffold may be used to increase lipophilicity, and modulate the activity of pharmacophores binding to the receptor subtypes, making carbohydrates more drug-like. In addition the use of GABA-esters allows reduction of the GABA's intrinsic high polarity, which prevents it from crossing the BBB. The methyl esters would easily be hydrolyzed by lipases commonly found in the brain.

1.5 Radioligand Technique^[3, 134]

The affinity of a drug for a receptor is a measure of how strongly that drug binds to the receptor. Efficacy is a measure of the maximum biological effect that a drug can produce as a result of receptor binding. It is important to appreciate the distinction between affinity and efficacy. A compound with high affinity does not necessarily have a high efficacy. For example, an antagonist can bind with high affinity but has no efficacy. The potency of a drug refers to the amount of drug required to achieve a defined biological effect. (i.e. active in small doses) but have a low efficacy. Affinity can be measure using a process known as **radioligand labeling**. A radioligand is a radioactively labelled drug that can associate with a receptor, transporter, enzyme, or any site of interest. Measuring the rate and extent of binding provides information on the number of binding sites, and their affinity and accessibility for various drugs. Radiolabelled ligand binding studies remain one of the most widely used techniques in characterizing the biochemical and pharmacological properties of receptors.

The introduction of radioligand binding techniques in the 1970s proved to be a watershed in the study of the interaction between ligands and the receptors to which they must bind in order to exert their biological effects. For more than three decades, radiolabelled ligand binding studies have been one of the most widely used approaches for the characterization of not only receptor –ligand interactions, but also the properties of the ligands and their receptors. The fundamental principle of the technique is simple: an isotopically labelled ligand (a known antagonist or agonist labeled with radioactivity) is allowed to bind to a receptor preparation in order to provide a tag for the receptor of interest. Once an equilibrium has been reached and the ligand-receptor complex is formed, the unbound ligands are removed by washing, filtration, or centrifugation. The extent of radioactivity can then be measured by detecting the amount of radioactivity present in the cells or tissues, and the amount of radioactivity that was removed. The properties of the receptor–ligand complex are explored directly using the radioactivity of the bound ligand as a marker. The use of

an appropriate radioligand binding methodology can provide many insights into the recognition characteristics of the receptor.

Currently, only distinct binding sites present on GABA_A R can be directly investigated by appropriate radioligand binding studies: the GABA/muscimol-, the benzodiazepine-, and the TBPS/picrotoxinin-binding site. Using these studies, compounds competitively interacting with the radioligand and thus, directly binding to the respective sites could be identified. The interactions of all the other drugs with GABA_A R can only be investigated by electrophysiology or by studying the allosteric effects of these drugs at the [³H]muscimol-, [³H]benzodiazepine-, or [³⁵S]TBPS-binding site. These techniques, however, in most cases do not allow to clarify whether the allosteric effects of different ligands are mediated *via* the same or distinct binding sites. Therefore the total number of allosteric binding sites present on GABA_A R is not known. Structure-activity studies of most of the allosteric modulators of GABA_A R are thus not possible at present, preventing a structurally guided development of novel ligands for the respective binding site.

1.5.1 Ligand Binding: Simple Theory

Measuring the rate and extent of binding provides information on the number of binding sites, and their affinity and accessibility for various drugs. There are three kinds of experimental protocols:

- **Competitive binding experiments:** measure equilibrium binding of a single concentration of radioligand at various concentrations of an unlabeled competitor (inhibitor). Analyse of these data provides a more understanding of the affinity of the receptor for the competitor.
- **Kinetics experiments:** measure binding at various times to determine the rate constants for radioligand association and dissociation.

- **Saturation binding experiments:** measure equilibrium binding of various concentrations of the radioligand. Analyse the relationship between binding and ligand concentration to determine the number of sites, **B_{max} (R₀)**, and the ligand affinity, **K_d**. Because this kind of experiment used to be analyzed with **Scatchard plots** they are sometimes called "Scatchard experiments". These analyses depend on the assumption that is allowed the incubation to proceed to equilibrium. This can take anywhere from a few minutes to many hours, depending on the ligand, receptor, temperature, and other experimental conditions. The lowest concentration of radioligand will take the longest to equilibrate. For testing equilibration time, it is better to use a low concentration of radioligand (such as 10-20% of the K_d).

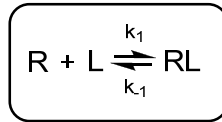
1.5.1.1 Equilibrium Binding: Saturation Analysis

The interaction between an endogenous or an exogenous^{xxiii} ligand and its receptor is responsible by a cellular functions rearrangement. Most ligands interact with the receptor through weak interactions, such as intermolecular bonds. The binding forces are strong enough to hold the ligand for a certain period of time to let it have an effect on the target, but weak enough to allow the drug to depart once it has done its purpose. They are several types of intermolecular bonding interactions, which differ in their bond strengths. The number and types of these interactions depend on the structure of the drug and the functional groups that are present. Thus, each ligand may use one or more of the following interactions, but not necessary all of them:

- Electrostatic or ionic bond
- Hydrogen bonds
- Van der Waals interactions
- Dipolo-dipole and ion-dipole interactions
- Repulsive interactions

^{xxiii} **Exogenous** substances are derived or developed from outside the body; originating externally.

In the simplest case, a reversible bimolecular association of a ligand with its receptor implies the formation of a complex receptor-ligand. This interaction may be described with the following equilibrium:



where **R** = receptor, **L** = ligand and **RL** = receptor–ligand complex, with k_1 and k_{-1} being the association and dissociation rate constants of the interaction, respectively.

At equilibrium, there is no net change in the concentration of RL. Thus the rate of the forward reaction is equal and opposite to the rate of the reverse reaction, i.e.,

$$k_1[\text{R}][\text{L}] = k_{-1}[\text{RL}] \quad \text{Eq. (1)}$$

This can be rearranged to:

$$\frac{[\text{R}][\text{L}]}{[\text{RL}]} = \frac{k_1}{k_{-1}} = K_d \quad \text{Eq. (2)}$$

where K_d is the equilibrium dissociation constant, i.e. the equilibrium constant for bound versus unbound radioligand (in radioligand labeling).

[L] and [RL] can be found by measuring the radioactivity of unbound ligand and bound ligand respectively. However, it is not possible to measure [R], and so we have to carry out some mathematical manipulations to remove [R] from the equations.

The Law of Mass Action dictates that the total concentration of receptor binding sites in the assay, designed R_0 or **Bmax**, is invariant and it is the sum of the concentrations of receptor that is bound to the ligand (RL), and the receptor that remains free (R), i.e.,

$$[R_0] = [R] + [RL] \quad \text{Eq. (3)}$$

So, the total number of receptors present must equal the number of receptors occupied by the ligand ([RL]) and those that are unoccupied ([R]).

Substitution for [R], from Eq. (3) into Eq. (2) yields:

$$\frac{([R_0]-[RL])[L]}{[RL]} = K_d \quad \text{Eq. (4)}$$

which, by simple rearrangement, gives the classical equation describing the formation of the receptor–ligand complex:

$$[RL] = \frac{[R_0][L]}{[L] + K_d} \quad \text{Eq. (5)}$$

There are two important conclusions that can be drawn from this equation. Firstly, when the ligand concentration, [L], is very much greater than the equilibrium dissociation constant, K_d ($[L] \gg K_d$), Eq. (5) simplifies to:

$$[RL] \approx [R_0] \quad \text{Eq. (6)}$$

illustrating that, at high ligand concentrations, the receptor sites will become saturated. Secondly when the ligand concentration, [L], equals the K_d , 50% of the available sites will be occupied by the ligand:

$$[RL] = \frac{[R_0]}{2} \quad \text{Eq. (7)}$$

Both of these conditions can readily be appreciated when [RL] is plotted against [L], as shown in Figure 32.

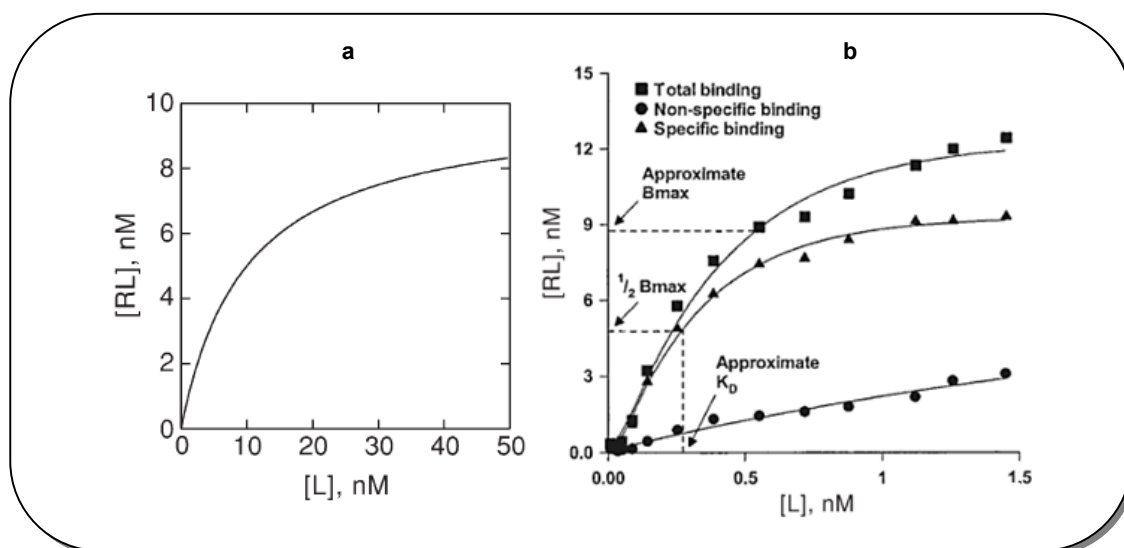


Figure 32. Graphic representations of the effects of ligand concentration on the formation of the receptor-ligand according to Eq. (5) in the text. (a) Stimulated data using values of 10 nM for both R_0 (B_{max}) and K_d (b) An example of a saturated isotherm with total, specific and nonspecific binding (nsb). The nsb was subtracted from the total to give the amount of specific binding. The specific binding saturates and an approximate value for the B_{max} for this experiment can be estimated from the ordinate. An approximate value for the K_d can be obtained from the abscissa, corresponding to 50% of the B_{max} .^[134, 135]

1.5.1.1.1 Nonspecific Binding

Experimentally, the ligand frequently binds not only to the receptor but also to other components present in the reaction mixture, such as the membrane in which the receptor of interest is embedded. Binding to the receptor of interest is called **specific binding**, while binding to the other sites is called **non-specific binding**. This nonspecific binding (nsb) exhibits quite distinct characteristics in saturation binding; it is generally of low affinity and non saturable (Fig. 32b). In practice, nonspecific binding can be determined experimentally by making use of the saturability of the specific binding to the receptor. This normally involves carrying out a parallel experiment in which a high concentration of a non-radiolabelled ligand for the receptor of interest (sufficient to saturate the specific receptor sites) is included. Under these conditions, the binding of the radioligand to the receptor population of interest will be reduced to zero while the nonspecific binding will remain unchanged

(since there are essentially an infinite number of nonspecific sites). Thus the concentration of the specifically bound complex, [RL] is the difference between the total and nonspecific binding curves, as shown in Figure 32b.

The appropriate definition of nonspecific binding is essential prior to characterization of the kinetic and equilibrium properties of the binding interaction. As a rule, nonspecific binding can be defined using a concentration of the unlabelled ligand that is 100 times its K_d value for the sites of interest. Failure to appropriately define nonspecific binding will invalidate the determination of the binding parameters.

1.5.1.1.2 Analysis of Saturation Binding Isotherms: Scatchard Plot

A historically important graphical technique to describe binding data is the Scatchard plot (Fig. 33).^[136] This is a graph based on a number of experiments where different concentrations of a known radioligand are used. [RL] and [L] are measured in each case and a Scatchard plot is drawn which compares the ratio [RL]/[L] versus [RL]. This gives a straight line, in which the ratio of bound and free radioligand is plotted on the ordinate against the amount of bound radioligand on the abscissa (line A; Fig. 32). A linear Scatchard plot indicates that the radioligand binds with a single affinity. The slope is a measure of the radioligand's affinity for the receptor and allows K_d to be determined, and the intercept of the line with the abscissa represents the total number of receptors available, i.e. R_0 (B_{max}). This latter parameter is generally standardized against a suitable reference that allows a direct comparison of receptor density in different tissues and in different studies.

The Scatchard plot is simply a linearization of the function:

$$K_d = \frac{[R][L]}{[RL]} = \frac{([R_0] - [RL])[L]}{[RL]} \quad \text{Eq. (8)}$$

for which rearrangement gives:

$$\frac{[RL]}{[L]} = \frac{[R_0]}{K_d} - \frac{[RL]}{K_d} \quad \text{Eq. (9)}$$

Since [RL] and [L] represent the bound and free ligand, respectively, this can be rewritten as:

$$\frac{[bound]}{[free]} = \frac{[R_0]}{K_d} - \frac{[bound]}{K_d} \quad \text{Eq. (10)}$$

Thus, for this simple binding reaction, a plot of [bound]/[free] versus [bound] will be a straight line with a slope of (-1/K_d) and will have an intercept on the x-axis of [R₀] or B_{max}.

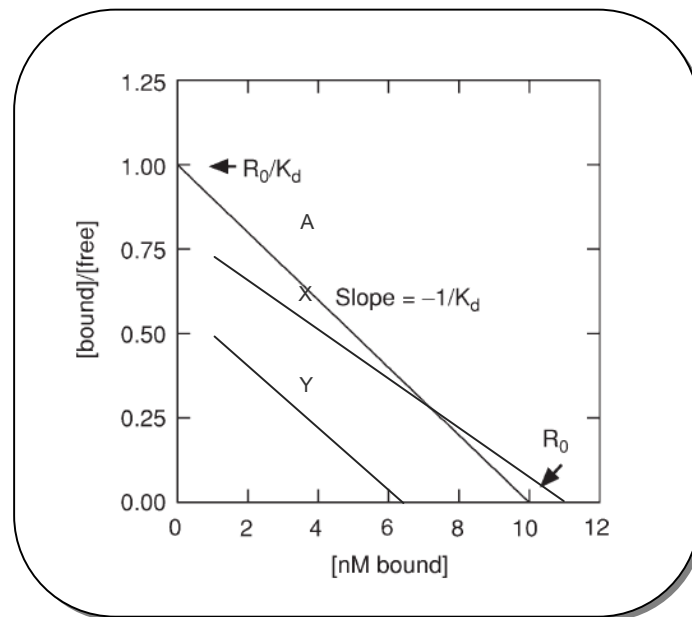


Figure 33. Graphic representation of Scatchard plot, y-axis:[bound]/[free]=[RL]/[L] and x-axis:[bound ligand]=[RL]. (A) radioligand only; (X), radioligand + competitive ligand; (Y), radioligand + non-competitive ligand. In scatchard plot (A) is illustrated how the K_d and R₀ (or B_{max}) can be obtained from a such a linearization procedure.^[3, 134]

The determination of the affinity of a novel drug that is not radioactively labelled is possible by repeating the radioligand experiments in the presence of the unlabelled test compound. The test compound competes with the radioligand for the receptor's binding sites and is called a **displacer**. The stronger the affinity of the test compound, the more effectively it will compete for binding sites and the less radioactivity will be measured for [LR]. This will result in a different line in the Scatchard plot.

If the test compound competes directly with the radiolabelled ligand for the same binding site on the receptor, then the slope is decreased but the intercept on the x-axis remains the same (line X in the graph, Figure 33). Meaning that, if the radioligand concentration is much greater than the test compound it will bind to all the receptors available. Although, agents that bind to the receptor at an allosteric binding site do not compete with the radioligand for the same binding site and so cannot be displaced by high levels of radioligand. However, by binding to an allosteric site they make the normal binding site unrecognizable to the radioligand and so there are less receptors available. This result in a line with an identical slope to line A, but crossing the x-axis at a different point, thus indicating a lower total number of available receptors (line Y, Fig. 33).

1.5.1.2 Equilibrium Binding: Competition Studies

The affinity of non-radiolabelled ligands may be estimated by their ability to compete with a radioligand for binding to the receptor of interest. Here the equations outlined above hold for both the radioactive and nonradioactive ligands. Receptor occupation can be determined only for the proportion which is tagged with the radioactive ligand. In these "displacement studies", the unlabelled ligand displaces the radioactive ligand from its binding sites and the concentration dependence of this effect can lead to an indirect measurement of its binding affinity.

The data from these displacement experiments can be used to plot a different graph which compares the percentage of the radioligand that is bound to a receptor versus the concentration of the test compound. This results in a sigmoidal curve termed the displacement or inhibition curve, which can be used to identify the IC_{50} value for the test compound (i.e. the concentration of compound that prevents 50% of radioactive ligand being bound) (Fig. 34).

Experimentally, it is common to use a concentration of the radiolabelled compound which is close to its K_d value. In these experiments, the IC_{50} value for the competing ligand is defined as the concentration at which it reduces the specific binding of the radioligand to 50% of that obtained in its absence (Fig. 33). Under equilibrium conditions, with a single homogeneous population of binding sites, the equilibrium dissociation constant for the competitor (test compound) (K_i) is defined by the Cheng-Prusoff equation:^[137]

$$[K_i] = \frac{IC_{50}}{1 + [L] / K_d} \quad \text{Eq. (11)}$$

where $[L]$ and K_d refer to the concentration of the radiolabelled ligand and its equilibrium dissociation constant for binding used in the experiment. K_i can be also referred to the inhibitory or affinity constant. This equation is valid only if the bound ligand is $< 10\%$ of the free ligand concentration and when $K_d \gg$ the concentration of the receptor sites. The IC_{50} is the intercept on the x-axis. This value can then be used with Eq. 14 to calculate the K_i of the displacer and the K_d for the radiolabelled ligand.

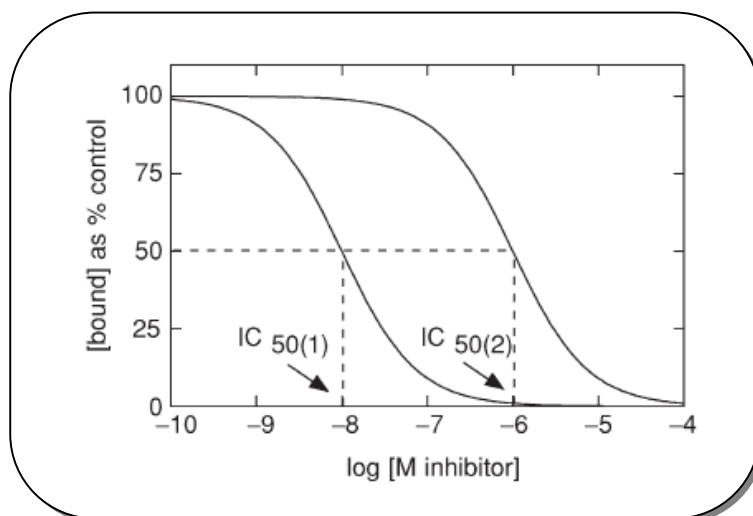


Figure 34. Graphic representation of competition curves for displacement of a radiolabelled ligand by two competitive inhibitors (displacers) having IC_{50} values of 10 nM and 1 μ M.^[134]

1.5.1.3 Limits on the Interpretation of Equilibrium Radioligand Binding Studies

Radioligand binding techniques have proved to be enormously valuable not only for the characterization of receptors that are responsible for the mediation of physiological and pharmacological responses, but also for the characterization of new chemical entities during development. While radioligand binding methods have proved to be of huge importance over many years, they do have several important limitations.

The interactions between the receptor and the ligand have the following standards:

- the receptor–ligand interaction is reversible,
- the association process is bimolecular,
- the dissociation process is monomolecular,
- receptors in the population are equivalent and independent of each other,
- measurements are made after the interaction has reached equilibrium,
- and the ligand can exist only free or bound to the receptor.

Using these assumptions, radiolabelled ligand binding techniques can provide specific information on binding site densities, ligand binding affinities, ligand–protein recognition and kinetic parameters. These approaches have proved priceless in studies of ligand–receptor interactions and, prior to molecular cloning, provided the first evidence for the existence of receptor subtypes. In more complex analyses, ligand binding studies can be useful for detecting cooperativity^{xxiv} between binding sites, for studying inhibitory mechanisms (e.g., competitive versus noncompetitive inhibitors) and for elucidating the effects of allosteric modulators that may be of both physiological or pharmacological importance.

Equilibrium binding assays do, however, suffer from a number of limitations. Many important ligand–receptor interactions, for example, may occur under pre-equilibrium conditions. In the case of ligand-gated ion channels, such as GABA_A R, the binding of an agonist to the receptor rapidly induces a conformational change to open the ion channel. If the agonist remains bound, the receptor undergoes further slow conformational transitions that lead to a refractory, desensitized state in which the ion channel is closed. Under equilibrium conditions only the desensitized receptor–agonist complex is accessible to measurement. Details of the kinetic process that leads to the final equilibrium state is therefore required, thus, is useful to have information on the agonist binding events that cause the channel to open. In only a few cases can the functionality of the ligands be implied from radioligand binding experiments. However, the consequences of binding site occupancy on the function of the protein can be ascertained in only a very few cases. Therefore, it is impossible to distinguish an agonist from an antagonist.

^{xxiv} **Cooperativity** is a biological phenomenon, displayed by receptors that have multiple binding sites, in which the shape of one subunit of the receptor consisting of several subunits is altered by the ligand.

1.5.2 Radiolabelled Ligand Binding Studies: Separation of Free From Bound Ligand

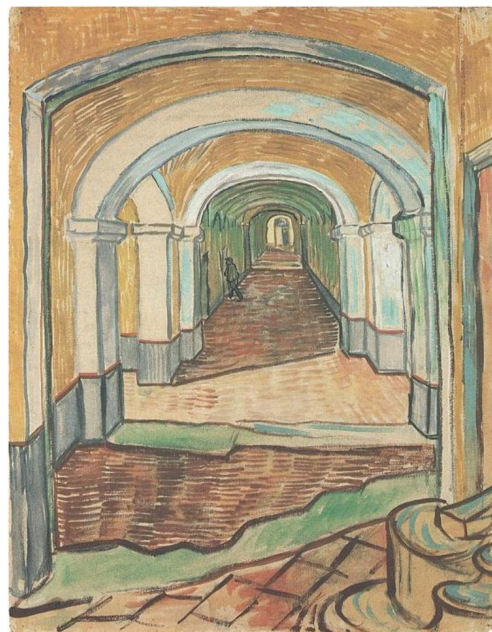
In radioligand binding studies, it is essential to experimentally distinguish between the ligand bound to the receptor and that which remains free in solution. There are three methods that are commonly used to accomplish this physical separation: equilibrium dialysis, centrifugation and filtration assays. It will be describe the last method in more detail since it was used in the present work. **Filtration assay** is one of the most commonly used methods for the separation of bound from free ligand. This method involves passing the reaction mixture through a filter made of, for example, glass fiber or cellulose. Particulate fractions, e.g., membranes and membrane-bound radioligand are selectively retained on the filter while the rest of the incubation mixture, containing free ligand, is allowed to pass through. Filtration is usually performed under reduced pressure in order to increase the speed of filtration, thus reducing nonspecific binding to the filter. To reduce further any nonspecific retention of free ligand by the filter, it is usually necessary to include one or more filter washing steps. A significant problem in such assays is that dissociation of bound ligand may occur during this washing. If, for example, washing of the filters takes 10 seconds, then a receptor–ligand complex whose dissociation half-time ($t_{1/2}$) is 10 seconds will have dissociated by 50% by the end of the wash. Manual filtration assays are thus limited to high affinity ligands with slow rates of dissociation. However, it is also possible to measure lower affinity binding using an automated modification of the filtration technique, which allows the filter washing times to be dramatically reduced, a “Biologic Rapid Filtration System”.^[138] This instrument, which relies on a microcomputer-controlled syringe to deliver a specific volume of wash buffer within a specified time, is capable of performing the washing step in tens of milliseconds. One disadvantage is that, since only one filter can be processed at a time, the experimental procedures can become very lengthy. However, the system has many advantages and being more useful not only for studying low affinity binding sites, but also for studies of rapid dissociation kinetics and ion efflux experiments.

*Um caminho, tantas portas,
além de cada porta tantos outros caminhos.
A certeza de que a busca foi incessante
testemunhou quem lá esteve
outros ouviram contar.*

*Ficaram guardadas as memórias
portas fechadas e caminhos sem fim.*

A certeza é só uma.

*Não há grito de dor
que no futuro
não tenha no fim
por eco uma alegria.*



*Corridor in Saint-Remy, 1889
Vincent van Gogh*

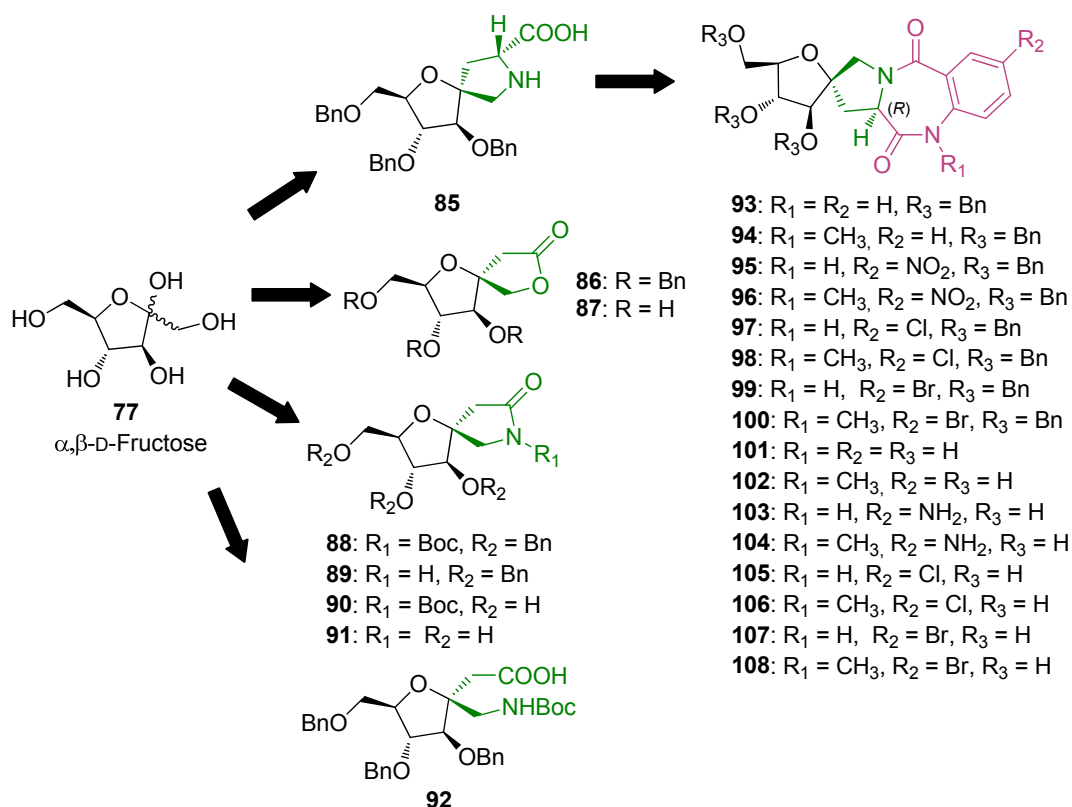
RESULTS AND DISCUSSION

Our first aim was to synthesize D-proline and L-proline analogues spiro-linked to a five-membered sugar (**85** in Scheme 1 and **112** in Scheme 2, respectively), in order to develop (*P*) and (*M*) conformers of 1,4-benzodiazepine-2,5-dione derivatives. Construction of the fructose-based proline moiety, prompt to further derivatization, is desirable to increase the conformational rigidity of the proline and consequently of the benzodiazepine template.

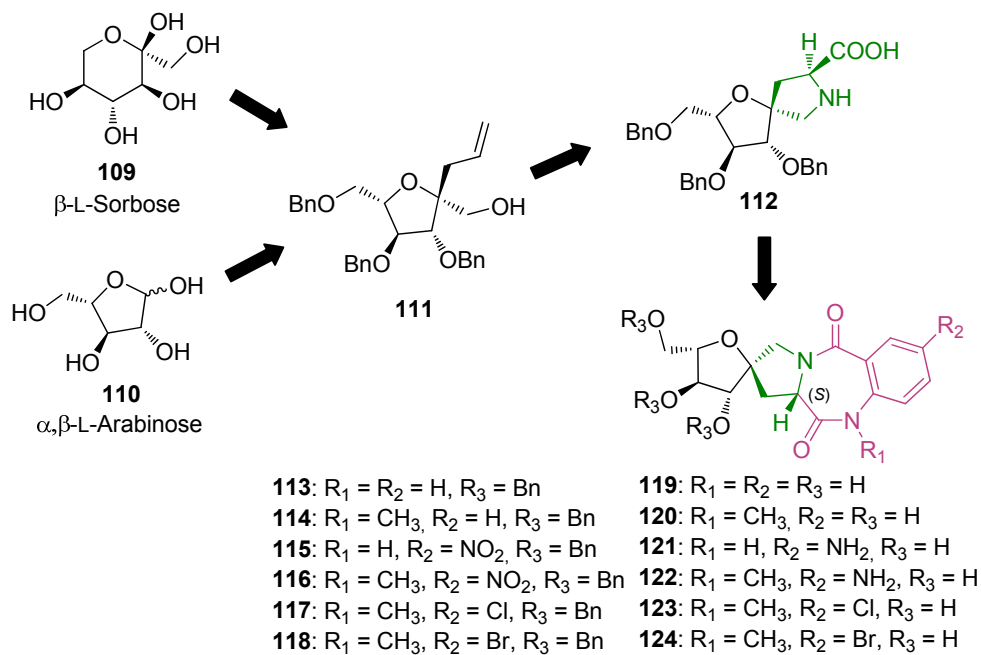
D-Fructose (**77**, Scheme 1) was used as starting material for the synthesis of the D-proline analogue (**85**, Scheme 1). However, the price of commercially available L-fructose does not encourage its use in the synthesis of the L-proline analogue. Preparation of 3-*C*-(3,4,6-tri-*O*-benzyl- α -L-fructofuranos-2-yl)propene (**111**), the key intermediate in the synthesis of the L-proline analogue, was performed through two different pathways. One of the pathways used L-sorbose (**109**, Scheme 1) as starting material^[139] and the other one L-arabinose (**110**, Scheme 2). The two proline analogues (compounds **85** in Scheme 1 and **112** in Scheme 2) were then used to create a sugar-based pyrrolobenzodiazepine library (compounds **93–108** in Scheme 1, and **113–124** in Scheme 2).

Moreover, taking advantage of some intermediates of the D-proline analogue synthesis, a library of GABA derivatives was developed, namely D-fructose-based β -disubstituted γ -butyrolactones and γ -butyrolactams (compounds **86–87** and **88–91** in Scheme 1, respectively) and a GABA analogue (compound **92**).

Conformational analysis of the sugar-based pyrrolobenzodiazepines was performed by molecular modelling calculations and experimental Dynamic NMR studies (DNMR). Biological evaluation of both libraries of compounds was performed with GABA_A R binding assays, using radioligand techniques.



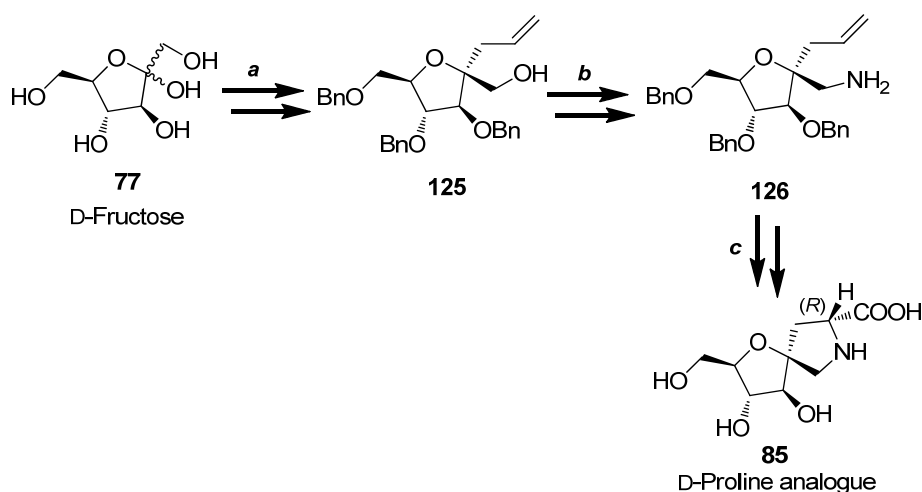
Scheme 1. Synthetic pathway for the production of pyrrolobenzodiazepines and GABA analogues starting from D-fructose.



Scheme 2. Synthetic pathway for pyrrolobenzodiazepines starting from L-sugars.

2.1 Synthesis of the Spiro D- and L-Proline Analogues

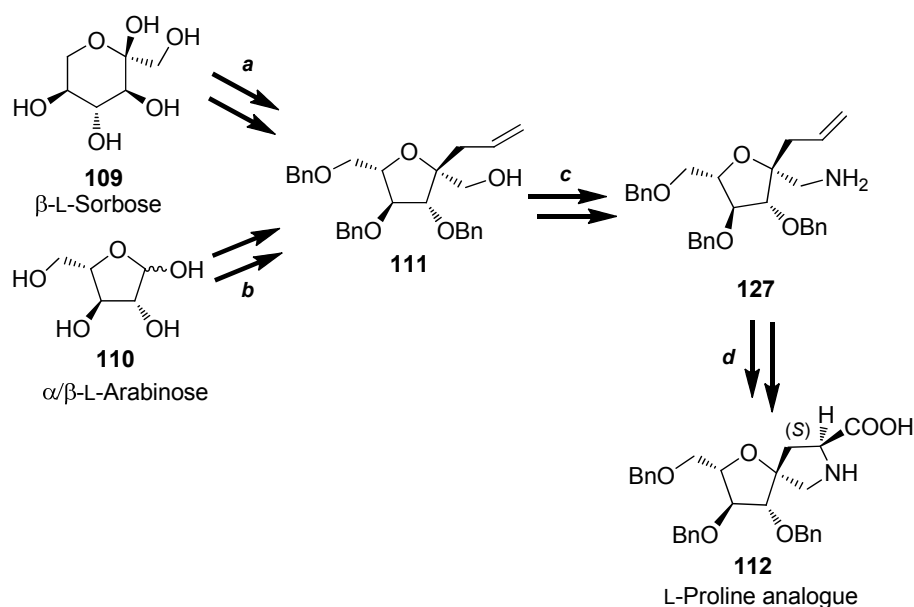
The construction of the (*R*)-proline ring in the D-proline analogue **85** was achieved by exploiting the anomeric position and the hydroxyl group at C-1 of D-fructose (Scheme 3). The synthetic plan involved firstly a three carbon chain elongation at the anomeric position by *C*-glycosylation (compound **125**). A pyrrolidine ring was then introduced *via* a 5-*exo*-iodocyclisation reaction between an amino function and an allylic group suitably positioned at the anomeric center of the sugar. Finally, the exocyclic iodomethylene group was converted into the desired carboxylic group in the final steps of the synthesis (compound **85**).



Scheme 3. Synthetic plan for the preparation of the D-proline analogue (see pathway *a* in Scheme 5 and pathways *b,c* in Scheme 7).

Several synthesis of L-proline and derivatives have been elaborated from other carbohydrates of the L-series; by chain elongation of the corresponding arabinonic acid, arabinose or glyceraldehydes, by inversion of configuration of OH-4 of sorbose, by enzymatic methods such as isomerization of mannose or by bacterial oxidation of mannitol.^[140-143]

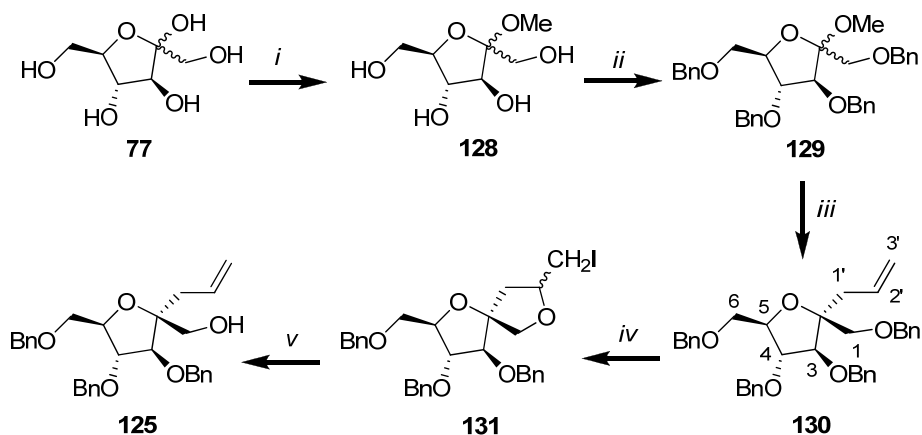
The key intermediate for the synthesis of the L-proline analogue **112**, 3-C-(3,4,6-Tri-O-benzyl- α -L-fructofuranos-2-yl)propene (**111**), was first synthesized from β -L-sorbose **109** (pathway *a*, Scheme 4).^[139] Inversion of configuration at C-3 and C-4 afforded the stereochemistry desired for L-fructose and a subsequent three carbon chain elongation at the anomeric position afforded the desired key intermediate **111**. Another synthetic route to **111** was also developed starting from α,β -L-arabinose (pathway *b*, Scheme 4). α,β -L-Arabinose **110** already has the furanose ring with the appropriate configuration, but lacks the extra carbon at the anomeric position. Hence, a one carbon chain elongation at the anomeric position followed by the same three carbon chain elongation as in pathway *a*, afforded compound **111**. Compound **111** was then used to obtain L-proline analogue **112** by the same synthetic procedure as the D-proline analogue **85** (pathways *b,c* in Scheme 3 \cong pathways *c,d* in Scheme 4).



Scheme 4. Synthetic plan for the L-proline analogues (see pathway *a* in Scheme 10, pathway *b* in Scheme 12 and pathways *c,d* in Scheme 17).

2.1.1 Synthesis of the Spiro D-Proline Analogue

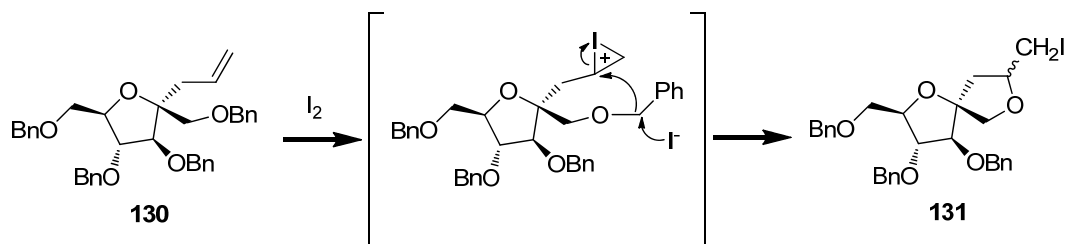
The first steps of this synthesis lead to the selective protection of position 3, 4 and 6, leaving the hydroxyl group at C-1 free (compound **125**, Scheme 5). The C-fructofuranosyl derivative **125** was generated starting from α,β -D-fructose, in which the anomeric position was selective protected as a methyl ether with methanol and sulphuric acid. Subsequent benzylation of the free hydroxyl groups was accomplished by treatment with benzyl bromide (BnBr) and sodium hydride (NaH) in dry dimethylformamide (DMF) leading to methyl 1,3,4,6-tetra-O-benzylfructofuranoside (**129**).^[144, 145]



Scheme 5. Reagents and conditions: *i*. dry CH₃OH, H₂SO₄, rt, 2h, 89% yield as a mixture of anomers; *ii*. BnBr, NaH, dry DMF, 0 °C then rt, 3h, quantitative yield; *iii*. AllSi(CH₃)₃, BF₃·Et₂O, dry CH₃CN, rt, 12h, 95%; *iv*. I₂, dry THF, rt, 1h, 98% yield as mixture of diastereoisomers (3:2 R:S ratio); *v*. Zn, AcOH, EtOH/Et₂O 1:1, rt, 24h, 80%.

Through Lewis acid [boron trifluoride etherate (BF₃·Et₂O)] mediated C-C bond formation in presence of allyltrimethylsilane [AllSi(CH₃)₃] the corresponding α -C-glycosyl compound **130** was obtained as the major compound in 95% yield (8:2 α : β ratio, as determined from the ratio in integrals of the ¹H-NMR signals of the crude mixture). The stereoselectivity of this reaction depends on the orientation of the benzyl group at C-3 which forces the nucleophilic attack mainly to the α -side of the cyclic oxonium intermediate which results mainly in the formation of the α -anomer,

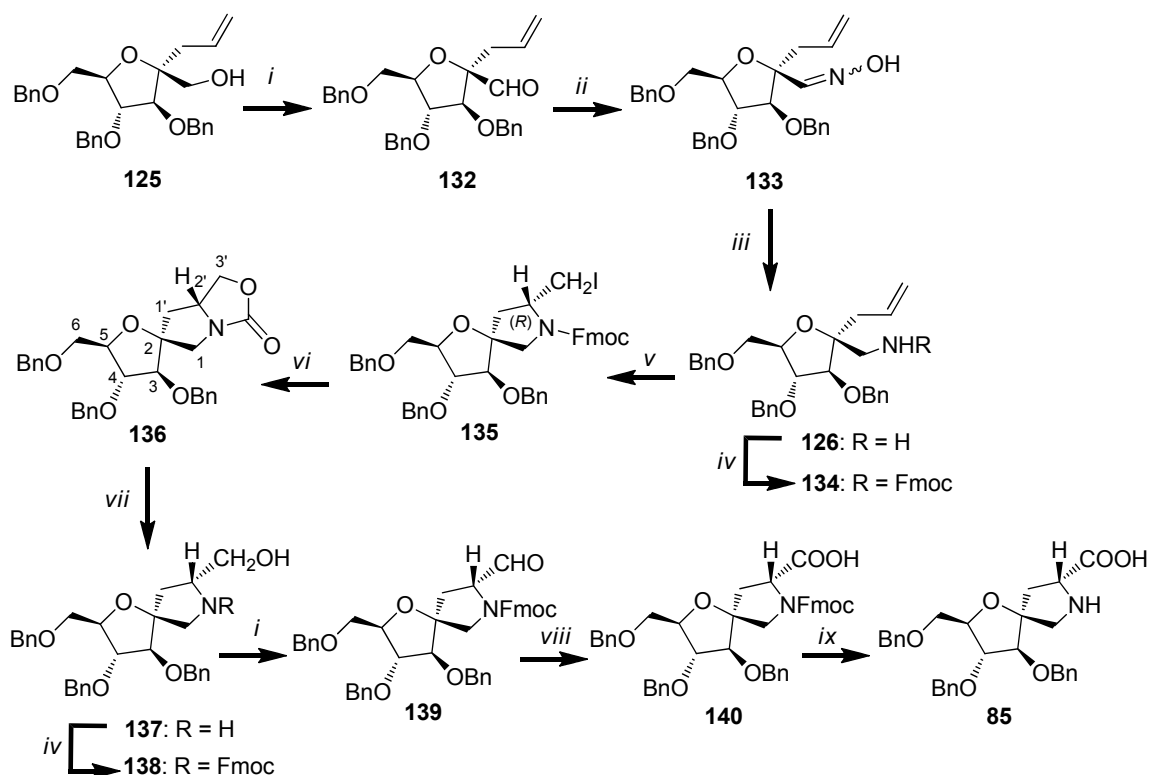
compound **130** (mechanism details described for a similar reaction in Scheme 11). The anomeric configuration of **130** was deduced by the chemical shift of C-1' (38.65 ppm) and compared to that of its β -epimer at C-1' (37.26 ppm), as reported in literature.^[144] As expected, for 3-*C*-(1,3,4,6-tetra-*O*-benzyl- α -D-fructofuranos-2-yl)propene (**130**), the ^{13}C chemical shift of the carbon atom attached to the anomeric position (C-1') is at higher field when it has a *cis* relationship with substituent on C-3 rather than when there is a *trans* relationship.^[144, 146] In order to selectively deprotect the C-1 benzyloxy group of compound **130**, an iodocyclization with iodine in tetrahydrofuran (THF) was performed affording the two spiro diastereoisomers in 98% yield (3:2 *R/S* ratio). This 5-*exo* cyclization can occur due to the correct spatial relationship between the double bond and the oxygen at C-1 in the benzylated fructosyl derivative **130**. The mechanism of the iodocyclization (Scheme 6) is initiated by the nucleophilic replacement of the benzyloxy-oxygen by iodide. The oxyanion formed then attacks the cyclic iodo-ether forming the five-membered ring. Cyclic iodoether **131** was treated with zinc in acetic acid leading to a reductive elimination, and regeneration of the original double bond, resulting in the deprotection at C-1 (compound **125**).



Scheme 6. Proposed mechanism of the 5-*exo* cyclization/debenzylation.^[147]

The second part of our synthetic plan consisted of the manipulation of the free hydroxyl group of 3-*C*-(3,4,6-tri-*O*-benzyl- α -D-fructofuranos-2-yl)propene (**125**) in order to obtain the bicyclic D-proline analogue **85** (Scheme 7). Thus, oxidation of primary alcohol **125** with iodoxybenzoic acid (IBX) in dry dimethyl sulfoxide (DMSO), followed by treatment with a 2.1 M buffer soln. of hydroxylamine hydrochloride ($\text{NH}_2\text{OH}\cdot\text{HCl}$ pH=4.5) gave the oxime **133** (92% yield as a mixture of *E/Z* isomers).

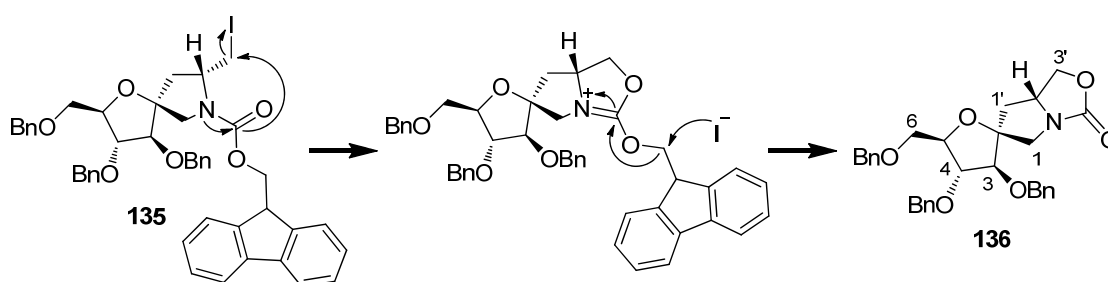
Further reduction with lithium aluminium hydride (LiAlH_4) produced a primary amine (compound **126**). In order to perform the iodocyclization reaction, the amino group required protection: in fact, reaction between amines and molecular iodine often results in *N*-iodination, the formation of molecular complexes and, in some cases, unusual oxidation processes.^[148-152] It seemed that a carbamate would be a good choice as amine protecting group, since 5-*exo* cyclisation of the carbamate derived from pent-4-enamines generally works well to give *N*-alkoxycarbonylpyrrolidines.^[153-156] Therefore, amine **126** was converted to the corresponding fluorenylmethoxycarbonyl derivative **134** with 9-fluorenylmethyl chloroformate (Fmoc-Cl) and *N,N*-diisopropylethylamine (DIPEA) in dry acetonitrile.



Scheme 7. Reagents and conditions: *i*. IBX, dry DMSO, rt, 2h; *ii*. 2.1 M Buffer soln. $\text{NH}_2\text{OH}\cdot\text{HCl}$ pH=4.5, $\text{CH}_3\text{OH}/\text{THF}$ 1:1, rt, 4h, 92% yield as mixture of *E/Z* isomers over two steps; *iii*. LiAlH_4 , dry THF, rt, 12h, quantitative yield; *iv*. Fmoc-Cl, DIPEA, dry CH_3CN , rt, 2h, 90% (**134**) and 96% (**138**); *v*. I_2 , dry DME, rt, 2h, 83%; *vi*. aq. soln. 1 M NaOH, CH_3CN , rt, 12h, quantitative yield; *vii*. aq. soln. 3M NaOH, EtOH, reflux, 4h, quantitative yield; *viii*. aq. soln. 1.25 M $\text{NaH}_2\text{PO}_4\cdot 2\text{H}_2\text{O}$, NaClO_2 , CH_3CN , rt, 7h, 76% yield over two steps; *ix*. Et_2NH , dry CH_3CN , rt, 2h, 74%.

The subsequent treatment with iodine in 1,2-dimethoxyethane (DME) afforded two diastereomeric spiro compounds; surprisingly, the diastereoselectivity of this iodocyclization reaction was extremely high in favour of the (*R*)-isomer, compound **135** (*d.e.*^{xxv} > 98 %). The stereochemistry of the new stereocenter in **135** was later determined by ¹H NMR on tricyclic compound **136**. Again, the spatial relationship between the double bond (allylic substituent) and the amino group at C-1 in compound **134**, allowed the formation of the bicyclic Fmoc-protected pyrrolidine **135**, through a stereoselective 5-*exo* cyclization.

The plan was then to substitute the iodide with a hydroxyl group, creating a primary alcohol, which could be oxidized to the corresponding carboxylic acid. Treatment of **135** with a 1M aq. soln. of NaOH in acetonitrile did, however, not produce the primary alcohol but instead, the tricyclic oxazolidinone **136** was the single reaction product isolated in quantitative yield. Similar results were obtained when amine **126** was protected with benzyloxycarbonyl or *tert*-butoxycarbonyl groups. The tricyclic compound **136** probably resulted from the attack of the carbamate carbonyl oxygen to the methylene group with iodide displacement to give a charged intermediate which is subsequently attacked by the iodide, as already reported for a similar reaction (Scheme 8). [157, 158]



Scheme 8. Proposed mechanism for the formation of the tricyclic compound **136**.

^{xxv} *d.e.* is the diastereoisomeric or diastereoisomer excess. $de = ([n^{\circ}\text{moles R} - n^{\circ}\text{moles S}] / [n^{\circ}\text{moles R} + \text{S}]) \times 100$.

A 2D NOESY experiment for the tricyclic oxazolidinone **136** (Fig. 35) showed a cross peak between H-2' and H-1'a, and between the H-3 and the H-1'b protons allowing to assign the stereochemistry of the corresponding compound. Therefore, the stereochemistry of the new stereocenter of compound **135** formed in the iodocyclization reaction was able to be determined through NOESY experiments on tricyclic compound **136**.

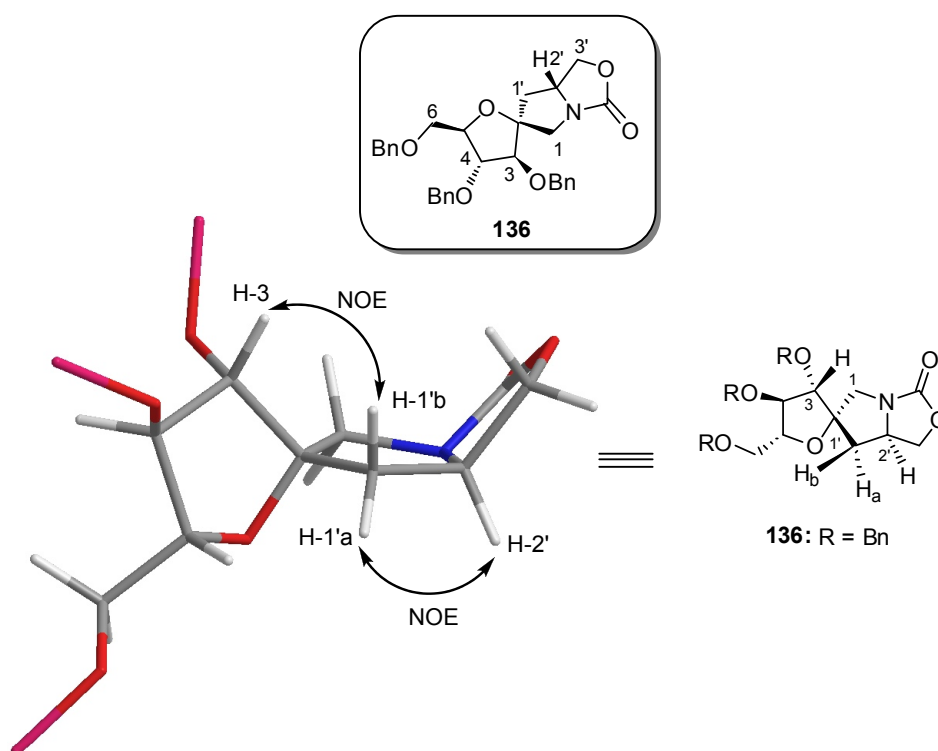


Figure 35. Correlations observed by 2D-NOESY for compound **136**.

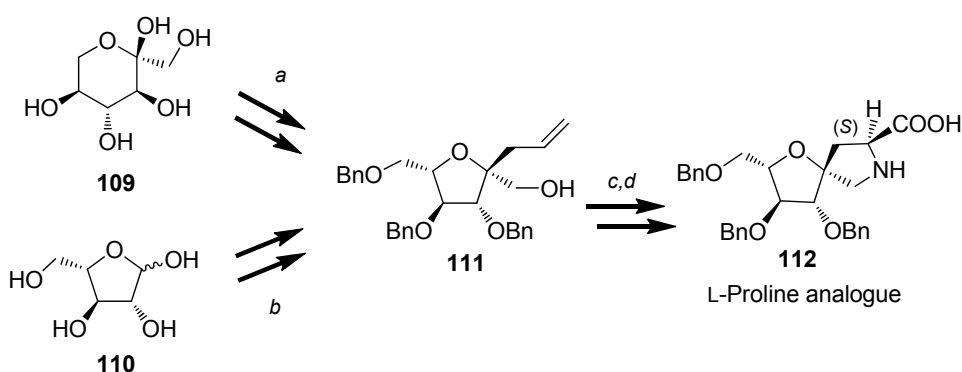
Ethylenediamine^[159] and lithium aluminium hydride^[160] were used for the hydrolysis of the oxazolidinone ring of compound **136**, however deficient results were obtained. Instead, refluxing compound **136** over night in an aq. soln. of 3 M NaOH with ethanol finally afforded the desired amino alcohol **137** in quantitative yield. Any attempt to convert compound **135** into **138** in a one-pot reaction failed. Protection of the amino function again with Fmoc-Cl, afforded Fmoc derivative **138** in 96% yield. Subsequent two oxidations, first with IBX, then with monosodium phosphate dihydrate (aq. soln. of 1.25 M NaH₂PO₄·2H₂O), gave rise to the D-proline analogue **140** (76% yield over

two steps). ^1H NMR experiments on Fmoc-protected amino acid **140** showed a very complex spectrum, possibly due to the presence of rotamers resulting from rotation over the amide bond of the carbamate group (N-C=O) (see Fmoc group on compound **135** in Scheme 8).^[161] Even at 70 °C, the ^1H NMR spectra showed only partial coalescence of the signals. Therefore, only ^{13}C NMR data is reported in the experimental section.

Final deprotection of the amino functionality with diethylamine (Et_2NH) in dry CH_3CN , afforded the free amino acid **85**. Further confirmation of the presence of rotamers in compound **140** was obtained by NMR observation of the free amino acid **85**. The ^1H NMR spectrum of compound **85**, recorded at 20 °C, showed the presence of only one product, contrary to compound **140**. In addition, the presence of different coupling constants between H-2' and H-1'a/H-1'b (13.9 and 7.1 Hz respectively) suggests a conformational rigidity of the proline ring **85**.

2.1.2 Synthesis of the Spiro L-Proline Analogue

Why two pathways? Considering the key intermediate **111** as the 'starting material' for the eleven steps synthesis of L-proline analogue **112** (pathways *c,d* in Scheme 9), a simple and highest overall yield approach for compound **111** was investigated. The use of β -L-sorbose **109** as a starting material (pathway *a* in Scheme 9) was based on a recent report given by Zhao *et al.*,^[139] which described the synthesis of L-fructose. Exploiting this procedure, with slight modifications, was developed the synthesis of compound **111** which involved various protection and deprotection, in addition to oxirane ring formation and opening to obtain the appropriate sugar stereochemistry (synthetic details in Scheme 10). However, not completely satisfied with this pathway, a novel approach was developed; pathway *b* in Scheme 9. This pathway takes advantage of the stereochemistry of α,β -L-arabinose **110** as starting material for the synthesis of intermediate **111** (synthetic details in Scheme 12).

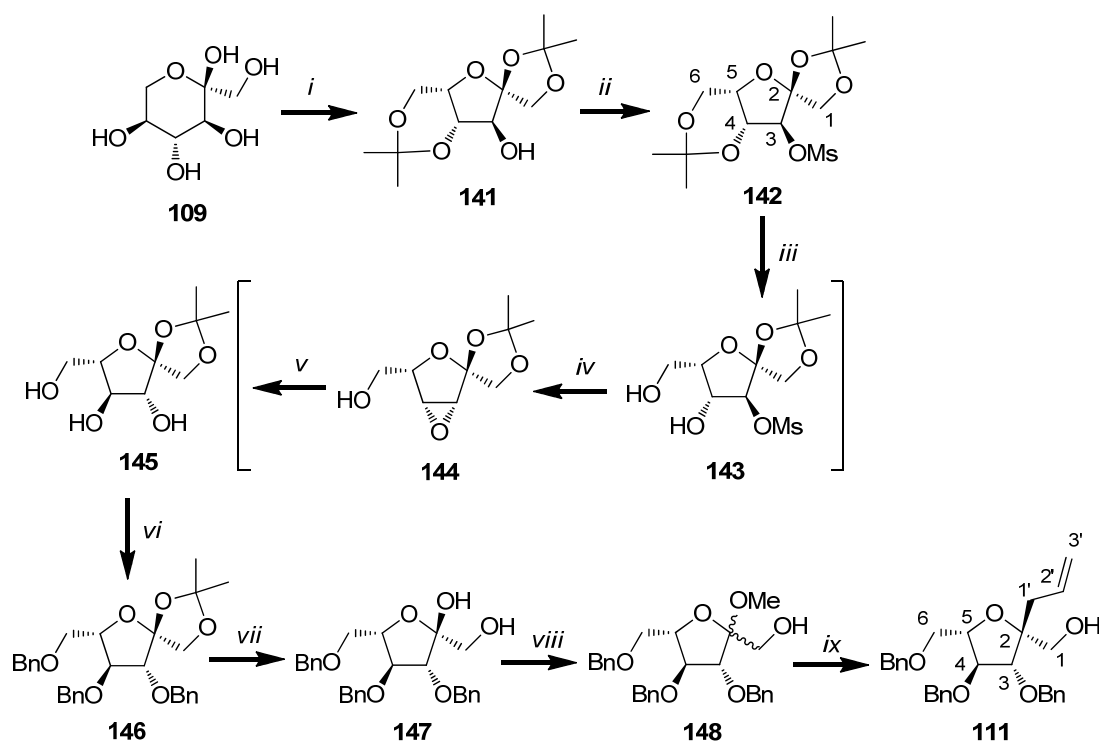


Scheme 9. Synthetic pathways for the synthesis of the L-proline analogue.

2.1.2.1 Synthesis of Compound 111 – Pathway *a*

Pathway *a* (Scheme 10) is an eight step synthesis starting from β -L-sorbose with an 8.5% overall yield. The strategy is comprised of diisopropylidene protection, mesylation, selective deprotection, oxirane formation and opening affording the inversion of configuration at C-3 and C-4 providing the stereochemistry of L-fructose.

In this synthesis, β -L-sorbose was selectively protected with 2,2-dimethoxypropane (DMP) in the presence of stannous chloride (SnCl_2) in 1,2-dimethoxyethane (DME). This reaction is very sensitive since compound **141** is likely to be a kinetic product and may easily isomerize with prolonged reaction time. Thus, the reaction is usually stopped once the solution becomes clear, i.e. before the L-sorbose is completely consumed. By reducing the reaction time, the isomerization of compound **141** can be minimized and the remaining L-sorbose can be readily recovered by filtration and reused. Hence, ketal **141** was used directly for mesylation to give compound **142** after recrystallization in 40% yield over two steps (Scheme 10).

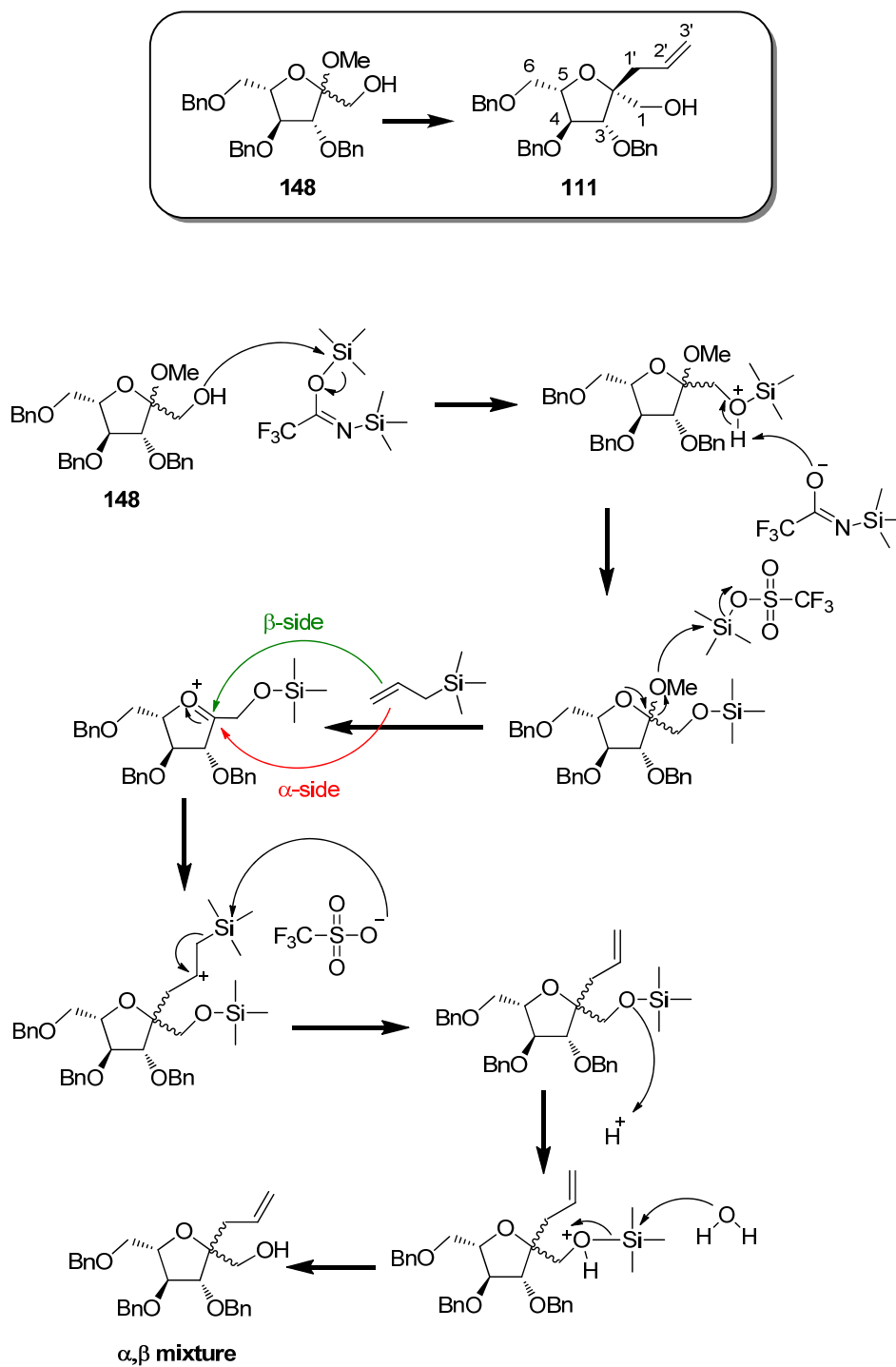


Scheme 10. Pathway *a*. Reagents and conditions: *i*. DMP, DME, SnCl₂, reflux, 2.5h; *ii*. MsCl, pyridine, 0 °C, 3h, 40% yield over two steps; *iii*. 4.5% H₂SO₄, rt, 3h; *iv*. NaOH, rt, 10 min; *v*. reflux, 12h, 55% yield over two steps; *vi*. BnBr, NaH 60%, rt, 3h, 77%; *vii*. acetic acid 60% (w), reflux, 20 min, 72%; *viii*. AcCl, CH₃OH, rt, 5h, 92% yield as a mixture of anomers (3:1 α:β ratio); *ix*. 1. BTSFA, CH₃CN, reflux 50°C, 6h; 2. AllSi(CH₃)₃, TMSOTf, 0°C then rt, 2h, 76% yield of α-anomer (8:2 α:β ratio).

The selective deprotection of the 4,6-*O*-isopropylidene group of **142** can be easily achieved using 4.5% H₂SO₄ at rt for 3h to give diol **143**. The conversion of compound **143** into epoxide **144** was quickly achieved in alkaline aq. soln. (9 M NaOH at rt) which, followed by refluxing at 90-100 °C, efficiently gave the white crystalline triol **145** in 55% yield over two steps. These reactions afforded the inversion of configuration at C-3 and C-4, necessary for the synthesis of the desired compound **111**. Benzylation of **145** according to the classical method (NaH, BnBr, DMF) afforded compound **146** (77% yield). The 1,2-*O*-isopropylidene group was then easily removed with acetic acid 60% (w) under reflux in 20 min (72% yield) giving compound **147**. Further methylation of the hemiacetal OH was needed in order to introduce the allyl

group. This reaction is very sensitive to humidity and a very dry environment is required, since in the presence of water in acidic conditions leads to other product formation. Acetal formation is usually performed in anhydrous conditions with Bronsted or Lewis acid, in excess alcohol. In this case, acetyl chloride (AcCl) in methanol (H^+ generated *in situ*) was used which generated compound **148** as a mixture of α,β -anomers (3:1 $\alpha:\beta$ ratio).

Silylation of the primary hydroxyl group in compound **148** using bis(trimethylsilyl)-trifluoroacetamide (BTSFA) was followed by *in situ* treatment with allyltrimethylsilane and catalytic trimethylsilyl trifluoromethanesulfonate (TMSOTf) to afford an α,β anomers mixture, which was separated to give the α -anomer, compound **111** in 76% yield (8:2 $\alpha:\beta$ ratio) (Scheme 11). As mentioned previously, the orientation of the benzyl group at C-3 position determines the preferred nucleophilic attack of the $AlSi(CH_3)_3$ from the opposite side, in this case the β -side of the cyclic oxonium intermediate and results in major formation of the desired α -anomer, compound **111**. A proposed mechanism for the allyl insertion is illustrated in Scheme 11, where the two possible nucleophilic attacks are shown.



Scheme 11. Proposed mechanism for the allyl insertion (the green arrow shows the favoured β -side attack while the red one indicates the unfavoured α -side attack).

The α,β -mixture (compounds **111** and **111'**) was separated and the compounds were analyzed by 2D-NOESY NMR experiments. The NOE effect was then calculated for the α - and β -anomers using Amber force field in CHCl_3 running ACROMODEL (integrated in the version 5.1 of the MAESTRO suite^{xxvi}) and the inter proton distances (in Ångstrom) were calculated (Fig. 36). When the distance is smaller than 4 Å, a NOE effect is expected between the protons in question. Thus, the expected NOE for the α -anomer **111** is between H-1'a and H-3/H-5, and between H-1a and H-4. For the β -anomer **111'**, a NOE is expected between H-1a and H-3/H-5, and between H-1'a and H-4.

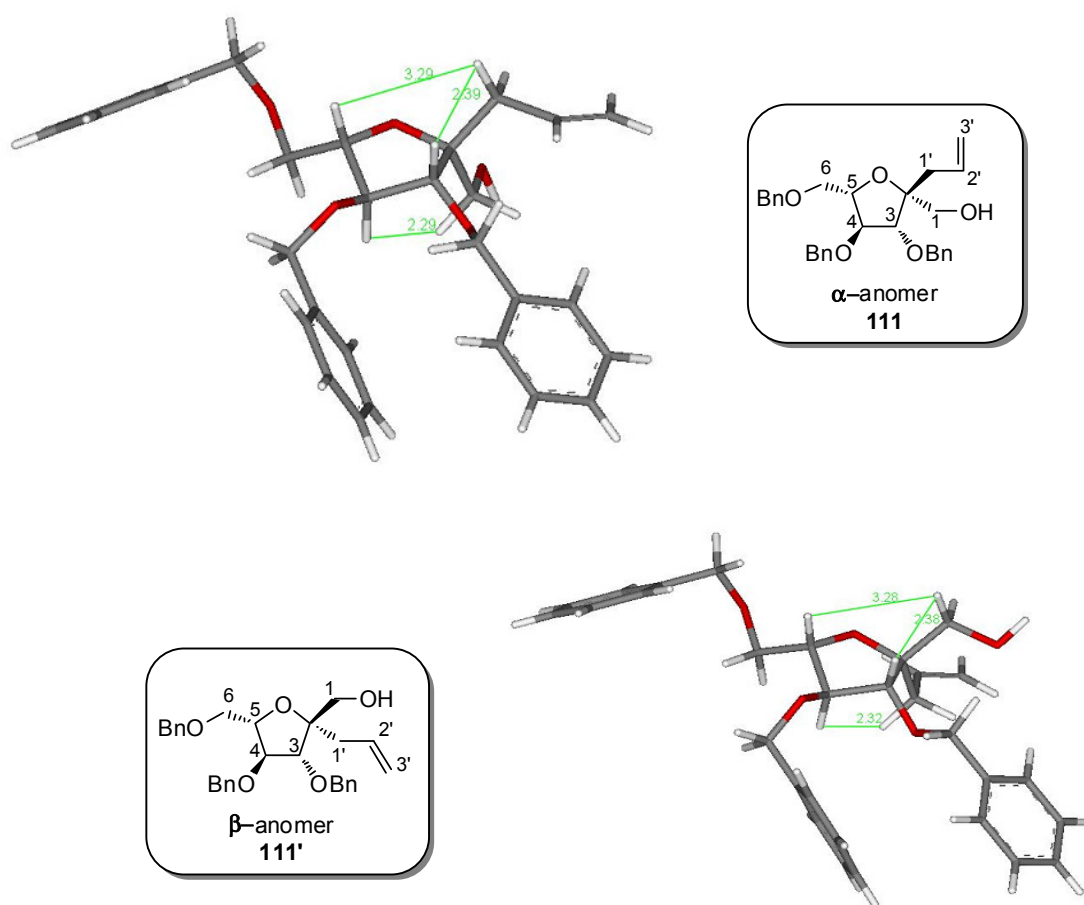


Figure 36. NOE effects and inter proton distances obtained by MacroModel® (Interactive Molecular Modeling System) for the α - and β -anomer **111** and **111'**, respectively.

^{xxvi} MacroModel, Schrödinger, LLC, New York, 2005.

The NOESY spectrum of compound **111** (α -anomer) is shown in Figure 37, where a clear NOE effect can be observed between H-1'a and H-3'a/H-3/H-1a as well as H-2'/H-5 (weak) and between H-1'b and H-2'/H-3/H-1b. These interactions together with the calculations confirmed the identity of the α -anomer. Furthermore, the chemical shift of C-1' was confirmed to be higher for the α -anomer (40.29 ppm) than for the β -anomer (37.19 ppm), in correlation with known effects (same for the enantiomer, compound **125**).

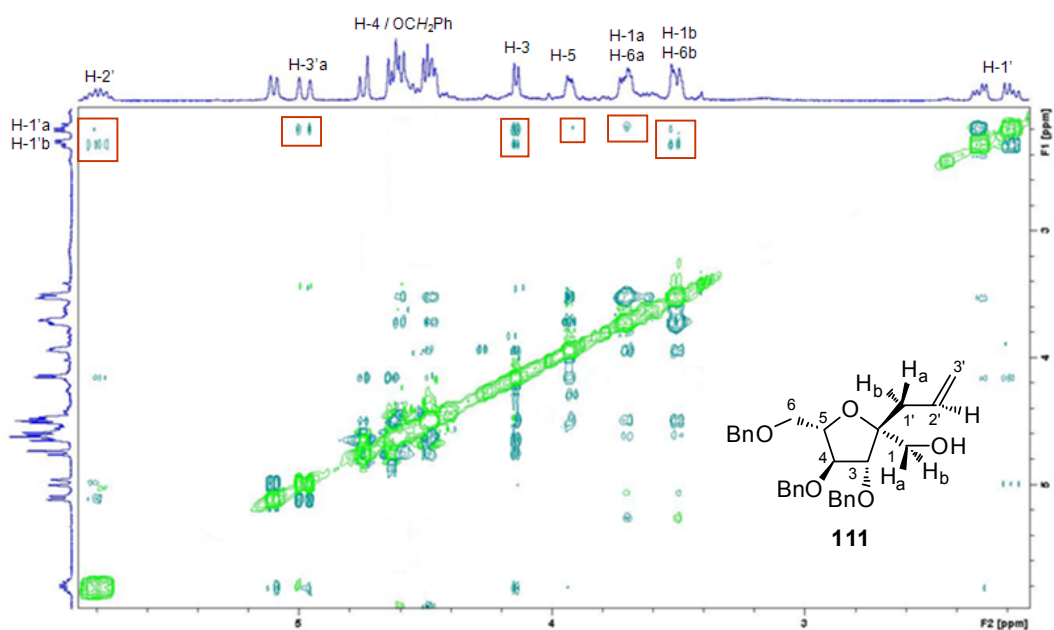
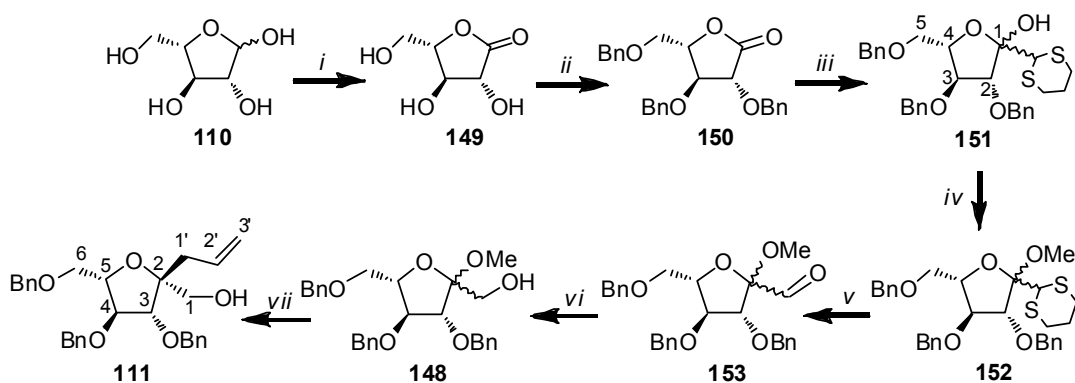


Figure 37. 2D NOESY spectrum of compound **111** (α -anomer).

2.1.2.2 Synthesis of Compound **111** – Pathway *b*

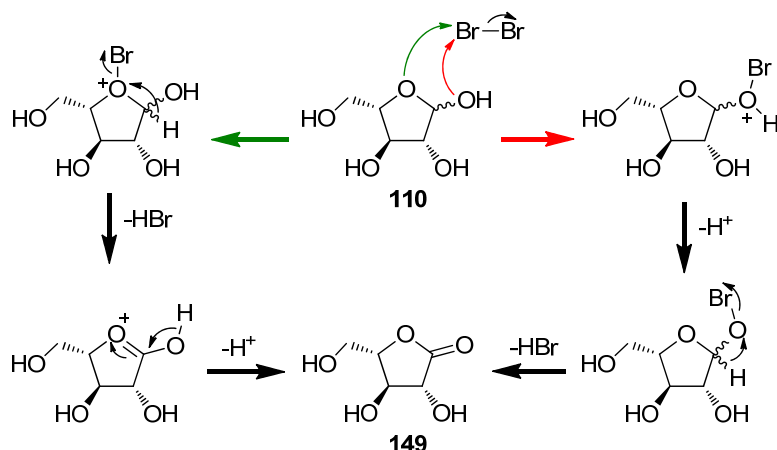
Pathway *b* (Scheme 12) is a seven-step synthesis which starts from α,β -L-arabinose **110**, and gives the target molecule **111** in 13.5% overall yield. This method is more straightforward and efficient than the previously mentioned pathway *a*. This approach takes advantage of the stereochemistry of the L-arabinose starting material and consists of oxidation of the anomeric position, protection with benzyl groups, chain elongation using 2-lithium-1,3-dithiane, oxidation of the dithioacetal to an aldehyde and finally reduction to an alcohol.



Scheme 12. Pathway *b*. Reagents and conditions: *i*. Br₂, K₂CO₃, H₂O, rt, 2h, 98%; *ii*. CCl₃C(=NH)OBn, TfOH, dioxane, 0 °C then rt, 3h, 65%; *iii*. 1,3 dithiane, n-BuLi (1.6 M hexane), THF, -78 °C, then NH₄Cl, 2h, 64% yield as a mixture of anomers (1:4 α:β ratio); *iv*. CH₃OH, H₂SO₄, m.s. 3Å, THF, reflux 40 °C, 12h, 67% yield as a mixture of anomers (1.5:1 α:β ratio); *v*. DBDMH, acetone, -20 °C, 15 min; *vi*. NaBH₄, EtOH, 0 °C, 30 min, 65% yield as a mixture of anomers over two steps (3:1 α:β ratio); *vii*. 1. BTSFA, CH₃CN, reflux 50°C, 6h; 2. AllSi(CH₃)₃, TMSOTf, 0 °C then rt, 2h, 76% yield for α anomer (8:2 α:β).

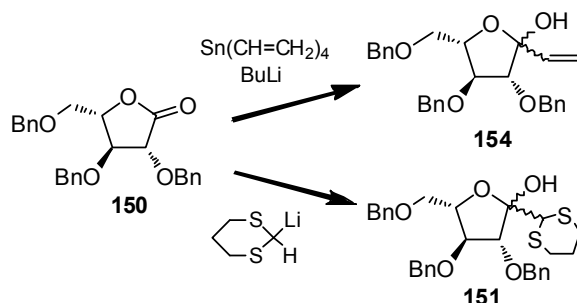
In this synthesis, α,β-L-arabinose **110** was selectively oxidized with bromine in water to give the desired aldonolactone **149** in 98% yield. Hypohalous acids (halogen in water) oxidise primary and secondary alcohols to aldehydes and ketones, respectively. The proposed mechanism for these reactions occurs *via* formation of a hypohalite followed by the E2 elimination of HX (in this case HBr) as shown in Scheme 13. However, in the presence of a hemiacetal, bromine is preferably attacked by O-1 or O-4, both pathways leading to the target lactone.^[162]

Aldonolactone **149** was subsequently benzylated, not according to the classical method (NaH, BnBr, DMF) since the presence of strong base promotes isomerization reactions or product decomposition. Therefore, benzylation was performed with benzyl 2,2,2-trichloroacetimidate [CCl₃C(=NH)OBn] under acidic conditions (TfOH) in dioxane^[163] and produced the perbenzylated derivative **150** in 65% yield (Scheme 12).

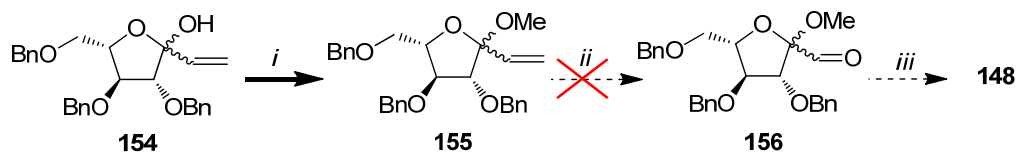


Scheme 13. Proposed mechanism for the oxidation of lactols by Br_2 in water.^[162]

Two synthetic approaches were envisaged for chain elongation starting from aldono-lactone **150** (Scheme 14). The first one was based on the reaction with vinyl lithium (tetravinyltin, BuLi , THF, -78°C , 2h)^[164] which afforded compound **154** in 82% yield. However, the subsequent oxidation of **155** with OsO_4 to obtain aldehyde **156** failed, probably due to steric hindrance (Scheme 15). Therefore, an alternative approach was developed starting with the reaction of **150** with 2-lithium-1,3-dithiane (formed *in situ* by 1,3-dithiane and *n*-butyllithium at -78°C in THF)^[165] which gave compound **151** as a α,β -anomers mixture in 64% yield (1:4 $\alpha:\beta$ ratio). The benzyl-group in position 3 should direct the attack from the β -side, however the presence of a bulky substituent in the anomeric position promotes the attack from the α -side, giving β -anomer as major product.

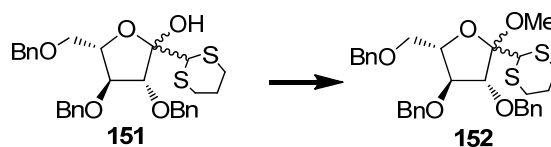


Scheme 14. Two proposed pathways for chain elongation.



Scheme 15. Reagents and conditions: *i.* dry CH₃OH, H₂SO₄, rt, 2h, 89% yield as a mixture of anomers; *ii.* 1. 0.016 M OsO₄ in *t*BuOH, NaIO₄, H₂O/acetone/*t*BuOH 1:1:1, rt; *iii.* NaBH₄.

Protection of the free hydroxyl group as a methyl ether was needed prior to the hydrolysis of the dithiane. However methylation of the α,β -mixture **151** proved to be problematic. The classical method (CH₃OH, conc. H₂SO₄, rt) could not be used due to solubility issues (Scheme 16). Other conditions were evaluated (Table 1) with the best results in entry 7 where 67% of compound **152** could be obtained.



Scheme 16.

Table 1. Experimental conditions for reaction of **151** with methanol.

Entry	Catalyst	Solvent	Temp.	Time	Yield mixture
1	Amberlite IR-120	THF	rt	3 days	20%
2	Amberlite IR-120	THF	reflux	3 days	20%
3	Acetic acid	THF	rt	3 days	30%
4	Acetic acid	THF	reflux	3 days	40%
5	H ₂ SO ₄ conc	THF	rt	24h	59%
6	H ₂ SO ₄ conc	CH ₂ Cl ₂	rt	2 days	52%
7	H ₂ SO ₄ conc	THF	reflux	12h	67%

The configuration of the stereocenter formed in compound **152** was determined by NOESY NMR experiments where a clear interaction between the OCH₃ and H-2/H-4 could be observed (Fig. 38).

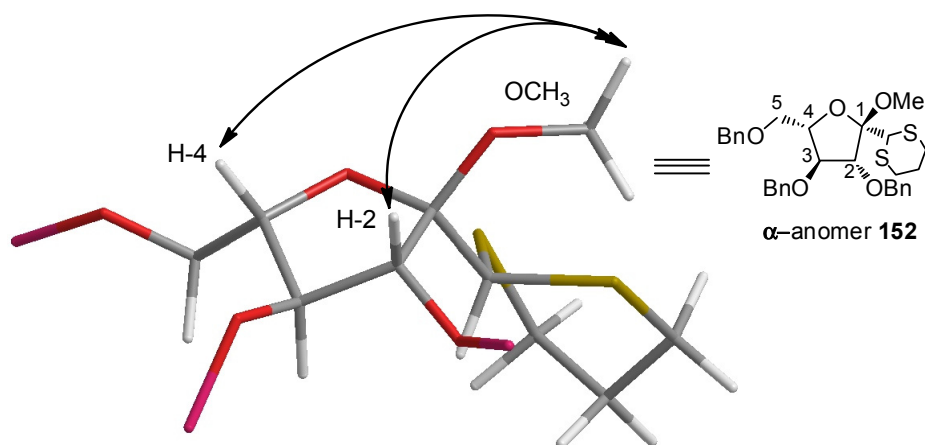


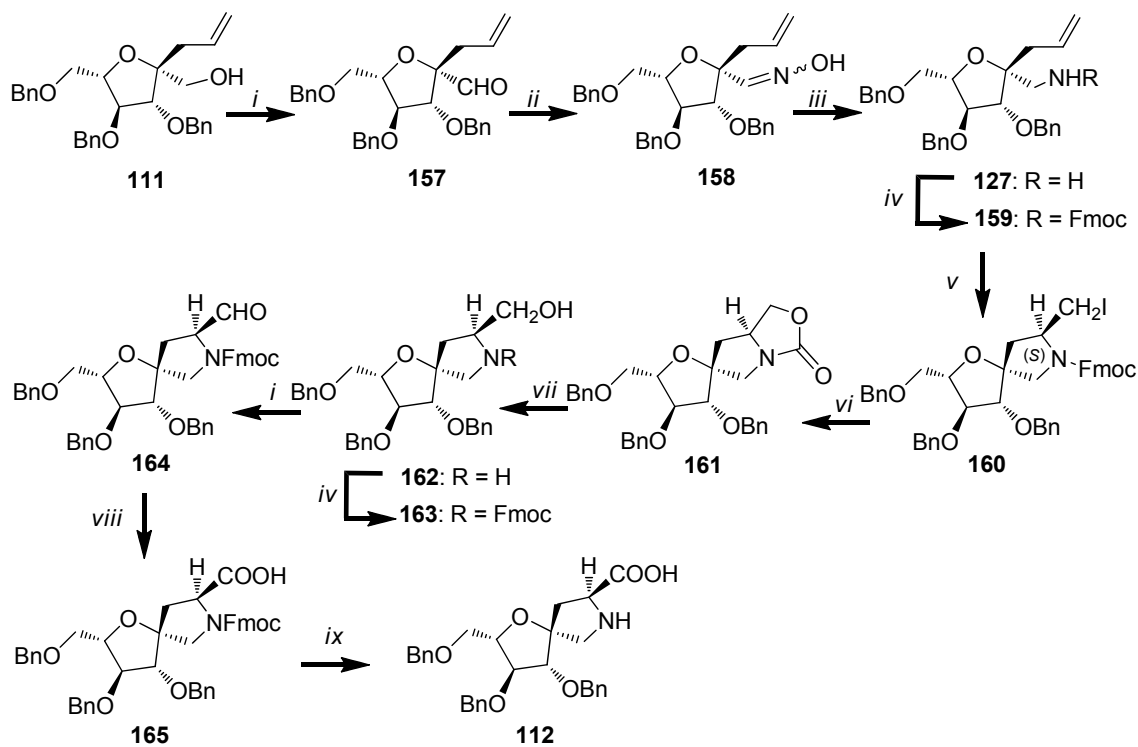
Figure 38. Correlations observed by 2D-NOESY for α -anomer **152**.

Reaction of **152** with 1,3-dibromo-5,5-dimethylhydantoin (DBDMH)^[165] resulted in the formation of aldehyde derivative **153**, which was treated with sodium borohydride (NaBH₄) in ethanol to afford **148** in 65% yield over two steps (3:1 α : β ratio). The allylic appendage was introduced at the anomeric position using the same procedure as in pathway *a* (Scheme 11).

The pathway *b* involved mainly a one carbon chain elongation at C-1 of a sugar with the appropriate stereochemistry, which can be considered a more elegant and direct method to obtain the L-fructose derivative, compound **111**. Compared to the method previously described (pathway *a*), pathway *b* proved to be more convenient and efficient regarding the number of reaction steps and the overall yield.

2.1.2.3 Synthesis of Compound **112**

The second part of the synthetic plan to obtain L-proline analogue **112** (Scheme 17) consists of an eleven step synthesis as presented for the D-proline analogue **85** (Scheme 7). A detailed description of the reactions will not be made in order to avoid redundant duplication of the experimental conditions. The product yield obtained in each step is indicated in Scheme 17 and no particular discrepancies were noticed compared to the synthesis of the D-proline analogue **85**.



Scheme 17. Reagents and conditions: *i*. IBX, dry DMSO, rt, 2h; *ii*. $\text{NH}_2\text{OH}\cdot\text{HCl}$, pH=4.5, $\text{CH}_3\text{OH}/\text{THF}$ 1:1, rt, 4h, 87% yield over two steps, as mixture of *E/Z* isomers; *iii*. LiAlH_4 , dry THF, rt, 12h, 92%; *iv*. Fmoc-Cl, DIPEA, dry CH_3CN , rt, 2h, 86% (**159**) and 90% (**163**); *v*. I_2 , dry DME, rt, 2h, 85%; *vi*. aq. soln. 1 M NaOH, CH_3CN , rt, 12h, 91%; *vii*. aq. soln. 3M NaOH, EtOH, reflux, 4h, 85%; *viii*. aq. soln. 1.25 M $\text{NaH}_2\text{PO}_4\cdot 2\text{H}_2\text{O}$, NaClO_2 , CH_3CN , rt, 7h, 70% yield over two steps; *ix*. Et_2NH , dry CH_3CN , rt, 2h, 85%.

The stereochemistry of the new stereocenter of compound **160** formed in the iodocyclization reaction was determined by NOESY experiments on tricyclic compound **161**. A 2D NOESY experiment for the tricyclic oxazolidinone **161** showed a cross peak between H-2' and H-1'a, and between H-1'b and H-3 (Fig. 39 and 40).

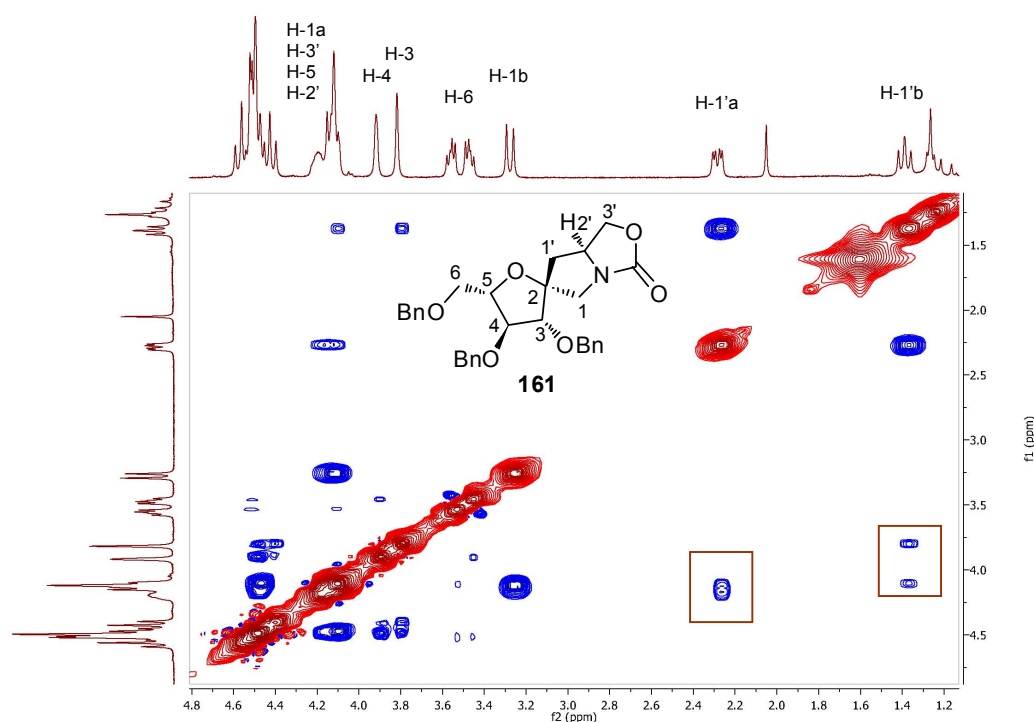


Figure 39. 2D NOESY spectrum of compound **161**.

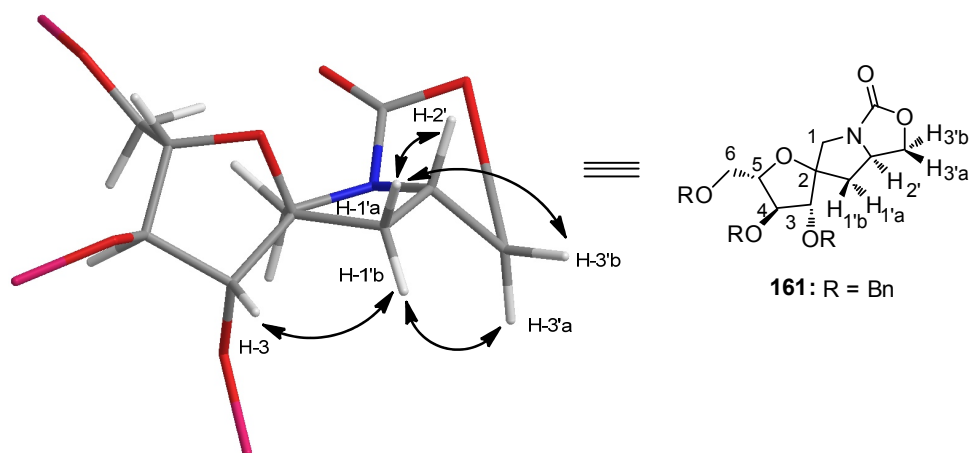


Figure 40. Correlation observed by 2D-NOESY for compound **161**.

2.1.3 Novel Rigid 1,4-Benzodiazepine-2,5-dione Scaffolds

Herein is describe the synthesis and conformational analysis of a library of novel enantiomeric conformationally constrained 1,4-benzodiazepine-2,5-diones scaffolds containing a fructose monosaccharide unit and a proline moiety (i.e. sugar-based pyrrolo[2,1-c][1,4]-benzodiazepine-5,11-diones, Fig. 41). Further, is describe the biological evaluation of these library as GABA_A receptor ligands.

These compounds were synthesized by coupling of D-fructose-D-proline derivative **85** or L-fructose-L-proline derivative **112** with the suitably functionalized isatoic anhydride **60**, by refluxing in DMF. Condensation of proline with isatoic anydride leads directly to the chiral benzodiazepine structure (see Fig. 21 in chapter 1.3.1). This reaction can be rationalized as a stepwise formation of a diazepine ring, amide formation of the proline nitrogen with the anhydride ester, followed by ring opening and loss of carbon dioxide from the carbamate, and subsequently the formation of a second amide with the proline carboxylate.

The free hydroxyl groups on the sugar offer the possibility of further functionalization for tuning of the pharmacokinetic properties and the biological activity. The proline moiety, connected to fructose through a spiro ring junction, gives high conformational rigidity to the benzodiazepine hybrid scaffolds, as confirmed by Molecular Modelling and DNMR data. The binding affinities of the rigid benzodiazepine enantiomers were measured in competition binding assays with GABA_A R in rat cortical membranes.

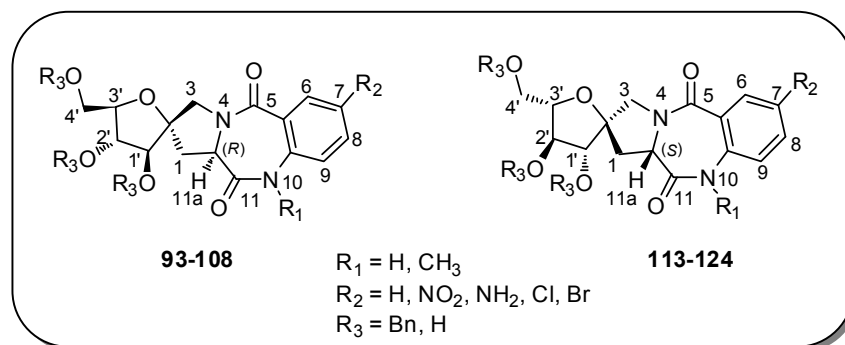
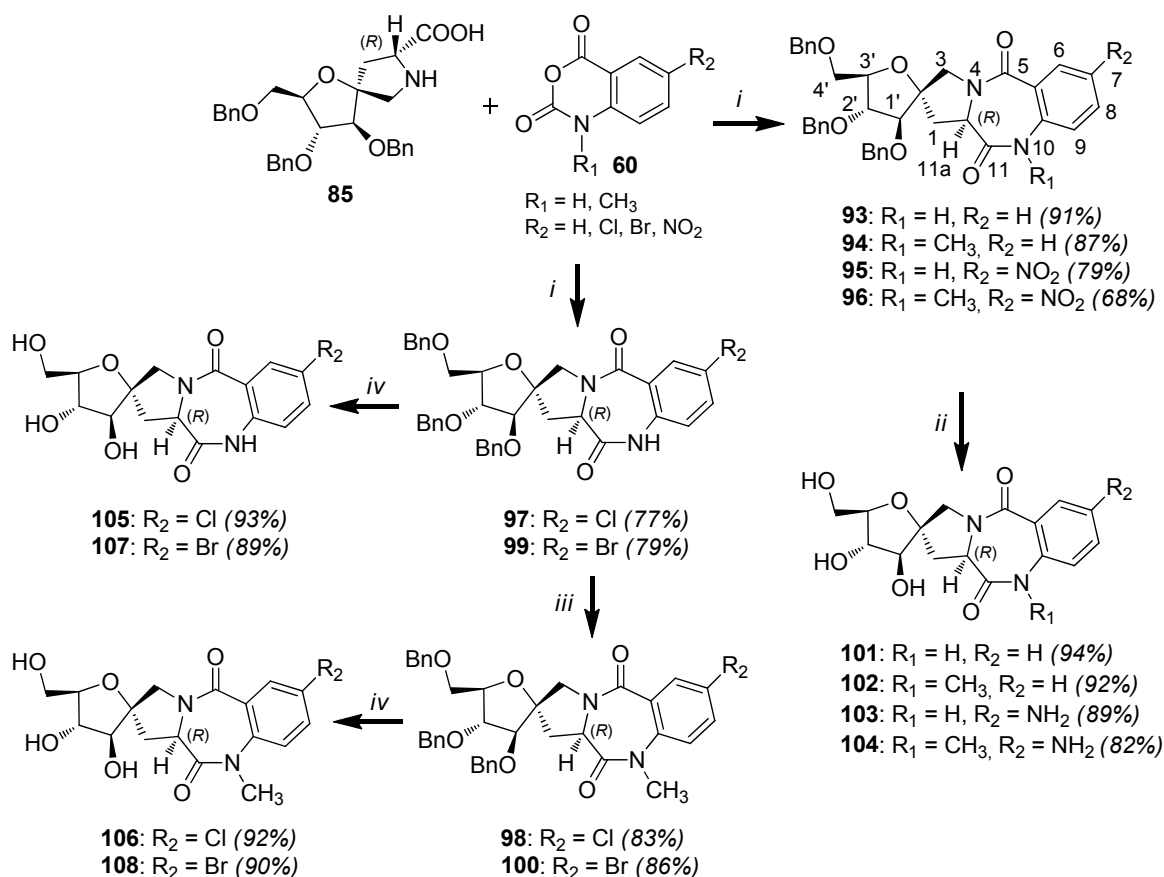


Figure 41. 1,4-Benzodiazepine-2,5-dione scaffolds.

The functionalization of the enantiomeric benzodiazepine scaffolds was based on previous mentioned QSAR studies (see chapter 1.3.4.3), which demonstrated that electronegative substituents at position seven and *N*-substitution contribute to higher receptor binding affinity. Therefore, -Cl, -Br, -NO₂, and also -NH₂ substituents were introduced at position seven and -CH₃ at position ten, using prefunctionalized isatoic anhydrides. Since *N*-methyl-5-bromoisatoic and *N*-methyl-5-chloroisatoic anhydrides were not commercially available, the corresponding benzodiazepine scaffolds were generated by *N*-methylation with iodomethane and cesium carbonate in DMF at rt. The subsequent deprotection of the benzodiazepine scaffolds was performed according to two different procedures. Since hydrogenolysis with palladium hydroxide on carbon [Pd(OH)₂/C] results in debenylation, reduction of nitro groups and dehalogenation of aromatic halides, the halo substituted benzodiazepine derivatives needed to be deprotected with a method that preserves the halide. The use of boron trichloride afforded the desired water soluble halogenated benzodiazepine scaffolds.

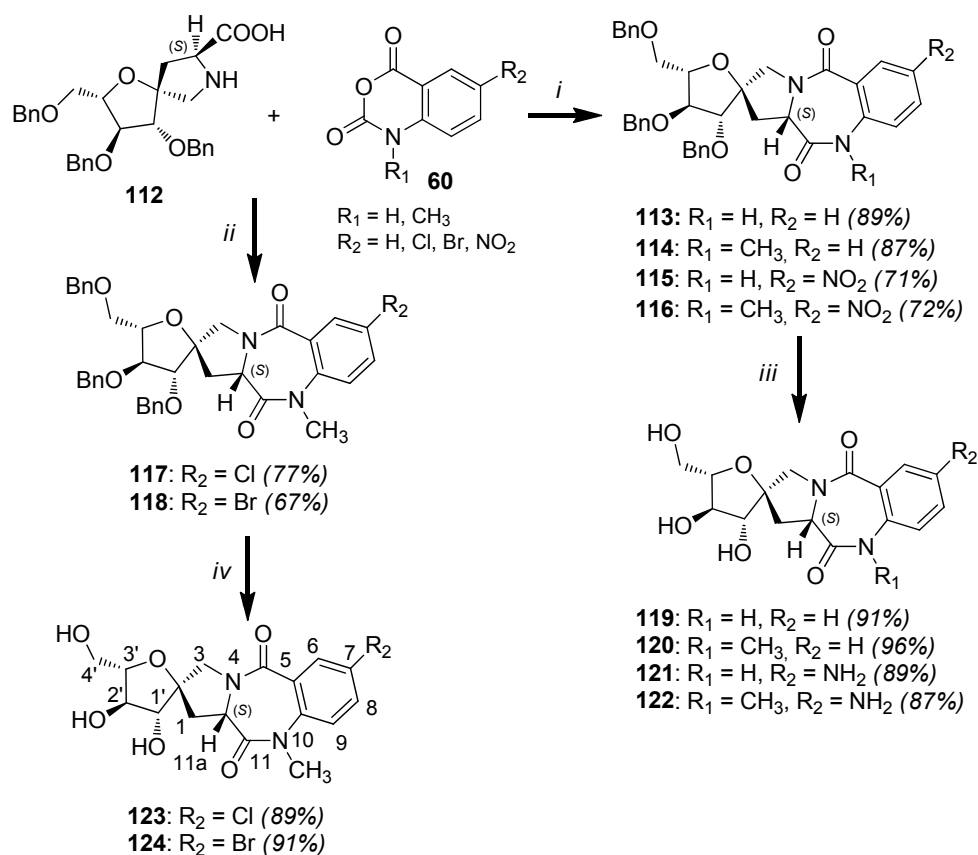
2.1.3.1 Synthesis

The synthesis of the D-fructose-based pyrrolobenzodiazepine scaffolds **93-96**, **97** and **99** was accomplished by heating suitably functionalised isatoic anhydride type **60** in dry DMF, with the D-proline analogue **85** (Scheme 18). Subsequent hydrogenolysis with Pd(OH)₂/C of compounds **93-96** resulted in both debenylation and reduction of the nitro group, affording benzodiazepines **101-104**. *N*-Methylation of compounds **97** and **99** afforded compounds **98** and **100** with 83% and 86% yield, respectively. Finally deprotection of compounds **97-100** with BCl₃ (1.0 M soln. in CH₂Cl₂) gave compounds **105-108** (Scheme 18).



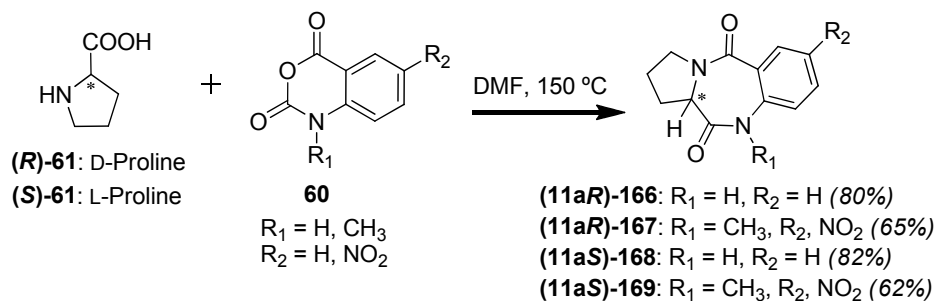
Scheme 18. Synthetic steps towards pyrrolobenzodiazepines derived from D-proline analogue. *Reagents and conditions:* *i.* dry DMF, reflux, 2h; *ii.* Pd(OH)₂/C (10% w/w), CH₃OH/EtOAc, 48h; *iii.* CH₃I, Cs₂CO₃, dry DMF, rt, 2h; *iv.* BCl₃ in 1M CH₂Cl₂, rt, 1h.

In addition, synthesis of L-fructose-based benzodiazepines scaffolds **113-118** was accomplished by heating suitably functionalised isatoic anhydride **60** in dry DMF, with the L-proline analogue **112** (Scheme 19); in the case of compounds **117** and **118** an *N*-methylation was also performed. Subsequent hydrogenolysis with Pd(OH)₂/C of compounds **113-116** resulted in debenzoylation and reduction of the nitro group, affording benzodiazepines **119-122**. The deprotection of the halo substituted benzodiazepine derivatives was performed with BCl₃ giving rise to compounds **123** and **124** in 89% and 91% yield, respectively (Scheme 19).



Scheme 19. Synthetic steps towards pyrrolobenzodiazepines derived from L-proline analogue. *Reagents and conditions:* *i.* dry DMF, reflux, 2h; *ii.* 1. dry DMF, reflux, 2h; 2. CH_3I , Cs_2CO_3 , dry DMF, rt, 2h; *iii.* $\text{Pd}(\text{OH})_2/\text{C}$ (10% w/w), $\text{CH}_3\text{OH}/\text{EtOAc}$, 48h; *iv.* BCl_3 in 1M CH_2Cl_2 , rt, 1h.

For further biological evaluation, pyrrolo[2,1-*c*][1,4]benzodiazepine-5,11-diones derived from the free amino acid D- and L-proline were also synthesized following the general procedure described in literature for compound **166**^[83] (Scheme 20).



Scheme 20. Synthesis of pyrrolo[2,1-*c*][1,4]benzodiazepine-5,11-diones derived from D- and L-proline.

2.1.3.2 Molecular Modelling and DNMR Experiments^{xxvii}

It has been reported that binding affinities at the GABA_A receptor are exquisitely sensitive to the conformation *M*- or *P*- of the benzodiazepine ring, which is governed by the pseudo-equatorial preference and absolute stereochemistry of the C-3 substituent, for 1,4-benzodiazepine-2,5-diones (R₂ in Fig. 42) or C-11a substituent, for pyrrolo[2,1-*c*][1,4]benzodiazepines. Therefore, great efforts have been devoted to the synthesis of conformationally constrained benzodiazepine derivatives, since conformational changes in the benzodiazepine ring system have shown strong effect on binding affinities to the receptor complex.

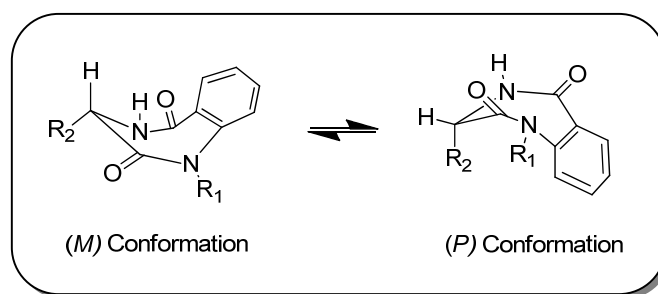


Figure 42. Conformational equilibrium present in the 1,4-benzodiazepine-2,5-dione ring.

In this context, in order to evaluate our sugar-based pyrrolobenzodiazepines, conformational analysis of sample water soluble D-fructose-based pyrrolobenzodiazepine **101** (R₁ = R₂ = R₃ = H) and **102** (R₁ = CH₃ and R₂ = R₃ = H) was performed by molecular modelling calculations and experimental NMR studies at variable temperature (Dynamic NMR, DNMR). Data showed a unique preferential conformation of the benzodiazepine ring, where H-11a adopts the pseudo-axial position, corresponding to the (*P*) helical conformation. However, conformers of the pyrrolo ring do exist, i.e. oxy-substituent can be pseudo-axial or pseudo-equatorial, as illustrated in Figure 43 for compound **101** and Figure 44 for compound **102**, but keeping always a (*P*)-conformation of the diazepine ring.

^{xxvii} These experiments were performed under the supervision of Dr. Cristina Airoidi in the Dept. of Biotechnology and Bioscience, University of Milano-Bicocca.

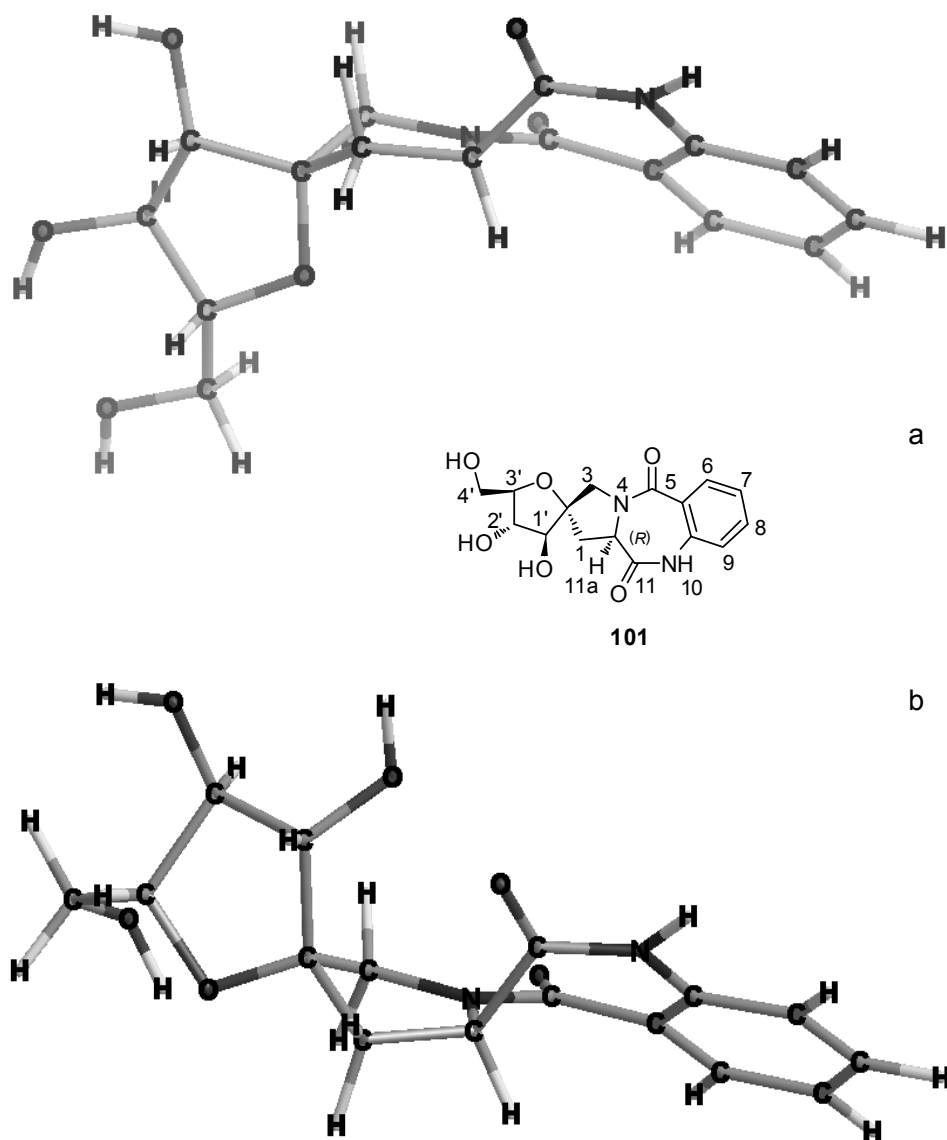


Figure 43. Oxy-substituent pseudo-axial (a) and pseudo-equatorial (b) conformers of pyrrolo ring in compound **101**. Pseudo-axial conformer: total energy = 25.028 kcal/mol, dihedral angle C5a-C9a-N10-C11 = +16.91°; pseudo-equatorial conformer: total energy = 22.319 kcal/mol, dihedral angle C5a-C9a-N10-C11 = +17.32°.

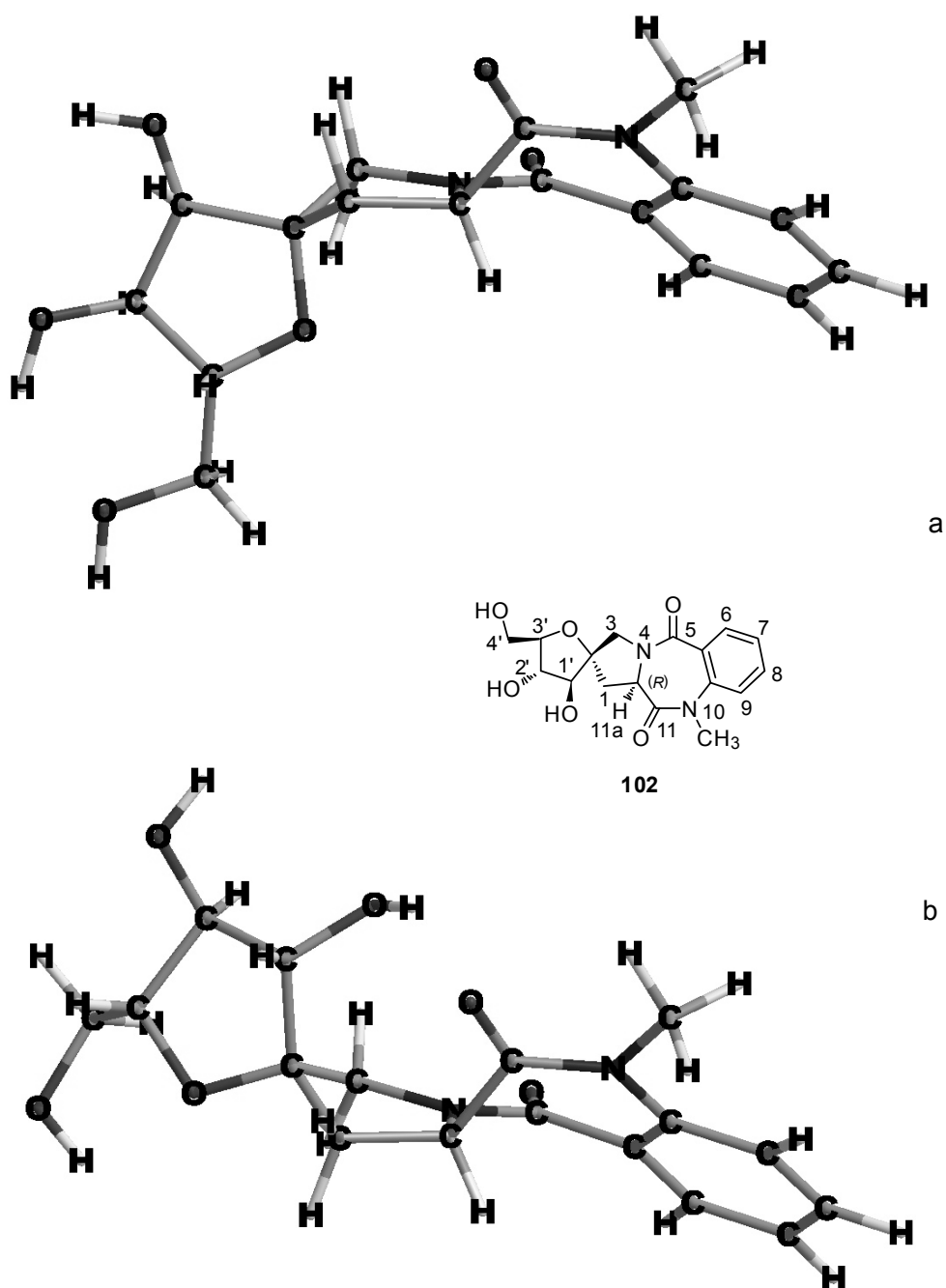


Figure 44. Oxy-substituent pseudo-axial (a) and pseudo-equatorial (b) conformers of compound **102** pyrrolo ring. Pseudo-axial conformer: total energy= 30.438 kcal/mol, dihedral angle C5a-C9a-N10-C11 = +22.73°; pseudo-equatorial conformer: total energy= 28.235 kcal/mol, dihedral angle C5a-C9a-N10-C11 = +24.57°.

The dihedral angle C5a–C9a–N10–C11 (average between the two conformers) was also determined, and resulted +17° for compound **101** and +24° for compound **102**, corresponding to the helical chirality (*P*), Table 2.

Table 2. Computational calculation of the dihedral angle C5a–C9a–N10–C11 by molecular mechanic and molecular dynamic.

Compound	Conformer (Oxy-substituent)	Total energy ¹	Dihedral Angle ^{1,2} C5a–C9a–N10–C11
101	pseudo-axial	25.028 kcal/mol	+16.91°
	pseudo-equatorial	22.319 kcal/mol	+17.32°
102	pseudo-axial	30.438 kcal/mol	+22.73°
	seudo-equatorial	28.235 kcal/mol	+24.57°

¹Calculated by ChemBio3D Ultra by applying an MM2 force field and Molecular Dynamics Computation (step interval = 2 fs; frame interval = 1 fs; heating/cooling rate = 1.000 kcal/atomp; target temperature = 300 K). Total energy and dihedral angle C5a–C9a–N10–C11 values calculated with the two methods are consistent.

²The dihedral angle average between the two conformers resulted +17° and +24° for compound **101** and **102**, respectively, corresponding to the helical chirality (*P*).

In addition, NMR experiments run at variable temperature, from 298 K (~ 25 °C) till a maximum value of 363 K (~ 90 °C), for compound **101** (Fig. 45) and compound **102** (Fig. 46), indicated that even at high temperature no conformational equilibrium of the benzodiazepine ring is present, in contrast to quaternary 1,4-benzodiazepin-2-ones, which exist as mixtures of the (*M*)- and (*P*)-conformers, as described in literature.^[102, 116, 118] Thus, D-fructose-based pyrrolbenzodiazepines synthesized retained always a single conformation of the seven-membered ring. In all reported cases, the coalescence temperature for the pseudo-equatorial/pseudo-axial equilibrium is always above 60°C (333 K).^[166, 167]

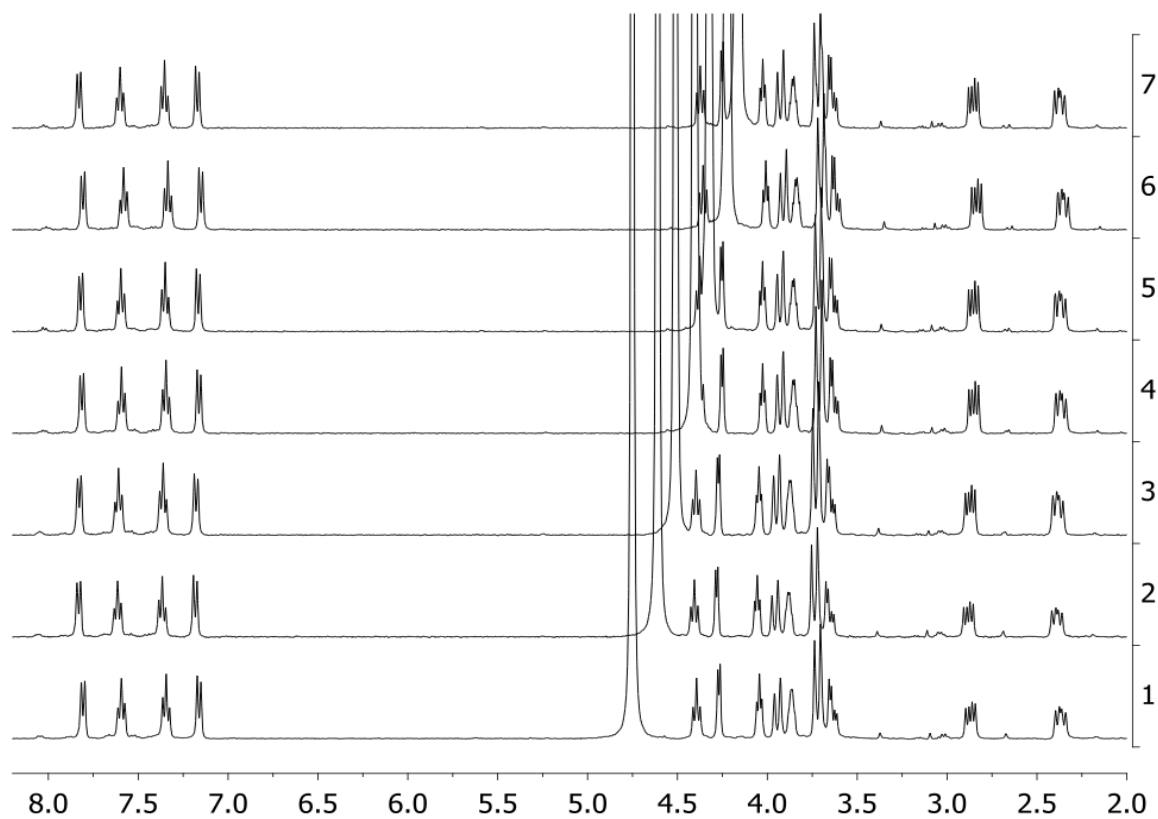
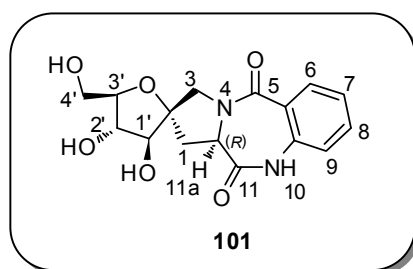


Figure 45. DNMR (298K – 363K) on molecule **101** dissolved in D₂O, 32 scans; spectrum **1**: 298 K, spectrum **2**: 313 K, spectrum **3**: 323 K, spectrum **4**: 333 K, spectrum **5**: 343 K, spectrum **6**: 353 K, spectrum **7**: 363 K. ¹H-NMR (D₂O): δ (ppm) 7.66 (d, 1H, *J* = 7.4 Hz, Ar-*H*), 7.44 (t, 1H, *J* = 7.4 Hz, Ar-*H*), 7.21 (t, 1H, *J* = 7.4 Hz, Ar-*H*), 7.01 (d, 1H, *J* = 7.4 Hz, Ar-*H*), 4.30 (t, 1H, *J* = 7.6 Hz, H-11a), 4.13 (d, 1H, *J* = 5.4 Hz, H-1'), 3.99 (t, 1H, *J* = 5.4 Hz, H-2'), 3.80 (d, 1H, *J* = 13.1 Hz, H-3a), 4.08 (bm, 1H, H-3'), 3.62-3.54 (m, 3H, H-3b, H-4'a, H-4'b), 2.70 (dd, 1H, *J* = 14.1, 7.6 Hz, H-1a), 2.23 (dd, 1H, *J* = 14.1, 7.6 Hz, H-1b).

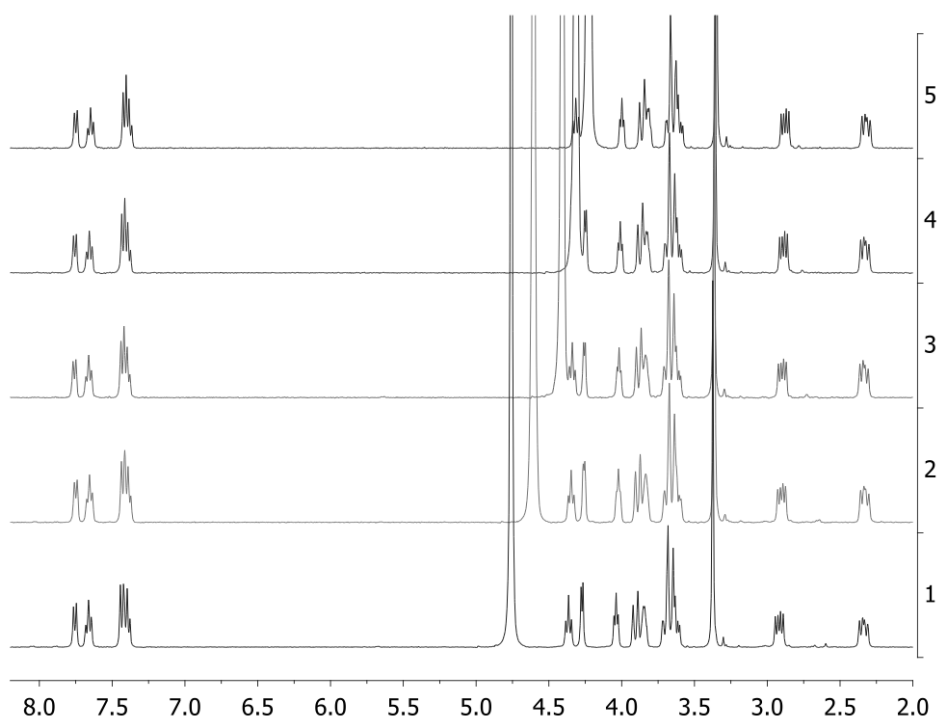
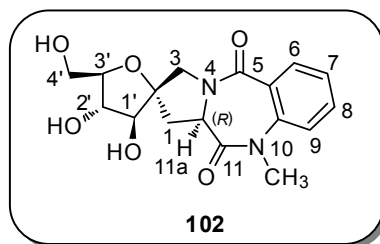


Figure 46. DNMR (298K – 353K) on molecule **102** dissolved in D₂O, 32 scans; spectrum **1**: 298K, spectrum **2** : 313K, spectrum **3**: 333K, spectrum **4**: 343K, spectrum **5**: 353K. ¹H-NMR (D₂O): δ (ppm) 7.72 (d, 1H, J = 7.7, Ar-*H*), 7.54 (t, 1H, J = 8.5 Hz, Ar-*H*), 7.48-7.40 (m, 2H, Ar-*H*), 4.38 (t, 1H, J = 8.1 Hz, H-11a), 4.22 (d, 1H, J = 4.3 Hz, H-1'), 3.98 (bt, 1H, H-2'), 3.92 (d, 1H, J = 13.4 Hz, H-3a), 3.90-3.78 (bm, 1H, H-3'), 3.72-3.53 (m, 3H, H-3b, H-4'a, H-4'b), 3.33 (s, 3H, NCH₃), 2.95 (dd, 1H, J = 13.9, 8.1 Hz, H-1a), 2.37 (dd, 1H, J = 13.9, 8.1 Hz, H-1b).

In order to best characterise these equilibrium, DNMR studies were performed also at low temperature for compound **101**, dissolved in CD₃CD₂OD, down to 173 K (~-10°C), illustrated in Figure 47. These studies indicate that the barrier for inversion of the pyrrolo ring is very low, as suggested also by Molecular Modelling (Fig. 43).

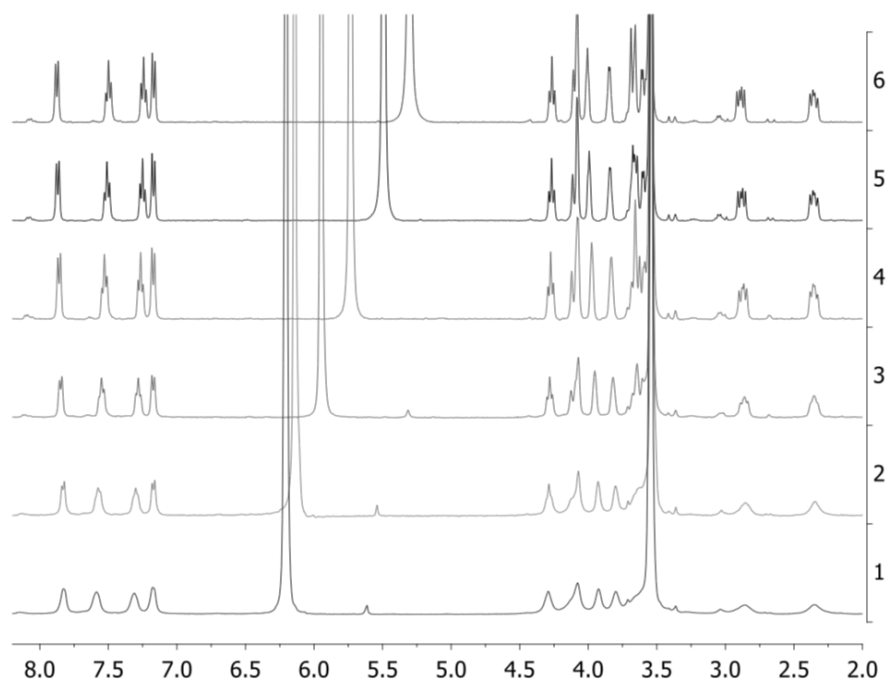


Figure 47. DNMR (173K – 293K) on molecule **101** dissolved in $\text{CD}_3\text{CD}_2\text{OD}$; spectrum **1**: 173K, 184 scans, spectrum **2** : 183K, 64 scans, spectrum **3**: 213K, 32 scans, spectrum **4**: 243K, 32 scans, spectrum **5**: 273K, 32 scans, spectrum **6**: 293K, 32 scans.

All previous data confirmed that the synthesised hybrid D-fructose-based pyrrolobenzodiazepines adopt a rigid conformation around the benzodiazepine ring, corresponding to helical chirality (*P*). Consequently, it is expected that L-fructose-based pyrrolobenzodiazepines adopt the opposite conformation, the (*M*)-helical chirality, since this conformation places the proline moiety to occupy a pseudo-equatorial orientation on the benzodiazepine ring (Fig. 48). Conformational analysis of L-fructose-based pyrrolobenzodiazepine **119** ($R_1 = R_2 = R_3 = \text{H}$) was performed using the same methodology used for its enantiomer, compound **101**.

Molecular Modelling performed on compound **119** showed a unique preferential conformation of the benzodiazepine ring, where R-11a adopts the pseudo-equatorial orientation (Fig. 48) in both conformers, as expected. Additional DNMR experiments also confirmed no conformational equilibrium around the benzodiazepine ring on

compound **119**, protons do not showed coalescence between temperatures of 298 K until 363 K (Fig. 49 and Fig. 50). Determination of dihedral angle C5a-C9a-N10-C11 determined resulted in -17° (average between conformers), corresponding to the helical chirality (*M*), Table 3.

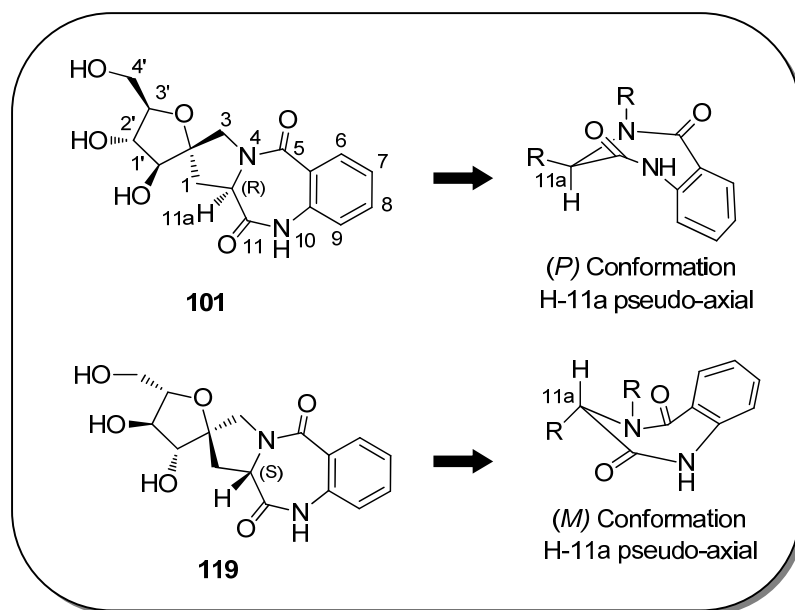


Figure 48. Conformation adopted by D- and L-fructose-based pyrrolobenzodiazepines. R represents fructose-proline analogue.

Table 3. Computational calculation of the dihedral angle C5a-C9a-N10-C11 by molecular mechanic and molecular dynamic.

Compound	Conformer (Oxy-substituent)	Total energy ¹ kcal/mol	Dihedral Angle ^{1,2} C5a-C9a-N10-C11
119	pseudo-axial	25.680	-16.58°
	pseudo-equatorial	22.838	-17.85°

¹Calculated by ChemBio3D Ultra by applying an MM2 force field and Molecular Dynamics Computation (step interval = 2 fs; frame interval = 1 fs; heating/cooling rate = 1.000 kcal/atombs; target temperature = 300 K). Total energy and dihedral angle C5a-C9a-N10-C11 values calculated with the two methods are consistent.

²The dihedral angle average between the two conformers resulted -17° for compound **119**, corresponding to the helical chirality (*M*).

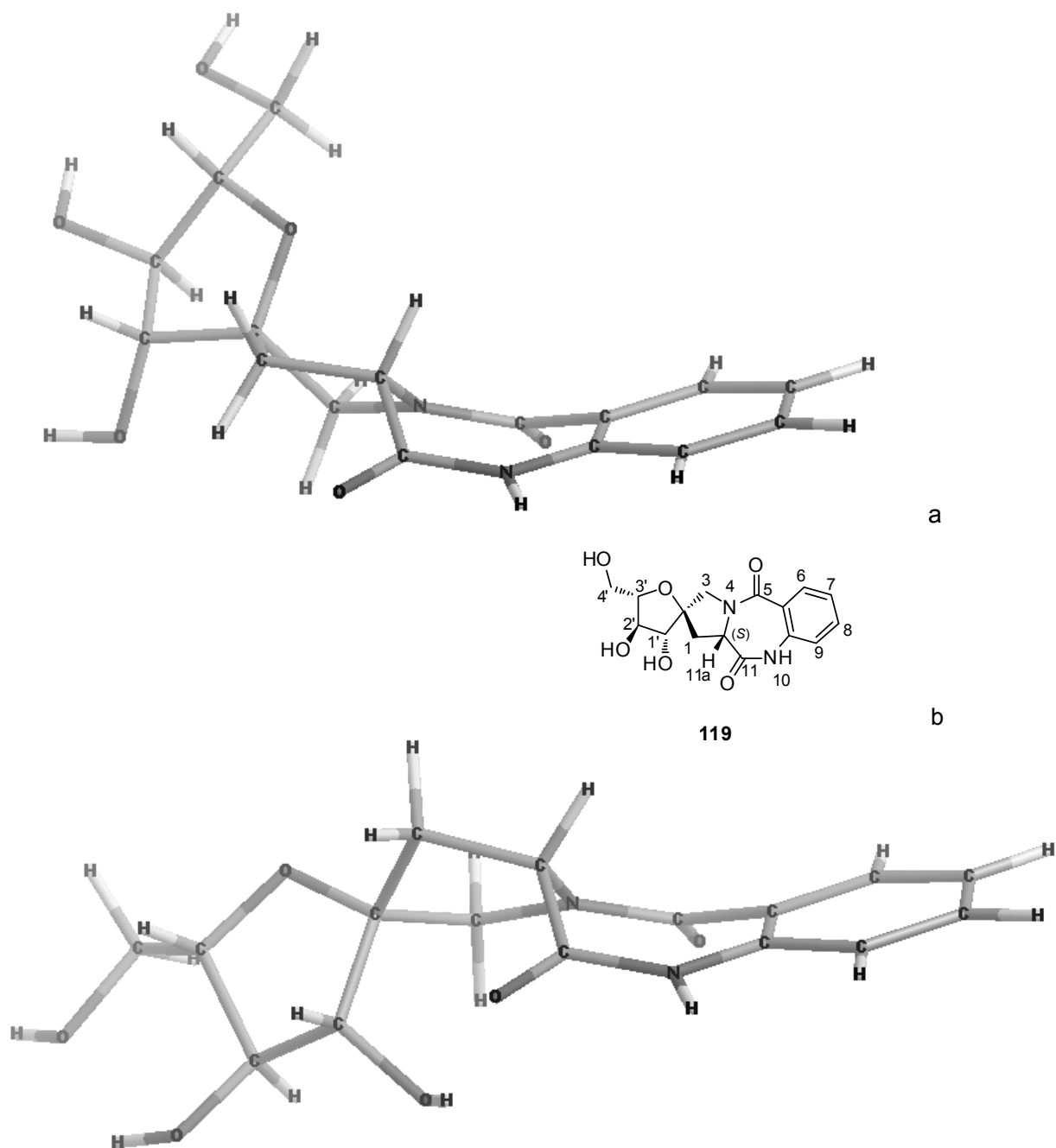


Figure 49. Oxy-substituent pseudo-axial (a) and pseudo-equatorial (b) conformers of the pyrrolo ring of compound **119**. Pseudo-axial conformer: total energy = 25.680 kcal/mol, dihedral angle C5a-C9a-N10-C11 = -16.58° ; pseudo-equatorial conformer: total energy = 22.838 kcal/mol, dihedral angle C5a-C9a-N10-C11 = -17.85° .

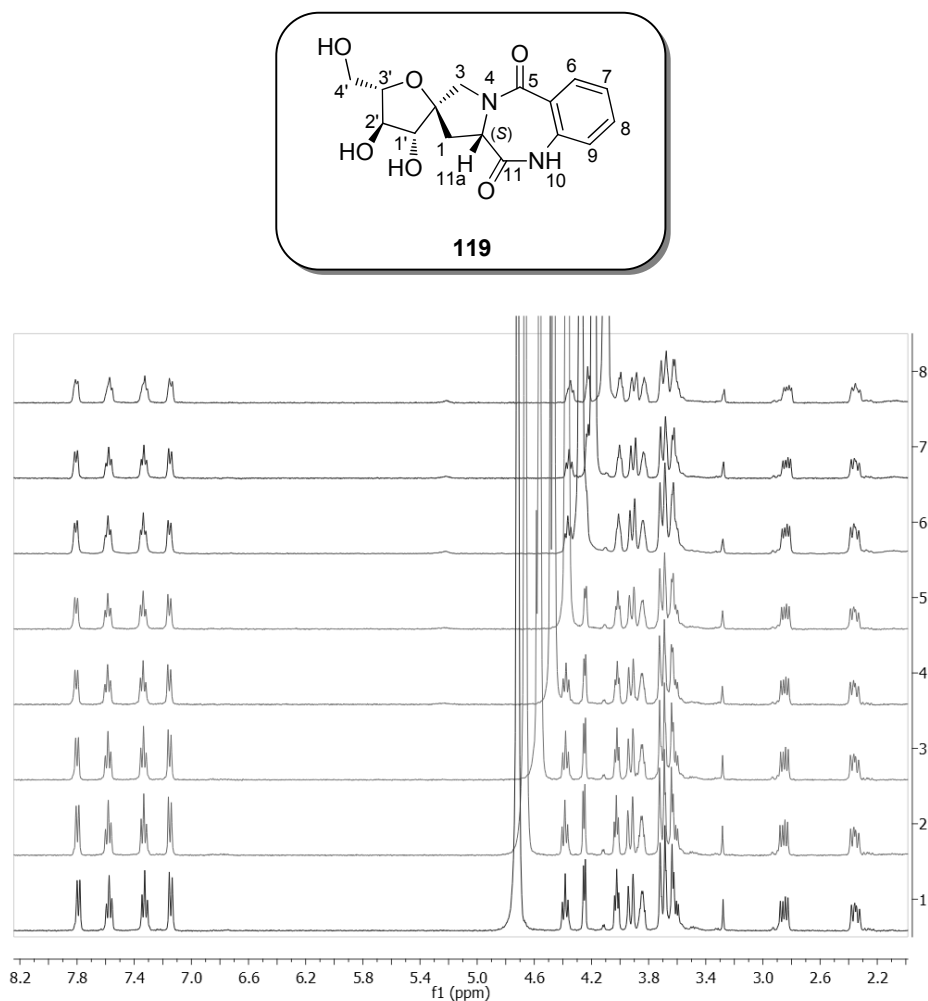


Figure 50. DNMR (298K – 363K) on molecule **119** dissolved in D_2O , 32 scans; spectrum **1**: 298 K, spectrum **2**: 303 K, spectrum **3**: 313 K, spectrum **4**: 323 K, spectrum **5**: 333 K, spectrum **6**: 343 K, spectrum **7**: 353 K, spectrum **8**: 363 K. 1H -NMR (D_2O): δ (ppm) 7.67 (d, 1H, $J = 7.7$ Hz, Ar- H), 7.46 (t, 1H, $J = 7.6$ Hz, Ar- H), 7.21 (t, 1H, $J = 7.6$ Hz, Ar- H), 7.03 (d, 1H, $J = 8.1$ Hz, Ar- H), 4.27 (t, 1H, $J = 7.9$ Hz, H-11a), 4.14 (d, 1H, $J = 5.3$ Hz, H-1'), 3.92 (dd, 1H, $J = 6.4, 5.4$ Hz, H-2'), 3.82 (dd, 1H, $J = 13.1, 1.1$ Hz, H-3a), 3.74 (bm, 1H, H-3'), 3.61-3.48 (m, 3H, H-3b, H-4'a, H-4'b), 2.74 (dd, 1H, $J = 14.1, 7.5$ Hz, H-1a), 2.24 (ddd, 1H, $J = 13.9, 8.5, 1.5$ Hz, H-1b).

The D- and L-sugar-based pyrrolobenzodiazepines synthesized appeared always as single conformers regarding the diazepine ring, and the sterically demanding substituent present on this ring, the pyrrolidine sugar-linked, assumes always a pseudo-equatorial orientation. This conformational homogeneity of the diazepine ring can be attributed to an amide resonance-imposed requirement for the proline moiety to occupy a pseudo-equatorial orientation on the benzodiazepine ring.

2.1.3.3 Biological Assays^{xxviii}

2.1.3.3.1 Evaluation of Total, Non-Specific and Specific Binding – Saturation Studies

The specific, non-specific and total binding were determined with increasing concentrations of [³H]flunitrazepam^{xxix} (**170**, Fig. 51), 0.05, 0.1, 0.2, 0.8, 1.6, 3.2, 6.4, 12.8, 25.6 nM, in the presence (500 μM) or absence of the non labelled flumazenil (**171**, Fig. 51), a benzodiazepine antagonist. Each test sample contained 50 μL of rat brain cortex membranes with a protein concentration of 0.3 mg/mL. The non-specific binding was determined on aliquots that had equal concentrations of [³H]flunitrazepam and non labelled flumazenil. However, the total binding was measured without the presence of non labelled flumazenil **171**. This non-specific binding represented about 1–2% of the total binding. The non-specific binding was subtracted from the total to give the amount of specific binding, for each concentration.

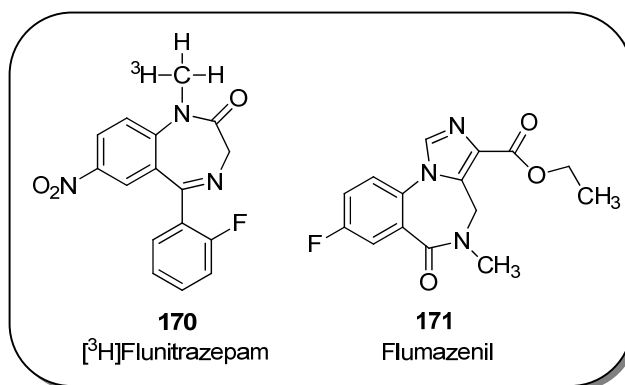


Figure 51. Chemical structure of labelled flunitrazepam and non labelled flumazenil.

^{xxviii} These experiments were performed under the supervision of Prof. Barbara Costa in the Dept. of Biotechnology and Bioscience, University of Milano-Bicocca.

^{xxix} **Flunitrazepam**, trade name Rohypnol®, is a CNS depressant ten times more potent than Valium® **67**, and while commonly prescribed for anxiety and sleep disorders in Europe, Latin America, and elsewhere, it was never approved for use or sale in the United States.

The quantity of [³H]flunitrazepam **170** present in each sample was expressed by the instrument in disintegrations per minute^{xxx} (dpm). Data were transformed from dpm to fmol/mg protein, according to the formula $1\text{nCi} = 2220\text{ dpm}$, i.e. dividing dpm by the specific activity of the radioligand ([³H]flunitrazepam = 80.0 nCi/pmoli) by 2220.

From the saturation binding experiments (Fig. 52) it could be deduced the relationship between binding and ligand concentration. This evaluation allowed to determinate the density of receptors for milligrams of protein, the B_{max} (R₀) (i.e. number of sites), and the equilibrium dissociation constant K_d, which measures the ligand affinity. The values of K_d and B_{max} are 3.324 nM and 38.72 fmol/mg protein, respectively, with a confidence interval of 1.039 nM – 5.609 nM for K_d and 30.10 a 47.33 fmol/mg protein for B_{max}. Therefore, the [³H]flunitrazepam concentration used in our assays fits into the range of K_d.

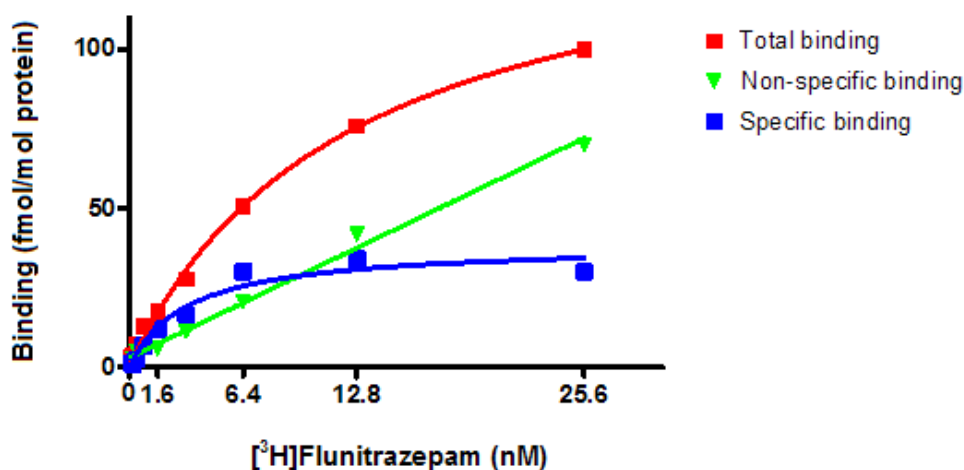


Figure 52. Graphic representation of total, non-specific and specific binding.

^{xxx} **Disintegrations per minute** (dpm) is a measure of radioactivity. Dpm is the number of atoms in a given quantity of radioactive material which had decayed in one minute, not the number of atoms that had been measured as decayed.

2.1.3.3.2 GABA_A R Binding Assays – Competition Studies

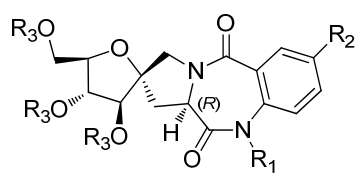
Preliminary biological evaluation of fructose-based pyrrolobenzodiazepines as GABA_A receptor ligands has been performed. In particular, was tested their ability to displace [³H]flunitrazepam from the receptor, using rat cortical membranes to perform a classical competition binding assay. The ability of these new benzodiazepines scaffolds, at a concentration of 100 μM, to bind to GABA_A receptor was determined using [³H]flunitrazepam at a concentration of 1 nM. The radioactivity values obtained from the spectrophotometer in dpm were convert into percentages, considering the value of specific binding 100%, given by the samples only with the [³H]flunitrazepam.

Initial binding assays were performed on D-fructose-based pyrrolobenzodiazepines, compounds **93-96** and **101-104**. The aim was to evaluate the effect of the *N*-methyl in the diazepine and the presence of –NO₂, –NH₂ substituents on the benzene ring. Data showed that compounds **96**, **101** and **104** possess affinity for GABA_A receptor significantly, inhibiting [³H]flunitrazepam binding in the μM range (Table 4). Therefore, we assume that methyl group at position ten together with a substituent on the benzene ring is essential for binding affinity. Subsequently, binding assays were performed on compounds **98**, **100**, **106** and **108** in order to evaluate the effect of halogens on the benzene ring. The exclusion of compounds **97-99** and **105-107** was based on previous data observations which resulted in the inexistent of non methylated compounds **117-118** and **123-124**.^{xxxi} Data showed that both halogens have significantly relevance on binding activity, being compound **106**, with –Cl substituent, more potent. Concerning the effect on binding affinities of free –OH or *O*-benzyl groups of the sugar, we can observe that, among the active compounds, namely **96**, **101**, **104**, **106** e **108**, only compound **96** has *O*-benzyl groups. Additional graphic representations of the binding data shown in Table 4 of benzylated and debenzylated benzodiazepine derivatives (R₁ = H, CH₃; R₂ = H, NO₂, NH₂ and R₃ = Bn, H) are

^{xxxi} In order to minimize the use of rat brain membranes, exclusion of some compounds for biological assays occurred. Animal tests were performed always with a moral scientific perspective.

illustrated in Figures 53 and 54. Almost all the sugar-based water soluble pyrrolobenzodiazepines presented higher binding affinities compared to those benzylated. Therefore, it seems that the hydrophilic groups on the potential drug are determinant on affinity for the benzodiazepine site on GABA_A R. However, the biological activity of these compounds is actually far from that of classical GABA_A modulators, such as the flumazenil **171** (see graphic representations below), which falls in the nM range; nevertheless, this result indicates that they can be considered as lead compounds.

Table 4. Binding competition studies of D-fructose-based pyrrolobenzodiazepines with [³H]flunitrazepam **170** at GABA_A R performed on rat cortical membranes.

Compound				% [³ H]Flunitrazepam specific binding ¹	Significance vs control ²
	R ₁	R ₂	R ₃		
170 (control)	-	-	-	100.00±2.00	—
93	H	H	Bn	111.81±2.33	n.s.
94	CH ₃	H	Bn	96.44±8.85	n.s.
95	H	NO ₂	Bn	101.01±2.10	n.s.
96	CH ₃	NO ₂	Bn	74.89±1.50	P<0.05
98	CH ₃	Cl	Bn	92.94±4.13	n.s.
100	CH ₃	Br	Bn	111.2±12.32	n.s.
101	H	H	H	78.22±7.43	P<0.05
102	CH ₃	H	H	93.04±12.77	n.s.
103	H	NH ₂	H	80.17±9.43	n.s.
104	CH ₃	NH ₂	H	70.63±2.36	P<0.01
106	CH ₃	Cl	H	73.74±7.31	P<0.05
108	CH ₃	Br	H	84.21±2.84	P<0.05

¹ Values are means±SEM determined from at least three independent experiments.

² Statistical analysis is performed with Kruskal-Wallis ANOVA for non parametric values followed by Dunns test; n.s. means not statistically significant and P, probability.

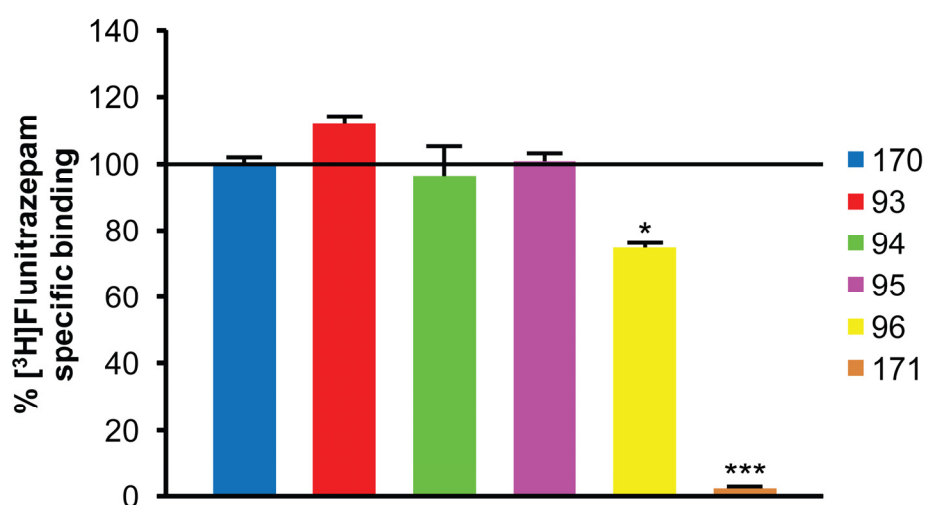


Figure 53. Graphic representation of binding competition studies of benzylated pyrrolobenzodiazepines ($R_1 = \text{H}, \text{CH}_3$ and $R_2 = \text{H}, \text{NO}_2$) derived from D-fructose, and flumazenil **171** with [³H]flunitrazepam **170** at GABA_A R performed on rat cortical membranes (Statistical analysis is performed with Kruskal-Wallis ANOVA).

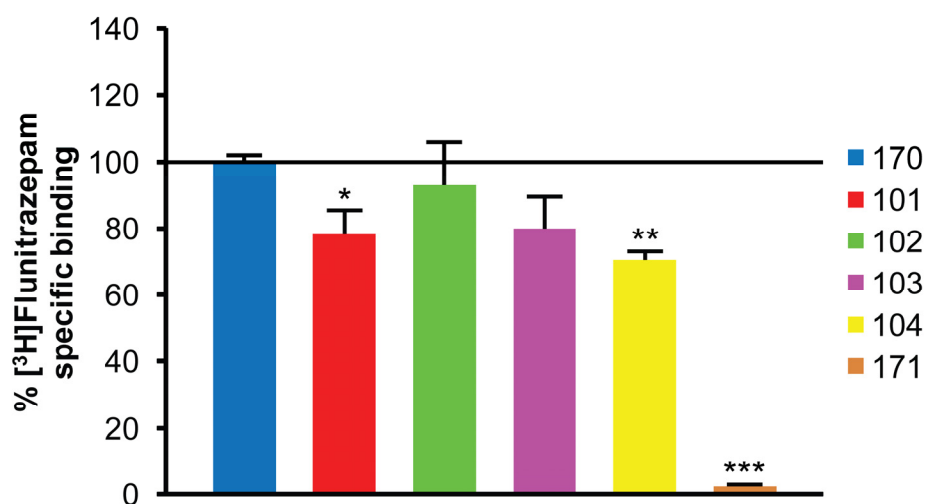
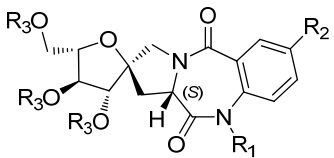


Figure 54. Graphic representation of binding competition studies of debenzylated pyrrolobenzodiazepines ($R_1 = \text{H}, \text{CH}_3$ and $R_2 = \text{H}, \text{NH}_2$) derived from D-fructose, and flumazenil **171** with [³H]flunitrazepam **170** at GABA_A R performed on rat cortical membranes (Statistical analysis is performed with Kruskal-Wallis ANOVA).

In addition, binding assays were performed also on L-fructose-based pyrrolobenzodiazepines, compounds **113-124**. Data illustrated in Table 5 reinforced the previous results obtained for the corresponding enantiomers. Hence, *N*-methyl and a substituent on the benzene ring are fundamental for GABA_A R binding affinity. However, a substituent on the benzene ring is definitely the most relevant effect on binding activity. Biological data demonstrate that -NO₂ and -NH₂ substituents are powerful enough to produce effect even in the absence of *N*-methyl and also with *O*-benzyl groups on the sugar (Figures 55-56). A possible explanation for the binding role of the amine compounds could be that this functional group is involved in hydrogen bonding either as a hydrogen bond acceptor or a hydrogen bond donor. The nitrogen atom has a lone pair of electrons and can act as a hydrogen bond acceptor for one hydrogen bond. In many cases, the amine may be protonated when it interacts with the target binding site. However, it can still act as hydrogen bond donor and formed a stronger hydrogen bond than if it was not ionized.^[3]

As mentioned previous, compounds with -Cl substituent presented highest biological activity respectively to those with -Br substituent. In addition, data showed (Table 5) that compounds **115 > 121 > 123 > 124 > 117 > 116 > 122** possess affinity for GABA_A receptor significantly inhibiting [³H]flunitrazepam binding in the μM range.

Table 5. Binding competition studies of L-fructose-based pyrrolobenzodiazepines with [³H]flunitrazepam **170** at GABA_A R performed on rat cortical membranes.

Compound				% [³ H]Flunitrazepam specific binding ¹	Significance vs control ²
	R ₁	R ₂	R ₃		
170 (control)	-	-	-	100.00±2.40	—
113	H	H	Bn	96.32±3.56	n.s.
114	CH ₃	H	Bn	105.90±4.62	n.s.
115	H	NO ₂	Bn	69.60±1.50	P<0.001
116	CH ₃	NO ₂	Bn	82.82±1.24	P<0.001
117	CH ₃	Cl	Bn	82.33±2.19	P<0.01
118	CH ₃	Br	Bn	93.20±4.88	n.s.
119	H	H	H	109.70±7.71	n.s.
120	CH ₃	H	H	112.20±8.17	n.s.
121	H	NH ₂	H	73.86±4.44	P<0.01
122	CH ₃	NH ₂	H	83.55±2.52	P<0.01
123	CH ₃	Cl	H	77.00±2.27	P<0.001
124	CH ₃	Br	H	82.17±1.69	P<0.01

¹ Values are means±SEM determined from at least three independent experiments.

² Statistical analysis is performed with Kruskal-Wallis ANOVA for non parametric values followed by Dunns test. n.s. means not statistically significant and P, probability.

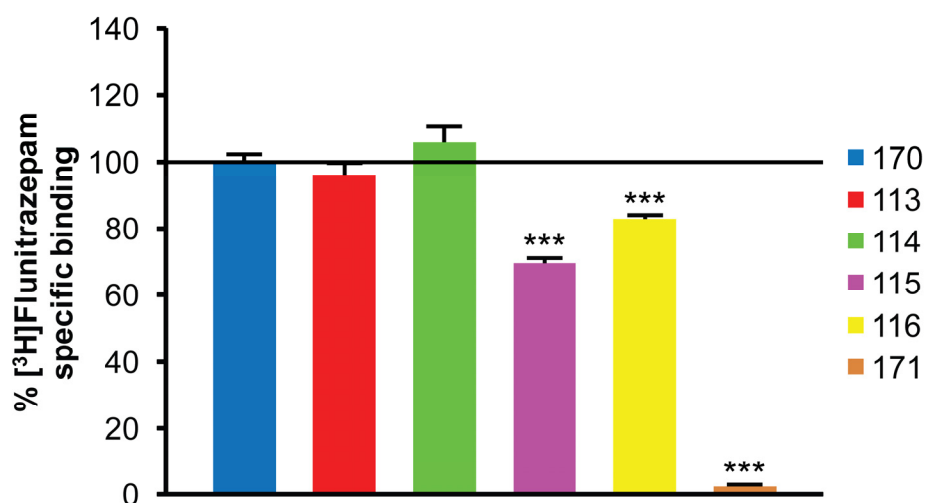


Figure 55. Graphic representation of binding competition studies of benzylated pyrrolobenzodiazepines ($R_1 = \text{H}, \text{CH}_3$ and $R_2 = \text{H}, \text{NO}_2$) derived from L-fructose, and flumazenil **171** with [³H]flunitrazepam **170** at GABA_A R performed on rat cortical membranes (Statistical analysis is performed with Kruskal-Wallis ANOVA).

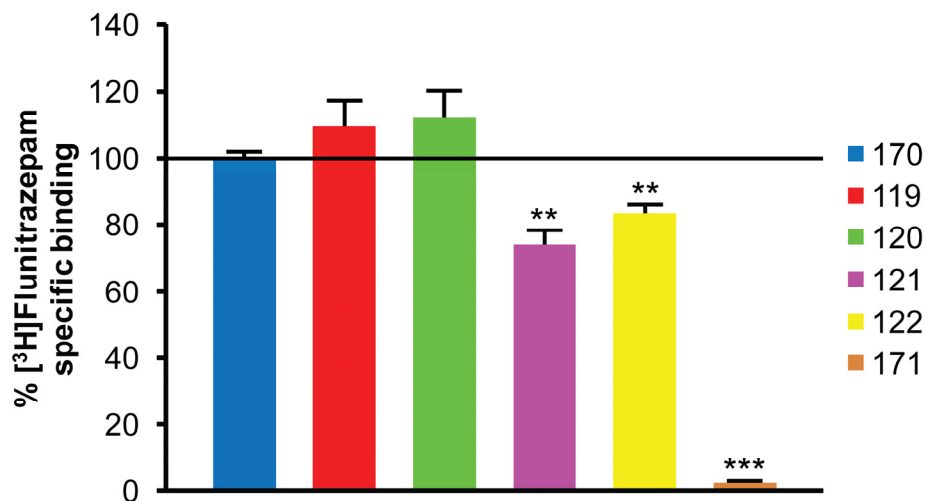


Figure 56. Graphic representation of binding competition studies of debenzylated pyrrolobenzodiazepines ($R_1 = \text{H}, \text{CH}_3$ and $R_2 = \text{H}, \text{NH}_2$) derived from L-fructose, and flumazenil **171** with [³H]flunitrazepam **170** at GABA_A R performed on rat cortical membranes (Statistical analysis is performed with Kruskal-Wallis ANOVA).

Additionally, Figures 57-58 illustrate the effects of the halogenated benzodiazepines derivated from D- and L-fructose, respectively, in the [³H]flunitrazepam specific binding to GABA_A receptor performed on rat cortical membranes. It is clearly perceptible that -Cl gives higher binding affinity compared to -Br substituent in both D- and L-fructose derived compounds. Hence, we can observe that benzodiazepines derived from L-fructose (Fig. 58), which adopt the (*M*) conformation, showed a small increase of their biological activity relative to benzodiazepines derived from D-fructose (Fig. 57).

Finally, to complete our evaluation we performed binding assays of the synthesized pyrrolobenzodiazepines derived from the free amino acid D- and L-proline (i.e. without the sugar moiety). Again the ability of these compounds (**166-169**, Fig. 59) to bind to GABA_A R was determined using [³H]flunitrazepam **170**. These compounds when compared to the corresponding benzodiazepine derivatives with the sugar moiety, namely compounds **93/101** and **96**, and **113/119** and **116**, showed binding activities slightly higher. In particular, the most potent fructose-proline-benzodiazepine derivative (compound **115**), showed 30% reduction of the radioligand specific binding, while the most active pyrrolobenzodiazepine, compound **169**, gave a 40% reduction (Table 6 and Fig. 60). This difference does not seem to be considerably relevant, so we can assume that the fructose moiety does not cause significant steric hindrance on binding to the receptor.

In addition, we can also observe that pyrrolobenzodiazepines without *N*-methyl or -NO₂ substituent, independently of being derived from D- or L-proline, show almost none binding affinity to the receptor. Once more we can observe that functionalization of the benzodiazepine scaffold is more relevant than the stereochemistry of the C-11a. Only with suitable substituents the pyrrolobenzodiazepines with (11a*S*) configuration show more binding affinity than those with (11a*R*) configuration.

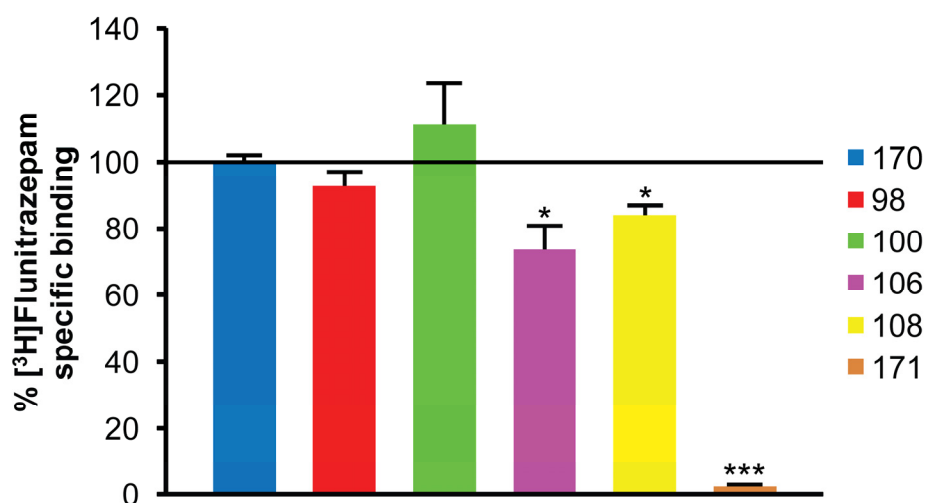


Figure 57. Graphic representation of binding competition studies of halogenated pyrrolobenzodiazepines derived from D-fructose, and flumazenil **171** with [³H]flunitrazepam **170** at GABA_A R performed on rat cortical membranes (Statistical analysis is performed with Kruskal-Wallis ANOVA).

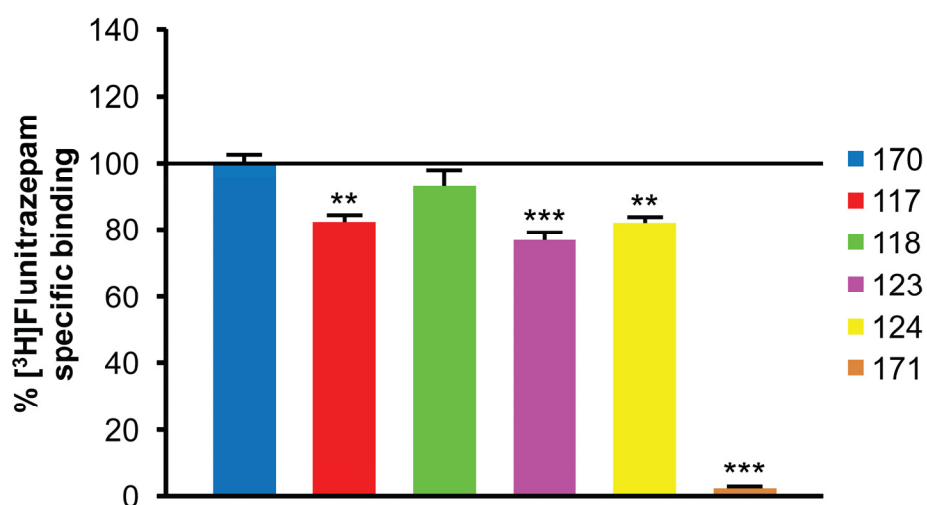


Figure 58. Graphic representation of binding competition studies of halogenated pyrrolobenzodiazepines derived from L-fructose, and flumazenil **171** with [³H]flunitrazepam **170** at GABA_A R performed on rat cortical membranes (Statistical analysis is performed with Kruskal-Wallis ANOVA).

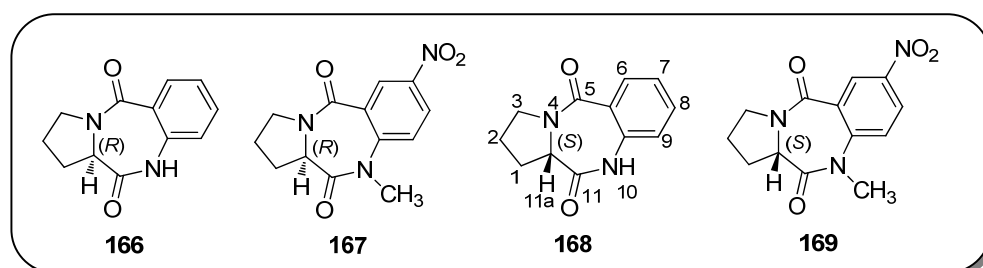


Figure 59. Chemical structure of synthesized pyrrolobenzodiazepines derived from the free amino acid D- and L-proline.

Table 6. Binding competition studies of pyrrolobenzodiazepines derived from D- and L-proline with [³H]flunitrazepam **170** at GABA_A R performed on rat cortical membranes.

Compound	% [³ H]Flunitrazepam specific binding ¹	Significance vs control ²
170 (control)	100.00±1.49	–
166	97.00±0.91	n.s.
167	80.25±3.68	P<0.05
168	95.50±2.47	n.s.
169	63.40±1.57	P<0.001

¹ Values are means±SEM determined from at least three independent experiments.

² Statistical analysis is performed with Kruskal-Wallis ANOVA for non parametric values followed by Dunns test.

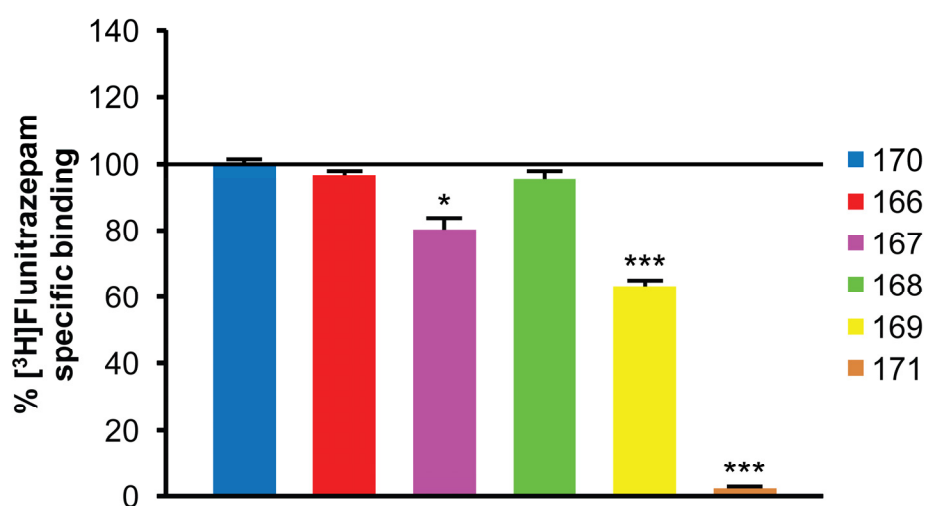


Figure 60. Graphic representation of binding competition studies of pyrrolobenzodiazepines derived from D- and L-proline, and and flumazenil **171** with [³H]flunitrazepam **170** at GABA_A R performed on rat cortical membranes (Statistical analysis is performed with Kruskal-Wallis ANOVA).

Summarizing, we observed that for D-fructose-based pyrrolobenzodiazepines, (*P*) conformers, a *N*-methyl in the diazepam and the presence of hydroxyl groups in the sugar favoured binding activity (hydrophilic effect predominant), and that substituents on the benzene ring increased affinity of the ligand for the binding site in the following order: $\text{NH}_2 > \text{Cl} > \text{NO}_2 > \text{Br}$. Although, the L-fructose-based pyrrolobenzodiazepines, (*M*) conformers, showed that *N*-methyl decreases binding activity, and benzyl groups in the sugar have slit increased on binding (lipophilic effect predominant). Concerning benzene ring substituents, the affinity increased in the following order: $\text{NO}_2 > \text{NH}_2 > \text{Cl} > \text{Br}$.

Moreover, we observed that the D-fructose-based pyrrolobenzodiazepines, which possess a (*P*)-helical conformation, presented binding affinities similar to those showed for the (*M*) conformers, the L-fructose-based pyrrolobenzodiazepines, even if in literature is reported as being the opposite conformation to that required for best binding to GABA_A receptor. The sugar moiety seemed to not cause significant steric hindrance on binding to the receptor in both conformers.

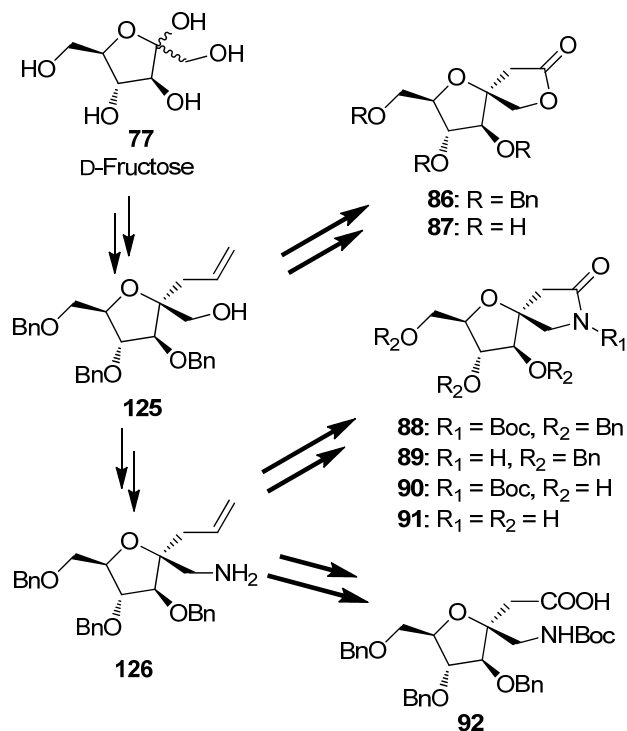
2.1.4 Fructose-Based γ -Butyrolactones and -Lactams, and a GABA Analogue

2.1.4.1 Synthesis

Synthesis of sugar-based β -disubstituted γ -butyrolactones **86-87** and γ -butyrolactams **88-91** are described here, as well as a lipophilic β -disubstituted GABA analogue **92**. These compounds are potential GABA receptor ligands, where the pharmacophore is engineered into the carbohydrate scaffold (Scheme 21).

The fructose moiety acts as a versatile scaffold, rich in stereochemistry and having a relatively rigid skeleton. For a GABA receptor ligand, penetration of BBB is required, and lipophilicity is the most important parameter that crucially influences this penetration, as previously discussed (see chapter 1.2.4). Therefore, the additional

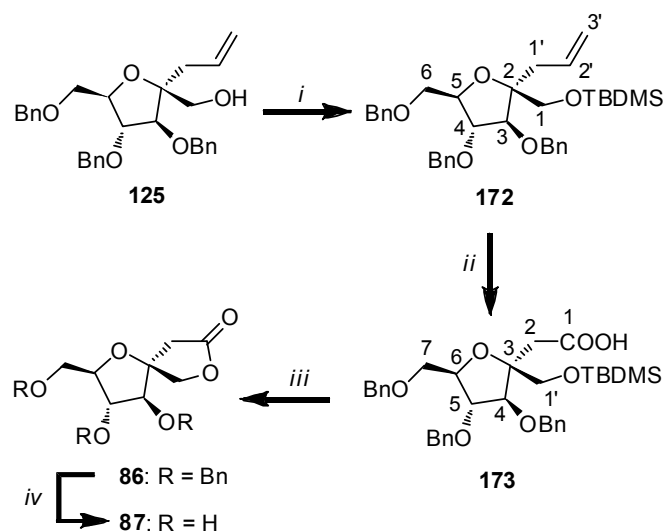
hydroxyl derivatization of the fructose scaffold may be used to increase lipophilicity, as well as to modulate the activity of pharmacophores or the receptor specificity.



Scheme 21. Synthetic pathway towards GABA receptor ligands **86–92**.

The synthesis of compounds **86–92** requires access to the key intermediates **125** and **126**, which synthesis was described in Schemes 5 and 7, respectively. The anomeric position and the hydroxyl group at C-1 of fructose were exploited for the construction of the butyrolactone or -lactam rings with a spiro junction to the carbohydrate scaffold.

GABA lactones **86–87** were synthesised *via* key intermediate 3-*C*-(3,4,6-tri-*O*-benzyl- α -D-fructofuranos-2-yl)propene (**125**), which was protected at the free hydroxyl group with *tert*-butyldimethylchlorosilane (TBDMSCl) and imidazole in dry DMF under reflux affording the corresponding *tert*-butyldimethylsilyl ether **172** (90% yield, Scheme 22).

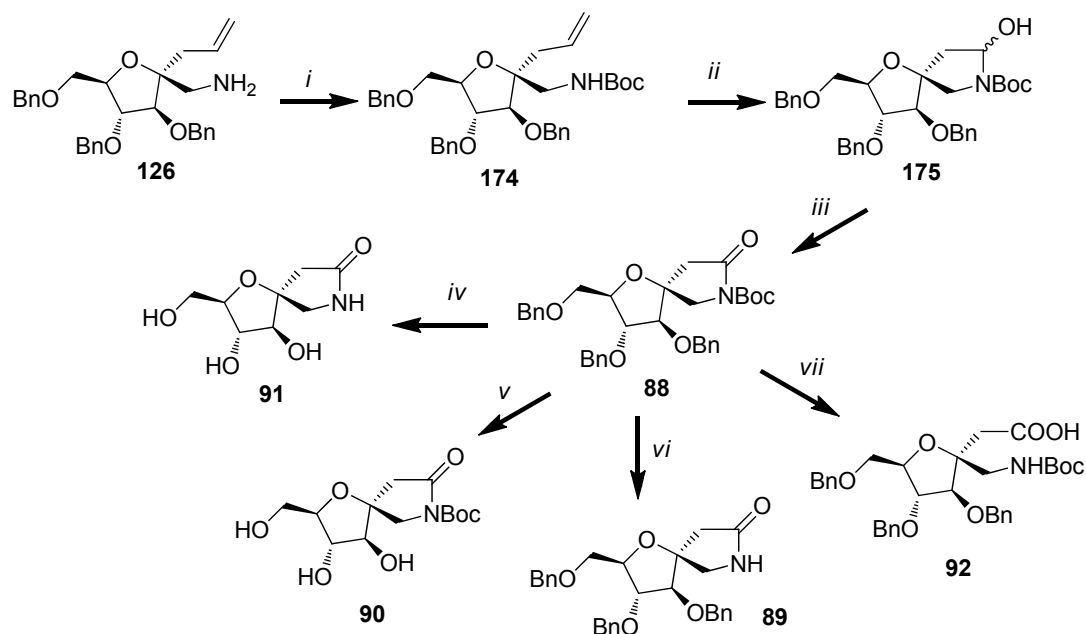


Scheme 22. Reagents and conditions: *i*. TBDMSCl, imidazole, dry DMF, reflux, 12h, 90%; *ii*. 1. 0.016 M OsO₄ in ^tBuOH, NaIO₄, H₂O/acetone/^tBuOH 1:1:1, rt, 2h 30 min; 2. 1.25 M NaH₂PO₄·2H₂O, NaClO₂, CH₃CN, rt, 3h, 71% yield over 2 steps; *iii*. TFA/H₂O 9:1, CH₂Cl₂, rt, 1h, 94% yield; *iv*. H₂, Pd(OH)₂/C, HCl 37%, CH₃OH/EtOAc 4:1, rt, 12h, 95%.

Oxidative cleavage of the double bond in the *C*-propenyl appendage of compound **172** in a two step degrading oxidation by reaction with osmium tetroxide/sodium periodate,^[168] followed by treatment with NaH₂PO₄/NaClO₂^[169] (71% yield over two steps) afforded the acid **173**, possessing the carboxylic function suitably positioned for the formation of the γ -butyrolactone ring. Attempts to oxidise the double bond of **125** without hydroxyl protection resulted in low yields of the desired product. Acidic hydrolysis of the silyl ether with aqueous trifluoroacetic acid in dichloromethane gave benzylated γ -lactone **86**. Debonylation by hydrogenolysis using palladium hydroxide as catalyst afforded fully deprotected hydrophilic lactone **87** (95% yield).

The synthesis of γ -butyrolactams **88–91** and GABA analogue **92** takes advantage, once again, of the *C*-propenyl substituent for the introduction of the carboxylic group. Replacement of the hydroxyl group at C-1 of fructose by the amino functionality is also required. To this end, the key intermediate **126** was synthesised from alcohol **125** (Scheme 7) and subsequently transformed into compounds **88–92** (Scheme 23).

The amine derivative **126** is a starting material for the synthesis of the key intermediate γ -butyrolactam **88**. Protection of amine **126** with Boc anhydride (or *tert*-butyldicarbonate) and triethyl amine afforded compound **174**. Oxidative cyclization of **174** to the corresponding lactam **88** proceeded in a two-step fashion by initial osmilation/ NaIO_4 oxidation to the hemiaminal **175**, followed by further oxidation using pyridinium chlorochromate (PCC).^[170] Hydrolysis of lactam **88** using 1M aq. soln. of lithium hydroxide provided the Boc-protected GABA analogue **92** in 61% yield. Any attempt to obtain a fully deprotected GABA analogue failed. Hydrogenolysis of lactam **88** using palladium hydroxide as catalyst in the presence of hydrochloric acid afforded fully deprotected and hydrophilic γ -lactam **91** (74% yield); on the contrary, hydrogenolysis with the same catalyst in the presence of acetic acid afforded the debenzylated *N*-Boc lactam **90** (70% yield). Finally, treatment of lactam **88** with aqueous trifluoroacetic acid gave sugar benzylated deprotected lactam **89** (76% yield).



Scheme 23. Reagents and conditions. *i.* Boc_2O , TEA, CH_2Cl_2 , rt, 12h, 87%; *ii.* 1. 0.016M OsO_4 in $t\text{-BuOH}$, NMO, $\text{THF}/\text{H}_2\text{O}$ 1:1, rt, 5h; 2. NaIO_4 , $\text{THF}/\text{H}_2\text{O}$ 1:1, 3h, 85% yield; *iii.* PCC, 4 Å m.s., CH_2Cl_2 , rt, 2h, 78% yield; *iv.* H_2 , $\text{Pd}(\text{OH})_2/\text{C}$, HCl 37%, $\text{CH}_3\text{OH}/\text{EtOAc}$ 4:1, rt, 12h, 74% yield; *v.* H_2 , $\text{Pd}(\text{OH})_2/\text{C}$, acetic acid, $\text{CH}_3\text{OH}/\text{EtOAc}$ 4:1, rt, 12h, 70% yield; *vi.* TFA/ H_2O 8:2, CH_2Cl_2 , rt, 2h, 76% yield; *vii.* aq. soln 1 M $\text{LiOH}\cdot\text{H}_2\text{O}$, THF, rt, 2h, 61% yield.

2.1.4.2 Biological Evaluation

2.1.4.2.1 Evaluation of Total, Non-Specific and Specific Binding – Saturation Studies

The specific, non-specific and total binding were determined with increasing concentrations of [³H]muscimol (**176**, Fig. 61), 0.05, 0.1, 0.2, 3.0, 10.0, 20.0, 30.0, 50.0, 75.0 nM, in the presence or absence of the non labelled muscimol **177** (500 μM). Each test sample contained 50 μL of rat whole brain membranes with a protein concentration of 0.1 mg/mL. The non-specific binding was determined on aliquots that had equal concentrations of [³H]muscimol and non labelled muscimol. Hence, the total binding was measured without the presence of non labelled muscimol **177** (Fig. 62). This non-specific binding represented about 30–40% of the total binding. The non-specific binding was subtracted from the total to give the amount of specific binding, for each concentration.

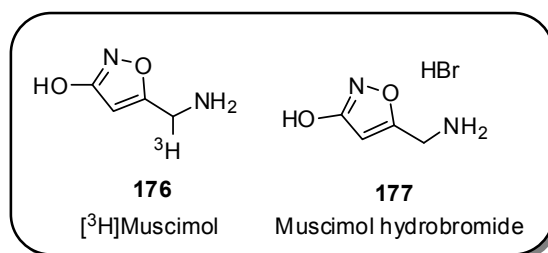


Figure 61. Chemical structure of [³H]muscimol and non labelled muscimol.

The quantity of [³H]muscimol **176** present in each sample was expressed by the instrument in disintegrations per minute (dpm). Data were transformed from dpm to fmol/mg protein, according to the formula $1\text{ nCi} = 2220\text{ dpm}$, i.e. dividing dpm by the specific activity of the radioligand ([³H]muscimol = 36.6 nCi/pmoli) by 2220.

From the saturation binding experiments (Fig. 62) we can deduce the relationship between binding and ligand concentration. This evaluation allows to determine the density of receptors for milligrams of protein, the B_{max} (R_0) (i.e. number of sites), and the equilibrium dissociation constant K_d , which measures the ligand affinity. The

values of K_d and B_{max} are 11.59 nM and 182.9 fmol/mg protein, respectively, with a confidence interval of 4.077 nM – 19.10 nM for K_d and 147.9 a 217.9 fmol/mg protein for B_{max} . Therefore, the [3H]muscimol concentration used in our assays fits into the range of K_d .

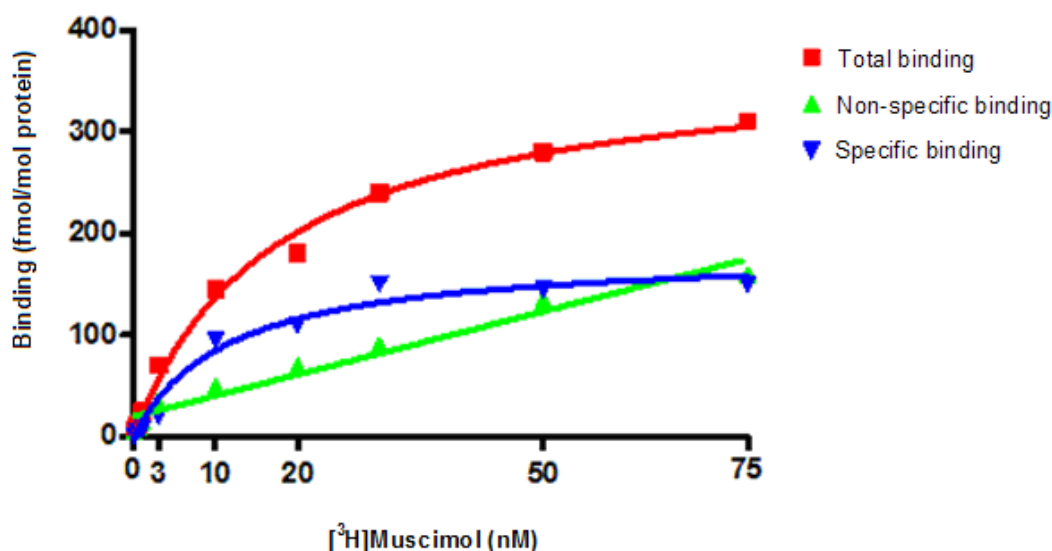


Figure 62. Graphic representation of total, non-specific and specific binding.

2.1.4.2.2 GABA_A R Binding Assays – Competition Studies

The ability of compounds **86-92** (Fig. 63) to bind to GABA_A receptor, at a concentration of 500 μ M, was determined using [3H]muscimol (a powerful agonist of GABA_A R, at a concentration of 10 nM) and rat brain membrane preparations. The results of this competition binding assay are reported in Table 7. The radioactivity values obtained from the spectrophotometer in dpm were converted into percentages, considering the value of specific binding 100%, given by the samples only with the [3H]muscimol.

Data show that compounds **86, 87, 88** and **90** possess affinity for GABA_A receptor significantly inhibiting [3H]muscimol binding in the μ M range. Particularly, the most

potent compound in the displacement binding study is the *N*-Boc protected lactam **90** with a 40% reduction of [³H]muscimol specific binding. Graphic representation of Table 7 data is illustrated in Figure 64.

Table 7. Binding competition studies of GABA derivatives with [³H]muscimol **176** at GABA_A R performed on rat cerebral membranes.

Compound	%[³ H]Muscimol specific binding ¹	Significance vs control ²
176 (control)	100.00±3.053	–
86	75.55±1.013	P<0.01
87	77.84±0.446	P<0.05
88	70.77±4.391	P<0.05
89	76.75±0.029	n.s.
90	60.42±6.668	P<0.05
91	96.80±1.976	n.s.
92	99.33±2.073	n.s.

¹ Values are means±SEM determined from at least three independent experiments.

² Statistical analysis is performed with Kruskal-Wallis ANOVA for non parametric values followed by Dunns test.

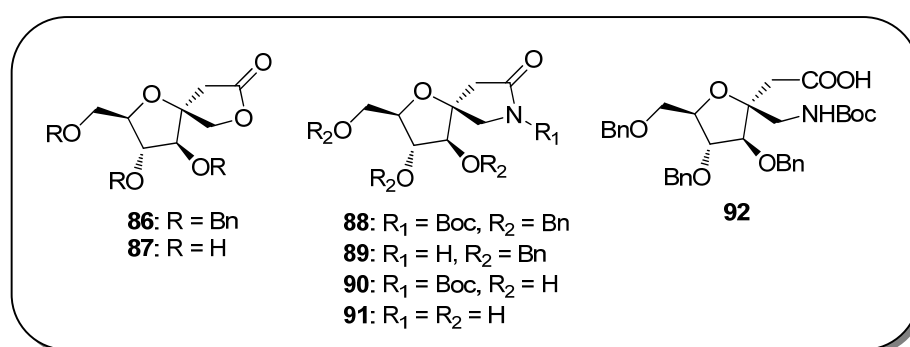


Figure 63. Chemical structure of synthesized sugar-based GABA analogues **86-92**.

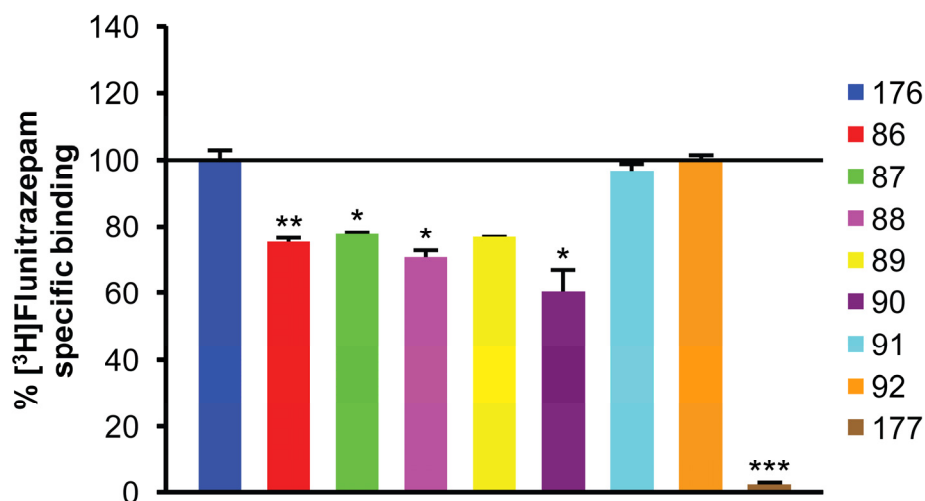


Figure 64. Graphic representation of binding competition studies of GABA analogues **86-92** derived from D-fructose, and non labelled muscimol **177** with [³H]muscimol **176** at GABA_A R performed on rat cerebral membranes (Statistical analysis is performed with Kruskal-Wallis ANOVA).

Biological data evidence that both butyrolactones **86-87**, and *N*-substituted lactams **88** and **89** are able to displace tritiated muscimol from the corresponding binding site in the GABA_A R. By this preliminary evaluation we can observed that the sugar moiety does not seem to hinder the binding, since both benzylated and deprotected lactones and lactams showed to have comparable activity. Hence, the carbohydrate moiety can effectively be used to modulate drug pharmacokinetic properties and lipophilicity. It is shown that the hydrophobic nature of benzyl groups can facilitate BBB crossing, which is one of the main issues to be addressed for CNS directed drugs. As mention previous, GABA receptor ligand action requires penetration of the BBB, so lipophilicity is one of the most important parameter that crucially influences its penetration. Another possible reason for these biological activities is that anticonvulsant activity can be increased by bulky side chains, in additional Boc, having an amide group are likely to interact with the binding site through hydrogen bonding, and the carbonyl oxygen atom can act as a hydrogen bond acceptor.

*Conclusão a sucata!...
Fiz o cálculo,
Saiu-me certo, fui elogiado...
Meu coração é um enorme estrada
Onde se expõe um pequeno animálculo...*

*A, microscópio de desilusões
Fizêi, prolixo nas minúcias fúteis...
Minhas conclusões práticas, inúteis...
Minhas conclusões teóricas, confusões...*

*Que teorias há para quem sente
O cérebro quebrar-se, como um dente
Dum pente de mendigo que emigrou?*

*Fecho o caderno dos apontamentos
E faço riscos moles e cinzentos
Nas costas do envelope do que sou...*

Álvaro de Campos



*Van Gogh's Chair, 1888
Vincent van Gogh*

CONCLUSIONS

Synthesis of novel and rigid 1,4-benzodiazepine-2,5-dione scaffolds derived from spiro bicyclic D- or L-proline analogues, containing a D-fructose or a L-fructose moiety, was accomplished. The D-proline analogue was synthesised from D-fructose in sixteen-steps and 24% overall yield through a three carbon chain elongation at the anomeric position, introduction of the amino function at C-1, cyclization to pyrrolidine and introduction of the carboxylic group. The spiro bicyclic L-proline analogue was obtained either starting from sorbose *via* a nineteen steps synthesis in 2% overall yield or starting from arabinose through a pathway involving eighteen steps in 3% overall yield. Both pathways make use of the key intermediate 3-*C*-(3,4,6-tri-*O*-benzyl- α -L-fructofuranos-2-yl)propene. In this work a new method was developed for its synthesis taking advantage of the stereochemistry of the arabinonolactone, easily obtained by oxidation of the anomeric position. Chain elongation was then accomplished by reaction with 2-lithium-1,3-dithiane, subsequent formation of the aldehyde and final reduction to the primary alcohol gave the target molecule in 13.5% overall yield. This method is more efficient than the procedure reported in the literature for L-fructose synthesis using sorbose. The latter pathway involved various protection and deprotection steps, in addition to oxirane ring formation and opening to build the appropriate sugar stereochemistry and led to the preparation of the key precursor in 8.5% overall yield. Starting from this key precursor, and using the methodology applied for the D-proline analogue, which requires subsequent eleven steps, the desired new spiro bicyclic L-proline analogue was obtained in 24% overall yield.

Conformational analysis, performed by Molecular Modelling calculations and DNMR data, established the absence of conformational equilibrium in the benzodiazepine ring of the fructose-proline-benzodiazepine scaffolds synthesized. These studies showed a unique preferential conformation of the benzodiazepine ring for each enantiomer. The D-proline analogue induced a rigid (*P*)-helical conformation and the L-proline analogue induced a rigid (*M*)-helical conformation on the 1,4-benzodiazepine-2,5-dione ring, where the fused bicyclic moiety is pseudo-

equatorial for both conformers. The conformational rigidity of the pyrrolobenzodiazepine *core* linked to the fructose by a spiro junction, allowed an accurate evaluation of the effect of conformational changes in the 1,4-benzodiazepine-2,5-dione ring on the ability of benzodiazepines to bind to the receptor complex, clarifying the stereoselectivity of this binding site.

Several literature reports showed that binding affinities at GABA_A R are sensitive to the helical chirality of the 1,4-benzodiazepine ring and that the (*M*)-helical conformation is required for best binding to GABA_A R. However, preliminary biological evaluation of the synthesized enantiomeric benzodiazepine derivatives showed that the conformation of the benzodiazepine ring was not the determining factor for best binding. We observed that both conformers have similar binding affinities. So, it appears that the receptor binding is governed mainly by the pseudo-equatorial preference of the C-11a substituent instead of (*M*) or (*P*) conformation.

In addition, we observed that binding is crucially dependent on the type of substituents present in the sugar (benzyl or hydrogen on the fructose moiety), in the nitrogen N10 (hydrogen or methyl) or in the benzene ring (halogen, nitro or amino). We concluded that substituents in position seven are essential for binding affinity, being -Br the less effective one. The D- and L-fructose-based pyrrolobenzodiazepines substituted with amino or nitro groups in the benzene ring showed the highest affinity for GABA_A R, in the range of μM . In general, benzodiazepines with an *N*-methyl in the diazepine and free hydroxyl groups in the sugar showed higher ability to displace tritiated flunitrazepam from the corresponding binding site in the GABA_A R.

Moreover, pyrrolobenzodiazepines synthesized without a sugar moiety showed binding activities slightly higher than those linked to a sugar moiety. In particular, the most potent fructose-proline-benzodiazepine derivative showed 30% reduction of the radioligand specific binding, while the most active pyrrolobenzodiazepine derivative without sugar moiety gave a 40% reduction. This difference does not seem to be

considerably relevant, so it can be assumed that the fructose moiety does not cause significant steric hindrance on binding to the receptor.

In addition, synthesis of novel D-fructose-based β -disubstituted γ -butyrolactones and γ -butyrolactam, and a lipophilic GABA analogue was also been accomplished in high overall yield (35%–58% yield range). The preliminary biological evaluation of such compounds as GABA receptor ligands showed that the γ -butyrolactone derivatives have the lowest binding activities when compared to γ -butyrolactam derivatives. However, they were able to displace 25% of tritiated muscimol from the corresponding binding site. *N*-Boc substituted γ -butyrolactone derivatives were more effective than the open chain GABA analogue. Substituents present on the fructose moiety did not seem to hinder the binding, as both benzylated and debenzylated lactones and lactams had comparable activity. The hydrophobic nature of benzyl groups may facilitate BBB crossing, which is one of the main issues to be addressed for CNS directed drugs.

In summary, this work generated the first library of pyrrolobenzodiazepines, lactones and lactams, spiro linked to a sugar moiety, significantly relevant for the elucidation of determinant aspects on GABA_A R binding.

*Nervos à flor da pele – desnudos
Eriçam-me o divino inconsciente
Da minha ignorância sabedora*

*Lutamos contra a maré viva da ciência
Teorizando especulações desconexas
E rangeram-me os dentes
Quis morder o cerne
Mordi antes a língua salgada*

*A paixão à razão morreu
Andava perdida nas teias do conhecimento
Estudava irreconhecível
E resultava em alienação perfeita!*

*Depois esperava ansiando a rapidez
Surpreendia-se por vezes
Num intuito sonhador resistia
Mas nunca baixou os braços
Tornou-se forte. Sabia?*



*Pair of Shoes, 1888
Vincent van Gogh*

EXPERIMENTAL SECTION

4.1 Organic Synthesis

4.1.1 General Methods

4.1.1.1 Dry Solvents and Reactions

All solvents were dried over molecular sieves (Fluka), for at least 24h prior to use. When dry conditions were required, the reactions were performed under argon atmosphere.

4.1.1.2 Preparation of 2-Iodoxybenzoic Acid (IBX)

The IBX is prepared from 2-iodobenzoic acid and potassium monopersulfate triple salt ($2\text{KHSO}_5\cdot\text{KHSO}_4\cdot\text{K}_2\text{SO}_4$). To a solution of 2-iodobenzoic acid (8 g, 0.032 mol) in H_2O (200 mL) at 100 °C, potassium monopersulfate triple salt (44 g, 0.143 mol) was added. The resulting suspension was vigorously stirred until complete dissolution of both reagents in the solvent. After 2h the resulting mixture was filtered with cold acetone and recrystallized.

4.1.1.3 Thin-Layer Chromatography

Thin-layer chromatography (TLC) was performed on Silica Gel 60-F254 plates (Merck) with detection with UV detection, or using a developing solution of conc. $\text{H}_2\text{SO}_4/\text{EtOH}/\text{H}_2\text{O}$ in a ratio of 5:45:45 followed by heating at 180 °C.

4.1.1.4 Flash Column Chromatography

Flash column chromatography was performed on Silica Gel 230-400 mesh (Merck). The boiling range of petroleum ether used as eluent in column chromatography is 40-60 °C.

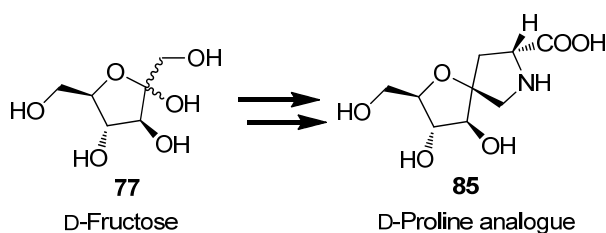
4.1.1.5 Mass Spectroscopy

Mass spectra were recorded on a MALDI2 Kompact Kratos instrument, with gentisic acid (DHB) as the matrix.

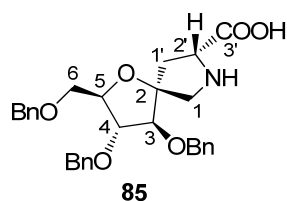
4.1.1.6 NMR Spectroscopy

NMR spectra were recorded at 400 MHz (^1H) and at 100.57 MHz (^{13}C) on a Varian MERCURY instrument and or on a Bruker Avance 400 spectrometer, at 300 K unless otherwise stated. Chemical shifts values (δ) are reported in ppm downfield from tetramethylsilane (TMS) as an internal standard and J values are given in Hz. The atoms of the sugar moiety were numbered for NMR purposes. Atoms numbering are represented in the chemical structure of each compound type and some of them do not follow the IUPAC rules.

4.1.2 Synthesis of the Spiro D-Proline Analogue

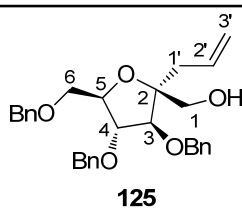


Scheme 24



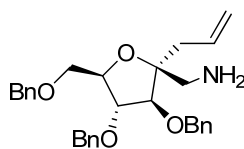
**Spiro{(1',4'-anhydro-2',3',5'-tri-O-benzyl-D-arabinitol)-1',4'-
-[(2R)-pyrrolidine-2-carboxylic acid]}**

Compound 85. To a solution of **140** (0.250 g, 0.344 mmol) in dry CH₃CN (15 mL) diethylamine (288 μL, 2.755 mmol) was added at rt under argon atmosphere. After 2h the reaction mixture was neutralized with acetic acid and concentrated. The crude was washed several times with petroleum ether, to removed Fmoc products, affording compound **85**, as an amorphous solid (0.128 g, 74 % yield). **MS (MALDI-TOF):** *m/z* 504 [M + H]⁺, 527 [M + Na]⁺, 543 [M + K]⁺. **Elemental analysis calcd (%)** for C₃₀H₃₃NO₆: C, 71.55; H, 6.60; N, 2.78; found: C, 71.58; H, 6.57; N, 2.81. **¹H NMR** (400 MHz, CDCl₃): δ (ppm) 7.80-6.92 (m, 15 H, OCH₂Ph), 4.52-4.37 (m, 6 H, OCH₂Ph), 4.25 (dd, 1 H, J = 13.9, 7.1 Hz, H-2'), 4.12 (bs, 1 H, H-5), 3.93-3.90 (m, 2H, H-3, H-4), 3.66 (d, 1 H, J = 12.9 Hz, H-1a), 3.55 (dd, 1H, J = 9.7, 5.5 Hz, H-6a), 3.42 (dd, 1H, J = 9.7, 6.8 Hz, H-6b), 3.29 (d, 1 H, J = 12.6 Hz, H-1b), 2.56 (dd, 1 H, J = 13.9, 7.1 Hz, H-1'a), 2.03 (dd, 1 H, J = 13.9, 12.2 Hz, H-1'b). **¹³C NMR** (100.57 MHz, CDCl₃): δ (ppm) 177.22 (C-3'), 138.15, 137.73, 137.47 (Cq Ph), 92.90 (C-2) 86.30, 83.40, 82.51 (C-3, C-4, C-5), 73.64, 72.02, 71.93, 70.61 (OCH₂Ph, C-6), 61.70 (C-2'), 43.04 (C-1), 30.11 (C-1').



3-C-(3,4,6-tri-O-benzyl-D-fructofuranos-2-yl)propene

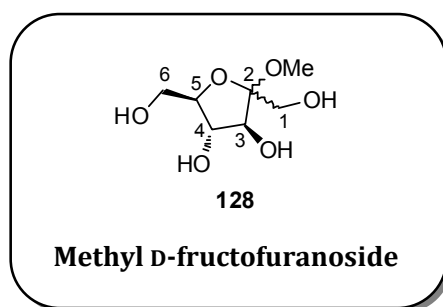
Compound 125. Iodoether mixture **131** (0.250 g, 0.416 mmol) was dissolved in 1:1 Et₂O/EtOH (15 mL) and dust Zn (0.136 g, 2.08 mmol) and acetic acid glacial (50 μL) were added. After stirring for 24 h, the suspension was filtered, and the solvent was evaporated. The residue was dissolved in CH₂Cl₂ and the solution was washed with 5% aqueous HCl. The organic layer was dried (Na₂SO₄), filtered and concentrated in vacuo. The crude residue was purified by flash chromatography (petroleum ether/EtOAc, 8:2) to afford **125** (0.158 g, 80%) as a colorless oil. **MS (MALDI-TOF):** *m/z* 498 [M + Na]⁺, 514 [M + K]⁺. **Elemental analysis calcd (%)** for C₃₀H₃₄O₅: C, 75.92; H, 7.22, found: C, 76.03; H, 7.25. **¹H-NMR** (400 MHz, CDCl₃): δ (ppm) 7.38-7.27 (m, 15H, OCH₂Ph), 5.83 (m, 1H, H-2'), 5.09 (d, 1H, *J* = 10.3 Hz, H-3'a), 4.97 (dd, 1H, *J* = 17.2 Hz, H-3'b), 4.72 (m, 6H, OCH₂Ph), 4.45 (t, 1H, *J* = 7.3 Hz, H-4), 4.12 (d, 1H, *J* = 7.3 Hz, H-3), 3.92 (td, 1H, *J* = 7.3, 3.2 Hz, H-5), 3.72 (m, 2H, H-1a, H-6a), 3.52 (m, 2H, H-1b, H-6b), 2.30 (dd, 1H, *J* = 13.9, 6.2 Hz, H-1'a), 2.18 (dd, 1H, *J* = 13.9, 8.0 Hz, H-1'b), 1.60 (bs, 1H, OH). **¹³C-NMR** (100.57 MHz, CDCl₃): δ (ppm) 132.98 (C-2'), 119.12 (C-3'), 84.33 (C-2), 86.71, 83.56, 79.40 (C-3, C-4, C-5), 73.70, 73.23, 73.21, 69.71, 66.43 (C-1, C-6, OCH₂Ph), 40.41 (C-1').



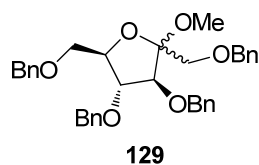
126

**1-Amino-2,5-Anhydro-3,4,6-tri-O-benzyl-1-deoxy-
-2-C-(prop-2-enyl)-D-glucitol**

Compound 126. Oxime derivative **133** (0.250 g, 0.513 mmol) was dissolved in dry THF (5 mL), and 800 μ L of 1M LiAlH₄ solution in THF were added. The reaction mixture was stirred overnight, and then quenched with EtOAc; the precipitate was filtered off, and the solvent evaporated under reduced pressure. Purification by flash chromatography (EtOAc/EtOH 6:4), afforded amine derivative **126** (quantitative yield) as a colourless oil. **MS (MALDI-TOF):** m/z 474.6 [M + H]⁺, 497.6 [M + Na]⁺, 512.6 [M + K]⁺. **Elemental analysis calcd (%)** for C₃₀H₃₅NO₄: C, 76.08; H, 7.45; N, 2.96, found: C, 76.10; H, 7.48; N, 2.93. **¹H-NMR** (400 MHz, CDCl₃): δ (ppm) 7.43-7.18 (m, 15H, OCH₂Ph), 5.85-5.77 (m, 1H, H-2'), 5.13 (d, 1H, J = 10.0 Hz, H-3'a), 5.07 (d, 1H, J = 17.8 Hz, H-3'b), 4.68-4.51 (m, 8H, OCH₂Ph, NH₂), 4.21 (dd, 1H, J = 7.0, 5.5 Hz, H-4), 4.09 (d, 1H, J = 5.5 Hz, H-3), 4.00 (dt, 1H, J = 7.0, 4.0 Hz, H-5), 3.68 (dd, 1H, J = 10.6, 4.0 Hz, H-6a), 3.58 (dd, 1H, J = 10.6 Hz, J = 4.0 Hz, H-6b), 2.90 (d, 1H, J = 14.1 Hz, H-1a), 2.70 (d, 1H, J = 14.1 Hz, H-1b), 2.39 (dd, 1H, J = 13.9, 7.1 Hz, H-1'a), 2.30 (dd, 1H, J = 13.9, 7.5 Hz, H-1'b). **¹³C-NMR** (100.57 MHz, CDCl₃): δ (ppm) 138.20, 138.14, 138.12 (Cq Ph), 133.49 (C-2'), 119.03 (C-3'), 85.27 (C-2) 87.97, 84.66, 79.39 (C-3, C-4, C-5), 73.74, 73.06, 72.94, 70.24 (OCH₂Ph, C-6), 47.50 (C-1), 41.99 (C-1').

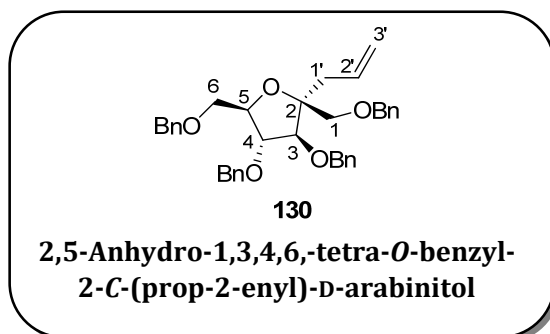


Compound 128. To a solution of α,β -D-fructose **77** (5 g, 0.028 mol) in dry CH_3OH (100 mL) was added conc H_2SO_4 (0.5 mL) at rt under argon atmosphere. After 2h stirring the reaction mixture was quenched by addition of Amberlite IR78 OH^- resin to neutralize the acid, the mixture was stirred for 5 min. Then, the resin was removed by filtration and the solvent was evaporated. The product was purified by flash column chromatography ($\text{EtOAc}/\text{CH}_3\text{OH}/\text{H}_2\text{O}$ 8:2:0.5) affording **128** (4.8 g, 89% yield) as a yellow oil mixture of α and β anomers. The anomers were not separable by chromatography, however a small amount of β anomer (R_f higher than the α anomer) was isolated to performed the following characterization. **β -anomer: MS (MALDI-TOF):** m/z 217.2 $[\text{M} + \text{Na}]^+$, 233.2 $[\text{M} + \text{K}]^+$. **Elemental analysis calcd (%)** for $\text{C}_7\text{H}_{14}\text{O}_6$: C, 43.30; H, 7.27, found: C, 42.60; H, 4.75. **$^1\text{H-NMR}$** (400 MHz, D_2O): δ (ppm) 4.64 (bm, 4H, OH), 3.95 (d, 1H, $J = 8.2$ Hz, H-3), 3.84 (t, 1H, $J = 8.2$ Hz, H-4), 3.65 (m, 1H, H-5), 3.60 (dd, 1H, $J = 12.2, 3.1$ Hz, H-6a), 3.52 (d, 1H, $J = 12.2$ Hz, H-1a), 3.44 (m, 2H, H-1b, H-6b), 3.12 (bs, 1H, OCH_3). **$^{13}\text{C-NMR}$** (100.57 MHz, D_2O): δ (ppm) 103.82 (C-1), 81.36 (C-5), 76.85 (C-3), 75.06 (C-4), 62.79 (C-6), 59.80 (C-1), 49.05 (OCH_3).

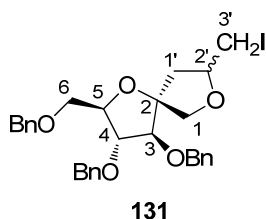


Methyl 1,3,4,6-tetra-*O*-benzyl-D-fructofuranoside

Compound 129. To a solution of **128** (5 g, 0.026 mol) in dry DMF (150 mL), NaH (1.3 g, 0.05 mol, 60% in mineral oil) was added portionwise at 0 °C. After stirring the mixture until release of H₂ stopped, benzyl bromide (11 mL, 0.123 mol) was added dropwise. The reaction mixture was left stirring at room temperature for 3h. After this time, the reaction was quenched by careful addition of EtOH at 0 °C to destroy the excess NaH. After addition of water and brine the product was extracted with EtOAc, and the combined organic layers were washed with brine, dried, filtered and concentrated. Purification of the crude product by flash chromatography on silica gel with petroleum ether/EtOAc 9:1 afforded **129** (quantitative yield) as a yellow oil mixture of α,β anomers. The isomers were not separated by chromatography.

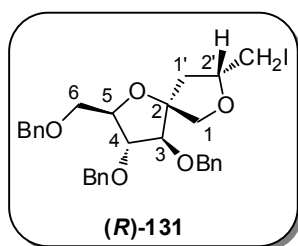


Compound 130. To a stirred solution of compound **129** (0.250 g, 0.451 mmol) in dry CH₃CN (10 mL) was added AllSi(CH₃)₃ (93 μL, 0.586 mmol) and BF₃·Et₂O (37 μL, 0.298 mmol) at rt under argon atmosphere. The reaction was monitored by TLC (eluent: petroleum ether/EtOAc 9:1) for 1.5h. After this time, the starting material was consumed; the mixture was neutralized with 5% NaHCO₃ and concentrated *in vacuo*. The residue was then extracted with CH₂Cl₂, the organic layer was dried on sodium sulphate, filtered and evaporated. Purification by flash chromatography (petroleum ether/EtOAc 9:1) afforded α-anomer **130** as a yellow oil (0.242 g, 95% yield) and a minor amount of the β-anomer (8:2 α:β ratio as determined from ratio in integrals of the ¹H-NMR of the mixture). **α-Anomer: MS (MALDI-TOF):** *m/z* 587.7 [M + Na]⁺, 603.7 [M + K]⁺. **Elemental analysis calcd (%)** for C₃₇H₄₀O₅: C, 78.69; H, 7.14, found: C, 76.73; H, 7.24. **¹H-NMR** (400 MHz, CDCl₃): δ (ppm) 7.37-7.24 (m, 15H, OCH₂Ph), Ph-H), 5.78 (bm, 1H, H-2'), 5.09 (d, 1H, *J* = 10.2 Hz, H-3'a), 4.97 (d, 1H, *J* = 17.3 Hz, H-3'b), 4.75-4.45 (m, 7H, OCH₂Ph, H-4), 4.13 (d, 1H, *J* = 7.7 Hz, H-3), 3.92 (bm, 1H, H-5), 3.70 (bm, 2H, H-1a, H-6a), 3.50 (m, 2H, H-1b, H-6b), 2.61 (bs, 1H, OH) 2.30 (dd, 1H, *J* = 14.0, 6.5 Hz, H-1'a), 2.17 (dd, 1H, *J* = 14.2, 7.6 Hz, H-1'b). **¹³C-NMR** (100.57 MHz, CDCl₃): δ (ppm) 138.06, 137.87, 137.71 (Cq Ph), 133.49 (C-2'), 128.23-127.48 (OCH₂Ph), 118.02 (C-3'), 86.52, 85.17 (C-4, C-5), 85.15 (C-2), 80.52 (C-3) 73.37, 73.20, 72.28, 72.01, 71.24, 70.98 (OCH₂Ph, C-6, C-1), 39.65 (C-1'). **β-Anomer: ¹³C-NMR** (100.57 MHz, CDCl₃), selected signals: δ (ppm) 134.00 (C-2'), 117.46 (C-3'), 37.26 (C-1').



Spiro[(1',4'-anhydro-2',3',5'-tri-*O*-benzyl-D-arabinitol)-1',4-(2-iodomethyltetrahydrofuran)]

Compound 131. Compound **130** (0.250 g, 0.443 mmol) was dissolved in dry THF (15 mL), and I₂ (0.337 g, 1.33 mmol) was added. The reaction mixture was stirred at rt for 1 h and then diluted with H₂O, and Na₂S₂O₃ was added until the organic phase turned colorless. The mixture was then extracted with AcOEt, the organic layer was separated, dried (Na₂SO₄), filtered, and concentrated to dryness *in vacuo*. The crude residue was purified by flash chromatography (petroleum ether/EtOAc 8.5:1.5) to afford a mixture *R/S* of cyclic iodoether derivative **131** (0.261 g, 98% yield, in 3:2 *R/S* ratio) as a clear oil. The following signal attributions were obtained from the separated mixture.^[123]



(R)-131: MS (MALDI-TOF): m/z 623 [M + Na]⁺, 639 [M + K]⁺.

Elemental analysis calcd (%) for C₃₀H₃₃O₅I: C, 60.00; H, 5.54,

found: C, 60.12; H, 5.58. **¹H-NMR** (400 MHz, CDCl₃): δ (ppm)

7.34-7.26 (m, 15H, OCH₂Ph), 4.59-4.48 (m, 5H, OCH₂Ph), 4.40 (d, 1H, $J = 11.6$ Hz, OCH₂Ph), 4.25 (d, 1H, $J = 10.3$ Hz, H-1a),

4.18-4.16 (m, 1H, H-5), 4.12-4.06 (m, 1H, H-2'), 3.94 (dd, 1H, $J = 3.3, 1.7$ Hz, H-4), 3.92

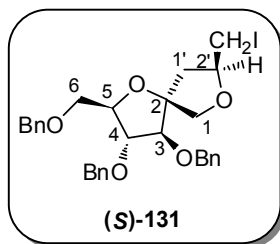
(d, 1H, $J = 1.7$ Hz, H-3), 3.88 (d, 1H, $J = 10.3$ Hz, H-1b), 3.58 (dd, 1H, $J = 9.9, 5.5$ Hz, H-

6a), 3.50 (dd, 1H, $J = 9.9, 6.6$ Hz, H-6b), 3.30-3.18 (m, 2H, H-3'), 2.34 (dd, 1H, $J = 12.8,$

5.1 Hz, H-1'a), 1.64 (dd, 1H, $J = 12.8, 9.9$ Hz, H-1'b). **¹³C-NMR** (100.57 MHz, CDCl₃): δ

(ppm) 92.94 (C-2), 86.80, 83.84, 82.00, 78.31 (C-3, C-4, C-5, C-2'), 74.46, 73.67, 72.06,

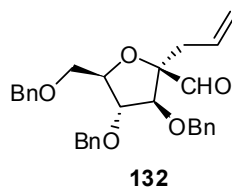
71.99, 70.83 (OCH₂Ph, C-1, C-6), 43.68 (C-1'), 10.31 (C-3').



(S)-131: MS (MALDI-TOF): m/z 623 [M + Na]⁺, 639 [M + K]⁺.

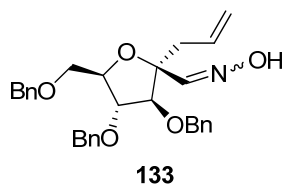
Elemental analysis calcd (%) for C₃₀H₃₃O₅I: C, 60.00; H, 5.54, found: C, 60.14; H, 5.55. **¹H-NMR** (400 MHz, CDCl₃): δ (ppm) 7.34-7.26 (m, 15H, OCH₂Ph), 4.68-4.47 (m, 5H, OCH₂Ph), 4.38 (d, 1H, J = 12.1 Hz, OCH₂Ph), 4.23-4.12 (m, 2H, H-5, H-2'), 4.11

(d, 1H, J = 10.3 Hz, H-1a), 4.03 (d, 1H, J = 10.3 Hz, H-1b), 3.96 (dd, 1H, J = 3.4, 1.5 Hz, H-4), 3.84 (d, 1H, J = 1.5 Hz, H-3), 3.58 (dd, 1H, J = 10.0, 5.4 Hz, H-6a), 3.48 (dd, 1H, J = 10.0, 6.5 Hz, H-6b), 3.34-3.22 (m, 2H, H-3'), 2.25 (dd, 1H, J = 9.9, 7.4 Hz, H-1'a), 2.06 (dd, 1H, J = 9.9, 5.1 Hz, H-1'b). **¹³C-NMR** (100.57 MHz, CDCl₃): δ (ppm) 91.96 (C-2), 86.59, 83.82, 81.91, 79.54 (C-3, C-4, C-5, C-2'), 73.46, 73.37, 71.75, 71.58, 70.30 (OCH₂Ph, C-1, C-6), 41.99 (C-1'), 9.33 (C-3').



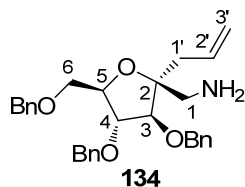
2,5-Anhydro-3,4,6-tri-*O*-benzyl-2-*C*-(prop-2-enyl)- α -D-glucose

Compound 132. Alcohol derivative **125** (0.250 g, 0.527 mmol) was dissolved in DMSO (20 mL) and IBX (0.294 g, 1.05 mmol) was added at rt under argon atmosphere. After 2h stirring, ice-cold water (20 mL) was added to the reaction mixture. The precipitate formed was filtered through a celite pad eluting with EtOAc, partial concentrated and extracted with H₂O/EtOAc. The organic layer was dried over Na₂SO₄, filtered, and evaporated to dryness. The crude aldehyde derivative **132** was used in the next step without further purification.



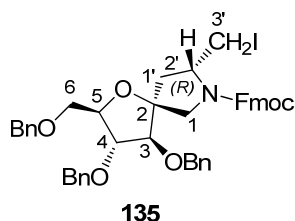
2,5-Anhydro-3,4,6-tri-*O*-benzyl-2-*C*-(prop-2-enyl)-*D*-glucose oxime

Compound 133. Aldehyde derivative **132** (≈ 0.527 mmol) was dissolved in a 1:1 THF/EtOH mixture (15 mL), and $\text{NH}_2\text{OH}\cdot\text{HCl}$ (0.052 g, 1.59 mmol) dissolved in a pH 4.5 acetate buffer (1.2 mL) were added. After 4h, the reaction mixture was extracted with CH_2Cl_2 , the organic layer dried over Na_2SO_4 , filtered, and evaporated to dryness. The crude was purified by flash chromatography (petroleum ether/EtOAc 8.5/1.5), affording oxime derivative **133**, as a colourless oil (0.236 g, 92% yield over two steps) and as a mixture of *E/Z* isomers. The isomers were not separable by chromatography. **MS (MALDI-TOF):** m/z 488.6 $[\text{M} + \text{H}]^+$, 510.6 $[\text{M} + \text{Na}]^+$, 526.6 $[\text{M} + \text{K}]^+$. **Elemental analysis calcd (%)** for $\text{C}_{30}\text{H}_{33}\text{NO}_5$: C, 73.90; H, 6.82; N, 2.87, found: 73.88; H, 6.80; N, 2.89. **$^1\text{H-NMR}$** (400 MHz, CDCl_3): δ (ppm) 7.51 (s, 1H, OH), 7.38-7.22 (m, 16H, OCH_2Ph , H-1), 5.95-5.82 (m, 1H, H-2'), 5.13 (d, 1H, $J = 10.2$ Hz, H-3'a), 5.09 (d, 1H, $J = 17.0$ Hz, H-3'b), 4.59-4.49 (m, 6H, OCH_2Ph), 4.16 (q, 1H, $J = 4.8$ Hz, H-5), 4.14-4.09 (m, 2H, H-3, H-4), 3.69-3.52 (m, 2H, H-6), 2.66 (bd, 2H, $J = 6.9$ Hz, H-1'). **$^{13}\text{C-NMR}$** (100.57 MHz, CDCl_3): δ (ppm) 152.14 (C-1), 138.25, 137.95, 137.71 (Cq Ph), 133.00 (C-2'), 119.31 (C-3'), 84.20 (C-2) 87.48, 84.72, 81.25 (C-3, C-4, C-5), 73.77, 72.71, 72.55, 70.67 (OCH_2Ph , C-6), 40.11 (C-1').



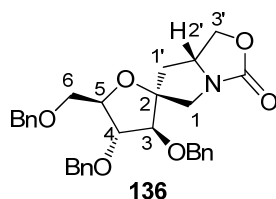
1-Amino-2,5-Anhydro-3,4,6-tri-*O*-benzyl-1-deoxy-2-*C*-(prop-2-enyl)-*N*-9H-fluoren-9-yl-methoxycarbonyl-D-glucitol

Compound 134. Amine derivative **126** (0.250 g, 0.528 mmol) was dissolved in dry CH₃CN (15 mL), and diisopropylethylamine (DIPEA, 46 μ L, 0.264 mmol) and Fmoc-Cl (0.164 g, 0.634 mmol) were added. After 2 h the reaction mixture was concentrated to dryness, and the residue purified by flash chromatography (petroleum ether/EtOAc 8.5:1.5). 0.330 g of compound **134** (90% yield) were obtained as a yellow oil. **MS (MALDI-TOF):** m/z 696.8 [M + H]⁺, 718.8 [M + Na]⁺, 734.8 [M + K]⁺. **Elemental analysis calcd (%)** for C₄₅H₄₅NO₆: C, 77.67; H, 6.52; N, 2.01; found: C, 77.72; H, 6.54; N, 2.06. **¹H-NMR** (400 MHz, CDCl₃): δ (ppm) 7.80-7.24 (m, 23H, OCH₂Ph, Ar-H Fmoc), 5.86-5.74 (m, 1H, H-2'), 5.66 (bt, 1H, J = 5.6 Hz, NH), 5.11 (dd, 1H, J = 10.3, 1.5 Hz, H-3'a), 5.02 (dd, 1H, J = 18.2, 1.5 Hz, H-3'b), 4.62-4.45 (m, 6H, OCH₂Ph), 4.36 (d, 2H, J = 7.0 Hz, CH₂-Fmoc), 4.23 (t, 1H, J = 5.9 Hz, H-4), 4.18 (t, 1H, J = 7.0 Hz, CH-Fmoc), 4.08 (d, 1H, J = 5.9 Hz, H-3), 4.97 (m, 1H, H-5), 3.61 (dd, 1H, J = 10.2, 4.0 Hz, H-6a), 3.52-3.46 (m, 2H, H-6b, H-1a), 3.38 (dd, 1H, J = 13.5, 5.5 Hz, H-1b), 2.38 (dd, 1H, J = 14.2, 6.6 Hz, H-1'a), 2.31 (dd, 1H, J = 14.2, 7.7 Hz, H-1'b). **¹³C-NMR** (100.57 MHz, CDCl₃): δ (ppm) 156.69 (CO-Fmoc), 144.30, 141.45 (Cq Ar Fmoc), 138.12, 137.97, 137.93 (Cq Ph), 133.02 (C-2'), 119.44 (C-3'), 87.02, 84.22 (C-3, C-4), 84.17 (C-2), 80.02 (C-5), 73.66, 73.03, 73.01, 69.89, 66.84 (OCH₂Ph, OCH₂-Fmoc, C-6), 47.77 (CH-Fmoc), 45.90 (C-1), 41.26 (C-1').



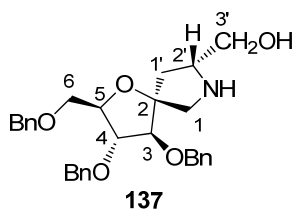
Spiro{[(1',4'-anhydro-2',3',5'-tri-O-benzyl-D-arabinitol)-1',4'-[(R)-(9H-fluoren-9-yl)methyl 2-iodomethylpyrrolidine-1-carboxylate]}

Compound 135. To a stirred solution of compound **134** (0.250 g, 0.359 mmol) in dry DME (15 mL) I₂ (0.274 g, 1.08 mmol) was added at room temperature under argon atmosphere. After 2h the reaction was quenched by adding H₂O and Na₂S₂O₃ to reduce excess iodine, the suspension was vigorously stirred until it became colourless. The mixture was then extracted with EtOAc, the organic layer was separated, dried (Na₂SO₄), filtered, and concentrated to dryness *in vacuo*. The crude was purified by flash chromatography (petroleum ether/EtOAc 8:2), affording bicyclic iodide **135** (*R*-isomer) as a colourless oil (0.245 g, 83 % yield). The diastereoselection of the iodocyclization reaction was extremely high in favour of the *R* isomer (*de* > 98%). **MS (MALDI-TOF):** *m/z* 822.7 [M + H]⁺, 844.7 [M + Na]⁺, 860.7 [M + K]⁺. **Elemental analysis calcd (%)** for C₄₅H₄₄INO₆: C, 65.77; H, 5.40; N, 1.70; found: C, 65.71; H, 5.46; N, 1.75. **¹H NMR** (400 MHz, CDCl₃): δ (ppm) 7.80-7.14 (m, 23H, OCH₂Ph, Ar-*H* Fmoc), 4.62-4.44 (m, 6H, OCH₂Ph) 4.36 (d, 2H, *J* = 7 Hz, CH₂-Fmoc), 4.23 (t, 1H, *J* = 5.9 Hz, H-4), 4.18 (t, 1H, *J* = 7.0 Hz, CH-Fmoc) 4.08 (d, 1H, *J* = 5.9 Hz, H-3), 3.97 (bm, 1H, H-5), 3.88-3.66 (m, 3H, H-2', CH₂I), 3.61 (dd, 1H, *J* = 10.2, 4.0 Hz, H-6a) 3.52-3.46 (m, 2H, H-6b, H-1a), 3.38 (dd, 1H, *J* = 13.5, 5.5 Hz, H-1b), 2.38 (dd, 1H, *J* = 14.2, 6.6 Hz, H-1'a), 2.31 (dd, 1H, *J* = 14.2, 7.7 Hz, H-1'b). **¹³C NMR** (100.57 MHz, CDCl₃): δ (ppm) 154.93 (CO-Fmoc), 144.13, 141.41 (Cq Ar Fmoc), 138.15, 137.82, 137.77 (Cq Ph), 89.54 (C-2) 86.45, 83.60, 81.85 (C-3, C-4, C-5), 73.64, 72.08, 72.02, 70.70, 67.56 (OCH₂Ph, OCH₂-Fmoc, C-6), 57.00 (C-2'), 54.91 (C-1), 47.52 (CH-Fmoc), 41.98 (C-1'), 14.30 (C-3').



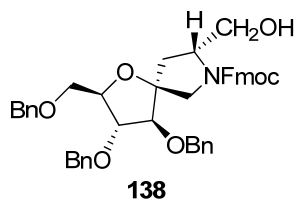
**Spiro{(1',4'-anhydro-2',3',5'-tri-O-benzyl-D-arabinitol)-
-1',6-[tetrahydropyrrolo[1,2-c]oxazol-3(1H)-one]}**

Compound 136. To a stirred solution of compound **135** (0.250 g, 0.304 mmol) in acetonitrile (15 mL) an aq. soln. of 1M NaOH (1.3 mL, 1.22 mmol) was added at rt. The reaction mixture was allowed to stir for 12h, after this time the solvent was concentrated, the residue was diluted with EtOAc and extracted. The organic layer was submitted to usual work-up and purified by flash chromatography (petroleum ether/EtOAc 7:3), affording 0.156 g of tricyclic compound **136** as a white solid (quantitative yield). **M.p.** 79-81 °C. **MS (MALDI-TOF):** m/z 516.6 [M + H]⁺, 538.6 [M + Na]⁺, 554.6 [M + K]⁺. **Elemental analysis calcd (%)** for C₃₁H₃₃NO₆: C, 72.21; H, 6.45; N, 2.72; found: C, 72.25; H, 5.50; N, 2.76. **¹H NMR** (400 MHz, CDCl₃): δ (ppm) 7.40-7.20 (m, 15H, OCH₂Ph), 4.59-4.39 (m, 6H, OCH₂Ph), 4.29-4.16 (m, 2H, H-2', H-3'a), 4.15-4.10 (m, 4H, H-1a, H-3'b, H-5), 3.92 (dd, 1H, $J = 3.2, 1.9$ Hz, H-4), 3.82 (d, 1H, $J = 1.9$ Hz, H-3), 3.56 (dd, 1H, $J = 9.9, 6.0$ Hz, H-6a), 3.47 (dd, 1H, $J = 9.9, 6.0$ Hz, H-6b), 3.28 (d, 1H, $J = 13.2$ Hz, H-1b), 2.29 (dd, 1H, $J = 12.9, 5.2$ Hz, H-1'a), 1.40 (dd, 1H, $J = 12.9, 10.9$ Hz, H-1'b). **¹³C NMR** (100.57 MHz, CDCl₃): δ (ppm) 144.80 (CO), 138.15, 137.82, 137.77 (Cq Ph), 93.93 (C-2) 86.82, 83.58, 82.42 (C-3, C-4, C-5), 73.70, 72.17, 72.17, 70.82, 67.12 (OCH₂Ph, C-6, C-3'), 59.19 (C-2'), 53.89 (C-1), 41.57 (C-1').



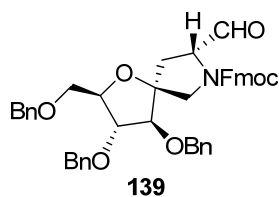
Spiro{(1',4'-anhydro-2',3',5'-tri-O-benzyl-D-arabinitol)-1',4-[(2R)-pyrrolidin-2-yl-methanol]}

Compound 137. To a stirred solution of compound **136** (0.250 g, 0.485 mmol) in ethanol (15 mL) an aq. sol. of 3M NaOH (1.6 mL, 4.85 mmol) was added at 60 °C. The reaction mixture was allowed to stir for 4h. After this time the solvent was concentrated, the residue was diluted with EtOAc and extracted. The organic layer was submitted to usual work-up and purified by flash chromatography (EtOAc/EtOH 7:3), affording 0.236 g amino alcohol derivative **137** as a yellow oil (quantitative yield). **MS (MALDI-TOF):** m/z 490.6 [M + H]⁺, 512.6 [M + Na]⁺, 528.6 [M + K]⁺. **Elemental analysis calcd (%)** for C₃₀H₃₅NO₅: C, 73.59; H, 7.21; N 2.86; found: C, 73.67; H, 7.23; N, 2.92. **¹H NMR** (400 MHz, CDCl₃): δ (ppm) 7.40-7.22 (m, 15H, OCH₂Ph), 4.59-4.40 (m, 6H, 3 OCH₂Ph), 4.15-4.10 (m, 1H, H-5), 3.93 (dd, 1H, $J = 3.7, 2.1$ Hz, H-4), 3.91 (d, 1H, $J = 2.1$ Hz, H-3), 3.59-3.49 (m, 4H, H-6a, H-2', OH or NH), 3.32 (d, 1H, $J = 11.9$ Hz, H-3'a), 3.30 (d, 1H, $J = 11.9$ Hz, H-3'b), 3.28 (bs, 1H, OH or NH), 3.14 (d, 1H, $J = 12.5$ Hz, H-1a), 3.08 (dd, 1H, $J = 12.5$ Hz, H-1b), 2.13 (dd, 1H, $J = 13.1, 6.4$ Hz, H-1'a), 1.53 (dd, 1H, $J = 13.1, 7.9$ Hz, H-1'b). **¹³C NMR** (100.57 MHz, CDCl₃): δ (ppm) 138.24, 137.97, 137.91 (Cq Ph), 93.58 (C-2), 86.57, 84.29, 81.44 (C-3, C-4, C-5), 73.65, 72.11, 72.00, 71.06 (OCH₂Ph, C-6), 64.17 (C-3'), 59.49 (C-2'), 53.11 (C-1), 38.61 (C-1').



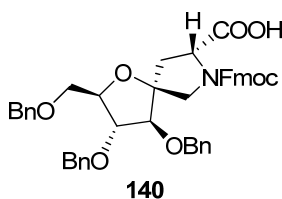
Spiro{(1',4'-anhydro-2',3',5'-tri-*O*-benzyl-*D*-arabinitol)-1',4'-[(*R*)-(9*H*-fluoren-9-yl)methyl 2-hydroxymethylpyrrolidine-1-carboxylate]}

Compound 138. The same experimental procedure reported for **134** was applied to the protection of the amine derivative **137** (0.250 g, 0.510 mmol) with DIPEA (44 μ L, 0.255 mmol) and Fmoc-Cl (0.158 g, 0.612 mmol) in dry CH₃CN (15 mL). Purified by flash chromatography (petroleum ether/EtOAc 6.5:3.5) afforded carbamate derivative **138** (0.350 g, 96% yield) as a yellow oil. **MS (MALDI-TOF):** m/z 712.8 [M + H]⁺, 734.8 [M + Na]⁺, 750.8 [M + K]⁺. **Elemental analysis calcd (%)** for C₄₅H₄₅NO₇: C, 75.93; H, 6.37; N, 1.97; found: C, 75.83; H, 6.43; N, 1.91. **¹H NMR** (400 MHz, CDCl₃): δ (ppm) 7.65-7.12 (m, 23H, OCH₂Ph, Ar-H Fmoc), 4.50-4.10 (m, 11H, OCH₂Ph, CH₂-Fmoc, CH-Fmoc, H-5, H-2'), 3.93 (bs, 1H, H-4), 3.76 (d, 1H, J = 1.5 Hz, H-3), 3.73 (d, 1H, J = 12.5 Hz, H-1a), 3.64 (d, 1H, J = 11.1 Hz, H-3'a), 3.59 (d, 1H, J = 12.5 Hz, H-1b), 3.53-3.41 (m, 4H, H-6, H-3'b, OH), 2.24 (dd, 1H, J = 13.1, 6.6 Hz, H-1'a), 1.46 (dd, 1H, J = 13.1, 10.6 Hz, H-1'b). **¹³C NMR** (100.57 MHz, CDCl₃): δ (ppm) 157.16 (CO-Fmoc), 144.19, 143.84, 141.49, 141.45 (Cq Ar Fmoc), 138.20, 137.82, 137.70 (Cq Ph), 89.33 (C-2) 86.54, 83.61, 82.11 (C-3, C-4, C-5), 73.70, 72.15, 71.93, 70.77, 68.07, 66.64 (OCH₂Ph, OCH₂-Fmoc, C-6, C-3'), 61.18 (C-2'), 54.86 (C-1), 47.54 (CH-Fmoc), 38.10 (C-1').



Spiro{(1',4'-anhydro-2',3',5'-tri-O-benzyl-D-arabinitol)-1',4'-[(R)-(9H-fluoren-9-yl)methyl 2-formylpyrrolidine-1-carboxylate]}

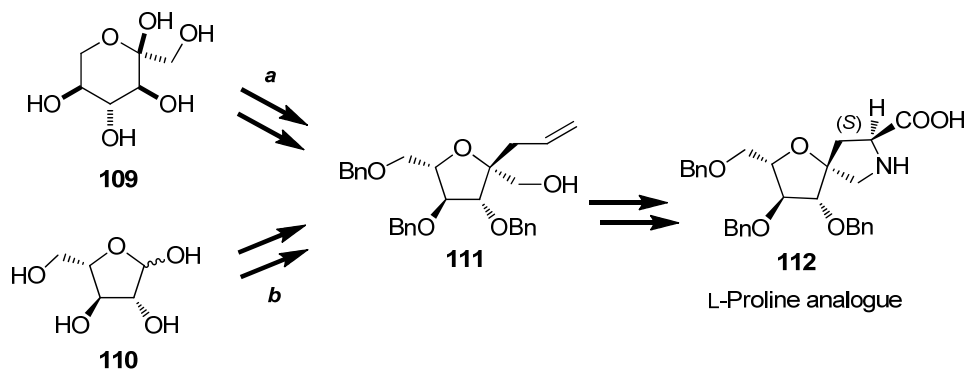
Compound 139. The same experimental procedure reported for **132** was applied to the oxidation of alcohol derivative **138** (0.250 g, 0.351 mmol) with IBX (0.056 g, 0.702 mmol) in DMSO (20 mL). The crude aldehyde derivative **139** (\approx 0.351 mmol) was used in the next step without further purification.



Spiro{(1',4'-anhydro-2',3',5'-tri-O-benzyl-D-arabinitol)-1',4'-[(R)-{[(9H-fluoren-9-yl)methoxy]carbonyl}pyrrolidine-2-carboxylic acid]}

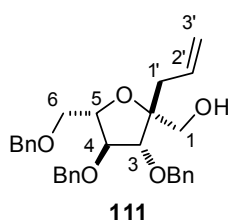
Compound 140. To a solution of crude aldehyde derivative **139** (\approx 0.351 mmol) in MeCN (15 mL) an aq. soln. of 1.25 M $\text{NaH}_2\text{PO}_4 \cdot 2\text{H}_2\text{O}$ (2.80 mL, 3.51 mmol) and NaClO_2 (0.317 g, 3.51 mmol) were added. After 7 hours the reaction mixture was concentrated, the residue suspended in CH_2Cl_2 and filtered, and the solvent evaporated under reduced pressure. Flash chromatography (petroleum ether/EtOAc 6:4 and then EtOAc/EtOH 9:1 + 0.1% AcOH) afforded compound **140** as a pink oil (76% yield over two steps). Due to the presence of rotamers only ^{13}C NMR is reported. **MS (MALDI-TOF):** m/z 748.8 $[\text{M} + \text{Na}]^+$, 764.8 $[\text{M} + \text{K}]^+$. **Elemental analysis calcd (%) for $\text{C}_{45}\text{H}_{43}\text{NO}_8$:** C, 74.46; H, 5.97; N, 1.93; found: C, 74.52; H, 6.01; N, 1.96. **^{13}C NMR** (100.57 MHz, CDCl_3): δ (ppm) 177.43 (C-3'), 155.70 (CO-Fmoc), 144.20, 143.89, 143.85, 141.49, (Cq Ar Fmoc), 138.08, 137.66, 137.44 (Cq Ph), 90.61 (C-2) 85.93, 83.69, 82.46 (C-3, C-4, C-5), 73.85, 72.46, 72.11, 71.95, 68.31 (OCH_2Ph , $\text{OCH}_2\text{-Fmoc}$, C-6), 61.18 (C-2'), 54.30 (C-1), 47.54 (CH-Fmoc), 38.87 (C-1').

4.1.3 Synthesis of the Spiro L-Proline Analogue



Scheme 25

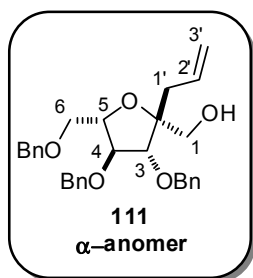
4.1.3.1 Synthesis of Compound 111 - Pathway *a*



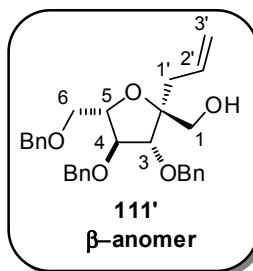
3-C-(3,4,6-tri-O-benzyl- α -L-fructofuranos-2-yl)propene

Compound 111. To a stirred solution of **148** (0.250 g, 0.538 mmol) in dry CH_3CN (2 mL) was added bis(trimethylsilyl) trifluoroacetamide (BTSFA) (0.144 mL, 0.538 mmol) at 100 °C under argon atmosphere. After 3h, analysis by thin-layer chromatography indicated that starting material **148** had been consumed. The reaction mixture clear and uniform was allowed to cool to rt, and $\text{AllSi}(\text{CH}_3)_3$ (0.128 mL, 0.81 mmol) and TMSOTf (48 μL , 0.264 mmol) were sequentially added at 0 °C and reaction was left stirring at rt for 1h. Water (3 mL) was added slowly to hydrolyze TMS ethers, and then the mixture was neutralized with an aq. soln. 1M NaOH and concentrated *in vacuo*. The residue was extracted with CH_2Cl_2 , the organic layer was

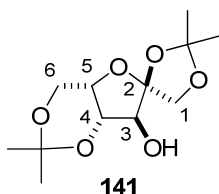
dried on sodium sulphate, filtered and evaporated. Purification by flash chromatography (petroleum ether/EtOAc 8:2) afforded the separation of the anomers being recovered 0.193g (76% yield) of the desired α -anomer **111** as a yellow oil. The 8:2 α : β ratio was determined from ratio integrals of the $^1\text{H-NMR}$ spectrum of the mixture.



α -Anomer: MS (MALDI-TOF): m/z 475.6 $[\text{M} + \text{H}]^+$, 497.6 $[\text{M} + \text{Na}]^+$, 513.6 $[\text{M} + \text{K}]^+$. **Elemental analysis calcd (%)** for $\text{C}_{30}\text{H}_{34}\text{O}_5$: C, 75.92; H, 7.22, found: C, 76.10; H, 7.35. **$^1\text{H-NMR}$** (400 MHz, CDCl_3): δ (ppm) 7.37-7.24 (m, 15H, OCH_2Ph), 5.78 (bm, 1H, H-2'), 5.09 (d, 1H, $J = 10.2$ Hz, H-3'a), 4.97 (d, 1H, $J = 17.3$ Hz, H-3'b), 4.75-4.45 (m, 7H, OCH_2Ph , H-4), 4.13 (d, 1H, $J = 7.7$ Hz, H-3), 3.92 (bm, 1H, H-5), 3.70 (bm, 2H, H-1a, H-6a), 3.50 (m, 2H, H-1b, H-6b), 2.30 (dd, 1H, $J = 14.0, 6.5$ Hz, H-1'a), 2.17 (dd, 1H, $J = 14.2, 7.6$ Hz, H-1'b), 1.83 (bs, 1H, OH). **$^{13}\text{C-NMR}$** (100.57 MHz, CDCl_3): δ (ppm) 138.32, 138.20, 137.73 (Cq Ph), 133.07 (C-2'), 128.71-127.07 (OCH_2Ph), 119.17 (C-3'), 84.29 (C-2), 86.65, 83.50, 79.34 (C-3, C-4, C-5), 73.65, 73.19, 72.15, 69.61, 64.41 (OCH_2Ph , C-6, C-1), 40.29 (C-1').



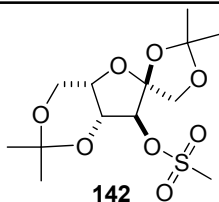
β -Anomer: MS (MALDI-TOF): m/z 475.6 $[\text{M} + \text{H}]^+$, 497.6 $[\text{M} + \text{Na}]^+$, 513.6 $[\text{M} + \text{K}]^+$. **Elemental analysis calcd (%)** for $\text{C}_{30}\text{H}_{34}\text{O}_5$: C, 75.92; H, 7.22, found: C, 76.04; H, 7.25. **$^1\text{H-NMR}$** (400 MHz, CDCl_3): δ (ppm) 7.33-7.26 (m, 15H, OCH_2Ph), 5.88 (bm, 1H, H-2'), 5.10 (d, 1H, $J = 17.0$ Hz, H-3'a), 5.07 (d, 1H, $J = 10.2$ Hz, H-3'b), 4.63-4.57 (m, 6H, OCH_2Ph), 4.15-4.07 (m, 3H, H-4, H-3, H-5), 3.61-3.55 (m, 4H, H-1, H-6), 2.48 (dd, 1H, $J = 14.1, 6.7$ Hz, H-1'a), 2.38 (dd, 1H, $J = 12.2, 6.7$ Hz, H-1'b), 1.93 (bs, 1H, OH). **$^{13}\text{C-NMR}$** (100.57 MHz, CDCl_3): δ (ppm) 138.04, 137.90, 137.80 (Cq Ph), 134.05 (C-2'), 128.39-127.55 (OCH_2Ph), 118.05 (C-3'), 85.69 (C-2), 84.71, 84.18, 80.53 (C-3, C-4, C-5), 73.37, 73.56, 72.17, 71.01, 64.62 (OCH_2Ph , C-6, C-1), 37.19 (C-1').



141

1,2:4,6-di-*O*-Isopropylidene- α -L-xylo-hex-2-ulo-2,5-furanose

Compound 141. A solution of dry 1,2-dimethoxyethane (2 mL) containing SnCl₂ (0.045 g, 0.25 mmol) was added to a suspension of β -L-sorbose **109** (10 g, 0.055 mol) in 2,2-dimethoxypropane (1200 mL) with vigorous stirring. The mixture was refluxed gently under argon atmosphere at 70 °C (bath temperature) for 2.5h. After this time, the reaction became clear and even without total consumed of β -L-sorbose the reaction was quenched with triethylamine (0.250 mL), filtered to remove the unreacted L-sorbose, and the solid was washed with EtOAc. The filtrate was concentrated to give compound **141** (\approx 0.055 mol) as a syrup, which was used in the next step without further purification.

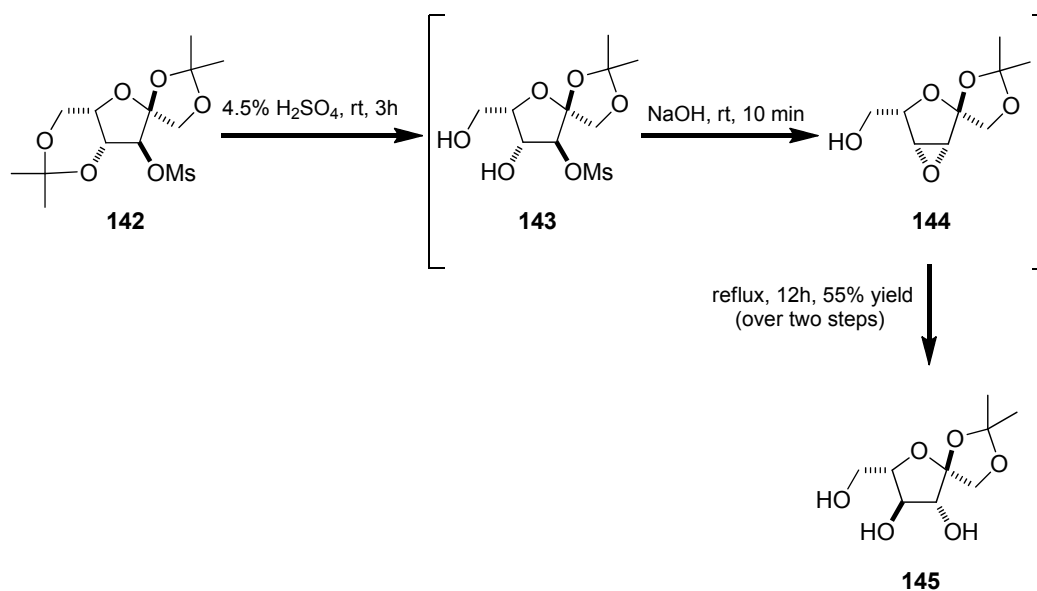


142

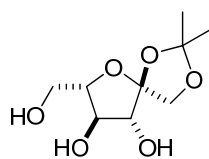
1,2:4,6-di-*O*-Isopropylidene-3-*O*-methanesulfonyl- α -L-xylo-hex-2-ulo-2,5-furanose

Compound 142. The above syrup **141** (\approx 0.055 mol) was dissolved in pyridine (24 mL). After cooling with an ice bath, methanesulfonyl chloride (MsCl, 5.4 mL, 0.069 mol) was added dropwise *via* an addition funnel over 20 min. After stirring at 0 °C for an additional 3h, the reaction mixture was poured into ice-water (150 mL), stirred for 30 min, and filtered. The filter cake was washed with several times and recrystallized from ethanol to give mesylate **141** as a white crystal (7.51 g, 40% yield over two steps

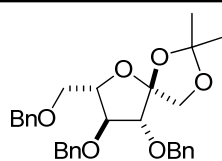
based on L-sorbose and 50% yield over two steps based on the recovered starting material). **M.p.** 120-122 °C. **Elemental analysis calcd (%)** for $C_{13}H_{22}O_8S$: C, 46.14; H, 6.55, found: C, 46.02; H, 6.42. **1H -NMR** (400 MHz, $CDCl_3$): δ (ppm) 4.88 (d, 1H, $J = 1.8$ Hz, H-3), 4.46 (dd, 1H, $J = 3.3, 1.8$ Hz, H-4), 4.25 (d, 1H, $J = 9.9$ Hz, H-1a), 4.22 (m, 1H, H-5), 4.20 (d, 1H, $J = 9.9$ Hz, H-1b), 4.01 (dd, 1H, $J = 13.2, 3.0$ Hz, H-6a), 3.92 (dd, 1H, $J = 13.2, 3.0$ Hz, H-6b), 3.16 (s, 3H, CH_3SO_3), 1.55 (s, 3H, CH_3), 1.47 (s, 3H, CH_3), 1.42 (s, 3H, CH_3), 1.38 (s, 3H, CH_3). **^{13}C -NMR** (100.57 MHz, $CDCl_3$): δ (ppm) 111.5 ($C(CH_3)_2$), 109.8 (C-2), 98.2 ($C(CH_3)_2$), 84.2, 73.3, 72.1 (C-3, C-4, C-5), 73.25, 60.4 (C-1, C-6), 38.9 (CH_3SO_3), 28.3, 26.0, 25.9, 20.1 (CH_3).



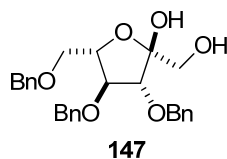
Scheme 26

**145****1,2-O-Isopropylidene- α -L-arabino-hex-2-ulo-2,5-furanose**

Compound 145. A suspension of mesylate **142** (10 g, 0.03 mol) in 4.5% (w) H₂SO₄ (100 ml) was stirred at rt until all the starting material had been consumed (monitored by TLC). After 3h, 9 M NaOH (20 ml) was added to the reaction mixture and left stirring at rt. After 10 min, compound **143** reacted completely and epoxide **144** was formed, according to TLC analysis (R_f **143** = 0.57, R_f **144** = 0.70, eluent: EtOAc)^[139]. At this point, the reaction mixture was heated at 90-100 °C for about 12h (R_f **145** = 0.30, eluent: EtOAc). The cooled mixture was neutralized with 4.5 M H₂SO₄ and evaporated. The syrupy residue was dissolved in warm excess CHCl₃, and the solvent mixture was kept at rt overnight to give white crystalline **145** (3.63 g, 55% yield over two steps). **M.p.** 83-85 °C. **MS (MALDI-TOF):** m/z 259.2 [M + K]⁺. **Elemental analysis calcd** (%) for C₉H₁₆O₆: C, 49.13; H, 7.33, found: C, 48.81; H, 7.41. **¹H-NMR** (400 MHz, D₂O): δ (ppm) 4.13 (d, 1H, J = 9.8 Hz, H-1a), 4.00 (d, 1H, J = 4.5 Hz, H-3), 3.86 (d, 1H, J = 9.9 Hz, H-1b), 3.83 (m, 1H, H-5), 3.77 (t, 1H, J = 4.7 Hz, H-4), 3.61 (dd, 1H, J = 12.4, 2.9 Hz, H-6a), 3.50 (dd, 1H, J = 12.4, 5.1 Hz, H-6b), 1.35 (s, 3H, CH₃), 1.26 (s, 3H, CH₃). **¹³C-NMR** (100.57 MHz, D₂O): δ (ppm) 114.53 (C(CH₃)₂), 114.44 (s, C-2), 85.28, 82.64, 77.79 (3d, C-3, C-4, C-5), 71.57, 63.57 (2t, C-1, C-6), 28.14, 27.61 (2q, CH₃).

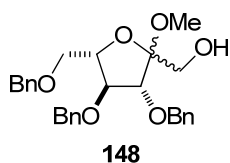
**146****3,4,6-Tri-O-benzyl-1,2-O-isopropylidene-
-α-L-arabino-hex-2-ulo-2,5-furanose**

Compound 146. To a solution of **145** (5 g, 0.023 mol) in dry DMF (150 mL), NaH (1.7 g, 0.07 mol, 60% in mineral oil) was added portionwise at 0 °C. After stirring the mixture until release of H₂ stopped, benzyl bromide (10 mL, 0.083 mol) was added dropwise. The reaction mixture was left stirring at rt for 3h. After this time, the reaction was quenched by careful addition of EtOH at 0 °C to destroy the excess NaH. After addition of water and brine the product was extracted with EtOAc, and the combined organic layers were washed with brine, dried, filtered and concentrated. Purification of the crude product by flash chromatography on silica gel with petroleum ether/EtOAc 9:1 afforded **146** as a yellow oil (8.7 g, 77% yield). **MS (MALDI-TOF):** *m/z* 491.6 [M + H]⁺, 529.6 [M + K]⁺. **Elemental analysis calcd (%)** for C₃₀H₃₄O₆: C, 73.45; H, 6.99, found: C, 73.38; H, 7.05. **¹H-NMR** (400 MHz, CDCl₃): δ (ppm) 7.37-7.25 (m, 15H, OCH₂Ph), 4.64-4.48 (m, 6H, OCH₂Ph), 4.32 (d, 1H, *J* = 9.6 Hz, H-1a), 4.22 (dd, 1H, *J* = 10.3, 4.6 Hz, H-5), 4.11 (d, 1H, *J* = 3.8 Hz, H-3), 4.02 (d, 1H, *J* = 9.6 Hz, H-1b), 3.92 (dd, 1H, *J* = 5.7, 3.9 Hz, H-4), 3.57 (d, 2H, *J* = 4.5 Hz, H-6), 1.54 (s, 3H, CH₃), 1.44 (s, 3H, CH₃). **¹³C-NMR** (100.57 MHz, CDCl₃): δ (ppm) 137.38, 138.20, 137.67 (Cq Ph), 128.71-127.83 (OCH₂Ph), 112.39, 111.21 (C-2, C[CH₃]₂), 87.70, 81.86, 80.50 (C-3, C-4, C-5), 73.54, 72.30, 72.19 (OCH₂Ph), 70.17, 69.92 (C-1, C-6), 26.82, 26.29 (CH₃).



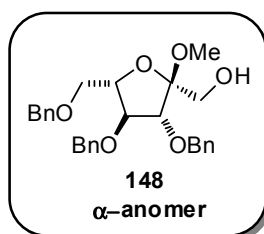
3,4,6-Tri-*O*-benzyl- α -L-arabino-hex-2-ulo-2,5-furanose

Compound 147. A solution of **146** (10 g, 0.02 mol) in 60% (w) of acetic acid (60 mL) was heated at 50 °C during 20 min. The solvent was evaporated and the residue was partitioned between CH₂Cl₂ and aqueous NaHCO₃. The organic layer was washed with brine, dried and concentrated to dryness. The residue was purified by column chromatography using petroleum ether/EtOAc 9:1 to give **147** as a yellow oil (6.49 g, 72% yield). **MS (MALDI-TOF):** m/z 451.5 [M + H]⁺, 489 [M + K]⁺. **Elemental analysis calcd (%)** for C₂₇H₃₀O₆: C, 71.98; H, 6.71, found: C, 72.03; H, 6.64. **¹H-NMR** (400 MHz, CDCl₃): δ (ppm) 7.35-7.25 (m, 15H, OCH₂Ph), 4.71-4.47 (m, 6H, OCH₂Ph), 4.17 (m, 2H, H-3, H-4), 4.12 (m, 1H, H-5), 3.80 (d, 1H, J = 11.9 Hz, H-1a), 3.70 (d, 1H, J = 11.8 Hz, H-1b), 3.52 (dd, 1H, J = 10.0, 4.5 Hz, H-6a), 3.51 (dd, 1H, J = 9.9, 4.2 Hz, H-6b). **¹³C-NMR** (100.57 MHz, CDCl₃): δ (ppm) 137.85, 137.67, 137.49 (Cq Ph), 128.77-128.01 (OCH₂Ph), 103.34 (C-2), 83.74, 83.54, 80.85 (C-3, C-4, C-5), 73.80, 73.12, 72.29 (OCH₂Ph), 70.92, 65.41 (C-1, C-6).

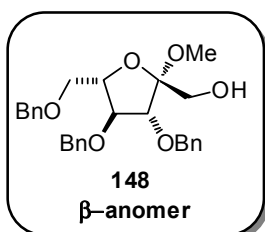


Methyl 3,4,6-tri-*O*-benzyl-L-arabino-hex-2-ulo-2,5-furanoside

Compound 148. A solution of **147** (5 g, 0.011 mol) in dry CH₃OH (200 mL), acetyl chloride was added dropwise at room temperature under argon atmosphere. After 5h, Amberlite IR78 OH⁻ resin was added to neutralize the acid and the mixture was stirred for 5 min. The resin was removed by filtration and the solvent was evaporated. The product was purified by flash column chromatography (petroleum ether/EtOAc 7:3) affording **148** (4.7 g, 92% yield) as a yellow oil mixture of α and β anomers (3:1 α:β ratio, as determined from the ratio integrals of the ¹H-NMR signals). The following signal attributions were obtained from the separated mixture.

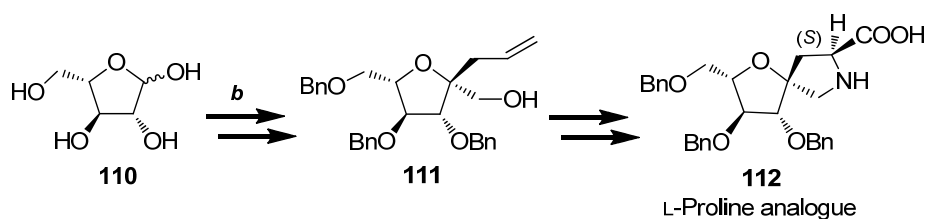


α-Anomer: MS (MALDI-TOF): m/z 487.5 [M + Na]⁺, 503.5 [M + K]⁺. **¹H-NMR** (400 MHz, CDCl₃): δ (ppm) 7.33-7.22 (m, 15H, OCH₂Ph), 4.67-4.46 (m, 6H, OCH₂Ph), 4.16 (bm, 2H, H-3, H-4), 4.09 (bm, 1H, H-5), 3.78 (dd, 1H, $J = 11.9, 6.7$ Hz, H-1a), 3.69 (dd, 1H, $J = 11.9, 5.2$ Hz, H-1b), 3.65 (dd, 1H, $J = 10.7, 3.4$ Hz, H-6a), 3.54 (dd, 1H, $J = 10.7, 3.9$ Hz, H-6b), 3.32 (s, 1H, OCH₃), 1.78 (bs, 1H, OH). **¹³C-NMR** (100.57 MHz, CDCl₃): δ (ppm) 137.86, 137.63, 137.42 (Cq Ph), 128.49-127.78 (OCH₂Ph), 107.69 (C-2), 86.33, 82.37, 80.21 (C-3, C-4, C-5), 73.82, 73.40, 72.42 (OCH₂Ph), 69.13 (C-6), 61.49 (C-1), 48.92 (OCH₃).

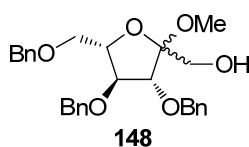


β -Anomer: MS (MALDI-TOF): m/z 487.5 [M + Na]⁺, 503.5 [M + K]⁺. **¹H-NMR** (400 MHz, CDCl₃): δ (ppm) 7.37-7.21 (m, 15H, OCH₂Ph), 4.62-4.46 (m, 6H, OCH₂Ph), 4.28 (d, 1H, J = 7.0, H-3), 4.14 (t, 1H, J = 6.9 Hz, H-4), 4.08 (bm, 1H, H-5), 3.79 (dd, 1H, J = 11.9, 6.7 Hz, H-1a), 3.69 (dd, 1H, J = 11.9, 6.7 Hz, H-1b), 3.63 (dd, 1H, J = 10.7, 3.5 Hz, H-6a), 3.50 (dd, 1H, J = 10.7, 3.9 Hz, H-6b), 3.30 (s, 1H, OCH₃), 2.05 (bs, 1H, OH). **¹³C-NMR** (100.57 MHz, CDCl₃): δ (ppm) 137.86, 137.80, 137.74 (Cq Ph), 128.38-127.76 (OCH₂Ph), 104.35 (C-2), 84.22, 83.67, 79.70 (C-3, C-4, C-5), 73.41, 72.97, 72.54 (OCH₂Ph), 71.80 (C-6), 62.53 (C-1), 49.57 (OCH₃).

4.1.3.2 Synthesis of Compound 111 - Pathway *b*



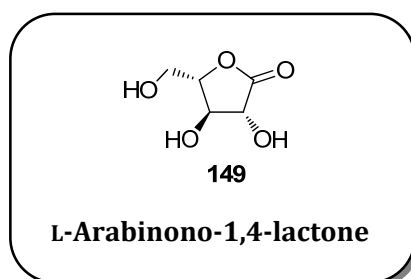
Scheme 27



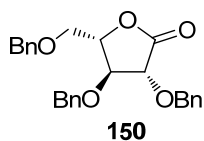
Methyl 3,4,6-tri-*O*-benzyl-L-arabino-hex-2-ulo-2,5-furanoside

Compound 148. To a 0 °C cooled solution of **153** (\approx 0.452 mmol) in dry EtOH (15 mL) was added NaBH₄ (0.205 g, 5.52 mmol) under argon atmosphere. The reaction mixture was left stirring for 30 min, and then quenched by addition of sat. aq. NH₄Cl soln. at 0 °C. The resulting mixture was extracted with EtOAc, the organic layer was

dried on sodium sulphate, filtered and evaporated. Purification by flash chromatography (petroleum ether/EtOAc 7:3) afforded **148** (0.137 g, 65% yield over two steps) as a yellow oil mixture of α and β anomers (3:1 α : β ratio, as determined from the ratio integrals of the $^1\text{H-NMR}$ signals). The NMR signal attributions were already shown in pathway *a*.

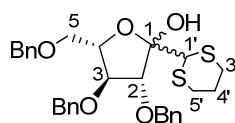


Compound 149. To a solution of α,β L-arabinose **110** (0.250 g, 1.66 mmol) in water (25 mL) potassium carbonate (0.321 g, 2.32 mmol) was added, the resulting mixture was cooled to 0 °C and bromine (0.170 ml, 3.32 mmol) was added dropwise with continues stirring. The reaction was left stirring in the dark for about 1h at rt. The solvent was then removed under reduced pressure. The crude residue was purified by silica gel flash chromatography (EtOAc/EtOH 8:2) to give the desired product **149** as a yellow oil (0.241 g, 98% yield). **MS (MALDI-TOF):** m/z 149.1 $[\text{M} + \text{H}]^+$, 171.1 $[\text{M} + \text{Na}]^+$, 187.1 $[\text{M} + \text{K}]^+$. **Elemental analysis calcd (%)** for $\text{C}_5\text{H}_8\text{O}_5$: C, 40.55; H, 5.44, found: C, 40.61; H, 5.40. **$^1\text{H-NMR}$** (400 MHz, CD_3OD): δ (ppm) 4.33 (d, 1H, $J = 8.5$ Hz, H-2), 4.14-4.09 (m, 2H, H-3, H-4), 3.87 (dd, 1H, $J = 13.0, 1.9$ Hz, H-5a), 3.65 (dd, 1H, $J = 13.0, 4.0$ Hz, H-5b). **$^{13}\text{C-NMR}$** (100.57 MHz, CD_3OD): δ (ppm) 176.41 (CO), 82.82, 75.66, 74.18 (C-2, C-3, C-4), 60.89 (C-5).



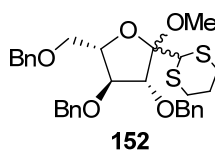
2,3,5-Tri-*O*-benzyl-L-arabinono-1,4-lactone

Compound 150. Benzyl trichloroacetimidate (1.9 mL, 10.14 mmol) and then trifluoromethanesulfonic acid (75 μ L, 0.84 mmol) were added at 0 °C, under argon atmosphere, to a soln. of **149** (0.250 g, 1.69 mmol) in dry dioxane (2.6 mL). The soln. was stirred for 3h, and then quenched with a sat. NaHCO₃ soln. and extracted with CH₂Cl₂. The organic layer was dried on sodium sulphate, filtered and evaporated. Flash column chromatography of the residue (petroleum ether/EtOAc 9:1) afforded **150** as a yellow oil (0.459 g, 65% yield). **MS (MALDI-TOF):** m/z 419.5 [M + H]⁺. **Elemental analysis calcd (%)** for C₂₆H₂₆O₅: C, 74.62; H, 6.26, found: C, 74.74; H, 6.22. **¹H-NMR** (400 MHz, CDCl₃): δ (ppm) 7.33-7.06 (m, 15H, OCH₂Ph), 5.00, 4.97, 4.71, 4.68 (AB, 2H, J = 11.6 Hz, PhCH₂O), 4.55 (d, 1H, J = 11.6 Hz, PhCH₂O), 4.49-4.41 (m, 2H, PhCH₂O) 4.28-4.24 (m, 3H, H-2, H-3, H-4), 3.63 (dd, 1H, J = 11.3, 1.8 Hz, H-5a), 3.50 (dd, 1H, J = 11.4, 3.3 Hz, H-5b). **¹³C-NMR** (100.57 MHz, CDCl₃): δ (ppm) 172.57 (CO), 137.41, 137.02, 136.72 (Cq Ph), 128.53-127.72 (OCH₂Ph), 79.20, 79.09, 78.81 (C-2, C-3, C-4), 72.48, 72.68, 72.47 (OCH₂Ph), 67.89 (C-5).

**151****2,3,5-Tri-O-benzyl-1-C-(1,3-dithiane-2-yl)-L-arabinose**

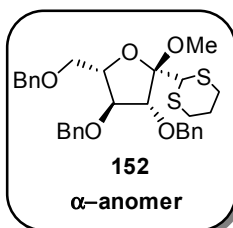
Compound 151. In a 25 mL, two-necked, round-botomed flask equipped with a magnetic stirring bar, a rubber septum, and an argon filled balloon was placed 1,3-dithiane (0.108 g, 0.90 mmol) in dry THF (6 mL). The soln. was cooled to -20 °C and *n*-BuLi (0.750 mL, 1.2 mmol, 1.6 M in hexane) was added slowly. After 1.5h the resulting mixture was cooled to -78 °C and added *via* cannula to a -78 °C soln. of **150** (0.250 g, 0.60 mmol) in dry THF (7 mL). The reaction was stirred for 20 min and quenched at -78 °C by addition of sat. NH₄Cl soln. (3 mL). To the reaction mixture was added EtOAc (20 mL) and then extracted. The organic layer was dried on sodium sulphate, filtered and evaporated. Flash column chromatography of the residue (petroleum ether/EtOAc 8:2) afforded **151** (0.205 g, 64% yield) as a yellow oil mixture of α and β anomers (1:4 α : β ratio, as determined from the ratio in integrals of the ¹H-NMR signals). The isomers were not separable by chromatography. The following signal attributions were assigned from a small amount, separated from the major product.

β -Anomer: MS (MALDI-TOF): m/z 539.7 [M + H]⁺, 577.7 [M + K]⁺. **¹H-NMR** (400 MHz, CDCl₃): δ (ppm) 7.38-7.18 (m, 15H, OCH₂Ph), 4.70 (s, 1H, H-1'), 4.62-4.41 (m, 7H, OCH₂Ph, H-3), 4.14 (bm, 2H, H-2, H-4), 3.60 (bm, 1H, H-5), 3.17 (bm, 2H, H-3'), 2.53 (bm, 2H, H-5'), 2.02 (bm, 2H, H-4'). **¹³C-NMR** (100.57 MHz, CDCl₃): δ (ppm) 137.86, 137.80, 137.50 (Cq Ph), 128.45-127.68 (OCH₂Ph), 110.10 (C-1), 84.11, 83.12, 80.23 (C-2, C-3, C-4), 73.32, 72.94, 72.30 (OCH₂Ph), 71.44 (C-5), 53.41 (C-1'), 27.48, 27.34 (C-3', C-5'), 25.16 (C-4').

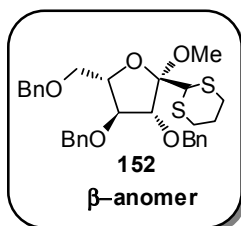


Methyl 2,3,5-Tri-O-benzyl-1-C-(1,3-dithiane-2-yl)-L-arabinoside

Compound 152. To a solution of **151** (0.250 g, 0.464 mmol) in dry THF (2 mL), m.s. 3\AA (0.250 g), MeOH (5 mL) and H_2SO_4 (10 μL) were added under argon atmosphere, and the resulting mixture was stirred under reflux (bath temperature 40 °C) for 12h. After this time, a soln. of 1M NaOH was added to the reaction to neutralize the acid, then the solvent was partial evaporated, and the residue was diluted with CH_2Cl_2 . The organic layer was dried on sodium sulphate, filtered and evaporated. Purification by flash chromatography (eluent (petroleum ether/EtOAc 8:2) afforded **152** (0.172 g, 67% yield) as a yellow oil mixture of α and β anomers (1.5:1 α : β ratio). The following signal attributions were obtained from a small amount of the separated α , β mixture. A 2D NOESY experiment for the α -anomer **152** showed a cross peak between OCH_3 and H-2, and between OCH_3 and H-4 allowing to the assignment of the corresponding stereochemistry.



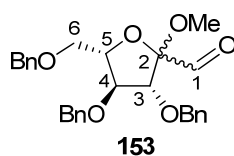
α -Anomer: MS (MALDI-TOF): m/z 553.7 $[\text{M} + \text{H}]^+$, 575.7 $[\text{M} + \text{Na}]^+$, 591.7. **$^1\text{H-NMR}$** (400 MHz, CDCl_3): δ (ppm) 7.32-7.26 (m, 15H, OCH_2Ph), 4.79 (s, 1H, H-1'), 4.59-4.45 (m, 6H, OCH_2Ph), 4.15 (dd, 1H, $J = 10.3, 4.5$ Hz, H-4), 3.97 (d, 1H, $J = 1.5$ Hz, H-2), 3.86 (d, 1H, $J = 4.2$ Hz, H-3), 3.68 (dd, 1H, $J = 10.4, 5.4$ Hz, H-5a), 3.54 (bm, 1H, H-5b), 3.52 (s, 3H, OCH_3), 2.91-2.75 (m, 2H, H-3', H-5'), 2.06 (bm, 1H, H-4'a), 1.90 (bm, 2H, H-4'b). **$^{13}\text{C-NMR}$** (100.57 MHz, CDCl_3): δ (ppm) 138.17, 137.88, 137.66 (Cq Ph), 128.87-127.57 (OCH_2Ph), 108.59 (C-1), 87.18, 84.33, 82.90 (C-2, C-3, C-4), 73.33, 72.61, 71.67 (OCH_2Ph), 70.11 (C-5), 51.46 (C-1'), 50.61 (OCH_3), 30.78, 29.68 (C-3', C-5'), 26.41 (C-4').



β-Anomer: MS (MALDI-TOF): m/z 553.7 [M + H]⁺, 575.7 [M + Na]⁺.

¹H-NMR (400 MHz, CDCl₃): δ (ppm) 7.34-7.26 (m, 15H, OCH₂Ph), 5.30 (s, 1H, H-1'), 4.58-4.47 (m, 6H, OCH₂Ph), 4.17 (dd, 1H, $J = 13.5$, 6.7 Hz, H-4), 4.12 (d, 1H, $J = 7.1$ Hz, H-2), 4.07 (d, 1H, $J = 6.6$ Hz, H-3),

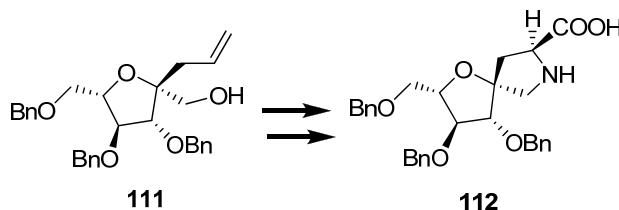
3.59 (dd, $J = 10.3$, 4.8 Hz, H-5a), 3.54 (dd, $J = 10.3$, 5.4 Hz, H-5b), 3.41 (s, 3H, OCH₃), 2.93-2.76 (m, 2H, H-3', H-5'), 2.05 (bm, 1H, H-4'a), 1.89 (bm, 2H, H-4'b). **¹³C-NMR** (100.57 MHz, CDCl₃): δ (ppm) 138.24, 137.97, 137.75 (C_q Ph), 128.87-127.60 (OCH₂Ph), 105.25 (C-1), 85.45, 83.94, 79.25 (C-2, C-3, C-4), 73.68, 72.23, 72.60 (OCH₂Ph), 70.39 (C-5), 52.15 (C-1'), 49.77 (OCH₃), 30.36, 29.69 (C-3', C-5'), 25.80 (C-4').



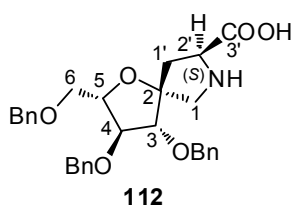
Methyl 3,4,6-Tri-*O*-benzyl-L-arabino-hexo-2-ulo-2,5-furanoside

Compound 153. To a solution of **152** (0.250 g, 0.452 mmol) in acetone (6 mL) at 25 °C was added to a solution of 1,3-dibromo-5,5-dimethylhydantion (DBDMH) (0.258 g, 0.904 mmol) in acetone (4 mL) at -20 °C. The solution quickly turned to red, but soon faded to yellow-orange, and was stirred for 15 min. At this time the solution was shaken with a mixture of sat. aq. sodium sulfite soln. and CH₂Cl₂. The organic phase was washed with sodium bicarbonate, water, brine, dried (NaSO₄), and concentrated to give a yellow oil, compound **153** (≈ 0.452 mmol) which was used in the next step without further purification.

4.1.3.3 Synthesis of Compound 112

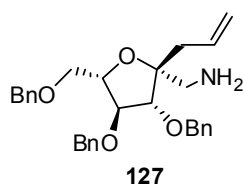


Scheme 28



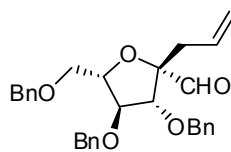
Spiro{(1',4'-anhydro-2',3',5'-tri-*O*-benzyl-L-arabinitol)-1',4'-[(2*S*)-pyrrolidine-2-carboxylic acid]}

Compound 112. The same experimental procedure reported for **85** was applied to the protected amino acid **165** (0.250 g, 0.344 mmol). Purification by flash chromatography afforded the free amino acid derivative **112** (0.147 g, 85 % yield), as an amorphous solid. **MS (MALDI-TOF):** m/z 504.6 $[M + H]^+$, 542.6 $[M + K]^+$. **Elemental analysis calcd (%)** for $C_{30}H_{33}NO_6$: C, 71.55; H, 6.60; N, 2.78; found: C, 71.60; H, 6.54; N, 2.83. **1H NMR** (400 MHz, $CDCl_3$): δ (ppm) 7.85-7.00 (m, 15 H, OCH_2Ph), 4.58-4.31 (m, 6 H, OCH_2Ph), 4.20 (dd, 1 H, $J = 13.0, 7.3$ Hz, H-2'), 4.11 (bs, 1 H, H-5), 3.96-3.84 (m, 2H, H-3, H-4), 3.76 (d, 1 H, $J = 13.8$ Hz, H-1a), 3.56 (dd, 1H, $J = 10.4, 6.2$ Hz, H-6a), 3.48 (dd, 1H, $J = 11.0, 5.9$ Hz, H-6b), 3.39 (d, 1 H, $J = 13.5$ Hz, H-1b), 2.60 (dd, 1 H, $J = 13.4, 6.9$ Hz, H-1'a), 2.05 (dd, 1 H, $J = 13.5, 12.2$ Hz, H-1'b). **^{13}C NMR** (100.57 MHz, $CDCl_3$): δ (ppm) 173.35 (C-3'), 137.93, 137.47, 137.17 (Cq Ph), 92.96 (C-2) 85.97, 83.02, 82.509 (C-3, C-4, C-5), 73.30, 71.78, 71.60, 70.33 (OCH_2Ph , C-6), 62.43 (C-2'), 42.63 (C-1), 29.66 (C-1').



**1-Amino-2,5-anhydro-3,4,6-tri-*O*-benzyl-
-1-deoxy-2-*C*-(prop-2-enyl)-L-glucitol**

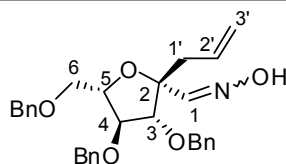
Compound 127. The same experimental procedure reported for **126** was applied to the oxime derivative **158** (0.250 g, 0.513 mmol). Purification by flash chromatography afforded **127** (0.223 g, 92% yield) as a colourless oil. **MS (MALDI-TOF):** m/z 474.6 [M + H]⁺, 497.6 [M + Na]⁺. **Elemental analysis calcd (%)** for C₃₀H₃₅NO₄ C, 76.08; H, 7.45; N, 2.96, found: C, 76.12; H, 7.50; N, 3.00. **¹H NMR** (400 MHz, CDCl₃): δ (ppm) 7.45-7.20 (m, 15H, OCH₂Ph), 5.83-5.75 (m, 1H, H-2'), 5.12 (d, 1H, J = 10.0 Hz, H-3'a), 5.06 (d, 1H, J = 17.8 Hz, H-3'b), 4.68-4.50 (m, 8H, OCH₂Ph, NH₂), 4.18 (dd, 1H, J = 7.0, 5.5 Hz, H-4), 4.06 (d, 1H, J = 5.5 Hz, H-3), 4.01 (dt, 1H, J = 7.0, 4.0 Hz, H-5), 3.68 (dd, 1H, J = 10.6, 4.0 Hz, H-6a), 3.57 (dd, 1H, J = 10.6, 4.0 Hz, H-6b), 2.90 (d, 1H, J = 14.1 Hz, H-1a), 2.70 (d, 1H, J = 14.1 Hz, H-1b), 2.41 (dd, 1H, J = 13.9, 7.1 Hz, H-1'a), 2.32 (dd, 1H, J = 13.9, 7.5 Hz, H-1'b). **¹³C NMR** (100.57 MHz, CDCl₃): δ (ppm) 138.26, 138.19, 138.14 (Cq Ph), 133.50 (C-2'), 119.10 (C-3'), 87.99 (C-3), 85.01 (C-2), 84.69, 80.03 (C-4, C-5), 73.84, 73.16, 72.99, 70.34 (OCH₂Ph, C-6), 47.55 (C-1), 42.05 (C-1').



157

2,5-Anhydro-3,4,6-tri-*O*-benzyl-2-*C*-(prop-2-enyl)- α -L-glucose

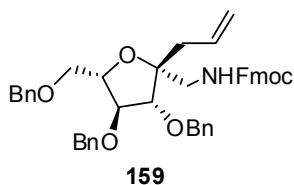
Compound 157. The same experimental procedure reported for **132** was applied to the oxidation of alcohol derivative **111** (0.250 g, 0.527 mmol). The crude aldehyde **157** (\approx 0.527 mmol) was used in the next step without further purification.



158

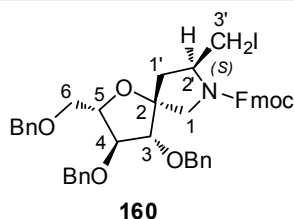
2,5-Anhydro-3,4,6-tri-*O*-benzyl-2-*C*-(prop-2-enyl)-L-glucose oxime

Compound 158. The same experimental procedure reported for **133** was applied to the aldehyde derivative **157** (\approx 0.527 mmol). Purification by flash chromatography afforded **158** (0.223 g, 87% yield over two steps) as a colourless oil (mixture of *E/Z* isomers). The isomers were not separable by chromatography. The following signal attributions were obtained from the mixture. **MS (MALDI-TOF):** m/z 488.6 [$M + H$]⁺, 510.6 [$M + Na$]⁺. **Elemental analysis calcd (%)** for C₃₀H₃₃NO₅: C, 73.90; H, 6.82; N, 2.87, found: C, 73.80; H, 6.91; N, 2.92. **¹H NMR** (400 MHz, CDCl₃): δ (ppm) 8.03 (s, 1H, OH), 7.49 (d, H-1), 7.34-7.24 (m, 15H, OCH₂Ph), 5.94-5.84 (m, 1H, H-2'), 5.12 (d, 1H, J = 10.6 Hz, H-3'a), 5.08 (d, 1H, J = 17.5 Hz, H-3'b), 4.59-4.43 (m, 6H, OCH₂Ph), 4.12 (bm, 1H, H-5), 4.09-4.06 (m, 2H, H-3, H-4), 3.64-3.57 (m, 2H, H-6), 2.67 (bd, 2H, H-1'). **¹³C NMR** (100.57 MHz, CDCl₃): δ (ppm) 154.13 (C-1), 138.36, 138.07, 137.86 (Cq Ph), 133.38 (C-2'), 119.17 (C-3'), 87.42 84.64 (C-3, C-4), 84.16 (C-2), 81.11 (C-5), 73.63, 72.54, 72.33, 70.51 (OCH₂Ph, C-6), 39.85 (C-1').



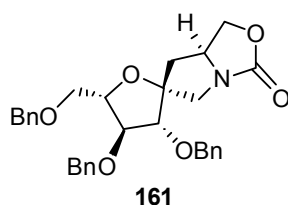
**1-Amino-2,5-Anhydro-3,4,6-tri-O-benzyl-1-deoxy-2-C-(prop-2-enyl)-
-N-9H-fluoren-9-yl-methoxycarbonyl-L-glucitol**

Compound 159. The same experimental procedure reported for **134** was applied to the amine derivative **127** (0.250 g, 0.528 mmol). Purification by flash chromatography afforded **159** (0.315 g, 86% yield) as a yellow oil. **MS (MALDI-TOF):** m/z 734.8 [M + K]⁺. **Elemental analysis calcd (%)** for C₄₅H₄₅NO₆: C, 77.67; H, 6.52; N, 2.01; found: C, 77.70; H, 6.50; N, 2.05. **¹H NMR** (400 MHz, CDCl₃): δ (ppm) 7.81-7.26 (m, 23H, OCH₂Ph, Ar-H Fmoc), 5.89-5.78 (bm, 2H, H-2', NH), 5.14 (dd, 1H, $J = 10.2, 1.5$ Hz, H-3'a), 5.06 (dd, 1H, $J = 17.2, 1.5$ Hz, H-3'b), 4.65-4.47 (m, 6H, OCH₂Ph), 4.40 (d, 2H, $J = 6.8$ Hz, CH₂-Fmoc), 4.27 (t, 1H, $J = 6.0$ Hz, CH-Fmoc), 4.11 (t, 1H, $J = 6.3$ Hz, H-4), 4.04 (d, 1H, $J = 6.3$ Hz, H-3), 4.00 (m, 1H, H-5), 3.64 (dd, 1H, $J = 10.5, 2.4$ Hz, H-6a), 3.52 (bm, 2H, H-6b, H-1a), 3.41 (dd, 1H, $J = 14.4, 5.0$ Hz, H-1b), 2.41 (dd, 1H, $J = 14.5, 6.6$ Hz, H-1'a), 2.32 (dd, 1H, $J = 14.5, 7.7$ Hz, H-1'b). **¹³C NMR** (100.57 MHz, CDCl₃): δ (ppm) 156.83 (CO-Fmoc), 144.38, 141.52 (Cq Ar Fmoc), 138.15, 138.02, 137.96 (Cq Ph), 133.05 (C-2'), 125.37, 125.00, 124.60, 120.17 (Ar Fmoc), 120.17 (C-3'), 86.86 (C-3), 84.13 (C-2), 84.09, 79.90 (C-4, C-5), 73.57, 72.95, 69.71, 66.75, 65.40 (OCH₂Ph, OCH₂-Fmoc, C-6), 50.60 (CH-Fmoc), 45.75 (C-1), 41.11 (C-1').



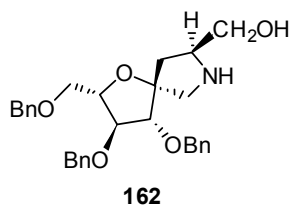
Spiro{(1',4'-anhydro-2',3',5'-tri-O-benzyl-L-arabinitol)-1',4'-[(S)-(9H-fluoren-9-yl)methyl 2-iodomethylpyrrolidine-1-carboxylate]}

Compound 160. The same experimental procedure reported for compound **135** was applied to the compound **159** (0.250 g, 0.359 mmol). Purification by flash chromatography afforded bicyclic iodide **160** (*S* isomer) as a colourless oil (0.251 g, 85 % yield). The diastereoselection of this iodocyclization reaction was extremely high in favour of the *S* isomer **160** (*d.e.* > 98 %). **MS (MALDI-TOF):** *m/z* 822.7 [*M* + *H*]⁺. **Elemental analysis calcd (%)** for C₄₅H₄₄INO₆: C, 65.77; H, 5.40; N, 1.70; found: C, 65.70; H, 5.43; N, 1.73. **¹H NMR** (400 MHz, CDCl₃): δ (ppm) 7.82-7.19 (m, 23H, OCH₂Ph, Ar-*H* Fmoc), 4.61-4.44 (m, 8H, OCH₂Ph, CH₂-Fmoc), 4.23 (t, 1H, *J* = 6.0 Hz, H-4), 4.13 (t, 1H, *J* = 7.1 Hz, CH-Fmoc), 4.08 (d, 1H, *J* = 6.0 Hz, H-3), 4.03 (bm, 1H, H-5), 3.88-3.66 (m, 3H, H-2', CH₂I), 3.46 (m, 2H, H-1), 2.82 (dd, 1H, *J* = 10.2, 2.5 Hz, H-6a), 2.76 (dd, 1H, *J* = 10.2, 2.3 Hz, H-6b), 2.38-2.22 (m, 1H, H-1'a) 1.90 (dd, 1H, *J* = 13.7, 8.5 Hz, H-1'b). **¹³C NMR** (100.57 MHz, CDCl₃): δ (ppm) 144.24 (CO-Fmoc), 141.56, 141.49 (Cq Ar Fmoc), 138.24, 137.91, 137.63 (Cq Ph), 125.40, 125.27, 124.86, 120.20 (Ar-Fmoc), 89.51 (C-2), 86.53, 83.58, 82.04 (C-3, C-4, C-5), 73.57, 71.95, 70.63, 67.66, 67.48 (PhCH₂O, OCH₂Fmoc, C-6), 60.67 (C-2'), 59.12 (C-1), 47.42 (CH-Fmoc), 29.96 (C-1'), 14.45 (C-3').



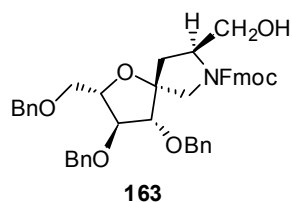
**Spiro{(1',4'-anhydro-2',3',5'-tri-O-benzyl-L-arabinitol)-
-1',6-[tetrahydropyrrolo[1,2-c]oxazol-3(1H)-one]}**

Compound 161. The same experimental procedure reported for compound **136** was applied to the compound **160** (0.250 g, 0.304 mmol). Purification by flash chromatography afforded tricyclic compound **161** as a white solid (0.143 g, 91 % yield). **M.p.** 78-80 °C. **MS (MALDI-TOF):** m/z 516.6 [M + H]⁺, 538.6 [M + Na]⁺. **Elemental analysis calcd (%)** for C₃₁H₃₃NO₆: C, 72.21; H, 6.45; N, 2.72; found: C, 72.19; H, 5.48; N, 2.75. **¹H NMR** (400 MHz, CDCl₃): δ (ppm) 7.34-7.23 (m, 15H, OCH₂Ph), 4.59-4.40 (m, 6H, OCH₂Ph), 4.21-4.17 (m, 1H, H-3'a), 4.15-4.10 (m, 4H, H-1a, H-3'b, H-5, H-2'), 3.92 (dd, 1H, $J = 3.2, 1.9$ Hz, H-4), 3.82 (d, 1H, $J = 1.9$ Hz, H-3), 3.56 (dd, 1H, $J = 9.7, 6.2$ Hz, H-6a), 3.47 (dd, 1H, $J = 9.8, 6.4$ Hz, H-6b), 3.28 (d, 1H, $J = 13.2$ Hz, H-1b), 2.28 (dd, 1H, $J = 12.8, 5.0$ Hz, H-1'a), 1.39 (dd, 1H, $J = 12.9, 10.5$, H-1'b). **¹³C NMR** (100.57 MHz, CDCl₃): δ (ppm) 161.76 (CO), 138.16, 137.77, 137.43 (Cq Ph), 128.81-127.89 (OCH₂Ph), 93.89 (C-2) 86.80, 83.51, 82.35 (C-3, C-4, C-5), 73.61, 72.07, 72.02, 70.72, 67.02 (OCH₂Ph, C-6, C-3'), 59.06 (C-2'), 53.72 (C-1), 41.38 (C-1').



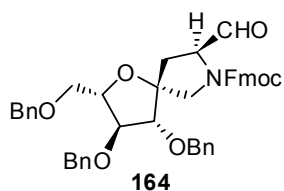
**Spiro{(1',4'-anhydro-2',3',5'-tri-O-benzyl-L-arabinitol)-1',4'-
-[(2S)-pyrrolidin-2-yl-methanol]}**

Compound 162. The same experimental procedure reported for compound **137** was applied to the compound **161** (0.250 g, 0.485 mmol). Purification by flash chromatography afforded amino alcohol **162** as a yellow oil (0.202 g, 85% yield). **MS (MALDI-TOF):** m/z 490.6 $[M + H]^+$, 512.6 $[M + Na]^+$, 528.6 $[M + K]^+$. **Elemental analysis calcd (%)** for $C_{30}H_{35}NO_5$: C, 73.59; H, 7.21; N, 2.86; found: C, 73.64; H, 7.18; N, 2.90. **1H NMR** (400 MHz, $CDCl_3$): δ (ppm) 7.35-7.21 (m, 15H, OCH_2Ph), 4.62-4.36 (m, 6H, OCH_2Ph), 4.16-4.10 (m, 1H, H-5), 4.05 (dd, 1H, $J = 6.6, 2.7$ Hz, H-4), 3.86 (d, 1H, $J = 2.7$ Hz, H-3), 3.68-3.60 (m, 2H, H-2'), 3.56-3.47 (m, 2H, H-6, *OH* or *NH*), 3.32 (d, 1H, $J = 11.9$ Hz, H-3'a), 3.30 (d, 1H, $J = 11.9$ Hz, H-3'b), 3.28 (bs, 1H, *OH* or *NH*), 3.14 (d, 1H, $J = 12.5$ Hz, H-1a), 3.08 (dd, 1H, $J = 12.5$ Hz, H-1b), 2.27 (dd, 1H, $J = 13.1, 6.4$ Hz, H-1'a), 1.47 (dd, 1H, $J = 13.1, 7.9$ Hz, H-1'b). **^{13}C NMR** (100.57 MHz, $CDCl_3$): δ (ppm) 138.20 137.95 137.88 (Cq Ph), 128.81-127.89 (OCH_2Ph), 93.50 (C-2), 86.53, 84.25, 81.40 (C-3, C-4, C-5), 73.61, 72.08, 71.98, 71.01 (OCH_2Ph , C-6), 64.12 (C-3'), 59.51 (C-2'), 53.12 (C-1), 38.57 (C-1').



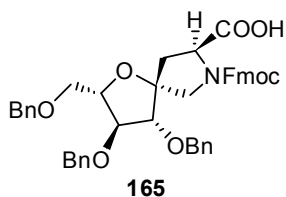
Spiro{(1',4'-anhydro-2',3',5'-tri-*O*-benzyl-L-arabinitol)-1',4'-[(*S*)-(9*H*-fluoren-9-yl)methyl 2-hydroxymethylpyrrolidine-1-carboxylate]}

Compound 163. The same experimental procedure reported for compound **138** was applied to the compound **162** (0.250 g, 0.510 mmol). Purification by flash chromatography afforded carbamate **163** (0.327 g, 90% yield) as a yellow oil. **MS (MALDI-TOF):** m/z 712.8 [M + H]⁺, 734.8 [M + Na]⁺. **Elemental analysis calcd (%)** for C₄₅H₄₅NO₇: C, 75.93; H, 6.37; N, 1.97; found: C, 75.87; H, 6.40; N, 1.90. **¹H NMR** (400 MHz, CDCl₃): δ (ppm) 7.75-7.22 (m, 23H, OCH₂Ph, Ar-Fmoc), 4.60-4.50 (m, 6H, OCH₂Ph), 4.39-4.31 (m, 3H, CH₂-Fmoc, CH-Fmoc), 4.24-4.15 (m, 2H, H-5, H-2'), 4.02 (bs, 1H, H-4), 3.85 (d, 1H, $J = 1.5$ Hz, H-3), 3.82 (d, 1H, $J = 12.3$ Hz, H-1a), 3.74 (d, 1H, $J = 10.6$ Hz, H-3'a), 3.68 (d, 1H, $J = 12.5$ Hz, H-1b), 3.62-3.50 (m, 4H, H-6, H-3'b, OH), 2.31 (dd, 1H, $J = 13.5, 6.9$ Hz, H-1'a), 1.55 (dd, 1H, $J = 13.2, 10.8$, H-1'b). **¹³C NMR** (100.57 MHz, CDCl₃): δ (ppm) 157.07 (CO-Fmoc), 144.05, 143.69, 141.33, 141.30 (Cq Ar Fmoc), 138.04, 137.65, 137.52 (Cq Ph), 125.22, 125.13, 124.72, 119.98 (Ar-Fmoc), 89.00 (C-2) 86.24, 83.31, 82.80 (C-3, C-4, C-5), 73.37, 71.82, 71.60, 70.44, 67.72, 66.65 (OCH₂Ph, OCH₂Fmoc, C-6, C-3'), 60.88 (C-2'), 54.48 (C-1), 47.16 (CH-Fmoc), 37.87 (C-1').



Spiro{(1',4'-anhydro-2',3',5'-tri-*O*-benzyl-L-arabinitol)-1',4-[(*S*)-(9*H*-fluoren-9-yl)methyl 2-formylpyrrolidine-1-carboxylate]}

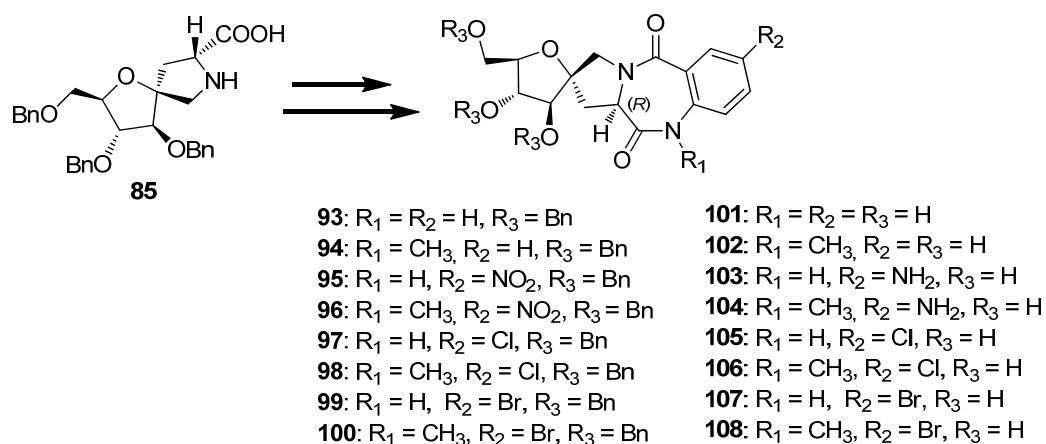
Compound 164. The same experimental procedure reported for alcohol **139** was applied to the compound **163** (0.250 g, 0.351 mmol). The crude aldehyde **164** (≈ 0.351 mmol) was used in the next step without further purification.



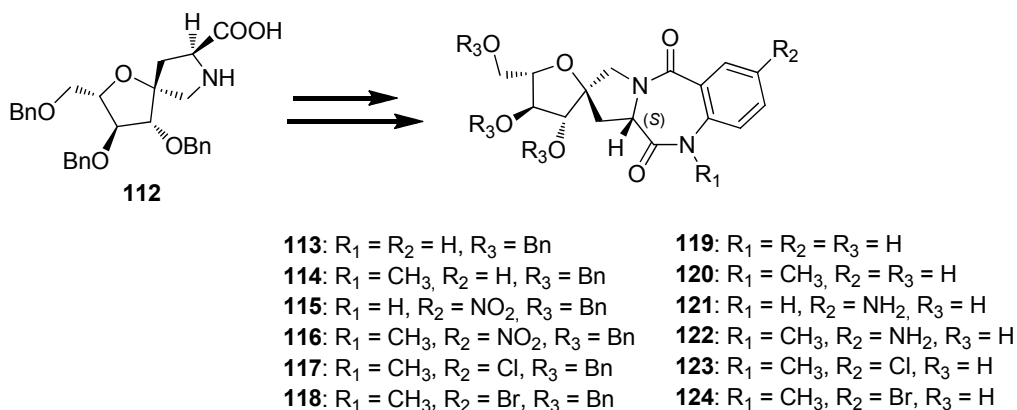
Spiro{(1',4'-anhydro-2',3',5'-tri-*O*-benzyl-L-arabinitol)-1',4-[(*S*)-{[(9*H*-fluoren-9-yl)methoxy]carbonyl}pyrrolidine-2-carboxylic acid]}

Compound 165. The same experimental procedure reported for **140** was applied to the crude aldehyde **164** (≈ 0.351 mmol). Purification by flash chromatography afforded compound **165** (0.178 g, 70% over two steps) as a pink oil. Due to conformational equilibrium only ^{13}C NMR is reported. **MS (MALDI-TOF):** m/z 726.8 $[\text{M} + \text{H}]^+$. **Elemental analysis calcd (%)** for $\text{C}_{45}\text{H}_{43}\text{NO}_8$: C, 74.46; H, 5.97; N, 1.93; found: C, 74.50; H, 6.00; N, 1.90. **^{13}C NMR** (100.57 MHz, CDCl_3): δ (ppm) 170.53 (C-3'), 156.07 (CO-Fmoc), 144.11, 143.78, 143.69, 141.83, (Cq Ar Fmoc), 138.01, 137.97, 137.53 (Cq Ph), 125.24, 125.14, 124.97, 119.97 (Ar-Fmoc), 90.19 (C-2) 85.61, 83.44, 82.13 (C-3, C-4, C-5), 73.37, 71.82, 71.77, 70.36, 68.14 (OCH₂Ph, OCH₂-Fmoc, C-6), 57.41 (C-2'), 53.31 (C-1), 47.10 (CH-Fmoc), 38.30 (C-1').

4.1.4 Synthesis of 1,4-Benzodiazepine-2,5-dione Scaffolds



Scheme 29. D-Fructose-based pyrrolobenzodiazepine scaffolds.



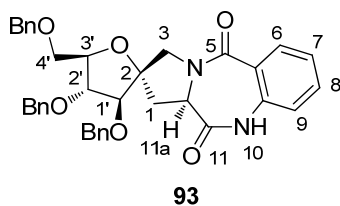
Scheme 30. L-Fructose-based pyrrolobenzodiazepine scaffolds.

General procedure for benzodiazepine synthesis. To a solution of the proline analogue (**85** or **112**) in dry DMF, suitably functionalized isatoic anhydride **60** was added under argon atmosphere, and the resulting mixture was stirred under reflux till complete consume of the starting material. The solvent was then removed under reduced pressure and the residue dissolved in CH₂Cl₂, filtered and evaporated. The crude halogenated benzodiazepines (R₂ = Cl, Br) derived from L-proline analogue were used in the next step (methylation) whereas the other crude products were purified by silica gel flash chromatography to give the desired product.

General procedure for methylation of halogenated benzodiazepines. Benzodiazepines (R₂ = Cl, Br) were dissolved in dry DMF, cesium carbonate (20 eq.) and iodomethane (10 eq.) were added under argon atmosphere, and the resulting mixture was stirred till complete consumption of the starting material. The solvent was then removed under reduced pressure and the residue dissolved in CH₂Cl₂ and filtered. The crude residue was purified by silica gel flash chromatography to give the desired product (compounds **98**, **99**, **117** and **118**).

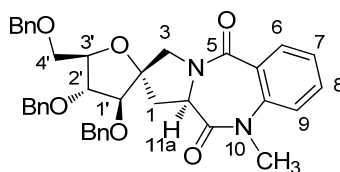
General hydrogenolysis procedure. Compounds derived from R₂ = H, NO₂ (**93-96** and **113-116**) were dissolved in 4:1 MeOH/AcOEt mixture and a few drops of HCl 37% and Pd(OH)₂/C (10% w/w) was added. The flask was purged three times with Ar and then filled with H₂. After 48 h, the catalyst was removed by filtration, and the filtrate concentrated under reduced pressure, affording compounds **101-104**, and **119-122**, respectively.

General debenylation procedure. Halogenated benzodiazepines **97-100**, **117** and **118** were dissolved in dry CH₂Cl₂ and boron trichloride solution 1M CH₂Cl₂ (7 eq.) was slowly added. The solvent was then removed under reduced pressure and the residue dissolved in water, filtered and evaporated. The crude residue was purified by silica gel flash chromatography (eluent AcOEt/EtOH 9:1) affording compounds **105-108**, **123** and **124**, respectively.



Spiro{[(1',4'-anhydro-2', 3', 5'-tri-*O*-benzyl-D-arabinitol)-1',2'-[(11a*R*)-pyrrolo[2,1-*c*][1,4]benzodiazepine-5,11-dione]}

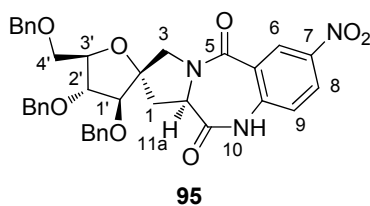
Compound 93. Reaction of **85** (0.250 g, 0.496 mmol) with isatoic anhydride (R = H, 96% pure) (0.101 g, 0.595 mmol), as describe above, after purification by silica gel flash chromatography (petroleum ether/EtOAc 5:5) afforded **93** as a dark brown oil (0.274 g, 91% yield). **MS (MALDI-TOF):** m/z 627 [M + Na]⁺, 643 [M + K]⁺. **Elemental analysis calcd (%)** for C₃₇H₃₆N₂O₆: C, 73.49; H, 6.00; N, 4.63, found: C, 73.46; H, 6.01; N, 4.65. **¹H-NMR** (400 MHz, CDCl₃): δ (ppm) 8.54 (bs, 1H, NH), 7.92 (d, 1H, $J = 7.8$ Hz, Ar-*H*), 7.30 (t, 1H, $J = 7.8$ Hz, Ar-*H*), 7.28-7.18 (m, 15 H, OCH₂Ph), 7.12 (t, 1H, $J = 7.8$ Hz, Ar-*H*), 6.88 (d, 1H, $J = 7.8$ Hz, Ar-*H*), 4.51-4.32 (m, 6H, 3 OCH₂Ph), 4.18 (t, 1H, $J = 6.8$ Hz, H-11a), 4.11 (dt, 1H, $J = 6.2, 3.1$ Hz, H-3'), 4.06 (d, 1H, $J = 13.4$ Hz, H-3a), 4.03 (d, 1H, $J = 1.5$ Hz, H-1'), 3.90 (dd, 1H, $J = 3.1, 1.5$ Hz, H-2'), 3.81 (d, 1H, $J = 13.4$ Hz, H-3b), 3.49 (dd, 1H, $J = 9.8, 6.2$ Hz, H-4'a), 3.42 (dd, 1H, $J = 9.8, 6.2$ Hz, H-4'b), 2.86 (dd, 1H, $J = 13.6, 6.8$ Hz, H-1a), 2.31 (dd, 1H, $J = 13.6, 6.8$ Hz, H-1b). **¹³C-NMR** (100.57 MHz, CDCl₃): δ (ppm) 171.0 (CO-11), 165.77 (CO-5), 138.18, 137.79, 137.56, 134.89 (Cq Ph, Ar), 132.64, 131.74 (C-6, C-8), 128.69-127.78 (OCH₂Ph), 126.62 (Cq Ar), 125.45, 121.06 (C-7, C-9), 89.50 (C-2), 85.06, 84.26, 82.53 (C-1', C-2', C-3'), 73.71, 72.06, 72.02, 70.96 (OCH₂Ph, C-4'), 56.55 (C-11a), 53.47 (C-3), 36.11 (C-1).



94

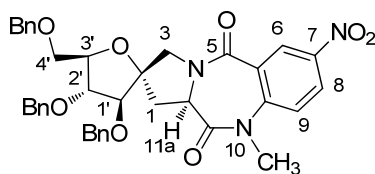
Spiro{[(1',4'-anhydro-2', 3', 5'-tri-*O*-benzyl-D-arabinitol)-1',2'-[(11a*R*)-10-methylpyrrolo[2,1-*c*][1,4]benzodiazepine-5,11-dione]}

Compound 94. Reaction of **85** (0.250 g, 0.496 mmol) with *N*-methylisatoic anhydride (90% pure) (0.117 g, 0.595 mmol), as describe above, after purification by silica gel flash chromatography (petroleum ether/EtOAc 5:5) afforded **94** as a yellow oil (0.267 g, 87 % yield). **MS (MALDI-TOF):** m/z 641 [M + Na]⁺, 657 [M + K]⁺. **Elemental analysis calcd (%)** for C₃₈H₃₈N₂O₆: C, 73.77; H, 6.19; N, 4.53, found: C, 73.72; H, 6.21; N, 4.56. **¹H-NMR** (400 MHz, CDCl₃): δ (ppm) 7.85 (d, 1H, J = 7.8, Hz, Ar-*H*), 7.42 (t, 1H, J = 8.2, Hz, Ar-*H*), 7.26-7.09 (m, 17H, OCH₂Ph, Ar-*H*), 4.56-4.28 (m, 6H, OCH₂Ph), 4.16 (t, 1H, J = 7.5 Hz, H-11a), 4.08 (dt, 1H, J = 6.2, 3.1 Hz, H-3'), 4.05-4.02 (m, 2H, H-3a, H-1'), 3.89 (dd, 1H, J = 3.1, 1.7 Hz, H-2'), 3.74 (d, 1H, J = 13.3 Hz, H-3b), 3.47 (dd, 1H, J = 9.8, 6.2 Hz, H-4'a), 3.40 (dd, 1H, J = 9.8, 6.2 Hz, H-4'b), 3.28 (s, 3H, NCH₃), 2.90 (dd, 1H, J = 13.9, 7.5 Hz, H-1a), 2.28 (dd, 1H, J = 13.9, 7.5 Hz, H-1b). **¹³C-NMR** (100.57 MHz, CDCl₃): δ (ppm) 169.38 (CO-11), 165.73 (CO-5), 140.47, 138.19, 137.81, 137.63 (Cq Ph, Cq Ar), 132.20, 130.75 (C-6, C-8), 129.30 (Cq Ar), 128.67-127.72 (OCH₂Ph), 125.89, 121.88 (C-7, C-9), 89.82 (C-2), 85.60, 84.07, 82.38 (C-1', C-2', C-3'), 73.69, 72.07, 72.01, 70.94 (OCH₂Ph, C-4'), 57.02 (C-11a), 53.39 (C-3), 36.78 (C-1), 36.65 (NCH₃).



Spiro{[(1',4'-anhydro-2', 3', 5'-tri-*O*-benzyl-D-arabinitol)-1',2'-[(11a*R*)-7-nitro-pyrrolo[2,1-*c*][1,4]benzodiazepine-5,11-dione]}

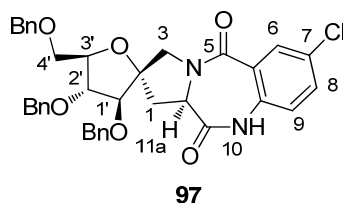
Compound 95. Reaction of **85** (0.250 g, 0.496 mmol) with 5-nitroisatoic anhydride (R = H, X = NO₂) (0.124 g, 0.595 mmol), as described above, after purification by silica gel flash chromatography (petroleum ether/EtOAc 6:4) afforded **95** as a brown amorphous solid (0.254 g, 79% yield). **MS (MALDI-TOF):** *m/z* 649.69 [M + H]⁺, 672 [M + Na]⁺. **Elemental analysis calcd (%)** for C₃₇H₃₅N₃O₈: C, 68.40; H, 5.43; N, 6.47, found: C, 68.47; H, 5.40; N, 4.65. **¹H-NMR** (400 MHz, CDCl₃): δ (ppm) 9.33 (bs, 1H, NH), 8.80 (d, 1H, *J* = 2.6 Hz, Ar-*H*), 8.06 (dd, 1H, *J* = 8.8, 2.6 Hz, Ar-*H*), 7.28-7.10 (m, 15H, OCH₂Ph), 7.02 (d, 1H, *J* = 8.8 Hz, Ar-*H*), 4.51-4.28 (m, 6H, OCH₂Ph), 4.21 (t, 1H, *J* = 8.2 Hz, H-11a), 4.13-4.09 (m, 2H, H-3', H-3a), 3.99 (d, 1H, *J* = 1.8 Hz, H-1'), 3.95 (dd, 1H, *J* = 2.8, 1.8 Hz, H-2'), 3.77 (d, 1H, *J* = 13.3 Hz, H-3b), 3.48 (dd, 1H, *J* = 9.8, 5.9 Hz, H-4'a), 3.42 (dd, 1H, *J* = 9.8, 6.2 Hz, H-4'b), 2.80 (dd, 1H, *J* = 13.0, 8.2 Hz, H-1a), 2.35 (dd, 1H, *J* = 13.5, 8.2 Hz, H-1b). **¹³C-NMR** (100.57 MHz, CDCl₃): δ (ppm) 170.67 (CO-11), 163.83 (CO-5), 144.63, 139.89, 138.02, 137.70, 137.44 (Cq Ph, Cq Ar), 128.74-126.71 (m, OCH₂Ph, Ar-*H*), 126.71 (s, Cq Ar), 121.99 (d, C-9), 88.98 (C-2), 85.25, 83.98, 82.54 (C-1', C-2', C-3'), 73.75, 72.15, 72.03, 70.76 (OCH₂Ph, C-4'), 56.65 (C-11a), 53.98 (C-3), 36.16 (C-1).



96

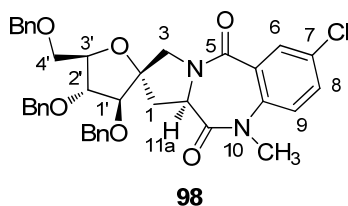
Spiro{(1',4'-anhydro-2', 3', 5'-tri-*O*-benzyl-D-arabinitol)-1',2'-[(11a*R*)-7-nitro-10-methylpyrrolo[2,1-*c*][1,4]benzodiazepine-5,11-dione}

Compound 96. Reaction of **85** (0.250 g, 0.496 mmol) with *N*-methyl-5-nitroisatoic anhydride (0.132 g, 0.595 mmol) afforded crude **96**, as described above. Purification by flash chromatography (eluent toluene/acetone 9:1) afforded **96** as a brown amorphous solid (0.223 g, 68% yield). **MS (MALDI-TOF):** m/z 686 [M + Na]⁺, 702 [M + K]⁺. **Elemental analysis calcd (%)** for C₃₈H₃₇N₃O₈: C, 68.77; H, 5.62; N, 6.33, found: C, 68.67; H, 5.67; N, 6.39. **¹H-NMR** (400 MHz, CDCl₃): δ (ppm) 8.75 (d, 1H, J = 2.7 Hz, Ar-*H*), 8.26 (dd, 1H, J = 9.0, 2.8 Hz, Ar-*H*), 7.27-7.14 (m, 16H, OCH₂Ph, Ar-*H*), 4.54-4.28 (m, 6H, OCH₂Ph), 4.21 (t, 1H, J = 8.0 Hz, H-11a), 4.10-4.06 (m, 2H, H-3', H-3a), 4.02 (d, 1H, J = 1.7 Hz, H-1'), 3.95 (dd, 1H, J = 3.2, 1.7 Hz, H-2'), 3.77 (d, 1H, J = 13.0 Hz, H-3b), 3.46 (dd, 1H, J = 9.9, 5.8 Hz, H-4'a), 3.41 (dd, 1H, J = 9.9, 6.0 Hz, H-4'b), 3.33 (s, 3H, NCH₃), 2.88 (dd, 1H, J = 13.2, 8.0 Hz, H-1a), 2.32 (dd, 1H, J = 13.2, 8.0 Hz, H-1b). **¹³C-NMR** (100 MHz, CDCl₃): δ (ppm) 169.74 (CO-11), 163.64 (CO-5), 145.13, 144.78, 138.08, 137.72, 137.50 (Cq Ph, Cq Ar), 129.98 (Cq Ar), 128.70-126.81 (OCH₂Ph, Ar), 122.69 (C-9), 89.44 (C-2), 85.51, 83.83, 82.43 (C-1', C-2', C-3'), 73.74, 72.16, 72.08, 70.96 (OCH₂Ph, C-4'), 58.99 (C-11a), 36.91 (C-3), 36.73 (C-1), 31.59 (NCH₃).



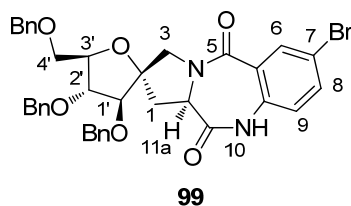
**Spiro{[(1',4'-anhydro-2', 3', 5'-tri-*O*-benzyl-D-arabinitol)-1',2'-
-[(11aR)-7-chloro-pyrrolo[2,1-*c*][1,4]benzodiazepine-5,11-dione]}**

Compound 97. Reaction of **85** (0.250 g, 0.496 mmol) with 5-chloroisatoic anhydride 97% (R = H, X = Cl) (0.147 g, 0.745 mmol), as described above, after purification by silica gel flash chromatography (petroleum ether/EtOAc 6:4) afforded **97** as a dark yellow amorphous solid (0.244 g, 77 % yield). **MS (MALDI-TOF):** m/z 662.1 [M + Na]⁺, 678.1 [M + K]⁺. **Elemental analysis calcd (%)** for C₃₇H₃₅ClN₂O₆: C, 69.53; H, 5.52; N, 4.38, found: C, 69.50; H, 5.54; N, 4.39. **¹H-NMR** (400 MHz, CDCl₃): δ (ppm) 8.78 (bs, 1H, NH), 7.90 (d, 1H, J = 2.5 Hz, Ar-*H*), 7.28-7.14 (m, 15H, OCH₂Ph), 7.10 (dd, 1H, J = 8.0, 1.8 Hz, Ar-*H*), 6.82 (d, 1H, J = 8.6 Hz, Ar-*H*), 4.50-4.28 (m, 6H, OCH₂Ph), 4.16 (t, 1H, J = 7.0 Hz, H-11a), 4.13-4.09 (m, 1H, H-3'), 4.05 (dd, 1H, J = 14, 1.3 Hz, H-3a), 4.01 (d, 1H, J = 1.6 Hz, H-1'), 3.90 (dd, 1H, J = 3.0, 1.9 Hz, H-2'), 3.8 (d, 1H, J = 13.3 Hz, H-3b), 3.48 (dd, 1H, J = 10.0, 6.1 Hz, H-4'a), 3.41 (dd, 1H, J = 10.0, 6.3 Hz, H-4'b), 2.82 (dd, 1H, J = 13.9, 6.8 Hz, H-1a), 2.31 (ddd, 1H, J = 13.6, 7.0, 1.2 Hz, H-1b). **¹³C-NMR** (100.57 MHz, CDCl₃): δ (ppm) 170.74 (CO-11), 164.27 (CO-5), 138.24, 137.76, 137.50, 133.61, 133.59 (Cq Ph, Cq Ar), 132.67, 131.41 (C-6, C-8), 131.08 (Cq Ar), 128.73-127.76 (OCH₂Ph), 122.57 (C-9), 89.19 (C-2), 85.07, 84.18, 82.54 (C-1', C-2', C-3'), 73.73, 72.08, 72.00, 70.88 (OCH₂Ph, C-4'), 56.63 (C-11a), 53.76 (C-3), 36.07 (C-1).



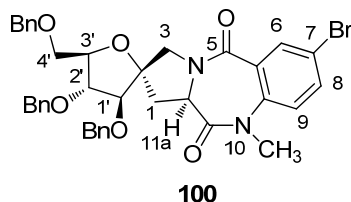
Spiro{(1',4'-anhydro-2', 3', 5'-tri-*O*-benzyl-D-arabinitol)-1',2-[(11a*R*)-7-chloro-10-methylpyrrolo[2,1-*c*][1,4]benzodiazepine-5,11-dione]}

Compound 98. Methylation of **97** (0.250 g, 0.391 mmol) was performed as described above. Purification by flash chromatography (eluent toluene/acetone 9:1) afforded **98** as a yellow amorphous solid (0.212 g, 83% yield). **MS (MALDI-TOF):** m/z 676.2 [M + Na]⁺, 692.2 [M + K]⁺. **Elemental analysis calcd (%)** for C₃₈H₃₇ClN₂O₆: C, 69.88; H, 5.71; N, 4.29, found: C, 69.85; H, 5.72; N, 4.31. **¹H-NMR** (400 MHz, CDCl₃): δ (ppm) 7.83 (d, 1H, $J = 2.4$ Hz, Ar-*H*), 7.38 (dd, 1H, $J = 8.7, 2.6$ Hz, Ar-*H*), 7.26-7.13 (m, 15H, OCH₂Ph), 7.05 (d, 1H, $J = 8.7$ Hz, Ar-*H*), 4.51-4.31 (m, 6H, OCH₂Ph), 4.14 (t, 1H, $J = 7.4$ Hz, H-11a), 4.10-4.06 (m, 1H, H-3'), 4.04-4.01 (m, 2H, H-3a, H-1'), 3.92 (dd, 1H, $J = 3.0, 1.8$ Hz, H-2'), 3.70 (d, 1H, $J = 13.3$ Hz, H-3b), 3.47 (dd, 1H, $J = 9.9, 6.9$ Hz, H-4'a), 3.41 (dd, 1H, $J = 9.9, 6.3$ Hz, H-4'b), 3.26 (s, 3H, NCH₃), 2.87 (dd, 1H, $J = 13.9, 7.1$ Hz, H-1a), 2.29 (ddd, 1H, $J = 14, 8.3, 1.7$ Hz, H-1b). **¹³C-NMR** (100 MHz, CDCl₃): δ (ppm) 169.04 (CO-11), 164.27 (CO-5), 138.95, 138.16, 137.78, 137.57 (Cq Ph, Cq Ar), 132.20, 130.52 (C-6, C-8), 131.59, 130.60 (Cq Ar), 128.68-127.73 (OCH₂Ph), 123.35 (C-9), 89.65 (C-2), 85.56, 83.96, 82.34 (C-1', C-2', C-3'), 73.71, 72.10, 71.90, 71.82 (OCH₂Ph, C-4'), 56.99 (C-11a), 53.53 (C-3), 36.72 (NCH₃), 36.66 (C-1).



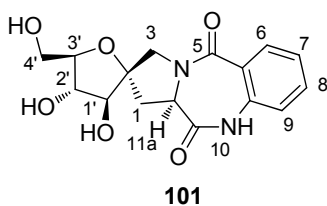
Spiro{(1',4'-anhydro-2', 3', 5'-tri-*O*-benzyl-D-arabinitol)-1',2'-[(11a*R*)-7-bromo-pyrrolo[2,1-*c*][1,4]benzodiazepine-5,11-dione]}

Compound 99. Reaction of **85** (0.250 g, 0.496 mmol) with 6-bromo anhydride 97% (R = H, X = Br) (0.180 g, 0.745 mmol), as described above, after purification by silica gel flash chromatography (petroleum ether/EtOAc 6:4) afforded **99** as a yellow amorphous solid (0.268 g, 79% yield). **MS (MALDI-TOF):** m/z 706.6 [M + Na]⁺, 722.6 [M + K]⁺. **Elemental analysis calcd (%)** for C₃₇H₃₅BrN₂O₆: C, 65.01; H, 5.16; N, 4.10, found: C, 65.04; H, 5.14; N, 4.09. **¹H-NMR** (400 MHz, CDCl₃): δ (ppm) 9.06 (bs, 1H, NH), 8.13 (d, 1H, $J = 2.4$ Hz, Ar-*H*), 7.43 (dd, 1H, $J = 8.5, 2.4$ Hz, Ar-*H*), 7.37-7.18 (m, 15H, OCH₂Ph), 6.85 (d, 1H, $J = 8.5$ Hz, Ar-*H*), 4.59-4.37 (m, 6H, OCH₂Ph), 4.24 (t, 1H, $J = 6.8$ Hz, H-11a), 4.21-4.18 (m, 1H, H-3'), 4.14 (dd, 1H, $J = 13.3, 1.4$ Hz, H-3a), 4.10 (d, 1H, $J = 1.7$ Hz, H-1'), 4.01 (dd, 1H, $J = 3.1, 1.7$ Hz, H-2'), 3.8 (d, 1H, $J = 13.2$ Hz, H-3b), 3.57 (dd, 1H, $J = 9.9, 6.9$ Hz, H-4'a), 3.51 (dd, 1H, $J = 9.8, 6.3$ Hz, H-4'b), 2.91 (dd, 1H, $J = 13.8, 6.8$ Hz, H-1a), 2.39 (ddd, 1H, $J = 13.8, 6.9, 1.4$ Hz, H-1b). **¹³C-NMR** (100.57 MHz, CDCl₃): δ (ppm) 171.24 (CO-11), 164.17 (CO-5), 138.12, 137.76, 137.50 (Cq Ph), 135.55, 134.33 (C-6, C-8), 134.01, 128.10 (Cq Ar), 128.73-127.76 (OCH₂Ph), 122.81 (C-9), 118.58 (Cq Ar), 89.19 (C-2), 85.03, 84.17, 82.53 (C-1', C-2', C-3'), 73.73, 72.08, 71.99, 70.77 (OCH₂Ph, C-4'), 56.53 (C-11a), 53.78 (C-3), 36.08 (C-1).



Spiro{(1',4'-anhydro-2', 3', 5'-tri-*O*-benzyl-D-arabinitol)-1',2'-[(11a*R*)-7-bromo-10-methylpyrrolo[2,1-*c*][1,4]benzodiazepine-5,11-dione]}

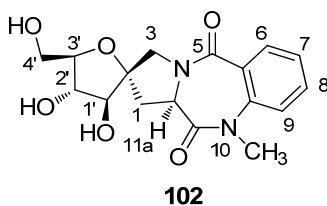
Compound 100. Methylation of **99** (0.250 g, 0.366 mmol) was performed as described previous. Purification by flash chromatography (eluent toluene/acetone 9:1) afforded **100** as a white amorphous solid (0.219 g, 86 % yield). **MS (MALDI-TOF):** m/z 720.6 [M + Na]⁺, 736.6 [M + K]⁺. **Elemental analysis calcd (%)** for C₃₈H₃₇BrN₂O₆: C, 65.42; H, 5.35; N, 4.02, found: C, 65.44; H, 5.34; N, 4.01. **¹H-NMR** (400 MHz, CDCl₃): δ (ppm) 7.98 (d, 1H, J = 2.4 Hz, Ar-*H*), 7.52 (dd, 1H, J = 8.7, 2.5 Hz, Ar-*H*), 7.26-7.13 (m, 15H, OCH₂Ph), 6.98 (d, 1H, J = 8.7 Hz, Ar-*H*), 4.51-4.32 (m, 6H, OCH₂Ph), 4.13 (t, 1H, J = 8.0 Hz, H-11a), 4.10-4.06 (m, 1H, H-3'), 4.04-4.00 (m, 2H, H-3a, H-1'), 3.92 (dd, 1H, J = 3.2, 1.9 Hz, H-2'), 3.69 (d, 1H, J = 13.3 Hz, H-3b), 3.46 (dd, 1H, J = 9.9, 5.9 Hz, H-4'a), 3.41 (dd, 1H, J = 9.9, 6.3 Hz, H-4'b), 3.26 (s, 3H, NCH₃), 2.87 (dd, 1H, J = 13.9, 7.2 Hz, H-1a), 2.29 (ddd, 1H, J = 14, 8.3, 1.9 Hz, H-1b). **¹³C-NMR** (100.57 MHz, CDCl₃): δ (ppm) 169.01 (CO-11), 164.27 (CO-5), 139.44, 138.16, 137.78, 137.57 (Cq Ph, Cq Ar), 135.12, 133.45 (C-6, C-8), 130.81 (Cq Ar), 128.67-127.73 (OCH₂Ph), 123.57 (C-9), 119.20 (Cq Ar), 89.62 (C-2), 85.55, 83.95, 82.37 (C-1', C-2', C-3'), 73.70, 72.10, 70.90, 70.82 (OCH₂Ph, C-4'), 56.97 (C-11a), 53.54 (C-3), 36.73 (NCH₃), 36.65 (C-1).



101

Spiro{(1',4'-anhydro-D-arabinitol)-1',2-[(11aR)-pyrrolo[2,1-c][1,4]benzodiazepine-5,11-dione]}

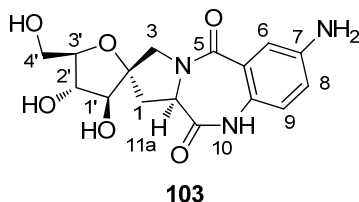
Compound 101. Hydrogenolysis of **93** (0.100 g, 0.165 mmol) afforded **101** as a clear brown amorphous solid (0.052 g, 94% yield). **MS (MALDI-TOF):** m/z 357 [M + Na]⁺, 373 [M + K]⁺. **Elemental analysis calcd (%)** for C₁₆H₁₈N₂O₆: C, 57.48; H, 5.43; N, 8.38, found: C, 57.55; H, 5.38; N, 8.44. **¹H-NMR** (400 MHz, D₂O): δ (ppm) 7.66 (d, 1H, J = 7.4 Hz, Ar-*H*), 7.44 (t, 1H, J = 7.4 Hz, Ar-*H*), 7.21 (t, 1H, J = 7.4 Hz, Ar-*H*), 7.01 (d, 1H, J = 7.4 Hz, Ar-*H*), 4.30 (t, 1H, J = 7.6 Hz, H-11a), 4.13 (d, 1H, J = 5.4 Hz, H-1'), 3.99 (t, 1H, J = 5.4 Hz, H-2'), 3.80 (d, 1H, J = 13.1 Hz, H-3a), 4.08 (bm, 1H, H-3'), 3.62-3.54 (m, 3H, H-3b, H-4'a, H-4'b), 2.70 (dd, 1H, J = 14.1, 7.6 Hz, H-1a), 2.23 (dd, 1H, J = 14.1, 7.6 Hz, H-1b). **¹³C-NMR** (100.57 MHz, D₂O): δ (ppm) 171.56 (CO-11), 168.43 (CO-5), 135.20 (Cq Ar), 133.50, 130.10, 125.65 (Ar), 125.14 (Cq Ar), 121.82 (Ar), 88.03 (C-2), 81.96, 79.21, 76.44 (C-1', C-2', C-3'), 61.36 (C-4'), 56.33 (C-11a), 52.94 (C-3), 34.95 (C-1).



102

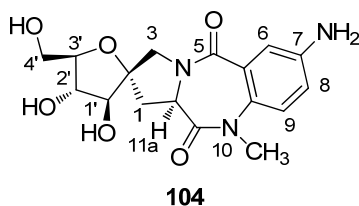
Spiro{(1',4'-anhydro-D-arabinitol)-1',2-[(11aR)-10-methylpyrrolo[2,1-c][1,4]benzodiazepine-5,11-dione]}

Compound 102. Hydrogenolysis of **94** (0.100 g, 0.161 mmol) afforded **102** as a yellow amorphous solid (0.052 g, 92% yield). **MS (MALDI-TOF):** m/z 371 [M + Na]⁺, 387 [M + K]⁺. **Elemental analysis calcd (%)** for C₁₇H₂₀N₂O₆: C, 58.61; H, 5.79; N, 8.04, found: C, 58.55; H, 5.84; N, 8.06. **¹H-NMR** (400 MHz, D₂O): δ (ppm) 7.72 (d, 1H, J = 7.7, Ar-*H*), 7.54 (t, 1H, J = 8.5 Hz, Ar-*H*), 7.48-7.40 (m, 2H, Ar-*H*), 4.38 (t, 1H, J = 8.1 Hz, H-11a), 4.22 (d, 1H, J = 4.3 Hz, H-1'), 3.98 (bt, 1H, H-2'), 3.92 (d, 1H, J = 13.4 Hz, H-3a), 3.90-3.78 (bm, 1H, H-3'), 3.72-3.53 (m, 3H, H-3b, H-4'a, H-4'b), 3.33 (s, 3H, NCH₃), 2.95 (dd, 1H, J = 13.9, 8.1 Hz, H-1a), 2.37 (dd, 1H, J = 13.9, 8.1 Hz, H-1b). **¹³C-NMR** (100.57 MHz, D₂O): δ (ppm) 170.76 (CO-11), 167.89 (CO-5), 140.58, 133.70 (Cq Ar), 129.64, 127.45, 126.74, 123.32 (Ar), 88.23 (C-2), 80.86, 79.21, 76.54 (C-1', C-2', C-3'), 60.86 (C-4'), 57.43 (C-11a), 52.74 (C-3), 37.58 (NCH₃), 36.99 (C-1).



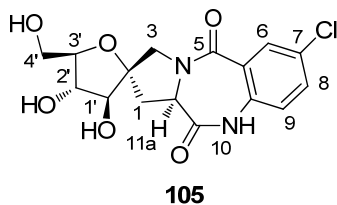
Spiro{[(1',4'-anhydro-D-arabinitol)-1',2-][(11aR)-7-amino-pyrrolo[2,1-c][1,4]benzodiazepine-5,11-dione]}

Compound 103. Hydrogenolysis of **95** (0.100 g, 0.154 mmol) afforded **103** as a brown oil (0.048 g, 89% yield). **MS (MALDI-TOF):** m/z 372 $[M + Na]^+$, 388 $[M + K]^+$. **Elemental analysis calcd (%)** for $C_{16}H_{19}N_3O_6$: C, 55.01; H, 5.48; N, 12.03, found: C, 55.05; H, 5.40; N, 12.09. **1H -NMR** (400 MHz, CD_3OD): δ (ppm) 7.69 (bs, 1H, Ar-*H*), 7.40 (bd, 1H, Ar-*H*), 7.15 (d, 1H, $J = 8.5$ Hz, Ar-*H*), 4.36 (t, 1H, $J = 7.7$ Hz, H-11a), 4.12 (d, 1H, $J = 4.2$ Hz, H-1'), 4.06 (d, 1H, 11.8 Hz, H-3a), 3.97 (t, 1H, $J = 4.2$ Hz, H-2'), 3.75-3.70 (m, 1H, H-3'), 3.68-3.65 (m, 2H, H-3b, H-4'a), 3.62 (dd, 1H, $J = 11.8, 5.1$ Hz, H-4'b), 2.81 (dd, 1H, $J = 13.7, 7.9$ Hz, H-1a), 2.27 (dd, 1H, $J = 13.7, 7.7$ Hz, H-1b). **^{13}C -NMR** (100.57 MHz, CD_3OD): δ (ppm) 174.12 (CO-11), 169.40 (CO-5), 139.87, 133.58, 130.98 (Cq Ar), 130.43, 128.11, 127.10 (Ar), 92.64 (C-2), 87.77, 84.08, 81.88 (C-1', C-2', C-3'), 66.27 (C-4'), 60.57 (C-11a), 57.44 (C-3), 39.68 (C-1).



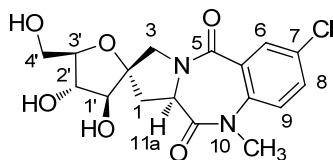
Spiro{(1',4'-anhydro-D-arabinitol)-1',2-[(11aR)-7-amino-10-methylpyrrolo[2,1-c][1,4]benzodiazepine-5,11-dione]}

Compound 104. Hydrogenolysis of **96** (0.100 g, 0.151 mmol) afforded **104** as a brown amorphous solid (0.045 g, 82% yield). **MS (MALDI-TOF):** m/z 386 [M + Na]⁺, 402 [M + K]⁺. **Elemental analysis calcd (%)** for C₁₇H₂₁N₃O₆: C, 56.19; H, 5.83; N, 11.56, found: C, 56.11; H, 5.80; N, 11.60. **¹H-NMR** (400 MHz, D₂O): δ (ppm) 7.80 (d, 1H, J = 2.9 Hz, Ar-*H*), 7.68 (dd, 1H, J = 9.0, 2.9 Hz, Ar-*H*), 7.48 (d, 1H, J = 9.0 Hz, Ar-*H*), 4.24 (t, 1H, J = 8.0 Hz, H-11a), 4.16 (d, 1H, J = 5.3 Hz, H-1'), 3.92 (dd, 1H, J = 6.4, 5.3 Hz, H-2'), 3.83-3.72 (m, 2H, H-3a, H-3'), 3.61-3.49 (m, 3H, H-3b, H-4'a, H-4'b), 3.26 (s, 3H, NCH₃), 2.94 (dd, 1H, J = 14.1, 8.0 Hz, H-1a), 2.25 (dd, 1H, J = 14.1, 8.0 Hz, H-1b). **¹³C-NMR** (100.57 MHz, D₂O): δ (ppm) 172.71 (CO-11), 168.10 (CO-5), 138.67, 129.74, 131.59 (Cq Ar), 127.87, 127.15, 123.68 (Ar), 91.03 (C-2), 84.56, 81.63, 78.92 (C-1', C-2', C-3'), 65.30 (C-4'), 59.34 (C-11a), 55.44 (C-3), 39.13 (NCH₃), 37.95 (C-1).



105
Spiro{[(1',4'-anhydro-D-arabinitol)-1',2-[(11a*R*)-7-chloro-pyrrolo[2,1-*c*][1,4]benzodiazepine-5,11-dione]}

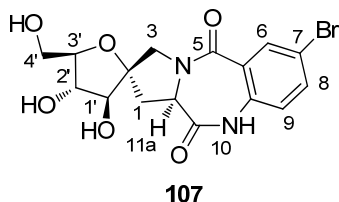
Compound 105. Debenzylation of **97** (0.250 g, 0.391 mmol) and further purification afforded compound **105** as a dark yellow amorphous solid (0.134 g, 93% yield). **MS (MALDI-TOF):** m/z 391.8 [M + Na]⁺, 407.8 [M + K]⁺. **Elemental analysis calcd (%)** for C₁₆H₁₇ClN₂O₆: C, 52.11; H, 4.65; N, 7.60, found: C, 52.09; H, 4.64; N, 7.63. **¹H-NMR** (400 MHz, CD₃OD): δ (ppm) 7.81 (d, 1H, J = 2.5 Hz, Ar-*H*), 7.52 (dd, 1H, J = 8.7, 2.5 Hz, Ar-*H*), 7.12 (d, 1H, J = 8.7 Hz, Ar-*H*), 4.33 (t, 1H, J = 8.0 Hz, H-11a), 4.12 (d, 1H, J = 4.4 Hz, H-1'), 4.03 (dd, 1H, J = 13.2, 1.6 Hz, H-3a'), 3.97 (t, 1H, J = 5.3 Hz, H-2'), 3.81 (dd, 1H, J = 8.6, 5.2 Hz, H-3'), 3.71-3.66 (m, 2H, H-3b, H-4'a), 3.61 (dd, 1H, J = 11.8, 5.2 Hz, H-4b), 2.89 (dd, 1H, J = 13.9, 7.9 Hz, H-1a), 2.34 (ddd, 1H, J = 13.8, 8.2, 1.5 Hz, H-1a). **¹³C-NMR** (100.57 MHz, CD₃OD): δ (ppm) 174.35 (CO-11), 169.58 (CO-5), 139.06 (Cq Ar), 136.51, 133.99 (C-6, C-8), 133.77, 131.29 (Cq Ar), 127.08 (C-9), 92.45 (C-2), 87.52, 83.93, 81.68 (C-1', C-2', C-3'), 66.11 (C-4'), 60.40 (C-11a), 57.23 (C-3), 39.50 (C-1).



106

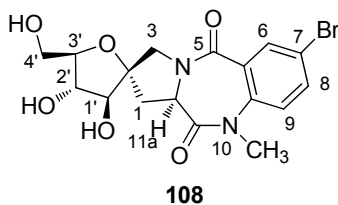
Spiro{[(1',4'-anhydro-D-arabinitol)-1',2-[(11aR)-7-chloro-10-methylpyrrolo[2,1-c][1,4]benzodiazepine-5,11-dione]}

Compound 106. Debenzylation of **98** (0.250 g, 0.383 mmol) and further purification afforded **106** as a white amorphous solid (0.134 g, 92% yield). **MS (MALDI-TOF):** m/z 405.8 $[M + Na]^+$, 421.8 $[M + K]^+$. **Elemental analysis calcd (%)** for $C_{17}H_{19}ClN_2O_6$: C, 53.34; H, 5.00; N, 7.32, found: C, 53.37; H, 4.98; N, 7.31. **1H -NMR** (400 MHz, D_2O): δ (ppm) 7.61 (d, 1H, $J = 2.5$ Hz, Ar- H), 7.51 (dd, 1H, $J = 8.8, 2.6$ Hz, Ar- H), 7.27 (d, 1H, $J = 8.8$ Hz, Ar- H), 4.22 (t, 1H, $J = 7.9$ Hz, H-11a), 4.15 (d, 1H, $J = 5.3$ Hz, H-1'), 3.92 (t, 1H, $J = 6.3$ Hz, H-2'), 3.78-3.71 (m, 2H, H-3a', H-3'), 3.61-3.48 (m, 3H, H-3b, H-4'a, H-4b), 3.32 (s, 3H, NCH_3), 2.78 (dd, 1H, $J = 14.2, 7.3$ Hz, H-1a), 2.22 (ddd, 1H, $J = 14.2, 8.5, 1.7$ Hz, H-1a). **^{13}C -NMR** (100.57 MHz, D_2O): δ (ppm) 172.90 (CO-11), 169.12 (CO-5), 141.70 (Cq Ar), 135.68 (C-6) 133.88 (Cq Ar) 131.47 (C-8), 131.36 (Cq Ar), 127.31 (C-9), 92.94 (C-2), 84.47, 81.63, 78.85 (C-1', C-2', C-3'), 63.78 (C-4'), 59.24 (C-11a), 55.20 (C-3), 39.06 (NCH_3), 37.81 (C-1).



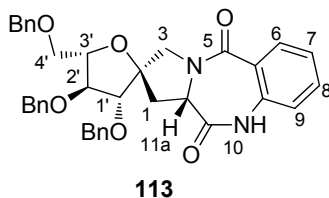
Spiro{[(1',4'-anhydro-D-arabinitol)-1',2-[(11aR)-7-bromo-pyrrolo[2,1-c][1,4]benzodiazepine-5,11-dione]}

Compound 107. Debenzylation of **99** (0.250 g, 0.366 mmol) and further purification afforded **107** as a white amorphous solid (0.134 g, 89% yield). **MS (MALDI-TOF):** m/z 436.2 $[M + Na]^+$, 452.2 $[M + K]^+$. **Elemental analysis calcd (%)** for $C_{16}H_{17}BrN_2O_6$: C, 46.51; H, 4.15; N, 6.78, found: C, 46.49; H, 4.16; N, 6.79. **1H -NMR** (400 MHz, CD_3OD): δ (ppm) 7.96 (d, 1H, $J = 2.3$ Hz, Ar- H), 7.65 (dd, 1H, $J = 8.6, 2.4$ Hz, Ar- H), 7.05 (d, 1H, $J = 8.6$ Hz, Ar- H), 4.33 (t, 1H, $J = 8.0$ Hz, H-11a), 4.10 (d, 1H, $J = 4.4$ Hz, H-1'), 4.03 (dd, 1H, $J = 13.1, 1.7$ Hz, H-3a'), 3.97 (t, 1H, $J = 5.3$ Hz, H-2'), 3.81 (ddd, 1H, $J = 10.5, 5.2, 3.4$ Hz, H-3'), 3.71-3.66 (m, 2H, H-3b, H-4'a), 3.61 (dd, 1H, $J = 11.8, 5.2$ Hz, H-4b), 2.89 (dd, 1H, $J = 14.0, 7.9$ Hz, H-1a), 2.34 (ddd, 1H, $J = 13.8, 8.2, 1.7$ Hz, H-1a). **^{13}C -NMR** (100.57 MHz, CD_3OD): δ (ppm) 174.33 (CO-11), 169.49 (CO-5), 139.50 (Cq Ar), 139.43, 136.97 (C-6, C-8), 131.56 (Cq Ar), 127.24 (C-9), 121.08 (Cq Ar), 92.42 (C-2), 87.48, 83.91, 81.67 (C-1', C-2', C-3'), 66.11 (C-4'), 60.38 (C-11a), 57.24 (C-3), 39.51 (C-1).



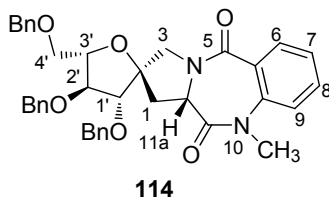
Spiro{[(1',4'-anhydro-D-arabinitol)-1',2-[(11aR)-7-bromo-10-methylpyrrolo[2,1-c][1,4]benzodiazepine-5,11-dione]}

Compound 108. Debenzylation of **100** (0.250 g, 0.358 mmol) and further purification afforded **108** as a white amorphous solid (0.138 g, 90% yield). **MS (MALDI-TOF):** m/z 450.3 $[M + Na]^+$, 466.3 $[M + K]^+$. **Elemental analysis calcd (%)** for $C_{17}H_{19}BrN_2O_6$: C, 47.79; H, 4.48; N, 6.56, found: C, 47.77; H, 4.49; N, 6.57. **1H -NMR** (400 MHz, D_2O): δ (ppm) 7.73 (d, 1H, $J = 2.4$ Hz, Ar-*H*), 7.62 (dd, 1H, $J = 8.8, 2.4$ Hz, Ar-*H*), 7.17 (d, 1H, $J = 8.8$ Hz, Ar-*H*), 4.19 (t, 1H, $J = 7.9$ Hz, H-11a), 4.12 (d, 1H, $J = 5.3$ Hz, H-1'), 3.90 (t, 1H, $J = 6.3$ Hz, H-2'), 3.76-3.69 (m, 2H, H-3a', H-3'), 3.59-3.44 (m, 3H, H-3b, H-4'a, H-4b), 3.20 (s, 3H, NCH_3), 2.76 (dd, 1H, $J = 14.3, 7.5$ Hz, H-1a), 2.19 (ddd, 1H, $J = 14.2, 8.4, 1.6$ Hz, H-1a). **^{13}C -NMR** (100.57 MHz, D_2O): δ (ppm) 172.62 (CO-11), 168.55 (CO-5), 142.09 (Cq Ar), 138.48 (C-6) 133.88 (C-8), 131.60 (Cq Ar) 127.29 (C-9), 121.36 (Cq Ar), 92.85 (C-2), 84.58, 81.69, 78.95 (C-1', C-2', C-3'), 63.81 (C-4'), 59.18 (C-11a), 55.26 (C-3), 39.01 (NCH_3), 37.90 (C-1).



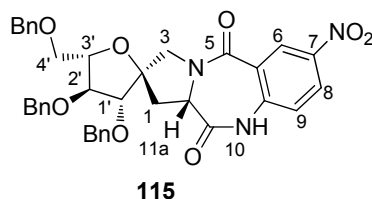
113
Spiro{(1',4'-anhydro-2', 3', 5'-tri-*O*-benzyl-L-arabinitol)-1',2'-[(11a*S*)-pyrrolo[2,1-*c*][1,4]benzodiazepine-5,11-dione]}

Compound 113. Reaction of **112** (0.250 g, 0.496 mmol) with isatoic anhydride (R = H, 96% pure) (0.101 g, 0.595 mmol), as describe above, after purification by silica gel flash chromatography (petroleum ether/EtOAc 5:5) afforded **113** as a yellow amorphous solid (0.281 g, 89% yield). **MS (MALDI-TOF):** m/z 627.7 [M + Na]⁺, 643.7 [M + K]⁺. **Elemental analysis calcd (%)** for C₃₇H₃₆N₂O₆: C, 73.49; H, 6.00; N, 4.63, found: C, 73.45; H, 6.02; N, 4.65. **¹H-NMR** (400 MHz, CDCl₃): δ (ppm) 8.80 (bs, 1H, NH), 7.93 (dd, 1H, $J = 7.9, 1.3$ Hz, Ar-*H*), 7.33-7.12 (m, 17 H, OCH₂Ph, Ar-*H*), 6.92 (d, 1H, $J = 7.7$ Hz, Ar-*H*), 4.52-4.30 (m, 6H, 3 OCH₂Ph), 4.19 (t, 1H, $J = 6.8$ Hz, H-11a), 4.12 (dt, 1H, $J = 6.2, 3.2$ Hz, H-3'), 4.07 (d, 1H, $J = 13.4$ Hz, H-3a), 4.03 (d, 1H, $J = 1.3$ Hz, H-1'), 3.90 (dd, 1H, $J = 2.8, 1.4$ Hz, H-2'), 3.81 (d, 1H, $J = 13.3$ Hz, H-3b), 3.49 (dd, 1H, $J = 9.9, 6.2$ Hz, H-4'a), 3.42 (dd, 1H, $J = 9.8, 6.2$ Hz, H-4'b), 2.86 (dd, 1H, $J = 13.9, 6.7$ Hz, H-1a), 2.31 (dd, 1H, $J = 13.7, 6.9$ Hz, H-1b). **¹³C-NMR** (100.57 MHz, CDCl₃): δ (ppm) 171.2 (CO-11), 165.94 (CO-5), 138.23, 137.85, 137.61, 135.05 (Cq Ph, Cq Ar), 132.69, 131.72 (C-6, C-8), 128.75-127.89 (OCH₂Ph), 126.61 (Cq Ar), 125.44, 121.19 (C-7, C-9), 89.50 (C-2), 84.94, 84.17, 82.47 (C-1', C-2', C-3'), 73.61, 71.93, 71.88, 70.87 (OCH₂Ph, C-4'), 56.42 (C-11a), 53.31 (C-3), 35.88 (C-1).



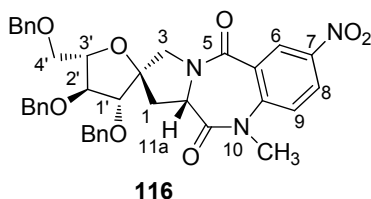
**Spiro{[(1',4'-anhydro-2', 3', 5'-tri-*O*-benzyl-L-arabinitol)-1',2'-
-[(11a*S*)-10-methylpyrrolo[2,1-*c*][1,4]benzodiazepine-5,11-dione]}**

Compound 114. Reaction of **112** (0.250 g, 0.496 mmol) with *N*-methyloisatoic anhydride (90% pure) (0.117 g, 0.595 mmol), after purification as described above, afforded **114** as a yellow amorphous solid (0.267 g, 87 % yield). **MS (MALDI-TOF):** m/z 641.7 [M + Na]⁺, 657.7 [M + K]⁺. **Elemental analysis calcd (%)** for C₃₈H₃₈N₂O₆: C, 73.77; H, 6.19; N, 4.53, found: C, 73.75; H, 6.20; N, 4.54. **¹H-NMR** (400 MHz, CDCl₃): δ (ppm) 7.94 (dd, 1H, $J = 7.8, 1.4$ Hz, Ar-*H*), 7.52 (dt, 1H, $J = 8.4, 1.6$ Hz, Ar-*H*), 7.34-7.19 (m, 17H, OCH₂Ph, Ar-*H*), 4.60-4.41 (m, 6H, OCH₂Ph), 4.24 (t, 1H, $J = 7.7$ Hz, H-11a), 4.17 (ddd, 1H, $J = 12.1, 6.1, 3.2$ Hz, H-3'), 4.13-4.10 (m, 2H, H-3a, H-1'), 3.97 (dd, 1H, $J = 2.9, 1.7$ Hz, H-2'), 3.81 (d, 1H, $J = 13.3$ Hz, H-3b), 3.55 (dd, 1H, $J = 9.9, 6.2$ Hz, H-4'a), 3.49 (dd, 1H, $J = 9.8, 6.2$ Hz, H-4'b), 3.37 (s, 3H, NCH₃), 2.98 (dd, 1H, $J = 14.0, 7.1$ Hz, H-1a), 2.37 (ddd, 1H, $J = 13.9, 7.5, 1.4$ Hz, H-1b). **¹³C-NMR** (100.57 MHz, CDCl₃): δ (ppm) 169.32 (CO-11), 165.59 (CO-5), 140.33, 138.04, 137.65, 137.47 (Cq Ph, Cq Ar), 132.05, 130.59 (C-6, C-8), 129.13 (Cq Ar), 128.51-127.49 (OCH₂Ph), 125.72, 121.70 (C-7, C-9), 89.57 (C-2), 85.29, 83.77, 82.11 (C-1', C-2', C-3'), 73.39, 71.76, 71.68, 70.63 (OCH₂Ph, C-4'), 56.66 (C-11a), 53.03 (C-3), 36.40 (NCH₃), 36.24 (C-1).



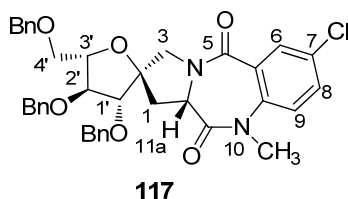
Spiro{(1',4'-anhydro-2', 3', 5'-tri-*O*-benzyl-L-arabinitol)-1',2'-[(11a*S*)-7-nitro-pyrrolo[2,1-*c*][1,4]benzodiazepine-5,11-dione]}

Compound 115. Reaction of **112** (0.250 g, 0.496 mmol) with 5-nitroisatoic anhydride (R = H, X = NO₂) (0.124 g, 0.595 mmol), as described above, after purification by silica gel flash chromatography (petroleum ether/EtOAc 6:4) afforded **115** as a brown amorphous solid (0.228 g, 71% yield). **MS (MALDI-TOF):** *m/z* 649.69 [M + H]⁺, 672 [M + Na]⁺, 688 [M + K]⁺. **Elemental analysis calcd (%)** for C₃₇H₃₅N₃O₈: C, 68.40; H, 5.43; N, 6.47, found: C, 68.45; H, 5.47; N, 4.53. **¹H-NMR** (400 MHz, CDCl₃): δ (ppm) 9.24 (bs, 1H, NH), 8.78 (d, 1H, *J* = 2.5 Hz, Ar-*H*), 8.07 (dd, 1H, *J* = 8.8, 2.5 Hz, Ar-*H*), 7.30-7.11 (m, 15H, OCH₂Ph), 7.03 (d, 1H, *J* = 8.8 Hz, Ar-*H*), 4.50-4.27 (m, 6H, OCH₂Ph), 4.22 (t, 1H, *J* = 8.4 Hz, H-11a), 4.15-4.10 (m, 2H, H-3', H-3a), 3.89 (d, 1H, *J* = 1.8 Hz, H-1'), 3.94 (dd, 1H, *J* = 2.8, 1.8 Hz, H-2'), 3.78 (d, 1H, *J* = 13.3 Hz, H-3b), 3.47 (dd, 1H, *J* = 9.8, 5.9 Hz, H-4'a), 3.40 (dd, 1H, *J* = 9.8, 6.2 Hz, H-4'b), 2.79 (dd, 1H, *J* = 13.0, 8.2 Hz, H-1a), 2.32 (dd, 1H, *J* = 13.5, 8.2 Hz, H-1b). **¹³C-NMR** (100.57 MHz, CDCl₃): δ (ppm) 170.65 (CO-11), 163.80 (CO-5), 144.61, 139.87, 137.89, 137.68, 137.40 (Cq Ph, Cq Ar), 128.70-126.69 (OCH₂Ph, Ar), 126.70 (Cq Ar), 121.98 (C-9), 88.97 (C-2), 85.22, 83.96, 82.52 (C-1', C-2', C-3'), 73.73, 72.13, 72.01, 70.73 (OCH₂Ph, C-4'), 56.63 (C-11a), 53.96 (C-3), 36.15 (C-1).



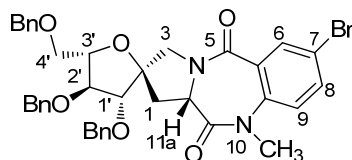
Spiro{(1',4'-anhydro-2', 3', 5'-tri-*O*-benzyl-L-arabinitol)-1',2'-[(11a*S*)-7-nitro-10-methylpyrrolo[2,1-*c*][1,4]benzodiazepine-5,11-dione]}

Compound 116. Reaction of **112** (0.250 g, 0.496 mmol) with *N*-methyl-5-nitroisatoic anhydride (R = CH₃, X = NO₂) (0.132 g, 0.595 mmol) afforded crude **116**. Purification by flash chromatography (eluent toluene/acetone 9:1) afforded **116** as a yellow amorphous solid (0.236 g, 72% yield). **MS (MALDI-TOF):** *m/z* 686.7 [M + Na]⁺, 702.7 [M + K]⁺. **Elemental analysis calcd (%)** for C₃₈H₃₇N₃O₈: C, 68.77; H, 5.62; N, 6.33, found: C, 68.67; H, 5.67; N, 6.39. **¹H-NMR** (400 MHz, CDCl₃): δ (ppm) 8.77 (d, 1H, *J* = 2.7 Hz, *Ar-H*), 8.28 (dd, 1H, *J* = 9.0, 2.8 Hz, *Ar-H*), 7.29-7.15 (m, 16H, OCH₂Ph, *Ar-H*), 4.53-4.32 (m, 6H, OCH₂Ph), 4.46 (t, 1H, *J* = 7.7 Hz, H-11a), 4.11-4.07 (m, 2H, H-3', H-3a), 4.03 (d, 1H, *J* = 1.6 Hz, H-1'), 3.95 (dd, 1H, *J* = 3.2, 1.8 Hz, H-2'), 3.72 (d, 1H, *J* = 13.3 Hz, H-3b), 3.47 (dd, 1H, *J* = 9.8, 5.9 Hz, H-4'a), 3.41 (dd, 1H, *J* = 9.8, 6.3 Hz, H-4'b), 3.34 (s, 3H, NCH₃), 2.88 (dd, 1H, *J* = 13.7, 7.2 Hz, H-1a), 2.33 (ddd, 1H, *J* = 14.1, 8.4, 1.6 Hz, H-1b). **¹³C-NMR** (100.57 MHz, CDCl₃): δ (ppm) 168.99 (CO-11), 163.77 (CO-5), 145.21, 144.81, 138.13, 137.77, 137.56, 130.01 (Cq Ph, Cq Ar), 128.77-127.77 (OCH₂Ph), 127.09, 126.86, 122.74 (Ar), 89.47 (C-2), 85.41, 83.73, 82.38 (C-1', C-2', C-3'), 73.65, 72.06, 71.91, 70.64 (OCH₂Ph, C-4'), 56.87 (C-11a), 53.61 (C-3), 36.51 (NCH₃), 31.59 (C-1).



**Spiro{(1',4'-anhydro-2', 3', 5'-tri-*O*-benzyl-L-arabinitol)-1',2'-
-[(11a*S*)-7-chloro-10-methylpyrrolo[2,1-*c*][1,4]benzodiazepine-5,11-dione]}**

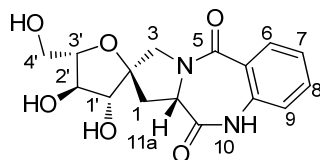
Compound 117. Reaction of **112** (0.250 g, 0.496 mmol) with 5-chloroisatoic anhydride 97% (R = H, X = Cl) (0.121 g, 0.595 mmol), afforded the respective crude benzodiazepine. Without further purification the previous compound was methylated. Purification by flash chromatography (eluent toluene/acetone 9:1) afforded **117** as a yellow amorphous solid (0.251 g, 77% yield). **MS (MALDI-TOF):** m/z 6532 [M + Na]⁺, 692.2 [M + K]⁺. **Elemental analysis calcd (%)** for C₃₈H₃₇ClN₂O₆: C, 69.88; H, 5.71; N, 4.29, found: C, 69.86; H, 5.72; N, 4.30. **¹H-NMR** (400 MHz, CDCl₃): δ (ppm) 7.85 (d, 1H, $J = 2.6$ Hz, Ar-*H*), 7.39 (dd, 1H, $J = 8.7, 2.6$ Hz, Ar-*H*), 7.27-7.15 (m, 15H, OCH₂Ph), 7.06 (d, 1H, $J = 8.7$ Hz, Ar-*H*), 4.52-4.33 (m, 6H, OCH₂Ph), 4.14 (t, 1H, $J = 7.7$ Hz, H-11a), 4.09 (ddd, 1H, $J = 12.2, 6.2, 3.3$ Hz, H-3'), 4.05-4.01 (m, 2H, H-3a, H-1'), 3.92 (dd, 1H, $J = 3.0, 2.0$ Hz, H-2'), 3.70 (d, 1H, $J = 13.3$ Hz, H-3b), 3.47 (dd, 1H, $J = 9.9, 5.9$ Hz, H-4'a), 3.41 (dd, 1H, $J = 9.9, 6.3$ Hz, H-4'b), 3.27 (s, 3H, NCH₃), 2.88 (dd, 1H, $J = 14.0, 7.2$ Hz, H-1a), 2.29 (ddd, 1H, $J = 13.9, 8.4, 1.6$ Hz, H-1b). **¹³C-NMR** (100.57 MHz, CDCl₃): δ (ppm) 169.17 (CO-11), 164.50 (CO-5), 139.01, 138.23, 138.84, 137.66 (Cq Ph, Cq Ar.), 132.24 (Ar), 131.63, 130.66 (Cq Ar), 130.55 (Ar), 128.71-127.76 (OCH₂Ph), 123.37 (Ar), 89.58 (C-2), 85.52, 83.90, 82.31 (C-1', C-2', C-3'), 73.61, 72.00, 71.92, 70.75 (OCH₂Ph, C-4'), 56.85 (C-11a), 53.40 (C-3), 36.56 (NCH₃), 36.48 (C-1).

**118**

**Spiro{(1',4'-anhydro-2', 3', 5'-tri-*O*-benzyl-L-arabinitol)-1',2-
-[(11a*S*)-7-bromo-10-methylpyrrolo[2,1-*c*][1,4]benzodiazepine-5,11-dione)}**

Compound 118. Reaction of **112** (0.250 g, 0.496 mmol) with 6-bromoisatoic anhydride 90% (R = H, X = Br) (0.160 g, 0.595 mmol) afforded the respective crude benzodiazepine. Without further purification the previous compound was methylated, and after purification afforded **118** as a white amorphous solid (0.231 g, 67 % yield).

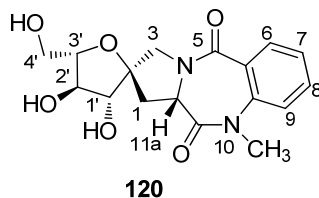
MS (MALDI-TOF): m/z 720.6 [M + Na]⁺, 736.6 [M + K]⁺. **Elemental analysis calcd** (%) for C₃₈H₃₇BrN₂O₆: C, 65.42; H, 5.35; N, 4.02, found: C, 65.39; H, 5.37; N, 4.03. **¹H-NMR** (400 MHz, CDCl₃): δ (ppm) 8.05 (d, 1H, J = 2.4 Hz, Ar-*H*), 7.60 (dd, 1H, J = 8.7, 2.5 Hz, Ar-*H*), 7.32-7.21 (m, 15H, OCH₂Ph), 7.06 (d, 1H, J = 8.7 Hz, Ar-*H*), 4.58-4.34 (m, 6H, OCH₂Ph), 4.21 (t, 1H, J = 7.7 Hz, H-11a), 4.15 (ddd, 1H, J = 3.2, 6.1, 12.0 Hz, H-3'), 4.10-4.07 (m, 2H, H-3a, H-1'), 4.00 (dd, 1H, J = 2.8, 1.9 Hz, H-2'), 3.76 (d, 1H, J = 13.1 Hz, H-3b), 3.53 (dd, 1H, J = 9.9, 6.0 Hz, H-4'a), 3.47 (dd, 1H, J = 9.9, 6.4 Hz, H-4'b), 3.32 (s, 3H, NCH₃), 2.94 (dd, 1H, J = 14.0, 7.2 Hz, H-1a), 2.35 (ddd, 1H, J = 13.8, 8.3, 1.6 Hz, H-1b). **¹³C-NMR** (100.57 MHz, CDCl₃): δ (ppm) 169.14 (CO-11), 164.38 (CO-5), 139.51, 138.23, 137.85, 137.64 (Cq Ph, Cq Ar), 135.16, 133.49 (C-6, C-8), 130.88 (Cq Ar), 128.71-127.76 (OCH₂Ph), 123.59 (C-9), 119.21 (Cq Ar), 89.57 (C-2), 85.51, 83.89, 82.31 (C-1', C-2', C-3'), 73.61, 72.00, 70.92, 70.73 (OCH₂Ph, C-4'), 56.84 (C-11a), 53.40 (C-3), 36.51 (NCH₃), 36.48 (C-1).



119

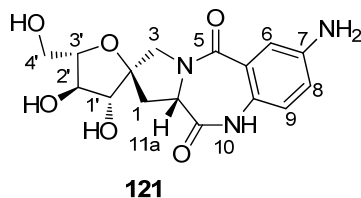
Spiro{(1',4'-anhydro-L-arabinitol)-1',2}-[(11aS)-pyrrolo[2,1-c][1,4]benzodiazepine-5,11-dione]}

Compound 119. Hydrogenolysis of **113** (0.100 g, 0.165 mmol) afforded compound **119** as a yellow amorphous solid (0.050 g, 91% yield). **MS (MALDI-TOF):** m/z 357.3 $[M + Na]^+$, 373.3 $[M + K]^+$. **Elemental analysis calcd (%)** for $C_{16}H_{18}N_2O_6$: C, 57.48; H, 5.43; N, 8.38, found: C, 57.53; H, 5.40; N, 8.36. **1H -NMR** (400 MHz, D_2O): δ (ppm) 7.67 (d, 1H, $J = 7.7$ Hz, Ar- H), 7.46 (t, 1H, $J = 7.6$ Hz, Ar- H), 7.21 (t, 1H, $J = 7.6$ Hz, Ar- H), 7.03 (d, 1H, $J = 8.1$ Hz, Ar- H), 4.27 (t, 1H, $J = 7.9$ Hz, H-11a), 4.14 (d, 1H, $J = 5.3$ Hz, H-1'), 3.92 (dd, 1H, $J = 6.4, 5.4$ Hz, H-2'), 3.82 (dd, 1H, $J = 13.1, 1.1$ Hz, H-3a), 3.74 (bm, 1H, H-3'), 3.61-3.48 (m, 3H, H-3b, H-4'a, H-4'b), 2.74 (dd, 1H, $J = 14.1, 7.5$ Hz, H-1a), 2.24 (ddd, 1H, $J = 13.9, 8.5, 1.5$ Hz, H-1b). **^{13}C -NMR** (100.57 MHz, D_2O): δ (ppm) 171.72 (CO-11), 168.67 (CO-5), 135.22 (Cq Ar), 133.48, 130.23, 125.85 (Ar), 125.34 (Cq Ar), 121.72 (Ar), 88.12 (C-2), 81.98, 79.24, 76.49 (C-1', C-2', C-3'), 61.51 (C-4'), 56.43 (C-11a), 53.03 (C-3), 35.01 (C-1).



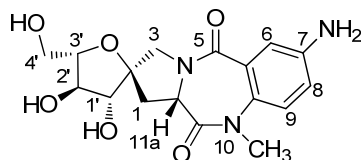
**Spiro{(1',4'-anhydro-L-arabinitol)-1',2-[(11aS)-
-10-methylpyrrolo[2,1-c][1,4]benzodiazepine-5,11-dione]}**

Compound 120. Hydrogenolysis of **114** (0.100 g, 0.161 mmol) afforded **120** as a yellow amorphous solid (0.054 g, 96% yield). **MS (MALDI-TOF):** m/z 371.4 $[M + Na]^+$, 387.4 $[M + K]^+$. **Elemental analysis calcd (%)** for $C_{17}H_{20}N_2O_6$: C, 58.61; H, 5.79; N, 8.04, found: C, 58.60; H, 5.83; N, 8.01. **1H -NMR** (400 MHz, D_2O): δ (ppm) 7.80 (dd, 1H, $J = 7.8, 1.4$, Ar- H), 7.71 (dt, 1H, $J = 8.3, 1.5$ Hz, Ar- H), 7.49-7.42 (m, 2H, Ar- H), 4.41 (t, 1H, $J = 7.9$ Hz, H-11a), 4.32 (d, 1H, $J = 5.4$ Hz, H-1'), 4.08 (dd, 1H, $J = 6.3, 5.5$ Hz, H-2'), 3.95 (dd, 1H, $J = 13.1, 1.7$ Hz, H-3a), 3.91-3.87 (bm, 1H, H-3'), 3.77-3.65 (m, 3H, H-3b, H-4'a, H-4'b), 3.42 (s, 3H, NCH_3), 2.96 (dd, 1H, $J = 14.3, 7.5$ Hz, H-1a), 2.38 (ddd, 1H, $J = 14.1, 8.5, 1.7$ Hz, H-1b). **^{13}C -NMR** (100.57 MHz, D_2O): δ (ppm) 170.44 (CO-11), 167.80 (CO-5), 140.27 (Cq Ar), 133.13, 129.04 (Ar), 127.14 (Cq Ar), 126.25, 122.76 (Ar), 88.23 (C-2), 81.67, 78.87, 76.03 (C-1', C-2', C-3'), 60.98 (C-4'), 56.46 (C-11a), 52.38 (C-3), 36.25 (NCH_3), 35.02 (C-1).



Spiro{[(1',4'-anhydro-L-arabinitol)-1',2'-[(11a*S*)-7-amino-pyrrolo[2,1-*c*][1,4]benzodiazepine-5,11-dione]}

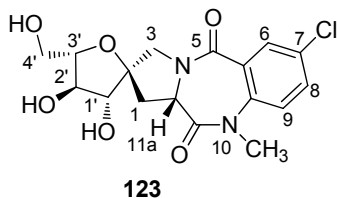
Compound 121. Hydrogenolysis of **115** (0.100 g, 0.154 mmol) afforded **121** as a brown oil (0.048 g, 89% yield). **MS (MALDI-TOF):** m/z 372 [M + Na]⁺, 388 [M + K]⁺. **Elemental analysis calcd (%)** for C₁₆H₁₉N₃O₆: C, 55.01; H, 5.48; N, 12.03, found: C, 55.10; H, 5.41; N, 12.12. **¹H-NMR** (400 MHz, CD₃OD): δ (ppm) 7.68 (bs, 1H, Ar-*H*), 7.37 (bd, 1H, Ar-*H*), 7.12 (d, 1H, $J = 8.5$ Hz, Ar-*H*), 4.34 (t, 1H, $J = 7.7$ Hz, H-11a), 4.10 (d, 1H, $J = 4.2$ Hz, H-1'), 4.03 (d, 1H, 11.8 Hz, H-3a), 3.98 (t, 1H, $J = 4.2$ Hz, H-2'), 3.74-3.70 (m, 1H, H-3'), 3.70-3.67 (m, 2H, H-3b, H-4'a), 3.63 (dd, 1H, $J = 11.8, 5.1$ Hz, H-4'b), 2.82 (dd, 1H, $J = 13.7, 7.9$ Hz, H-1a), 2.26 (dd, 1H, $J = 13.7, 7.7$ Hz, H-1b). **¹³C-NMR** (100.57 MHz, CD₃OD): δ (ppm) 174.08 (CO-11), 169.39 (CO-5), 139.86, 133.54, 130.97 (Cq Ar), 130.42, 128.10, 127.11 (Ar), 92.66 (C-2), 87.79, 84.09 81.89 (C-1', C-2', C-3'), 66.26 (C-4'), 60.56 (C-11a), 57.46 (C-3), 39.69 (C-1).



122

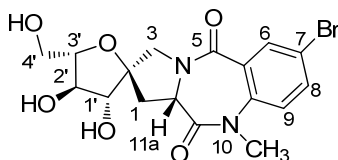
Spiro{[(1',4'-anhydro-L-arabinitol)-1',2-[(11a*S*)-7-amino-10-methylpyrrolo[2,1-*c*][1,4]benzodiazepine-5,11-dione]}

Compound 122. Hydrogenolysis of **116** (0.100 g, 0.151 mmol) afforded **122** as a dark yellow amorphous solid (0.048 g, 87% yield). **MS (MALDI-TOF):** m/z 385.7 [M + Na]⁺, 401.7 [M + K]⁺. **Elemental analysis calcd (%)** for C₁₇H₂₁N₃O₆: C, 56.19; H, 5.83; N, 11.56, found: C, 56.15; H, 5.86; N, 11.57. **¹H-NMR** (400 MHz, D₂O): δ (ppm) 7.01 (d, 1H, $J = 2.4$ Hz, Ar-*H*), 6.89 (dd, 1H, $J = 8.6, 2.4$ Hz, Ar-*H*), 6.84 (d, 1H, $J = 8.6$ Hz, Ar-*H*), 4.23 (t, 1H, $J = 7.9$ Hz, H-11a), 4.13 (d, 1H, $J = 5.3$ Hz, H-1'), 3.91 (dd, 1H, $J = 6.4, 5.4$ Hz, H-2'), 3.79 (dd, 1H, $J = 13.1, 1.3$ Hz, H-3a), 3.75-3.71 (bm, 1H, H-3'), 3.60-3.48 (m, 3H, H-3b, H-4'a, H-4'b), 3.17 (s, 3H, NCH₃), 2.71 (dd, 1H, $J = 14.2, 7.4$ Hz, H-1a), 2.21 (ddd, 1H, $J = 14.1, 8.0, 1.2$ Hz, H-1b). **¹³C-NMR** (100.57 MHz, D₂O): δ (ppm) 172.14 (CO-11), 167.71 (CO-5), 144.61, 132.25, 128.04 (Cq Ar), 124.08, 120.87, 114.73 (Ar), 88.28 (C-2), 81.67, 78.87, 76.02 (C-1', C-2', C-3'), 60.99 (C-4'), 56.48 (C-11a), 52.27 (C-3), 36.30 (NCH₃), 34.99 (C-1).



Spiro{[(1',4'-anhydro-L-arabinitol)-1',2-[(11a*S*)-7-chloro-10-methylpyrrolo[2,1-*c*][1,4]benzodiazepine-5,11-dione]}

Compound 123. Debenzylation of **117** (0.250 g, 0.383 mmol) and further purification afforded **123** as a white amorphous solid (0.129 g, 89% yield). **MS (MALDI-TOF):** m/z 405.8 [M + Na]⁺, 421.8 [M + K]⁺. **Elemental analysis calcd (%)** for C₁₇H₁₉ClN₂O₆: C, 53.34; H, 5.00; N, 7.32, found: C, 53.40; H, 4.97; N, 7.29. **¹H-NMR** (400 MHz, D₂O): δ (ppm) 7.63 (d, 1H, $J = 2.4$ Hz, Ar-*H*), 7.52 (dd, 1H, $J = 8.8, 2.5$ Hz, Ar-*H*), 7.28 (d, 1H, $J = 8.9$ Hz, Ar-*H*), 4.24 (t, 1H, $J = 7.9$ Hz, H-11a), 4.15 (d, 1H, $J = 5.3$ Hz, H-1'), 3.92 (t, 1H, $J = 6.2$ Hz, H-2'), 3.79-3.71 (m, 2H, H-3a', H-3'), 3.61-3.49 (m, 3H, H-3b, H-4'a, H-4b), 3.24 (s, 3H, NCH₃), 2.79 (dd, 1H, $J = 14.3, 7.5$ Hz, H-1a), 2.23 (ddd, 1H, $J = 14.2, 8.0, 1.4$ Hz, H-1a). **¹³C-NMR** (100.57 MHz, D₂O): δ (ppm) 170.37 (CO-11), 166.57 (CO-5), 139.16 (Cq Ar), 133.08 (C-6) 131.31 (Cq Ar) 128.89 (C-8), 128.83 (Cq Ar), 124.70 (C-9), 89.39 (C-2), 81.92, 79.10, 76.32 (C-1', C-2', C-3'), 61.25 (C-4'), 56.66 (C-11a), 52.61 (C-3), 36.43 (NCH₃), 35.25 (C-1).



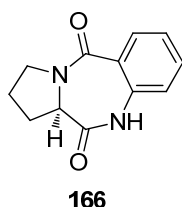
124

Spiro{(1',4'-anhydro-L-arabinitol)-1',2-[(11a*S*)-7-bromo-10-methylpyrrolo[2,1-*c*][1,4]benzodiazepine-5,11-dione]}

Compound 124. Debenzylation of **118** (0.250 g, 0.358 mmol) and further purification afforded **124** as a white amorphous solid (0.139 g, 91% yield). **MS (MALDI-TOF):** m/z 450.2 $[M + Na]^+$, 466.2 $[M + K]^+$. **Elemental analysis calcd (%)** for $C_{17}H_{19}BrN_2O_6$: C, 47.79; H, 4.48; N, 6.56, found: C, 47.70; H, 4.51; N, 6.62. **1H -NMR** (400 MHz, D_2O): δ (ppm) 7.80 (d, 1H, $J = 2.3$ Hz, Ar-*H*), 7.67 (dd, 1H, $J = 8.8, 2.4$ Hz, Ar-*H*), 7.22 (d, 1H, $J = 8.8$ Hz, Ar-*H*), 4.26 (t, 1H, $J = 7.8$ Hz, H-11a), 4.16 (d, 1H, $J = 5.3$ Hz, H-1'), 3.92 (t, 1H, $J = 6.3$ Hz, H-2'), 3.80-3.72 (m, 2H, H-3a', H-3'), 3.61-3.50 (m, 3H, H-3b, H-4'a, H-4b), 3.24 (s, 3H, NCH_3), 2.80 (dd, 1H, $J = 14.2, 7.5$ Hz, H-1a), 2.23 (ddd, 1H, $J = 14.2, 8.5, 1.7$ Hz, H-1a). **^{13}C -NMR** (100.57 MHz, D_2O): δ (ppm) 170.37 (CO-11), 166.51 (CO-5), 139.66 (Cq Ar), 136.02 (C-6) 131.89 (C-8), 129.07 (Cq Ar) 124.86 (C-9), 118.89 (Cq Ar), 88.39 (C-2), 81.91, 79.09, 76.30 (C-1', C-2', C-3'), 61.25 (C-4'), 56.66 (C-11a), 52.61 (C-3), 35.39 (NCH_3), 35.24 (C-1).

4.1.5 Synthesis of the Pyrrolobenzodiazepines

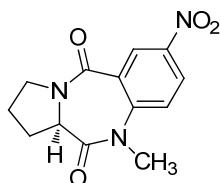
General procedure for pyrrolobenzodiazepine synthesis. To a solution of (*R*)-**61** or (*S*)-**61** in dry DMF, suitably functionalised isatoic anhydride **60** (1.2 eq.) was added under argon atmosphere, and the resulting mixture was stirred under reflux (bath temp. 120°C) till complete consume of the starting material. The reaction mixture was cooled and added to iced water (15 mL), the precipitate was isolated and recrystallised from ethanol.



166

(11aR)-Pyrrolo[2,1-c][1,4]benzodiazepine

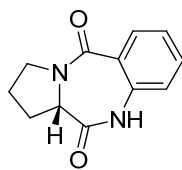
Compound 166. ¹H-NMR (400 MHz, CDCl₃): δ(ppm) 8.56 (bs, 1H, NH), 8.01 (d, 1H, *J* = 7.8 Hz, H-6), 7.48 (t, 1H, *J* = 7.8 Hz, H-8), 7.27 (t, 1H, *J* = 7.8 Hz, H-7), 7.03 (d, 1H, *J* = 8.0 Hz, H-9), 4.09 (d, 1H, *J* = 6.2 Hz, H-11a), 3.82 (bm, 1H, H-2a), 3.61 (bm, 1H, H-2b), 2.77 (bm, 1H, H-1a), 2.06 (m, 3H, H-1b, H-3). ¹³C-NMR (100.57 MHz, CDCl₃): δ (ppm) 171.23 (CO-11), 165.35 (CO-5), 135.18 (Cq Ar), 132.43, 131.13 (C-6, C-8), 127.13 (Cq Ar), 125.09, 120.96 (C-7, C-9), 56.65 (C-2), 47.31 (C-11a), 26.25 (C-3), 23.48 (C-1). **M.p.** 213-215 °C, 82% yield.



167

(11aR)-7-nitro-10-methylpyrrolo[2,1-c][1,4]benzodiazepine

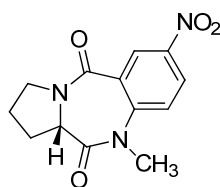
Compound 167. $^1\text{H-NMR}$ (CDCl_3): δ (ppm) 8.80 (d, 1H, $J = 2.1$ Hz, H-6), 8.35 (dd, 1H, $J = 8.9, 2.2$ Hz, H-8), 7.36 (d, 1H, $J = 9.0$ Hz, H-9), 4.06 (d, 1H, $J = 5.2$ Hz, H-11a), 3.83 (bm, 1H, H-2a), 3.58 (bm, 1H, H-2b), 3.46 (3H, NCH_3), 2.77 (bm, 1H, H-1a), 2.07 (m, 3H, H-1b, H-3). 62% yield.



168

(11aS)-Pyrrolo[2,1-c][1,4]benzodiazepine

Compound 168. $^1\text{H-NMR}$ (400 MHz, CDCl_3): δ (ppm) 8.58 (bs, 1H, NH), 8.01 (d, 1H, $J = 7.8$ Hz, H-6), 7.48 (t, 1H, $J = 7.9$ Hz, H-8), 7.27 (t, 1H, $J = 8.5$ Hz, H-7), 7.03 (d, 1H, $J = 8.0$ Hz, H-9), 4.09 (d, 1H, $J = 6.2$ Hz, H-11a), 3.82 (bm, 1H, H-2a), 3.61 (bm, 1H, H-2b), 2.76 (bm, 1H, H-1a), 2.05 (m, 3H, H-1b, H-3). $^{13}\text{C-NMR}$ (100.57 MHz, CDCl_3): δ (ppm) 171.24 (CO-11), 165.35 (CO-5), 135.18 (Cq Ar), 132.43, 131.13 (C-6, C-8), 127.13 (Cq Ar), 125.08, 120.96 (C-7, C-9), 56.65 (C-2), 47.31 (C-11a), 26.25 (C-3), 23.48 (C-1). **M.p.** 204-206 °C. 80% yield.

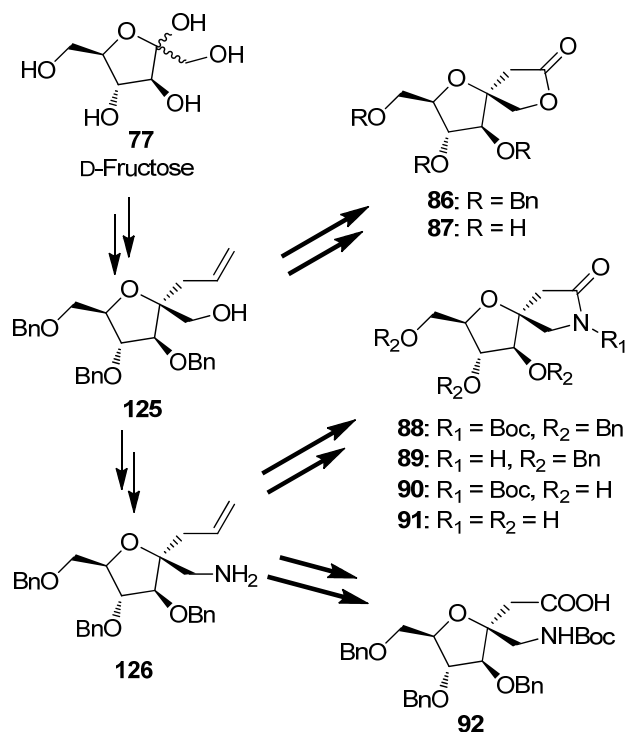


169

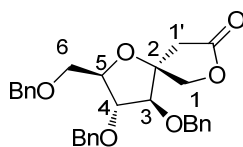
(11aS)-7-nitro-10-methylpyrrolo[2,1-c][1,4]benzodiazepine

Compound 169. $^1\text{H-NMR}$ (400 MHz, CDCl_3): δ (ppm) 8.80 (d, 1H, $J = 2.6$ Hz, H-6), 8.34 (dd, 1H, $J = 9.0, 2.7$ Hz, H-8), 7.36 (d, 1H, $J = 9.0$ Hz, H-9), 4.05 (d, 1H, $J = 6.0$ Hz, H-11a), 3.82 (bm, 1H, H-2a), 3.58 (bm, 1H, H-2b), 3.45 (3H, NCH_3), 2.78 (bm, 1H, H-1a), 2.08 (m, 3H, H-1b, H-3). 65% yield.

4.1.6 Synthesis of the Fructose-Based γ -Butyrolactones and -Lactams, and a GABA analogue



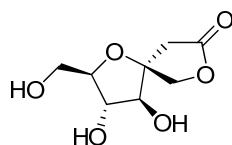
Scheme 31



86

**3,6-Anhydro-4,5,7-tri-O-benzyl-2-deoxy-3-C-(hydroxymethyl)-
-D-manno-heptonic acid lactone**

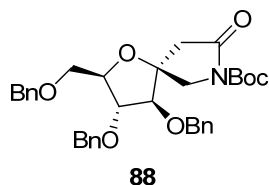
Compound 86. To a solution of **173** (0.250 g, 0.412 mmol) in CH₂Cl₂ (8 mL), a mixture of 9:1 TFA/H₂O (0.3 mL) was added at 0 °C. The reaction mixture was allowed to warm at room temperature and stirred for 1h. The reaction was quenched by slowly adding NaHCO₃ until neutral pH. The product was extracted with CH₂Cl₂ and the organic layer was dried on sodium sulphate, filtered and evaporated. Flash column chromatography of the residue (petroleum ether/EtOAc 8:2) afforded **86** (0.184 g, 94% yield) as a dark yellow oil. **MS (MALDI-TOF):** *m/z* 498 [M + Na]⁺, 514 [M + K]⁺. **Elemental analysis calcd (%)** for C₂₉H₃₀O₆: C, 73.40; H, 6.37, found: C, 73.38; H, 6.39. **¹H NMR** (400 MHz, CDCl₃): δ (ppm) 7.40-7.22 (m, 15H, OCH₂Ph), 4.63-4.51 (m, 6H, OCH₂Ph), 4.39 (d, 1H, *J* = 9 Hz, H-1'a), 4.37 (d, 1H, *J* = 9 Hz, H-1'b), 4.23 (dt, 1H, *J* = 6.1, 3 Hz, H-6), 4.04 (dd, 1H, *J* = 3, 1.7 Hz, H-5), 3.94 (d, 1H, *J* = 1.7 Hz, H-4), 3.60 (dd, 1H, *J* = 10, 5.5 Hz, H-7a), 3.52 (dd, 1H, *J* = 10, 6.4 Hz, H-7b), 2.77 (d, 1H, *J* = 18 Hz, H-2a), 2.63 (d, 1H, *J* = 18 Hz, H-2b). **¹³C NMR** (100.57 MHz, CDCl₃): δ (ppm) 175.12 (CO), 138.02, 137.53, 137.09 (Cq Ph), 87.36 (C-3), 85.81, 82.89, 82.77 (C-4, C-5, C-6), 73.74 (C-1'), 72.38, 72.18, 72.02, 70.42 (OCH₂Ph, C-7), 39.60 (C-2).



87

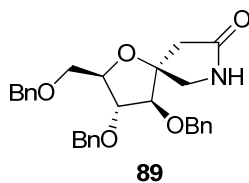
**3,6-Anhydro-2-deoxy-3-C-(hydroxymethyl)-
-D-manno-heptonic acid lactone**

Compound 87. Compound **86** (0.250 g, 0.527 mmol) was dissolved in 4:1 MeOH/EtOAc mixture (15 mL) and a few drops of HCl 37% and catalytic Pd(OH)₂/C (10% w/w) were added. The flask was purged three times with Ar and then filled with H₂. After 12h, the catalyst was removed by filtration, and the filtrate concentrated under reduced pressure. The crude residue was purified by silica gel flash chromatography (EtOAc) affording compound **87** as a yellow oil (0.102 g, 95% yield). **MS (MALDI-TOF):** *m/z* 227 [M + Na]⁺, 243 [M + K]⁺. **Elemental analysis calcd (%)** for C₈H₁₂O₆: C, 47.06; H, 5.92, found: C, 47.04; H, 5.97. **¹H NMR** (400 MHz, D₂O): δ (ppm) 4.50 (d, 1H, *J* = 10.6 Hz, H-1'a), 4.23 (d, 1H, *J* = 10.6 Hz, H-1'b), 4.07 (d, 1H, *J* = 3.8 Hz, H-4), 3.89 (dd, 1H, *J* = 5.1, 3.8 Hz, H-5), 3.80 (dt, 1H, *J* = 5.1, 3.5 Hz, H-6), 3.60 (dd, 1H, *J* = 12.3, 3.5 Hz, H-7a), 3.52 (dd, 1H, *J* = 12.3, 5.3 Hz, H-7b), 2.81 (d, 1H, *J* = 18 Hz, H-2a), 2.68 (d, 1H, *J* = 18 Hz, H-2b). **¹³C NMR** (100.57 MHz, D₂O): δ (ppm) 178.83 (CO), 87.47 (C-3), 83.69, 79.48, 76.64 (C-4, C-5, C-6), 74.88 (C-1'), 61.42 (C-7), 38.70 (C-2).



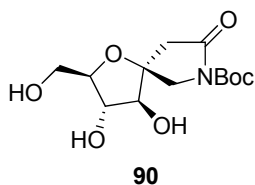
**3,6-Anhydro-4,5,7-tri-*O*-benzyl-2-deoxy-3-*C*-
-(aminomethyl(*N*-tertbutoxycarbonyl))-*D*-manno-heptonic acid lactam**

Compound 88. To a solution of **175** (0.250 g, 0.434 mmol) and molecular sieves (4 Å, 300 mg) in dry CH₂Cl₂ (8 mL) PCC (0.187 g, 0.868 mmol) was added and the mixture was stirred for 2h. The resulting mixture was filtered through a celite pad eluting with EtOAc. The filtrate was concentrated and purified by silica gel flash chromatography (petroleum ether/EtOAc 7:3) to give the lactam **88** as a white solid (0.194 g, 78% yield). **M.p.** 82-85 °C. **MS (MALDI-TOF):** *m/z* 597 [M + Na]⁺, 613 [M + K]⁺. **Elemental analysis calcd (%)** for C₃₄H₃₉NO₇: C, 71.18; H, 6.85; N, 2.44, found: C, 71.20; H, 6.90; N, 2.40. **¹H NMR** (400 MHz, CDCl₃): δ (ppm) 7.37-7.22 (m, 15H, OCH₂Ph), 4.60-4.37 (m, 6H, OCH₂Ph), 4.2-4.15 (m, 1H, H-6), 4.02 (d, 1H, *J* = 12.4 Hz, H-1'a), 3.99 (dd, 1H, *J* = 3.2, 1.8 Hz, H-5), 3.85 (d, 1H, *J* = 12.4 Hz, H-1'b), 3.82 (d, 1H, *J* = 1.8 Hz, H-4), 3.57 (dd, 1H, *J* = 10, 5.6 Hz, H-7a), 3.49 (dd, 1H, *J* = 10, 6.1 Hz, H-7b), 2.77 (d, 1H, *J* = 18 Hz, H-2a), 2.64 (d, 1H, *J* = 18 Hz, H-2b), 1.5 (s, 9H, ^tBu). **¹³C NMR** (100.57 MHz, CDCl₃): δ (ppm) 171.70 (CO-1), 149.97 (CO), 138.12, 137.66, 137.34 (Cq Ph), 85.9, 83.21, 82.23 (C-4, C-5, C-6), 83.2, 83.0 (C-3, C(CH₃)₃), 73.60, 72.11, 71.95, 70.44 (OCH₂Ph, C-7), 53.06 (C-2), 43.92 (C-1'), 28.96, 28.27, 27.75 (^tBu).



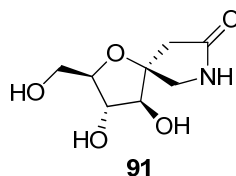
3,6-Anhydro-4,5,7-tri-*O*-benzyl-2-deoxy-3-*C*-(aminomethyl)-*D*-manno-heptonic acid lactam

Compound 89. A solution of **88** (0.250 g, 0.436 mmol) in dry CH₂Cl₂ (7 mL) and 80% aq. TFA (13 mL) was stirred for 2h at rt. Then, the mixture was neutralised with an aq. sat. soln. of NaHCO₃, and extracted with CH₂Cl₂. The organic layer was dried (Na₂SO₄), filtered, concentrated to dryness, and then purified by silica gel flash chromatography (petroleum ether/EtOAc 5:5) to give **89** as a yellow oil (0.157 g, 76% yield). **MS (MALDI-TOF):** *m/z* 497 [M + Na]⁺, 513 [M + K]⁺. **Elemental analysis calcd (%)** for C₂₉H₃₁NO₅: C, 73.55; H, 6.60; N, 2.96, found: C, 73.50; H, 6.64; N, 2.99. **¹H NMR** (400 MHz, CDCl₃): δ (ppm) 7.3-7.14 (m, 15H, OCH₂Ph), 5.5 (s, 1H, NH), 4.52-4.31 (m, 6H, OCH₂Ph), 4.12-4.10 (m, 1H, H-6), 3.91 (dd, 1H, *J* = 3.5, 1.9 Hz, H-5), 3.8 (d, 1H, *J* = 1.9 Hz, H-4), 3.7 (d, 1H, *J* = 12 Hz, H-1'a), 3.5 (dd, 1H, *J* = 10, 5.6 Hz, H-7a), 3.42 (dd, 1H, *J* = 10, 6.1 Hz, H-7b), 3.4 (d, 1H, *J* = 12 Hz, H-1'b), 2.52 (d, 1H, *J* = 17.5 Hz, H-2a), 2.44 (d, 1H, *J* = 17.5 Hz, H-2b). **¹³C NMR** (100.57 MHz, CDCl₃): δ (ppm) 175.4 (CO), 138.16, 137.74, 137.44 (Cq Ph), 87.45 (C-3), 86.14, 83.41, 82.10 (C-4, C-5, C-6), 73.59, 72.06, 71.89, 70.52 (OCH₂Ph, C-7), 48.74 (C-2), 41.45 (C-1').



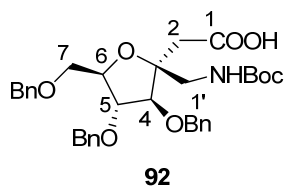
3,6-Anhydro-2-deoxy-3-C-(aminomethyl(*N*-tertbutoxycarbonyl))-*D*-manno-heptonic acid lactam

Compound 90. Compound **88** (0.250 g, 0.436 mmol) was dissolved in 4:1 CH₃OH/EtOAc mixture (15 mL) and a few drops of acetic acid and catalytic Pd(OH)₂/C (10% w/w) were added. The flask was purged three times with Ar and then filled with H₂. After 12h, the catalyst was removed by filtration, and the filtrate concentrated under reduced pressure. The crude residue was purified by silica gel flash chromatography (EtOAc/CH₃OH 9:1) affording compound **90** as a yellow oil (0.093g, 70% yield). **MS (MALDI-TOF):** *m/z* 326 [M + Na]⁺, 342 [M + K]⁺. **Elemental analysis calcd (%)** for C₁₃H₂₁NO₇: C, 51.48; H, 6.98; N, 4.62, found: C, 51.53; H, 6.92; N, 4.65. **¹H NMR** (400 MHz, D₂O): δ (ppm) 3.97 (d, 1H, *J* = 4.4 Hz, H-4), 3.93 (d, 1H, *J* = 12.4 Hz, H-1'a), 3.88 (m, 1H, H-5), 3.8-3.76 (m, 1H, H-6), 3.66 (d, 1H, *J* = 12.4 Hz, H-1'b), 3.56 (dd, 1H, *J* = 12.4, 5.3 Hz, H-7a), 3.5 (dd, 1H, *J* = 12.4, 5.4 Hz, H-7b), 2.77 (d, 1H, *J* = 18 Hz, H-2a), 2.62 (d, 1H, *J* = 18 Hz, H-2b), 1.34 (s, 9H, ^tBu). **¹³C NMR** (100.57 MHz, D₂O): δ (ppm) 178.19 (CO-1), 153.52 (CO), 87.94, 85.3 (C-3, C(CH₃)₃), 85.55, 82.38, 81.99 (C-4, C-5, C-6), 63.90 (C-7), 56.27 (C-2), 45.68 (C-1'), 28.94, 28.54, 27.85 (^tBu).



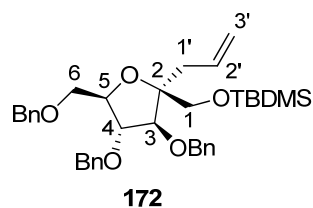
**3,6-Anhydro-2-deoxy-3-C-(aminomethyl)-
-D-manno-heptonic acid lactam**

Compound 91. Compound **88** (0.250 g, 0.436 mmol) was dissolved in 4:1 CH₃OH/EtOAc mixture (15 mL) and a few drops of HCl 37% and catalytic Pd(OH)₂/C (10% w/w) were added. The flask was purged three times with Ar and then filled with H₂. After 12h, the catalyst was removed by filtration, and the filtrate concentrated under reduced pressure. The crude residue was purified by silica gel flash chromatography (EtOAc/CH₃OH/H₂O 7.5:2:0.5) affording compound **91** as a yellow oil (0.066 g, 74% yield). **MS (MALDI-TOF):** *m/z* 226 [M + Na]⁺, 242 [M + K]⁺. **Elemental analysis calcd (%)** for C₈H₁₃NO₅: C, 47.29; H, 6.45; N, 6.89, found: C, 47.20; H, 6.40; N, 6.91. **¹H NMR** (400 MHz, D₂O): δ (ppm) 4.24 (s, 1H, NH), 3.99 (d, 1H, *J* = 4 Hz, H-4), 3.88 (dd, 1H, *J* = 5.3, 4 Hz, H-5), 3.8-3.76 (m, 1H, H-6), 3.66 (d, 1H, *J* = 12 Hz, H-1'a), 3.6 (dd, 1H, *J* = 12.3, 3.6 Hz, H-7a), 3.51 (dd, 1H, *J* = 12.3, 5.4 Hz, H-7b), 3.24 (d, 1H, *J* = 12 Hz, H-1'b), 2.58 (d, 1H, *J* = 18 Hz, H-2a), 2.42 (d, 1H, *J* = 18 Hz, H-2b). **¹³C NMR** (100.57 MHz, D₂O): δ (ppm) 180.72 (CO), 89.85 (C-3), 85.58, 82.38, 79.20 (C-4, C-5, C-6), 63.99 (C-7), 52.15 (C-2), 43.41 (C-1').



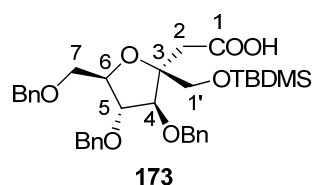
**3,6-Anhydro-4,5,7-tri-*O*-benzyl-2-deoxy-3-*C*-
-(aminomethyl(*N*-tertbutoxycarbonyl))-*D*-manno-heptonic acid**

Compound 92. To a solution of **88** (0.250 g, 0.436 mmol) in dry THF (7 mL) 1 M LiOH·H₂O (1.74 mL, 1.74 mmol) was added, and the resulting solution was stirred at room temperature for 2h. THF was evaporated, and the resulting residue was dissolved in diethyl ether and filtered. The resulting filtrate was washed with Et₂O and the aqueous layer was acidified with 1 M HCl and extracted with Et₂O. The combined organic layers were dried (Na₂SO₄), filtered, concentrated to dryness providing **92** as a yellow oil (0.157 g, 61% yield). **MS (MALDI-TOF):** *m/z* 615 [M + Na]⁺, 631 [M + K]⁺. **Elemental analysis calcd (%)** for C₃₄H₄₁NO₈: C, 69.02; H, 6.98; N, 2.37, found: C, 69.08; H, 6.95; N, 2.40. **¹H NMR** (400 MHz, CDCl₃): δ (ppm) 7.25-7.16 (m, 15H, OCH₂Ph), 5.05 (t, 1H, *J* = 6.3 Hz, NH), 4.53-4.33 (m, 6H, OCH₂Ph), 4.23 (d, 1H, *J* = 3.9 Hz, H-4), 4.11-4.07 (m, 1H, H-6), 3.97 (dd, 1H, *J* = 6.8, 3.9 Hz, H-5), 3.47 (dd, 1H, *J* = 10.3, 4.6 Hz, H-7a), 3.45-3.42 (m, 2H, H-1'), 3.40 (dd, 1H, *J* = 10.3, 4.6 Hz, H-7b), 2.64 (d, 1H, *J* = 14 Hz, H-2a), 2.57 (d, 1H, *J* = 14 Hz, H-2b), 1.48 (s, 9H, ^tBu). **¹³C NMR** (100.57 MHz, CDCl₃): δ (ppm) 178.24 (CO-1), 156.76 (CO), 138.04, 137.83, 137.63 (Cq Ph), 86.63, 85.51, 83.89 (C-4, C-5, C-6), 85.48, 80.48 (C-3, C(CH₃)₃), 77.62, 77.30, 76.98, 69.99 (OCH₂Ph, C-7), 44.20 (C-1'), 40.42 (C-2), 28.65, 28.58, 27.98 (^tBu).



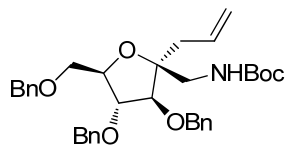
**2,5-Anhydro-3,4,6-tri-*O*-benzyl-2-*C*-(prop-2-enyl)-
-1-*O*-tertbutyldimethylsilyl-*D*-glucitol**

Compound 172. To a solution of **125** (0.250 g, 0.527 mmol) in dry DMF (10 mL), TBDMSCl (0.198 g, 1.32 mmol) and imidazole (0.106 g, 1.58 mmol) were added under argon atmosphere, and the resulting mixture was stirred under reflux for 12h. The solvent was then removed under reduced pressure and the residue dissolved in CH₂Cl₂ and washed with brine. The organic layer was dried (Na₂SO₄), filtered and evaporated. The crude residue was purified by silica gel flash chromatography (petroleum ether/EtOAc 9:1), affording **172** as a yellow oil (0.279 g, 90% yield). **MS (MALDI-TOF):** *m/z* 611 [M + Na]⁺, 627 [M + K]⁺. **Elemental analysis calcd (%)** for C₃₆H₄₈O₅Si: C, 73.43; H, 8.22; Si, 4.77, found: C, 73.46; H, 8.20; Si, 4.73. **¹H NMR** (400 MHz, CDCl₃): δ (ppm) 7.38-7.25 (m, 15H, OCH₂Ph), 5.81-5.79 (m, 1H, H-2'), 5.10 (d, 1H, *J* = 10.2 Hz, H-3'a), 4.98 (d, 1H, *J* = 17 Hz, H-3'b), 4.75-4.46 (m, 6H, OCH₂Ph), 4.10 (dq, 1H, *J* = 5.3, 1.3 Hz, H-5), 4.04 (dd, 1H, *J* = 5.3, 3.6 Hz, H-4), 3.96 (d, 1H, *J* = 3.6 Hz, H-3), 3.69 (dd, 1H, *J* = 10.0, 1.4 Hz, H-6a), 3.63 (dd, 1H, *J* = 10.0, 1.2 Hz, H-6b), 3.60-3.52 (m, 2H, H-1), 2.52-2.41 (m, 2H, H-1'), 0.88 (s, 9H, C(CH₃)₃), 0.04 (s, 3H, SiCH₃), -0.08 (s, 3H, SiCH₃). **¹³C NMR** (100.57 MHz, CDCl₃): δ (ppm) 138.27, 138.16, 137.69 (Cq Ph), 133.05 (C-2'), 119.18 (C-3'), 84.40 (C-2), 86.69, 83.58, 79.46 (C-3, C-4, C-5), 73.74, 73.25, 70.96, 69.72 (OCH₂Ph, C-6), 66.51 (C-1), 40.45 (C-1'), 26.94, 25.17, 24.53 (C(CH₃)₃), 20.15 (C(CH₃)₃), -4.6, -4.8 (SiCH₃).



3,6-Anhydro-4,5,7-tri-*O*-benzyl-2-deoxy-3-C-(hydroxymethyl(*O*-tertbutyldimethylsilyl))-D-manno-heptonic acid

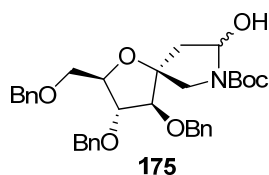
Compound 173. To a solution of **172** (0.250 g, 0.424 mmol) in 1:1:1 H₂O/acetone/*tert*BuOH (10 mL), 0.016M OsO₄ in *tert*BuOH (1.3 mL, 0.021 mmol) was added. After 30 min the mixture was treated with sodium periodate (0.181 g, 0.848 mmol) and 2h later the reaction solution was filtered and the solvents evaporated *in vacuo* without heating, affording the desired aldehyde that was used without further purification. To a solution of the aldehyde (\approx 0.424 mmol) in dry CH₃CN (8 mL) a soln. of NaH₂PO₄·2H₂O 1.25 M (3.4 mL, 4.24 mmol) and sodium chlorite (0.383 g, 4.24 mmol) were added at r.t. After 3h the solvents were evaporated *in vacuo* and the resulting residue was dissolved in CH₂Cl₂, filtered and evaporated. The residue was purified by flash column chromatography (petroleum ether/EtOAc 8:2) affording **173** as a yellow oil (0.182 g, 71% yield). **MS (MALDI-TOF):** *m/z* 630 [M + Na]⁺, 646 [M + K]⁺. **Elemental analysis calcd (%)** for C₃₅H₄₆O₇Si: C, 69.27; H, 7.64; Si, 4.63, found: C, 69.29; H, 7.60; Si, 4.60. **¹H NMR** (400 MHz, CDCl₃): δ (ppm) 7.30-7.19 (m, 15H, OCH₂Ph), 4.54-4.45 (m, 6H, OCH₂Ph), 4.28-4.26 (m, 1H, H-6), 3.98 (dd, 1H, *J* = 5.6, 2.2 Hz, H-5), 3.96 (d, 1H, *J* = 2.2 Hz, H-4), 3.84 (d, 1H, *J* = 10.3 Hz, H-1'a), 3.73 (d, 1H, *J* = 10.3 Hz, H-1'b), 3.56 (dd, 1H, *J* = 9.8, 6.0 Hz, H-7a), 3.46 (dd, 1H, *J* = 9.8, 6.1 Hz, H-7b), 2.92 (d, 1H, *J* = 15 Hz, H-2a), 2.74 (d, 1H, *J* = 15 Hz, H-2b), 0.86 (s, 9H, C(CH₃)₃), 0.03 (s, 3H, SiCH₃), -0.02 (s, 3H, SiCH₃). **¹³C NMR** (100.57 MHz, CDCl₃): δ (ppm) 173.5 (CO), 138.77, 138.68, 137.91 (Cq Ph), 83.95 (C-3), 86.19, 82.45, 78.93 (C-4, C-5, C-6), 73.17, 72.95, 72.07, 70.25 (OCH₂Ph, C-7), 63.43 (C-1'), 36.50 (C-2), 26.21, 25.95, 23.43 (C(CH₃)₃), 21.25 (C(CH₃)₃), -3.9, -4.2 (SiCH₃).



174

1-Amino-2,5-Anhydro-3,4,6-tri-O-benzyl-1-deoxy-2-C-(prop-2-enyl)-N-tertbutoxycarbonyl-D-glucitol

Compound 174. To a solution of **126** (0.250 g, 0.528 mmol) and triethylamine (0.223 ml, 1.58 mmol) in dry CH_2Cl_2 (7 ml) was added Boc anhydride (0.138 g, 0.634 mmol) at 0 °C. Then the mixture was warmed to room temperature and stirred at r.t. overnight. Volatiles were removed, and the residue was dissolved in EtOAc and washed with H_2O . The organic layer was dried (Na_2SO_4), filtered, concentrated to dryness, and then purified by silica gel flash chromatography (petroleum ether/EtOAc 9:1) to give the desired product **174** as a yellow oil (0.264 g, 87% yield). **MS (MALDI-TOF):** m/z 597 $[\text{M} + \text{Na}]^+$, 613 $[\text{M} + \text{K}]^+$. **Element analysis calcd (%)** for $\text{C}_{35}\text{H}_{43}\text{NO}_6$: C, 73.27; H, 7.55; N, 2.44, found: C, 73.31; H, 7.50; N, 2.54. **$^1\text{H NMR}$** (400 MHz, CDCl_3): δ (ppm) 7.38-7.24 (m, 15H, OCH_2Ph), 5.89-5.79 (m, 1H, H-2'), 5.37 (t, 1H, $J = 5.6$ Hz, NH), 5.13 (dd, 1H, $J = 10.2, 2.1$ Hz, H-3'a), 5.06 (dd, 1H, $J = 17.1, 2.1$ Hz, H-3'b), 4.63-4.47 (m, 6H, OCH_2Ph), 4.20 (dd, 1H, $J = 6.7, 5.4$ Hz, H-4), 4.09 (d, 1H, $J = 5.4$ Hz, H-3), 3.99 (m, 1H, H-5), 3.61 (dd, 1H, $J = 10.5, 4.0$ Hz, H-6a), 3.49 (dd, 1H, $J = 10.5, 4.0$ Hz, H-6b), 3.38 (m, 2H, H-1), 2.43 (dd, 1H, $J = 14.2, 7.0$ Hz, H-1'a), 2.34 (dd, 1H, $J = 14.2, 7.6$ Hz, H-1'b), 1.45 (s, 9H, ^tBu). **$^{13}\text{C NMR}$** (100.57 MHz, CDCl_3): δ (ppm) 161.74 (CO), 138.45, 138.34, 138.22 (Cq Ph), 132.89 (C-2'), 119.94 (C-3'), 88.17, 85.18, 79.74 (C-3, C-4, C-5), 85.67, 85.11 (C-2, $\text{C}(\text{CH}_3)_3$), 73.54, 73.09, 72.59, 69.64 (OCH_2Ph , C-6), 40.85 (C-1), 38.46 (C-1'), 28.20, 26.7, 25.6 (^tBu).



**3,6-Anhydro-4,5,7-tri-*O*-benzyl-2-deoxy-3-*C*-
-(aminomethyl(*N*-tertbutoxycarbonyl))-*D*-manno-heptonic acid lactol**

Compound 175. To a solution of **174** (0.250 g, 0.436 mmol) in dry THF (6 ml) NMO (0.147 g, 1.09 mmol) and 0.016 M OsO₄ in *tert*BuOH (1.38 ml, 0.022 mmol) were added at 0 °C, and the resulting mixture was stirred at room temperature for 5h. Additional NMO (0.071 g) was added, and stirring was continued overnight. The mixture was poured into 1 M Na₂S₂O₃ and extracted with EtOAc. The organic layer was dried (Na₂SO₄), filtered, concentrated to dryness to give the diol intermediate that was used without further purification. To a solution of the previous crude diol (≈ 0.436 mmol) in THF (5 mL) aqueous solution of NaIO₄ (158 mg, 0.741 mmol in 1 mL) was added at 0 °C, and the mixture was stirred for 3h, poured into ice/water, and extracted with EtOAc. The organic layer was dried (Na₂SO₄), filtered, concentrated to dryness, and then purified by silica gel flash chromatography (petroleum ether/EtOAc 7:3) to give the compound **175** as a yellow oil (0.213 g, 85% yield). **MS (MALDI-TOF):** *m/z* 599 [M + Na]⁺, 615 [M + K]⁺. **Elemental analysis calcd (%)** for C₃₄H₄₁NO₇: C, 70.93; H, 7.18; N, 2.43, found: C, 71.00; H, 7.20; N, 2.40. **¹H NMR** (400 MHz, CDCl₃): δ (ppm) 7.28-7.12 (m, 15H, OCH₂Ph), 5.37 (t, 1H, *J* = 6 Hz, H-1), 4.51-4.30 (m, 6H, OCH₂Ph), 4.10-4.02 (m, 1H, H-6), 4.0 (d, 1H, *J* = 1.6 Hz, H-4), 3.85 (dd, 1H, *J* = 3.5, 1.6 Hz, H-5), 3.81 (d, 1H, *J* = 12 Hz, H-1'a), 3.51 (dd, 1H, *J* = 17, 5.8 Hz, H-7a), 3.40 (dd, 1H, *J* = 17, 7 Hz, H-7b), 3.37 (d, 1H, *J* = 12 Hz, H-1'b), 2.2 (dd, 1H, *J* = 14, 5.2 Hz, H-2a), 1.9 (dd, 1H, *J* = 14, 6.8 Hz, H-2b), 1.15 (s, 9H, ^tBu). **¹³C NMR** (100.57 MHz, CDCl₃): δ (ppm) 151.15 (CO), 138.54, 138.78, 137.25 (C_q Ph), 85.87, 83.54, 82.31 (C-4, C-5, C-6), 83.60, 83.38 (C-3, C(CH₃)₃), 73.55, 72.63, 71.97, 70.50 (OCH₂Ph, C-7), 54.43 (C-1'), 39.54 (C-2), 28.94, 28.35, 27.80 (^tBu).

4.2 Molecular Modelling and DNMR Experiments

Molecular modelling. Conformational analysis of compounds **101**, **102** and **119** was performed applying an MM2 force field in vacuum. Each model was built with ChemDraw, energy was minimized (minimum RMS gradient=0.010), and the dihedral angle C5a-C9a-N10-C11 value calculated using ChemBio3D Ultra. A Molecular Dynamics Computation was performed (step interval=2 fs; frame interval=1 fs; heating/cooling rate=1.000 kcal/atom/ps; target temperature=300 K) monitoring the same dihedral angle. The average value was calculated; in both the cases it corresponded to that found by MM calculations.

DNMR Experiments: 0.5 mg of compound **101**, **102** or **119** was dissolved in 0.6 mL of D₂O (363–293 K) or CD₃CD₂OD (293–173 K). ¹H and selective 1D-NOESY (data not shown) spectra were recorded at different temperatures and then processed with MestreNova (MestreLab Research s.r.l.). For spectra recorded in D₂O, the HDO chemical shift was calculated according to the equation $\delta = 5.060 - 0.0122T + (2.11 \times 10^{-5})T$.^[171]

4.3 In Vitro Pharmacology: GABA_A R binding assays

4.3.1. Chemicals

- [³H]Flunitrazepam **170** (M.W. unlabelled at this specific activity 313.28, C₁₆H₁₂FN₃O₃), flunitrazepam[methyl-³H], has a specific activity of 80.0 Ci/mmol and was purchased from International PBI SPA (Milan, Italy), American Radiolabeled Chemicals, Inc.
- Flumazenil **171** (M.W. 303.39, C₁₅H₁₄FN₃O₃), 8-fluoro-5,6-dihydro-5-methyl-6-oxo-4H-imidazo[1,5-a][1,4]benzodiazepine-3-carboxylic acid, ethyl ester, was purchased from TOCRIS Bioscience, Tocris Cooksoon Ltd. (Bristol, U.K.)

- [³H]Muscimol **176** (M.W. unlabelled 114.10, C₄H₆N₂O₂), [methylene-³H(N)]-(3-hydroxy-5-aminomethylisoxazole), has a specific activity of 36.6 Ci/mmol and was purchased from PerkinElmer (Boston, U.S.A.).
- Muscimol hydrobromide 98% **177** (M.W. 195.01, C₄H₆N₂O₂·HBr), 5-aminomethyl-3-hydroxyisoxazole hydrobromide), was purchased from Sigma-Aldrich (Milan, Italy).

4.3.2 Instruments

Centrifugation assays were performed on a centrifuge Biofuge Primo R-Heraeus and on an ultracentrifuge Beckman XL-90. Filtration assays were performed using Whatman GF/B glass fiber filters ($\varnothing = 1\text{-}2$ cm). Liquid scintillation counting^{xxxii} was performed on a Spectrophotometer Beckman LS65000 with 40% of efficiency for Tritium and was used the scintillation fluid UltimaGold™ F from PerkinElmer (Boston, U.S.A.).

4.3.3 Methods

The Investigations using experimental animals were conducted in accordance with the internationally accepted principles for laboratory animal use and care as found in for example the European Community guidelines (EEC Directive of 1986; 86/609/EEC).

^{xxxii} **Liquid scintillation counting** is an analytical technique for the measure of radiation from beta-emitting nuclides. It's an instrument capable of converting the kinetic energy of nuclear emissions into light energy. Samples are dissolved or suspended in a "cocktail", the **scintillation fluid**, containing an aromatic solvent and small amounts of other additives known as fluorophores. Beta particles emitted from the sample transfer energy to the solvent molecules, which transfer their energy to the fluorophores; the excited fluor molecules dissipate the energy by emitting light. In this way, each beta emission (ideally) results in a pulse of light, which is detected by the counter.

4.3.3.1 Benzodiazepine Derivatives

4.3.3.1.1 Membrane Preparation

Membranes were prepared from rat cortex as described by Ahboucha *et al.*^[172] The rat frontal cortex was homogenized, through a glass/teflon potter at 1000 rpm, in ice-cold 0.32 M sucrose, pH 7.4 (20 mL/gr of tissue) and the homogenate was centrifuged at $2000 \times g$ for 10 min at 4 °C. The supernatant was then ultracentrifuged at $140000 \times g$ for 30 min at 4 °C and the pellet was resuspended in Tris-HCl 50 mM pH 7.4 (2mL/g wet weight) and again centrifuged at $140000 \times g$ for 30 min at 4 °C. After the final centrifugation, the pellet was suspended in 1ml of ice-cold Tris-HCl buffer (50 mM pH 7.4) and was manually homogenized through a glass/teflon potter, and stored frozen at -80 °C. On the day of the assay, the tissue was thawed and the pellet, resuspended in Tris-HCl in order to obtain a final protein concentration of 2 mg/mL, was used for displacement binding studies.

4.3.3.1.2 Radioligand Binding Assay

[³H]Flunitrazepam **170** (1nM) served as radioligand and non specific binding was determined in the presence of flumazenil **171** (100μM) and represented about 1-2% of the total binding. The water soluble benzodiazepine derivatives synthesized were diluted in TrisHCl buffer 50mM pH 7.4 to obtain the final concentration of 100μM, whereas stock solutions of the benzodiazepine derivatives with the benzyl group in the sugar were prepared in ethanol and then diluted in TrisHCl buffer to obtain the final concentration of 100μM. The binding reaction consisted in 0.3 mg of membranes incubated with the radioligand in the presence or absence of the test compounds for 90 min at 4 °C. During this incubation period, the appropriate number of filters were soaked in ice cold buffer. The binding reaction was then stopped by rapid filtration under vacuum through a glass-fiber filter. The filters were mounted in the filtration manifold, vacuum was applied and an aliquot of the first sample was applied to the

first filter. Once the sample compartment drains, the filter was washed immediately by the rapid addition of 2 mL portions of ice cold Tris-HCl buffer (two times). After being washed twice the filters were dried under a heat lamp for 10 min, and then were transferred to scintillation vials and dissolved in 8 mL of scintillation fluid. Filter bound radioactivity was determined by scintillation counter, 20 min for each filter. The radioactivity values obtained from the spectrophotometer in dpm were converted into percentages, considering the value of specific binding 100%, given by the samples only with the [³H]flunitrazepam **170**. For all compounds three independent experiments were performed in triplicate.

4.3.3.1.3 Data Analysis

Results are expressed in terms of percentage of control [³H]flunitrazepam **170** specific binding and analyzed by GraphPad Prism, using the Kruskal-Wallis ANOVA for non parametric data followed by Dunns test for specific comparisons.

4.3.3.2 GABA Derivatives

4.3.3.2.1 Membrane Preparation

Rat brain membranes were prepared and assayed for GABA_A receptor binding by using the method described by Frosini *et al.*^[173] with slight modifications. The whole brain was homogenized in 10 vol. of cold 0.32 M sucrose and the homogenate was centrifuged at 2500 × *g* for 10 min at 4 °C. The supernatant was then ultracentrifuged at 48000 × *g* for 30 min at 4 °C and the pellet (crude synaptic membranes) was resuspended in Tris-HCl 50 mM pH 7.4 (1mL/g wet weight) and frozen (-20 °C) for 24h. Thawed membranes were then resuspended in Tris-HCl containing Triton X-100 (0.05% w/v) in order to obtain a final protein concentration of 1 mg/ml. The mixture was incubated for 30 min at 37 °C and then ultracentrifuged at 48000 × *g* for 20 min at

4 °C. The pellet was then washed three times with Tris-HCl 50 mM pH 7.4 and frozen at -20 °C before use. The pellet, resuspended in Tris-HCl in order to obtain a final protein concentration of 2 mg/mL, was used for displacement binding studies.

4.3.3.2.2 Radioligand Binding Assay

[³H]Muscimol **176** (10 nM) served as radioligand and non specific binding was determined in the presence of non labelled muscimol **177** (500 μM) and represented about 30–40% of the total binding. For Scatchard analysis, 50 μM aliquots (0.1 mg protein) of membrane preparation were incubated in Tris-HCl buffer (50 mM, pH 7.4) in a final volume of 500 μM in the presence of [³H]muscimol 10 nM. Compounds **87**, **90** and **91** were diluted only in Tris-HCl buffer to obtain the final concentration of 500 μM, whereas stock solutions of compounds **86**, **88**, **89** and **92** were prepared in ethanol and then diluted in Tris-HCl to obtain the final concentration of 500 μM. The binding reaction consisted in 0.1 mg of membranes incubated with the radioligand in the presence or absence of the test compounds for 30 min at 4 °C. During this incubation period, the appropriate number of filters was soaked in ice cold buffer. The binding reaction was then stopped by rapid filtration under vacuum through a glass-fiber filter. The filters were mounted in the filtration manifold, vacuum was applied and an aliquot of the first sample was applied to the first filter. Once the sample compartment drains, the filter was washed immediately by the rapid addition of 2 mL ice cold Tris-HCl buffer (two times). After being washed twice the filters were dried under a heat lamp for 10 min, and then were transferred to scintillation vials and dissolved in 8 mL of scintillation fluid. Filter-bound radioactivity was determined by a scintillation counter (20 min for each filter), to estimate the amount of bound radioligand. The radioactivity values obtained from the spectrophotometer are dpm, which were convert into percentages, considering the value of specific binding 100%, given by the samples only with the [³H]muscimol. For all compounds three independent experiments were performed in triplicate. Filtration assay was performed as described by Frosini *et al.*^[173]

4.3.3.2.3 Data Analysis

Results are expressed as percentage of control [^3H]muscimol **176** specific binding and analyzed by Graph Pad Prism, using the Kruskal-Wallis ANOVA for non parametric data followed by Dunns test for specific comparisons.

4.3.3.3 Lowry Protein Assay^[174]

The Lowry procedure is one of the most venerable and widely-used protein assays, being first described in 1951. Under alkaline conditions, the divalent copper ion forms a complex with peptide bonds in which it is reduced to monovalent ion. Monovalent copper ion and the radical groups of tyrosine, tryptophan, and cysteine react with Folin reagent (phospho-molybdic-phosphotungstic reagent) to produce an unstable product that becomes reduced to molybdenum/tungsten, and changes colour from yellow to blue.

There is much protein-to-protein variation in the intensity of colour development. Ideally, the standard should be similar to the unknown. In our protein assay we used bovine serum albumin (BSA) as a standard since albumin is a major component of serum.

Stock Solutions:

- Standard solution of bovine serum albumin 1 mg/mL;
- Cooper reagent: Na_2CO_3 , CuSO_4 and $\text{NaKC}_4\text{H}_4\text{O}_6 \cdot 4\text{H}_2\text{O}$
- Folin Ciocalteau reagent

Samples:

The rat cortex membrane samples were diluted three times:

- Dilution 1:100;
- Serial dilution 1:500 to 1:100;
- Dilution 1:500

Procedure:

In a ninety six wells microplate were added 1, 2, 4, 8, 12, 15, 20, 30 and 50 μL of BSA (1 mg/mL) and 50 μL of rat cortex membrane for each dilution. The albumin is diluted in distilled H_2O to obtain the final volume. To each well was added 150 μL of Cooper reagent, and after 10 min of incubation, 15 μL of Folin Ciocalteu reagent was added. The plate with the samples was manual agitated and another incubated of 45 min in the dark was performed. After two incubations the samples were ready to be read in a spectrophotometer at 630 nm. The control samples (blank) were prepared in same way as the standard, but the 100 μL of albumin were substituted by distillate water. All analyses are performed in triplicate.

Analysis:

A standard curve of absorbance versus micrograms protein was prepared. The determination of the concentrations of the original samples is made through the amount protein in the curve.

REFERENCES



-
- [1] World Health Organization, <http://www.who.int/en/>.
- [2] Europa - The European Union On-Line, <http://europa.eu>.
- [3] G. L. Patrick (Ed.), *An Introduction to Medicinal Chemistry*, Oxford University Press Inc., New York, U.S., **2005**.
- [4] E. R. Kandel, J. H. Schwartz, T. M. Jessel (Eds.), *Principles of Neural Science*, Appleton & Lange, **2000**.
- [5] W. A. Catterall, *Science* **1984**, 223(4637), 653-661.
- [6] Anthropology.net, (Ed.: K. Kamrani), <http://anthropology.net>.
- [7] H. R. Arias (Ed.), *Biological and biophysical aspects of ligand-gated ion channel receptor superfamilies*, Research Signpost, India, **2006**.
- [8] D. A. Lauffenburger, J. J. Linderman (Eds.), *Receptors: Models for Binding, Trafficking, and Signalling*, Oxford University Press, **1996**.
- [9] S. J. Enna (Ed.), *GABA*, Elsevier, London, UK, **2006**.
- [10] A. N. Bateson, *Sleep Medicine* **2004**, 5 Suppl.(1), S9-S15.
- [11] J. Bormann, A. FeigenSPAN, *Trends Neurosci.* **1995**, 18, 515-519.
- [12] A. Couve, S. J. Moss, M. N. Pangalos, *Mol. Cell. Neurosci.* **2000**, 16, 296-312.
- [13] B. Bettler, J. Y. Tiao, *Pharmacol. Ther.* **2006**, 110, 533-543.
- [14] E. Roberts, S. Frankel, *J. Biol. Chem.* **1950**, 187, 55-63.
- [15] S. Udenfriend, *J. Biol. Chem.* **1950**, 187, 65-69.
- [16] J. Awapara, A. J. Landua, R. Fuerst, B. Seale, *J. Biol. Chem.* **1950**, 187, 35-39.
- [17] O. A. C. Petroff, *The Neuroscientist* **2002**, 8(6), 562-573.
- [18] E. Roberts, D. G. Simonsen, *Biochem. Pharmacol.* **1963**, 12, 113-134.
- [19] J.-Y. Wu, T. Matsuda, E. Roberts, *J. Biol. Chem.* **1973**, 248, 3038-3034.
- [20] W. Löscher, *Prog. Neurobiol.* **1999**, 58, 31-59.
- [21] D. F. Owens, A. R. Kriegstein, *Nature Reviews Neuroscience* **2002**, 3, 715-727.
- [22] S. J. Enna, N. G. Bowery (Eds.), *Diversity in structure, pharmacology, and regulation of GABA(A) receptors in "The GABA Receptors"*, Humana Press, Totowa, New Jersey, **1997**.
- [23] T. C. Jacob, S. J. Moss, R. Jurd, *Nature Reviews Neuroscience* **2008**, 9, 331-343.
- [24] Wikipedia, www.en.wikipedia.org.
- [25] E. B. Gonzales, C. L. Bell-Horner, M. A. M. d. l. Cruz, J. A. Ferrendelli, D. F. Covey, G. H. Dillon, *J. Pharmacol. Exp. Therap.* **2003**, 309(2), 677-683.
- [26] K. L. Williams, J. B. Tucker, G. White, D. S. Weiss, J. A. Ferrendelli, D. F. Covey, J. E. Krause, S. M. Rothman, *Mol. Pharmacol.* **1997**, 52, 114-119.
- [27] P. Krosggaard-Larsen, B. Frolund, U. Kristiansen, K. Frydenvang, B. Elbert, *European Journal of Pharmaceutical Sciences* **1997**, 5, 355-384.
- [28] G.-D. Li, C.-S. S. Chang, R. W. Olsen, *International Congress Series* **2005**, 1283, 61-66.
- [29] U. Rudolph, H. Mohler, *Ann. Rev. Pharmacol. Toxicol.* **2004**, 44, 475-498.
- [30] I. Bruning, E. Scotti, C. Sidler, J. M. Fritschy, *J. Comp. Neurol.* **2002**, 443, 43-55.
- [31] A. V. Kalueff, *Neurochem. Int* **2007**, 50, 61-68.
- [32] B. Frolund, B. Ebert, U. Kristiansen, T. Liljefors, P. Krosggaard-Larsen, *Curr. Top. Med. Chem.* **2002**, 2, 817-832.
- [33] P. Krosggaard-Larsen, H. Hjeds, D. R. Curtis, D. Lodge, G. A. R. Johnston, *J. Neurochem.* **1979**, 32, 1717-1724.

- [34] M. Mortensen, U. Kristiansen, B. Ebert, B. Frølund, P. Krogsgaard-Larsen, T. G. Smart, *J. Physiol. (London)* **2004**, 557, 393-417.
- [35] N. Gulyaeva, A. Zaslavsky, P. Lechner, M. Chlenov, O. McConnell, A. Chait, V. Kipnis, B. Zaslavsky, *Eur. J. Med. Chem.* **2003**, 38, 391-396.
- [36] P. Krogsgaard-Larsen, B. Frølund, U. Kristiansen, K. Frydenvang, B. Elbert, *Eur. J. Pharm. Sci.* **1997**, 5, 355-384.
- [37] C. Bernard, R. Cossart, J. C. Hirsch, M. Esclapez, Y. Ben-Ari, *Epilepsia* **2000**, 41(Suppl. 6), S90-S95.
- [38] C. G. T. Wong, T. Bottiglieri, O. C. Snead, *Ann. Neurol.* **2003**, 54, S3-S12.
- [39] R. B. Lydiard, *J. Clin. Psychiat.* **2003**, 64, 21-27.
- [40] L. Hosak, J. Libiger, *J. Eur. Psychiatry* **2002**, 17, 371-378.
- [41] L. M. Levy, M. C. Dalakas, M. K. Floeter, *Ann. Intern. Med.* **1999**, 131, 522-530.
- [42] J. R. Cooper, F. E. Bloom, R. H. Roth (Eds.), *Amino acid transmitters. In The biochemical basis of neuropharmacology*, Oxford University Press, Oxford, UK, **1991**.
- [43] S. Vemulapalli, M. Barletta, *Arch. Int. Pharmacodyn. Ther.* **1984**, 267, 46-58.
- [44] J. I. Nurnberger., W. H. Berrettini, S. Simmons-Alling, J. I. Guroff, E. S. Gershon, *Psychiatry Res.* **1986**, 19, 113-117.
- [45] S. Hog, J. R. Greenwood, K. B. Madsen, O. M. Larsson, B. Frolund, A. Schousboe, P. Krogsgaard-Larsen, R. Calusen, *Curr. Top. Med. Chem.* **2006**, 6, 1861-1882.
- [46] M. Chebib, G. A. R. Johnston, *J. Med. Chem.* **2000**, 43(8), 1427-1447.
- [47] R. W. Olsen, C.-S. S. Chang, G. Li, H. J. Hanchar, M. Wallner, *Biochem. Pharmacol.* **2004**, 68, 1675-1684.
- [48] E. R. Korpi, G. Grunder, H. Luddens, *Prog. Neurobiol.* **2002**, 67, 113-159.
- [49] G. A. R. Johnston, *Pharmacol. Therapeut.* **1996**, 69, 173-198.
- [50] J. S. Bryans, D. J. Wustrow, *Med. Res. Rev.* **1999**, 19, 149-177.
- [51] A. Sarup, O. M. Larsson, T. Bolvig, B. Frolund, P. Krogsgaard-Larsen, A. Schousboe, *Neurochem. Int* **2003**, 43, 445-451.
- [52] M. W. Hill, M. A. M. Cruz, D. F. Covey, S. M. Rothman, *Epilepsy Res.* **1999**, 37, 121-131.
- [53] G. Maksay, P. Molnár, L. Gruber, *Eur. Pharmacol. Mol. - Mol. Pharmacol. Sect* **1994**, 288, 61-68.
- [54] M. W. Hill, P. A. Reddy, D. F. Covey, S. M. Rothman, *J. Neurosci* **1998**, 18, 5103-5111.
- [55] L. R. McMahon, A. Coop, C. P. France, G. Winger, W. L. Woolverton, *Eur. J. Pharm.* **2003**, 466, 113-120.
- [56] T. Kapferer, R. Bruckner, *Eur. J. Org. Chem.* **2006**, 2119-1233 and refs cited therein.
- [57] M. Ghosh, *Tetrahedron* **2007**, 63, 11710-11715.
- [58] E. Takano, *Curr. Opin. Microbiol.* **2006**, 9, 287-294.
- [59] A. Kar, S. Gogoi, N. P. Argade, *Tetrahedron* **2005**, 61, 5297-5302.
- [60] M. I. Konaklieva, B. J. Plotkin, *Mini Rev. Med. Chem.* **2005**, 5, 73-95.
- [61] N. Ghoshala, P. K. Mukherjeeb, *Bioorg. Med. Chem. Lett.* **2004**, 14, 103-109.
- [62] R. Razet, U. Thomet, R. Furtmueller, F. Jursky, E. Sigel, W. Sieghart, R. H. Dodd, *Bioorg. Med. Chem. Lett.* **2000**, 10, 2579-2583.

- [63] D. J. Canney, H.-F. Lu, A. C. McKeon, K.-W. Yoon, K. Xu, K. D. Holland, S. M. Rothman, J. A. Ferrendelli, D. F. Covey, *Bioorg. Med. Chem.* **1998**, *6*, 43-55.
- [64] K. D. Holland, G. C. Mathews, A. M. Bolos-Sy, J. B. Tucker, P. A. Reddy, D. F. Covey, J. A. Ferrendelli, S. M. Rothman, *Mol. Pharmacol.* **1995**, *47*, 1217-1223.
- [65] P. A. Reddy, B. C. Hsiang, T. N. Latifi, M. W. Hill, K. E. Woodward, S. M. Rothman, J. A. Ferrendelli, D. F. Covey, *J. Med. Chem.* **1996**, *39*, 1898-1906.
- [66] P. A. Reddy, K. E. Woodward, S. M. McIlheran, B. C. Hsiang, T. N. Latifi, M. W. Hill, S. M. Rothman, J. A. Ferrendelli, D. F. Covey, *J. Med. Chem.* **1997**, *40*, 44-49.
- [67] E. M. Peterson, K. Xu, K. D. Holland, A. C. McKeon, S. M. Rothman, J. A. Ferrendelli, D. F. Covey, *J. Med. Chem.* **1994**, *37*, 275-286.
- [68] K. D. Holland, A. C. McKeon, D. F. Covey, J. A. Ferrendelli, *J. Pharmacol. Exp. Ther.* **1990**, *254*, 578 - 583.
- [69] G. C. Mathews, A. M. Bolos-Sy, D. F. Covey, S. M. Rothman, J. A. Ferrendelli, *Neuropharmacology* **1995**, *35*(2), 123-136.
- [70] G. V. Rekatas, E. K. Tani, V. J. Demopoulos, P. N. Kourounakis, *Drug. Develop. Res.* **2000**, *51*, 143-148.
- [71] M. W. Hill, P. A. Reddy, D. F. Covey, S. M. Rothman, *J. Pharmacol. Exp. Therap.* **1998**, *285*, 1303-1309.
- [72] H. Sasaki, Y. Mori, J. Nakamura, J. Shibasaki, *J. Med. Chem.* **1991**, *34*, 628-633.
- [73] G. M. Wall, J. K. Baker, *J. Med. Chem.* **1989**, *32*, 1340-1348.
- [74] T. Jehle, T. J. Feuerstein, W. A. Lagreze, *Ophthalmologie* **2001**, *98*, 237-241.
- [75] A. L. L. Garcia, M. J. S. Carpes, A. C. B. M. d. Oca, M. A. G. d. Santos, C. C. Santana, C. R. D. Correia, *J. Org. Chem.* **2004**, *70*, 1050-1053.
- [76] S. Roller, C. Siegers, R. Haag, *Tetrahedron* **2004**, *60*, 8711-8720.
- [77] M. W. Hill, P. A. Reddy, D. F. Covey, S. M. Rothman, *J. Pharmacol. Exp. Therap.* **1998**, *285*(3), 1303-1309.
- [78] B. M. Kenda, A. C. Matagne, P. E. Talaga, P. M. Pasau, E. Differding, B. I. Lallemand, A. M. Frycia, F. G. Moureau, H. V. Klitgaard, M. R. Gillard, B. Fuks, P. Michel, *J. Med. Chem.* **2004**, *47*, 530-549.
- [79] S. Bhutoria, N. Ghoshal, *QSAR Comb. Sci.* **2008**, *27*(7), 876-889.
- [80] D. A. Horton, G. T. Bourne, M. L. Smythe, *Chem. Rev.* **2003**, *103*, 893-930.
- [81] D. H. Kim, *J. Heterocycl. Chem.* **1975**, *12*, 1323-1324.
- [82] M. R. Peia, J. K. Stille, *J. Am. Chem. Soc.* **1989**, *111*, 5417-5424.
- [83] W. B. Wright, H. J. Brabander, E. N. Greenblatt, I. P. Day, R. A. Hardy, *J. Med. Chem.* **1978**, *21*, 1087-1089.
- [84] L. Moroder, J. Lutz, F. Grams, S. Rudolph-Bohner, G. Osapay, M. Goodman, W. Kolbeck, *Biopolymers* **1996**, *38*, 295-300.
- [85] M. Chorev, M. Goodman, *Acc. Chem. Res.* **1993**, *26*, 266-277.
- [86] S. A. W. Gruner, E. Locardi, E. Lohof, H. Kessler, *Chem. Rev.* **2002**, *102*, 491-524.
- [87] Y. Brouillette, J. Martinez, V. Lisowski, *Eur. J. Org. Chem.* (in press).
- [88] B. E. Evans, K. E. Rittle, M. G. Bock, R. M. DiPardo, R. M. Freidinger, W. L. Whitter, G. F. Lundell, D. F. Veber, P. S. Anderson, R. S. L. Chang, V. J. Lotti, D. J. Cerino, T. B. Chen, P. J. Kling, K. A. Kunkel, J. P. Springer, J. Hirshfield, *J. Med. Chem.* **1988**, *31*, 2235-2246.

- [89] R. G. Sherrill, J. M. Berman, L. Birkemo, D. K. Croom, M. Dezube, G. N. Ervin, M. K. Grizzle, M. K. James, M. F. Johnson, K. L. Queen, T. J. Rimele, F. Vanmiddlesworth, E. E. Sugg, *Bioorg. Med. Chem. Lett.* **2001**, *11*, 1145-1148.
- [90] M. G. Bock, R. M. Dipardo, B. E. Evans, K. E. Rittle, W. L. Whitter, V. M. Garsky, K. F. Gilbert, J. L. Leighton, K. L. Carson, E. C. Mellin, D. F. Veber, R. S. L. Chang, V. J. Lotti, S. B. Freedman, A. J. Smith, S. Patel, P. S. Anderson, R. M. Freidinger, *J. Med. Chem.* **1993**, *36*, 4276-4292.
- [91] G. Hirst, C. Aquino, L. Birkemo, D. Croom, M. Dezube, R. Dougherty, G. Ervin, M. Grizzle, B. Henke, M. James, M. Johnson, T. Momtahan, K. Queen, R. Sherrill, J. Szewczyk, T. Willson, E. Sugg, *J. Med. Chem.* **1996**, *39*, 5236-5245.
- [92] D. Dumas, G. Leclerc, J.J. Baldwin, S. Dale Lewis, M. Murcko, A. M. Naylor-Olsen, *Eur. J. Med. Chem.* **1998**, *33*, 471-488.
- [93] A. Kamal, K. L. Reddy, V. Devaiah, N. Shankaraiah, G. S. Kumar Reddy, S. Raghavan, *J. Comb. Chem.* **2007**, *9*, 29-42.
- [94] M. H. Bolli, J. Marfurt, C. Grisostomi, *J. Med. Chem.* **2004**, *47*, 2776-2795.
- [95] T. M. Francis, T. B. Sundberg, J. Cleary, T. Groendyke, A. W. Opiari, J. G. D. Glicka, *Bioorg. Med. Chem. Lett.* **2006**, *16*, 2423-2427.
- [96] D. Neidle, M. J. Waring, D. E. Thurston (Eds.), *Advances in the Study of Pyrrolo[2,1-c][1,4]benzodiazepine (PBD) Antitumour Antibiotics, in Molecular Aspects of Anticancer Drug-DNA Interactions*, The Macmillan Press Ltd., London, **1993**.
- [97] E. D. Clercq, *Antiviral Res.* **1998**, *38*, 153-179.
- [98] J. M. Samanen, F. E. Ali, L. S. Barton, W. E. Bondinell, J. L. Burgess, J. F. Callahan, R. R. Calvo, W. Chen, L. Chen, K. Erhard, G. Feuerstein, R. Heys, S-M. Hwang, D. R. Jakas, R. M. Keenan, T. W. Ku, C. Kwon, C-P. Lee, W. H. Miller, K. A. Newlander, A. Nichols, M. Parker, C. E. Peishoff, G. Rhodes, S. Ross, A. Shu, R. Simpson, D. Takata, T. O. Yellin, I. Uzsinskas, J. W. Venslavsky, C-K. Yuan, W. F. Huffman, *J. Med. Chem.* **1996**, *39*, 4867-4870.
- [99] P. Verdié, G. Subra, L. Feliu, P. Sanchez, G. Bergé, G. Garcin, J. Martinez, *J. Comb. Chem.* **2007**, *9*, 254-262.
- [100] M. D. Cummings, C. Schubert, D. J. Parks, R. R. Calvo, L. V. La France, J. Lattanze, K. L. Milkiewicz, T. Lu, *Chem. Biol. Drug Des.* **2006**, *67*, 201-205.
- [101] N. Cabedo, X. Pannecoucke, J.-C. Quirion, *Eur. J. Org. Chem.* **2005**, 1590-1596.
- [102] S. MacQuarrie-Hunter, P. R. Carlier, *Org. Lett.* **2005**, *7*, 5305-5308.
- [103] W. Zhang, Y. Lu, C. Hiu-Tung Chen, D. P. Curran, S. Geib, *Eur. J. Org. Chem.* **2006**(9), 2055-2059.
- [104] L. Cipolla, A. C. Araújo, C. Airoidi, D. Bini, *Anti-Cancer Agents in Medicinal Chemistry* **2009** *9*, 1-31.
- [105] T. Nagasaka, Y. Koseki, F. Hamaguchi, *Tetrahedron Lett.* **1989**, *30*, 1871-1872.
- [106] S. C. Wilson, P. W. Howard, S. M. Forrow, J. A. Hartley, L. J. Adams, T. C. Jenkins, L. R. Kelland, D. E. Thurston, *J. Med. Chem.* **1999**, *42*, 4028-4041.
- [107] X. Li, J. Yu, J. R. Atack, J. M. Cook, *Med. Chem. Res.* **2004**, *13*, 259-281.
- [108] E. Halapy, N. Kreiger, M. Cotterchio, M. Sloan, *Annals Epidemiology* **2006**, *16*(8), 632-636.
- [109] A. Terletskaia, N. Shvets, A. Dimoglo, Y. Chumakov, *J. Mol. Struct. (Theochem)* **1999**, *463*, 99-103.

- [110] L. J. Pym, S. M. Cook, T. Rosahl, R. M. McKernan, J. R. Atack, *British J. Pharmacology* **2005**, 1-9.
- [111] E. Costa, *Ann. Rev. Pharmacol. Toxicol.* **1998**, *38*, 321-250.
- [112] D. B. Williams, M. H. Akabas, *Mol. Pharmacol.* **2000**, *58*(5), 1129-1136.
- [113] J. F. Blount, R. I. Fryer, N. W. Gilman, L. J. Todaro, *Mol. Pharmacol.* **1983**, *24*, 425-428.
- [114] G. Maksay, Z. Tegyei, M. Simonyi, *Mol. Pharmacol.* **1991**, *39*, 725-732.
- [115] M. Simonyi, G. Maksay, I. Kovács, Z. Tegyei, L. Párkányi, A. Kálmán, L. Ötvös, *Bioorg. Chem.* **1990**, *18*(1), 1-12
- [116] P. R. Cartier, H. Zhao, S. L. MacQuarrie-Hunter, J. C. DeGuzman, *J. Am. Chem. Soc.* **2006**, *128*(47), 15215-15220.
- [117] A. Konowal, G. Snatzke, T. Alebic-Kolbah, F. Kajfez, S. Rendic, V. Sunjic, *Biochem. Pharmacol.* **1979**, *28*, 3109-3113.
- [118] P. C.-H. Lam, P. R. Carlier, *J. Org. Chem.* **2005**, *70*, 1530-1538.
- [119] Q. Huang, X. He, C. Ma, R. Liu, D. Yu, C. A. Dayer, G. R. Wenger, R. McKernan, J. M. Cook, *J. Med. Chem.* **2000**, *43*, 71-95.
- [120] D. Hadjipavlou-Litina, R. Garg, C. Hansch, *Chem. Rev.* **2004**, *104*, 3751-3793.
- [121] Q. Wang, Y. Han, H. Xue, *CNS Drug Reviews* **1999**, *5*(2), 125-144.
- [122] K. C. Nicolaou, H. J. Mitchell, *Angew. Chem. Int. Ed.* **2001**, *40*, 1576-1624.
- [123] L. Cipolla, E. Formi, J. Jiménez-Barbero, F. Nicotra, *Chem. Eur. J.* **2002**, *8*(17), 3976-3983.
- [124] C. A. Lipinski, F. Lombardo, B. W. Dominy, P. J. Freeney, *Adv. Drug Delivery Rev.* **1997**, *23*, 3-25.
- [125] G. Wess, M. Urmann, B. Sickenberger, *Angew. Chem. Int. Ed.* **2001**, *40*, 3341-3350.
- [126] D. Bouhlal, P. Godé, G. Goethals, M. Massoui, P. Villa, P. Martin, *Carbohydr. Res.* **2000**, *329*, 207-214.
- [127] D. Bouhlal, P. Martin, M. Massoui, G. Nowogrocki, S. Pilard, P. Villa, G. Goethals, *Tetrahedron: Asymm.* **2001**, *12*, 1573-1577.
- [128] N. Nishimura, H. Hisamitsu, M. Sugiura, I. Maeba, *Carbohydr. Res.* **2000**, *329*, 681-686.
- [129] L. Abrous, P. A. Jokiel, S. R. Friedrich, J. H. Jr., A. B. S. III, R. Hirschmann, *J. Org. Chem.* **2004**, *69*, 280-302.
- [130] L. Abrous, J. H. Jr., S. R. Friedrich, A. B. S. III, R. Hirschmann, *Org. Lett.* **2001** *3*(7), 1089-1092.
- [131] R. Kumar, J. W. Lown, *Org. Biomol. Chem.* **2003**, *1*, 3327-3342.
- [132] F. Schweizer, A. Otter, O. Hindsgaul, *Synlett* **2001**, *11*, 1743-1746.
- [133] F. Schweizer, O. Hindsgaul, *Carbohydr. Res.* **2006**, *341*, 1730-1736.
- [134] A. Lajtha (Ed.), *Handbook of Neurochemistry and Molecular Neurobiology - Practical Neurochemistry Methods*, Springer, Berlin, **2007**.
- [135] A. P. Davenport (Ed.), *Methods in Molecular Biology, Receptor Binding Techniques*, Humana Press, Cambridge, U.K., **2005**.
- [136] G. Scatchard, *Ann. NY Acad. Sci* **1949**, *51*, 660-666.
- [137] Y. C. Cheng, W. H. Prusoff, *Biochem. Pharmacol.* **1973**, *22*(23), 3099-3108.
- [138] Y. Dupont, *Anal. Biochem.* **1984**, *142*, 504-510.
- [139] M.-X. Zhao, Y. Shi, *J. Org. Chem.* **2006**, *71*, 5377-5379.

- [140] B. Bessières, C. Morin, *J. Org. Chem.* **2003**, *68*, 4100-4103.
- [141] T. Matsumoto, T. Enomoto, T. Kurosaki, *J. Chem. Soc., Chem. Commun.* **1992**, 610-611.
- [142] M. Sugiyama, Z. Hong, L. J. Whalen, W. A. Greenberg, C.-H. Wong, *Adv. Synth. Catal.* **2006**, *348*, 2555 - 2559.
- [143] Y. Gizaw, J. N. BeMiller, *Carbohydr. Res.* **1995**, *266*, 81-85.
- [144] F. Nicotra, L. Panza, G. Russo, *J. Org. Chem.* **1987**, *52*, 5627-5630.
- [145] E. Forni, L. Cipolla, E. Caneva, B. L. Ferla, F. Peri, F. Nicotra, *Tetrahedron Lett.* **2002**, *43*, 1355-1357.
- [146] A. S. Serrianni, R. Barker, *J. Org. Chem.* **1984**, *49*, 3292-3300.
- [147] F. Peri, L. Cipolla, E. Forni, F. Nicotra, *Monatshefte fur Chemie* **2002**, *133*, 369-382.
- [148] H. Tsubomura, S. Nagakura, *J. Chem. Phys.* **1957**, *27*, 819.
- [149] S. Nagakura, *J. Am. Chem. Soc.* **1958**, *80*, 520-524.
- [150] C. D. Schmulbach, D. M. Hart, *J. Am. Chem. Soc.* **1964**, *86*, 2347.
- [151] C. Biselx, J.-J. Schaer, D. Janjic, *Helv. Chim. Acta* **1978**, *61*, 832-836.
- [152] A. Goosen, C. W. McClelland, A. W. Sipamla, *J. Chem. Res. (M)* **1995**, *18*, 311.
- [153] K. C. Nicolaou, D. A. Claremon, W. E. Barnette, S. P. Seitz, *J. Am. Chem. Soc.* **1979**, *101*, 3704-3706.
- [154] K. C. Nicolaou, *Tetrahedron* **1981**, *37*, 4097-4109.
- [155] D. L. J. Clive, V. Farina, A. Singh, C. K. Wong, W. A. Kiel, S. M. Menchen, *J. Org. Chem.* **1980**, *45*, 2120-2126.
- [156] R. R. Webb, S. Danishefsky, *Tetrahedron Lett.* **1983**, *24*, 1357-1360.
- [157] L. Cipolla, C. Redaelli, F. Nicotra, *Letters in Drug Design and Discovery* **2005**, *2*(4), 291-293.
- [158] A. L. Williams, T. A. Grillo, D. L. Comin, *J. Org. Chem.* **2002**, *67*, 1972-1973.
- [159] S. J. Katz, S. C. Bergmeier, *Tetrahedron Lett.* **2002**, *43*, 557-559.
- [160] M. Takebayashi, S. Hiranuma, Y. Kanie, T. Kajimoto, O. Kanie, C.-H. Wong, *J. Org. Chem.* **1999**, *64*, 5280-5291.
- [161] P. V. Murphy, *Eur. J. Org. Chem.* **2007**, 4177-4187.
- [162] V. G. S. Box, *J. Mol. Struct.* **2001**, *569*, 167-178.
- [163] H. S. Jensen, G. Limberg, C. Pedersen, *Carbohydr. Res.* **1997**, *302*, 109-112.
- [164] S. Canesi, G. Berthiaume, P. Deslongchamps, *Eur. J. Med. Chem.* **2006**, 3681-3686.
- [165] F. A. Davis, T. Ramachandar, J. Chai, E. Skucas, *Tetrahedron Lett.* **2006**, *47*, 2743-2746.
- [166] A. Avdagic, A. Lesac, V. Sunjic, *Tetrahedron* **1999**, *55*, 1407-1416.
- [167] A. Avdagič, A. Lesac, Z. Majer, M. Hollosi, V. Sunjic, *Helv. Chim. Acta* **1998**, *81*, 1567-1582.
- [168] R. Pappo, D. S. Allen, R. U. Lemieux, W. S. Johnson, *J. Org. Chem.* **1956**, *21*, 478-479.
- [169] G. W. J. Fleet, J. C. Son, *Tetrahedron* **1988**, *44*, 2637-2647.
- [170] K. Lee, M. Zhang, H. Liu, D. Yang, T. R. J. Burke, *J. Med. Chem.* **2003**, *46*, 2621-2630.
- [171] H. E. Gottlieb, V. Kotlyar, A. Nudelman, *J. Org. Chem.* **1997**, *62*, 7512-7515.

- [172] S. Ahboucha, F. Araqi, G. P. Layrargues, R. F. Butterworth, *Neurochem. Int.* **2005**, *47*, 58-63.
- [173] M. Frosini, C. Sesti, S. Dragoni, M. Valoti, M. Palmi, H. B. F. Dixon, F. Machetti, G. Sgaragli, *Br. J. Pharmacol.* **2003**, *138*, 1163-1171.
- [174] O. H. Lowry, N. J. Rosebrough, A. L. Farr, R. J. Randall, *J. Biol. Chem.* **1951**, *193*, 265-275.